Loughborough University

FETUS SAFETY IN MOTOR VEHICLE ACCIDENTS

by

Moustafa Moustafa

A Doctoral Thesis

Submitted in partial fulfilment of the requirements for the award of

Doctor of Philosophy of Loughborough University

May 2014

ABSTRACT

Motor vehicle accidents are statistically the major cause of accidental severe injuries for pregnant women and fetuses fatality. Volunteers, post mortem human surrogates, anthropomorphic crash test devices and computational occupant models are used to improve human safety in motor vehicle accidents. However, due to the ethical issues, pregnant women and their fetuses cannot be used as volunteers or post mortem human surrogates to investigate the effects of crashes on them. The only anthropomorphic test device representing pregnant women is very limited in design and lacks a fetus. There is no computational pregnant occupant model with a fetus other than 'Expecting'.

This thesis focuses on understanding the risk of placental abruption for pregnant drivers involved in road accidents, hence assessing the risk to fetus fatality. An extensive review of existing models in general and pregnant women models in particular is reported. The time line of successive development of crash test dummies and their positive effect on automotive passive safety design are examined. 'Expecting', the computational pregnant occupant model with a finite element uterus and a multibody fetus, is used in this research to determine the strain levels in the uteroplacental interface. External factors, such as the effect of restraint systems and crash speeds are considered. Internal factors, such as the effect of placental location in the uterus, and the inclusion and exclusion of a fetus are investigated. The head of the multibody fetus is replaced with a deformable head model to investigate the effects of a deformable fetus head on strain levels.

The computational pregnant driver model with a fetus offers a more realistic representation of the response to crash impact hence provides a useful tool to investigate fetus safety in motor vehicle accidents. Seat belt, airbag and steering wheel interact directly with the pregnant abdomen and play an important role on fetus safety in motor vehicle accidents. The results prove that the use of a three-point seat belt with the airbag offer the greatest protection to the fetus for frontal crash impacts. The model without a fetus underestimates the strain levels. The outcome of this research should assist automobile manufacturers to address the potential safety issues at the design level.

Key Words: Motor vehicle safety, fetus, pregnant, Expecting, placenta, airbag, computational occupant models, anthropomorphic test devices.

To My Mother, Sabire
My Mother-in-law, Sezer
And My Dear Wife, Sena

ACKNOWLEDGEMENTS

I would like to express my gratefulness and appreciation to *Prof Dr Serpil Acar*, who accepted me as her PhD student and introduced me to the long exciting journey of 'Expecting'. Without her guidance, kind encouragement and care regarding every aspect of my PhD studentship, this thesis would not have been possible. Her knowledge, patience and understanding made possible the successful completion of the thesis.

I would like to express my deepest gratitude and appreciation to *Prof Dr Memis Acar*, who considered my PhD application, inspired, encouraged and supported me for this study. He has helped me at various stages during my PhD studies and willingly sharing his knowledge and ideas with me.

I am particularly grateful to *Dr Volkan Esat* from Middle East Technical University for his invaluable help, contributions and never ending support. I would like to extend my sincere thanks to *Dr Firat Batmaz and Dr Mostafa Aldah* for their unique friendship and help. Many thanks to *Dr Alix Weekes* from the Thatcham Motor Insurance Repair Research Centre for her assistance in the experimental tests.

I would also like to thank to *Dr Emrah Demirci* and *Dr Murat Demiral* from the Mechanical and Manufacturing Engineering School for their invaluable fellowship. My best wishes to Loughborough and Leicester Turkish communities for their strong fellowship and enthusiasm.

Very special thanks to Loughborough University for giving me the opportunity to carry out my doctoral research and for their financial support. Funding from the Loughborough University during my study is gratefully acknowledged.

Lastly, I would like to appreciate my parents, *Sefaettin and Sabire Mustafa*, and my brother *Serhat* for their patience, love, encouragement and unique support during my studies. And most of all for my loving, supportive, encouraging, and patient wife *Fatma Sena* whose faithful support during the final stages of this PhD is so appreciated. Thank you for being in my life. You are all loved deeply.

CONTENTS

LIST OF FIGURES

LIST OF TABLES

LIST OF SYMBOLS AND ABBREVIATIONS

ABAQUS	: Finite element analysis and computer aided engineering software
AC	: Abdominal circumference
AM50	: 50^{th} percentile American Male
ATB	: Articulated Total Body
ATD	: Anthropomorphic Test Device
BioRID	: Biofidelic Rear Impact Dummy
BPD	: Fetus head biparietal diameter
CAD	: Computer Aided Design
CAL3D	: Skeletal based 3d character animation library
CFD	: Computational Fluid Dynamics
CPU	: Central Processing Unit
CRABI	: Child Restraint Air Bag Interaction
CT	: Computed tomography
CVS	: Crash Victim Simulation
DfT	: Department for Transport
DOF	: Degree of Freedom
ESI	: Software and Service Company for virtual prototyping
EuroNCAP	: European New Car Assessment Programme
EuroSID	: European Side Impact Dummy
'Expecting'	: The first Computational Pregnant Occupant Model with a Fetus
FEA	: Finite Element Analysis
FMVSS	: Federal Motor Vehicle Safety Standards
FTSS	: First Technology Safety Systems
GEBOD	: Generator of Body Data
H-ARB	: Human Articulated Rigid Body
HC	: Fetus head circumference
HIC	: Head Injury Criteria

HIII	: Hybrid III Dummy
H-Model	: Computational human model developed by ESI
HSRI	: Highway Safety Research Institute
HUMOS	: Human Model for Safety
HyperMesh	: Finite element pre-processor
JAMA	: Japan Automotive Manufacturers Association
LS-DYNA	: General purpose multiphysics simulation software
MADYMO	: Mathematical DYnamical Models software
MAMA2B	: Maternal Anthropometry Apparatus Version 2B
MRI	: Magnetic Resonance Imaging
MVMA-2D	: Two dimensional crash victim simulation
NHTSA	: National Highway Traffic Safety Administration
OoP	: Out of Position
OPD	: Fetus head occipito-frontal diameter
Pam-Crash	: Crash simulation and design of occupant safety systems
PMHS	: Post Mortem Human Subject
POLAR	: Pedestrian dummy
Q10	: Q series older child dummy
RADIOSS	: Multidisciplinary finite element solver
RAMSIS	: 3D human solution software
RID	: Rear Impact Dummy
SID	: Side Impact Dummy
TfF	: Time to Fire, airbag firing time
THOR	: Test Device for Human Occupant Restraint
THUMS	: Total Human Model for Safety
TNO	: Netherlands Organization for Applied Scientific Research
TNOP6	: 6 years old TNO child dummy
UPI	: Uteroplacental Interface
VC	: Viscous Criteria
WHIPS	: Whiplash Protection System
WHO	: World Health Organization
WorldSID	: Side Impact Dummy

CHAPTER 1

INTRODUCTION

Motor vehicle accidents are the leading cause of death for young people aged 15-29, and the eighth leading cause of death globally. The WHO (World Health Organisation) report in 2013 shows that worldwide the total number of road traffic deaths remain unacceptably high at 1.24 million per year. This indicates that approximately 3400 people die on the world's roads every day and tens of millions of people are injured or disabled every year. The WHO report also highlights that road traffic deaths are increasing notably in low and middle income countries, whilst decreasing in some high income countries. Furthermore, the WHO estimates that by 2030 road traffic fatalities will become the fifth leading cause of death unless immediate action is taken (WHO, 2013).

The latest reports from the Department for Transport (DfT) for 2013 indicate there is a 5% reduction in the number of people killed or seriously injured in road accidents in the UK (DfT, 2013) (Acar and Weekes, 2013). In this report, approximately 1,730 people were killed in road accidents, 3% drop from 1,785 in the

year ending June 2012. Motor vehicle traffic levels rose slightly by 0.4% compared with the 12 month period ending June 2012.

National Statistics Office (2003) reports that UK women make an average 613 trips per year by car, which is similar to men. According to Department for Transport (DfT), women in the UK travels 4,573 miles a year on average. Increasing safety of vulnerable road users such as pregnant women, children, elderly, pedestrians, cyclists and motorcyclists play a significant role in reducing the total number of global road accidental deaths. Specifically, for pregnant women, motor vehicle accidents are the leading cause of accidental death (Pearlman, 1997). Women of childbearing age travel by car more often than men (Acar and Weekes, 2013). Worldwide, the number of female drivers and distances driven have increased more than ever before in the last two decades. The level of exposure among women of a reproductive age to road accidents increased (Haapaniemi, 1996). It has been estimated that during pregnancy the incidence of trauma varies between 6% and 7% (Pearlman, 1997). In the USA, motor vehicle accidents are the leading cause of accidental fetal death (Weiss *et al.,* 2001). It has been indicated that around 130,000 women in the second half of their pregnancy are involved in road accidents each year in the USA. Of these, around 30,000 sustain treatable injuries. Approximately 160 women die and between 300-3,800 fetuses die when the mother survives (Klinich *et al.,* 1999a). Statistics show that in the UK each year, there are approximately 750,000 new maternities and women are likely to be passengers or drivers during their pregnancy (Acar and Esat, 2010). It has been estimated that around 3400 women in the second half of pregnancy are involved in car crashes annually (Acar BS and Acar M, 2006). These facts indicate that pregnant women and their fetuses safety at road accidents is an important issue to investigate.

1.1 Occupant Safety

Car manufacturers and research institutes have been continuously working to design safer cars. Data collected from real world accidents and controlled experimental crash tests are used to investigate occupant safety in motor vehicle accidents. Computational crash test simulations have also become an effective

method for improving occupant safety within the car design industry. Real world accident data should provide the most realistic information.

Experimental crash tests play a significant role to improve occupant safety in motor vehicle accidents. Post mortem human surrogates, sandbags, window mannequins, animals, and even humans are used as test subjects in these experimental crash tests. First test devices did not meet expectations of car manufacturers when vehicles are improved into high speed advanced automobiles. Experimental studies with cadavers have contributed the greatest amount of knowledge about the human response to crashes at various speeds. However, there are ethical issues related to working with post mortem human surrogates, animals and humans. Translating an animal's anatomy and injuries into human injury criteria generates significant problems. Using humans also present unacceptable risks in conducting experiments as the human tolerance limits are reached and exceeded.

Anthropomorphic test devices (ATDs) make significant contributions to improve vehicle design and occupant safety over the years. Mechanical response data obtained from humans involved in real world accidents, and from post mortem human surrogates and animals from experimental crash tests to impacts have been collected and used to develop crash test dummies. Seat belts, vehicle crumple zones, side door beams, airbags, head restraints are some of the occupant safety developments which are routinely tested with ATDs. However, using ATDs in experimental crash tests has several limitations. Crash test dummies are designed for repeatable conditions to reproduce predefined load deformation corridors. But they have limited capability for assessment of injury of the soft tissue such as internal organs, ligaments etc. Furthermore, ATD's are very expensive devices requiring regular maintenance and calibration and many tests may become impractical due to the costs and time consumption involved in testing.

Computational modelling of an occupant and its environment offers an effective alternative method to physical experimental crash tests to improve occupant safety in motor vehicle accidents. Computational models can simulate vehicle collisions and dynamic motion of occupants and most importantly help to determine injury risk to the occupants. Occupants with different anatomical details can be

modelled to investigate possible injuries on the human body due to road accidents. Computational simulations can also provide additional information not readily available in experimental tests. Several crash scenarios can be analysed quickly and inexpensively with computational modelling. However, computational simulation cannot totally replace physical tests as legal certification of new car models is still required to be tested using anthropomorphic test devices in vehicles.

1.1.1 Injury

Injury has been defined as physical harm to a biological organism, resulting from acute exposure to energy such as mechanical, electrical, thermal, chemical (Baker *et al.*, 1984). Common types of physical injuries are broken bones, cuts, burns, wound. Langley and Brenner (2004) defined injury as damage to the body produced by energy exchanges that have relatively sudden discernible effects. Physical injury occurs if the biomechanical response is of such a nature that the biological system deforms beyond a tolerable limit resulting in damage to anatomical structures and/or alteration in normal function (Wismans, 1994). An injury occurs, for example, sudden deceleration, wounding by a projectile, or crushing by a heavy object. For the impact injury, the damage caused by the collision of a body with a moving or stationary object. The higher the speed of a vehicle, the shorter the time a driver has to stop and avoid a crash. When the object is brought to a sudden halt, deceleration injury to a body within or upon a rapidly moving object caused by the forces exerted. Deceleration injury can occur in high-speed vehicles when they stop or slow down abruptly or when the occupants of the vehicle are propelled from it while it is moving. The extent of injury depends upon the velocity, duration of impact, direction of impact, distance travelled, absorption of stresses by the body or objects struck. Impact injuries can occur in any accident involving moving vehicles, such as automobiles, trains, motorcycles.

A road traffic injury is a fatal or non-fatal injury incurred as a result of a collision on a public road involving at least one moving vehicle. Road traffic injuries are the leading cause of death among young people, aged 15-29 years (WHO, 2013). Vehicle accidents cause many different injuries such as brain, head, neck, spinal

cord, back, facial, internal injuries, to virtually any part of body, depending on the crash and the severity of the impact. Injury Criteria is created to correlate human injuries with accelerations, deflections and intrusions of certain body parts during the crash test simulation. Injury criteria is mostly statistical and is often based on real life accident or experimental test results. While outcome for a fatally injured road user is obvious, the outcomes for the survivors can only be classified to match the spread of injury from minor to' life-threatening'.

1.2 Pregnant Driver Safety

Motor vehicle accidents are the leading cause of accidental death for pregnant women (Pearlman, 1997). Placental abruption is the most common cause of all fetal deaths in motor vehicle accidents (Klinich *et al.*, 1998, 1999a; Rupp, 2001). Weiss *et al.*, (2001) estimated that each year 90-369 fetal loss occurs resulting from automotive crashes in the United States. In the UK, approximately 3400 women in the second half of pregnancy are involved in car crashes annually.

Seat belts and airbags prevent tens of thousands of deaths and serious injuries in the UK each year according to the Royal Society for the Prevention of Accidents safety publications report (Rospa, 2003). Wearing the seat belt is a legal requirement during pregnancy. The seat belt is designed to protect pregnant women and should be worn at all times, unless women are certified medically exempt. Crash test investigations have shown the effectiveness of using seat belts in reducing injury risk for pregnant women and their fetuses. However, seat belts appear to be one of the biggest problem areas for women during pregnancy. Safety guidelines from the UK Department for Transport and the National Highway Traffic Safety Administration in the USA describe the correct position of wearing seat belt such as 'the lap belt strap should go across the hips, fitting comfortably under the bump, while the diagonal strap should be placed between the breasts and around the bump' (DfT, 2003).

Johnson and Pring (2000) surveyed 159 pregnant women and found 98% were using seat belts in the front, and 48% in the rear. 48% correctly identified how to position the seat belt correctly. Brake (2005) surveyed 1,010 pregnant women and

found that 92% were using their seat belts. However, nearly a quarter (23%) of the pregnant women did not know for sure that it was safer to wear a seat belt in pregnancy both for the mother and for their fetuses. McGwin et al. (2004) reported a survey of pregnant women about seat belt usage. In this report, while the seat belt usage was 95%, correct positioning was only 72.5%.

Acar and Weekes did survey about the problems that pregnant women experience during car travel using a questionnaire. From the 584 responses from pregnant women, only 35 were not wearing their seat belt (7%). 37% had stopped wearing the seat belt because they believed it was a safety risk. The correct positioning of the seat belt is fundamental to providing protection in a collision. Acar and Weekes reported that only 13% of pregnancy women are actually wearing their seat belts in the correct position.

Department for Transport guidelines recommend that the 'distance between the centre of the steering wheel to the breast-bone should be at least 10 in (25 cm)' (Department for Transport, 2010). However, the advice given is not specific to pregnant women. The National Highway Traffic Safety Administration in the USA (2002) advise pregnant women to sit as far back as possible from the steering wheel or dashboard. Acar and Weekes reported that 75% of pregnant women reported that they were seated with their abdomen 15 cm or less away from the steering wheel. 10% of the pregnant women said they were driving with their abdomen less than 3 cm from the steering wheel or nearly touching. Only 10% of women are seated with a clearance distance of 25 cm or greater.

Adverse fetal outcome is associated with crash severity, maternal injury and maternal restraint (Klinich *et al.,* 1999a). However, pregnant women and their fetuses safety in road accidents are not easy to investigate, because there are several factors which cause fetal loss in motor vehicle accidents. These factors can be classified as external and internal factors. The external factors are such as crash speed, impact direction, restraint systems, occupant position. Crash speed contributes to about 30% of deaths on the road (WHO, 2004). Speed also contributes to the severity of the impact when a collision does occur. Different restraint systems play important role on occupant safety in motor vehicle accidents. The internal factors are

such as placenta locations in the uterus, inclusion and exclusion of a fetus in the uterus, effect of amniotic fluid. Collecting detailed data after a road accident and broad investigation for a fetus fatalities and pregnant occupant injuries in road accidents is very limited and almost impossible due to ethical issues. Therefore, investigation based on real world crash data of pregnant women and their fetuses is scarce. Experimental crash tests using pregnant baboons were conducted in the late 1960s to evaluate the effectiveness of the three-point seat belt for pregnant women (Crosby *et al.,* 1968).

Pregnant women have completely different anatomy to that of a 50th percentile adult male (Acar and Weeks, 2005). In addition to that, abdominal measurements of a pregnant woman vary regionally (Loftis *et al.,* 2008). Characterization of material properties for tissues in pregnant woman's abdomen is also difficult to investigate (Hu *et al.,* 2009; Manoogian *et al.,* 2008).

The safety of pregnant women was not seriously considered by car manufacturers until the 1990s. The only anthropomorphic test device, MAMA2B (Maternal Anthropometry Apparatus Version 2B) representing pregnant women is very limited in design (Rupp *et al.,* 2001). The fetus and placenta do not exist in this dummy. 30 weeks of pregnancy is represented with a water filled silicon bladder which is inserted in the Hybrid III 5th percentile female dummy (FTSS). The size and weight of the Hybrid III 5th percentile dummy represents the smallest segment of average adult USA population. The dummy was upgraded in 1997. The total weight of the Hybrid III 5th female dummy is 108+/-2 lbs, 49 +/-1 kg (User Manual MAMA2B Rev B, 2007). Anatomy of a pregnant abdomen is based on data collected from only twenty-two pregnant women. However, use of a bladder for a uterine insert provides an internal pressure measurement to investigate fetal injury and to assess restraint systems effect on fetal survivability.

Experimental crash tests with the pregnant ATD are both costly, time consuming and have limitations. Accurate humanlike response cannot be achieved. Computational human modelling can offer an improved biofidelic and realistic response over ATDs. Although several computational adult human models were

developed in the late 1990s, there were not any computational pregnant women models until early 2000s and pregnant occupant models were simple.

A finite element model of a pregnant crash test dummy was developed by Volvo in 2002. The model is called 'Linda' and it is a combination of a real human body and a Hybrid III dummy. A 36 week-old fetus, placenta and amniotic fluid are represented as a human body while the rest of the body is represented by the Hybrid III crash test dummy (Volvo Press, 2004). The fetus model was designed as a lump without extremities of the 36 week-old fetus. Furthermore, the model is limited by the anatomy of the Hybrid III dummy.

A computational pregnant woman model was developed by Moorcroft *et al.*, (2003) using the crash analysis software package MADYMO (Mathematical DYnamical Models). MADYMO is a computer program that simulates the dynamic behaviour of a physical system emphasizing the analysis of vehicle collisions and assessing injuries sustained by passengers. An existing 5th percentile female facet 30th week of gestation. The anthropometry of the adult facet occupant models has been obtained from the database of the RAMSIS software package (RAMSIS 1997). The Western European population aged 18 to 70 years of 1984 was used. For the facet mid-size male occupant model simply medium typologies were selected for height, weight and sitting height. For the small female a very short and very slim model was selected in RAMSIS. The resulting body mass and sitting height were considered to be somewhat extreme also in comparison to the small female Hybrid III crash dummy. The finite element placenta and uterus are filled with amniotic fluid while a fetus is not included in the model; which is a significant omission.

A computational model of the whole human body with a uterus was developed by Delotte *et al.*, (2006). The finite element uterus model is integrated in the HUMOS (Human Model for Safety) model (Serre *et al.*, 2002) which is a computational 3D model of a male human cadaver created from MRI (Magnetic Resonance Imaging) scan data. In order to do that, the abdomen of the HUMOS model is modified. A fetus of 32-week of gestation was developed from MRI on a woman close to a "European 50th percentile" (Delotte *et al.*, 2008). There is not enough information about fetus mass and its details. The post mortem human subject

were three women who died naturally and whose morphological characteristics were close to the 50th percentile (165 cm, 60 kg). Although the model details bones, internal organs, and contains an integrated uterus, it does not represent the anatomy of a pregnant woman. The model was validated under very low speed impact conditions, frontal impact at a speed of 20 km/h.

The geometry of the HUMOS 50th percentile male model is scaled to the anatomy of a 50th percentile woman with a specific focus on the pelvis (Peres *et al.*, 2011). The Humos model is a complete human body model resulting from a European project. It is based on a seated 50th percentile male human body (176 cm, 78 kg) and was obtained from a frozen cadaver in driving position. This model was scaled to represent the anatomy of a 50th percentile woman (162cm, 62 kg). Anatomy of a 7 months uterus is represented with a scaling method from MRI images. The fetus geometry is also extracted from the MRI images. Therefore, detailed anatomy of the fetus is not modelled and upper and lower extremities do not exist. A post mortem human subject is used to validate the model. An artificial silicone uterus is inserted into a woman's body. In this study, low impact speed (20 km/h) is used to validate the model.

Detail and accurate representation of anatomy of pregnant women is crucial to investigate injuries and fatalities of fetus and pregnant occupant in road accidents realistically. In 2006, Acar and Lopik created the first computational pregnant occupant model with a realistic fetus (Acar and Lopik, 2009, 2012) using the MADYMO which combines in one simulation program the capabilities offered by multibody and finite element techniques for the simulation of structural behaviour. The model is called 'Expecting' and developed by enclosing a multibody fetus within a finite element uterus model, both of which are integrated with an existing MADYMO 5th percentile small female model. In order to represent the pregnant anatomy in the 38th week of pregnancy, a MADYMO 5th percentile female model is modified according to Acar and Weeks research findings (Acar and Weekes, 2005). The anthropometry of the existing 5th percentile female facet MADYMO model were used from the Western European population aged 18 to 70 years of 1984. For the small female a very short and very slim model was selected in RAMSIS. The resulting body mass and sitting height were considered to be somewhat extreme also

in comparison to the small female Hybrid III crash dummy. As an injury criteria, placental abruption failure is considered. The threshold strain value for the occurrence of placental abruption is widely accepted to be 0.6 at the UPI (Utero-placental interface) (Rupp *et al.,* 2001). The placenta attaches to the internal surface of the uterus and connects the fetus to the mother. This interface is named uteroplacental interface (UPI). This more biofidelic model of a pregnant occupant with realistic hip, breasts, thighs and abdomen dimensions and a fetus within the uterus simulates the dynamic response of a pregnant woman and her fetus to impacts. The 38 week-old fetus, which has a mass of approximately 3.3 kg, changes the dynamic motion of the pregnant abdomen and interacts with internal organs such as amniotic fluid and placenta in the uterus. Inclusion of a fetus model in the uterus makes the pregnant occupant model to be more life-like and assists to realistically investigate fetus fatalities and injuries in road accidents. The abdomen of the pregnant driver also interacts with several external vehicle parts such as the seat belt, airbag, and steering wheel. Understanding of these interactions and factors is important to understand the risks of placental abruption.

1.3 Motivation

Only a few researchers have tried to study the impact of vehicle collisions on pregnant occupants and their fetuses although road accidents are the leading cause of accidental fetal fatalities. Only a few pregnant occupant models have been developed. Furthermore, most models do not represent pregnant women realistically and have several significant omissions such as a lack of a fetus in the uterus. The possible effects of the restraint systems and vehicle interior parts, such as the steering wheel on pregnant drivers involved in vehicle crashes are therefore still poorly understood. In addition, due to the coarse and simple representation of a pregnant abdomen, investigation of the fetus fatalities at road accidents still have several limitations. Improvements to the pregnant occupant models are necessary for more realistic crash test simulations. An improved ‘Expecting’ should assist car manufacturers and researchers to realistically investigate road accidents involving pregnant women and their unborn babies.

1.4 Aim of the Research

This research aims to enhance the existing 'Expecting' pregnant occupant model and to investigate the effects of internal and external factors on fetus fatalities by understanding the risk of placental abruptions in road accidents where a pregnant driver involved.

1.5 Research Questions and Methodology

The research starts with the investigation of the chronological development of ATDs, computational models are studied, the relation between their development and vehicle safety design are found through a literature survey. 'Expecting', is used as the main tool. It is modified and improved to achieve the following research questions;

- What is the effectiveness of airbag firing times on well-being of the fetus ?. Airbag deployment times were changed at crash test simulations with 'Expecting'. Strains and displacements in the uterus were calculated to predict the fetus fatalities due to abdominal loadings.
- What is the effectiveness of inclusion of the fetus model in the uterus on the risk of placental abruption ?. Drop tests of uterus with and without the fetus were simulated and effects of the fetus in the uterus on the strain levels were evaluated. Then, crash test simulations with and without the fetus were performed. Results of maximum strain levels on uteroplacental interface were compared.
- What is the role of placenta locations on the risk of placental abruption in road accidents ?. Placenta at different possible locations in the uterus was considered and the placenta was remodelled when the original placenta model for fundus location was not suitable for the alternative locations. 'Expecting' model with new placenta locations was applied in several crash scenarios and results were compared with the original model.
- What is the effectiveness of finite element amniotic fluid model developed between the multibody fetus and the finite element uterus on fetus safety ?. 'Expecting' model with the finite element amniotic fluid was validated with

rigid bar impact and belt loading tests. The fetus, amniotic fluid and uterus interactions were investigated and crash test scenarios were conducted with the model.

- What is the effect of a deformable fetus head on the risk of placental abruption in motor vehicle accidents ?. A computational fetus head model was developed and a hybrid fetus was created. A deformable skull was simulated in the uterus during the crash test simulations. Strain levels on uteroplacental interface were calculated and compared with the rigid head model results.

A modified 'Expecting' model was used in several crash scenarios. Crash test severities imbedded in all investigations above. The complete new models were used to simulate a range of frontal impacts of increasing severities such as from 15-35 km/h. In addition, several restraint system combinations; 'seat belt only', 'airbag only', 'seat belt and airbag', and 'no restraint' systems were applied.

CHAPTER 2

EVOLUTION OF ATDS, COMPUTATIONAL MODELLING AND VEHICLE SAFETY

2.1 Introduction

Car manufacturers and research institutes have been working to improve occupant safety for more than 80 years. In order to predict injuries induced during road accidents, dynamics of occupant body during collision events must be studied. Researchers use information from real world events, controlled experimental tests, and computational models, to study the occupant's safety and their risk of injuries in automobile accidents.

Experimental testing can provide much more extensive quantitative information, but there are a number of limitations in terms of creating real world conditions. In the experimental crash tests, human volunteers, cadavers, animals, or physical Anthropomorphic Test Devices can be used. Results in the experimental tests are affected by limited instrumentation and devices.

The first experimental test subjects were live people. Engineers, researchers and inventors used themselves as human test subjects. John P. Stapp was a well-known researcher who conducted live occupant tests from 1946 to 1958. He studied the effects of deceleration on both human and animal bodies. The great contribution of Stapp was to show that the primary deceleration forces acting in the majority of vehicle crashes are entirely survivable if the packaging of the human frame is satisfactory. He showed that humans can tolerate high loads for short periods, accelerations of 30 g for up to 0,5 second were entirely tolerable, with only reversible soft tissue bruising occurring. At 45 g signs of mild concussion and retinal haemorrhage begin to show. This was the highest known acceleration voluntarily encountered by a human. These were decelerations measured on the seat of a dynamic sled. The accelerations experienced by the head itself were much greater. John Stapp became interested in the implications of his work for vehicle safety. At the time, seat belts were generally not fitted in vehicles. Stapp had revealed that a properly restrained occupant could survive at higher impacts than an unrestrained one. Use of automobile crash test dummies was demonstrated at his conferences for the first time.

One of the most difficult problems in determining the benefits of a safety countermeasure is how to translate measurements from a test dummy to humans. For this analysis, some of the injury curves that it has used in the past and has developed many new injury assessment reference values are used. Injury risk curves are used to define the injury risk for a given human body response. Validity of the risk curves depend on the boundary conditions for which the injury criteria or models were developed. Injury risk curves are mostly based on data from real case studies and experiments using animals, post mortem human surrogates (PMHS) or human volunteers.

Injury mechanisms are usually distinguished in impact:

Elastic injury mechanisms: Compression and tension of the body causing injury if elastic tolerances are exceeded. Injury can occur in case of slow deformation of the body or in the case of high velocity impacts.

Viscous injury mechanisms: Impulsive type of loading causing mechanical waves in the body, which results in internal injuries.

Inertial injury mechanisms: Acceleration type of loading causing tearing of internal structures due to inertia effects.

An injury criterion is defined as a physical parameter or a function of several physical parameters which correlates well with the injury severity of the body region under consideration. Tolerance level is defined as the magnitude of loading indicated by the threshold of the injury criterion, which produces a specific type severity and risk.

The injury severity can be defined using injury scaling which is defined as the numerical classification of the type and severity of an injury. There are few coding systems in existence on a worldwide scale used in everyday practice to code injuries. the most well known anatomical scale is the Abbreviated Injury Scale (AIS) .

Table 2.1 The Abbreviate Injury Scale (AIS, 1990)

AIS Code	**Injury Description**
1	Minor
2	Moderate
3	Serious
4	Severe
5	Critical
6	Maximum (currently untreatable)
9	Unknown

The relation between threat-load-injury is presented in the TLI model by van der Horst (Horst, 2005). If an injury risk curve is available, it can be used for injury assessment. This means that with information of the human body response it can be determined what the injury risk is for a specific load on that body part. An injury risk curve can be used to define the tolerance levels for a specific criterion.

Injury assessment reference values (IARVs) were developed by Mertz in 1978 to assess the efficacy of restraint system designs using the Hybrid III midsize

adult male dummy as the vehicle occupant. The risk of the associated injury was defined as ' Unlikely' as risk levels less than 5% and IARV was not exceeded in the prescribed test. Head, neck, thoracic injury risk curves and viscous criterion were defined (Mertz, 1978). Injuries are complex and have varying outcomes although there are methods to classify injury for research purposes.

In order to demonstrate compliance with domestic vehicle safety standards, some crash testing became a mandatory as a government requirement. However, passing these tests became a main goal and something to be exceeded by as little as possible. Compliance testing has been performed by car manufacturers, insurance-funded companies, research laboratories. Mandatory compliance testing showed that one purpose might reveal other safety information. Therefore, success on some tests may not predict success on other tests.

When powerful high speed engines were inserted into the vehicles, using humans in crash tests became serious risk at this high severity range. For ethical reasons, human volunteer experiments cannot be performed. In order to facilitate vehicle safety tests, cadavers have been employed as test subjects. For instance, the injury effects of the windscreen on unrestrained cadavers were studied in the 1960s (Patrick, 1966). The experimental work on cadavers has supplied important information about variation of human occupant response to crash tests since the 1960s (Hodgson and Thomas, 1972), (Webster and Newman, 1976). However, work with cadavers presents a number of problems. The first problem is the moral and ethical issue related to working with the post mortem human surrogate. Secondly, while crash testing has become more routine, suitable cadavers have become scarce. Another problem is that no two cadavers are the same and tests conducted with them are not repeatable. There are also research concerns that the majority of available cadavers are old adults who do not represent the average population. Post mortem human surrogates have no active muscles as well. In addition to that, deceased accident victims could not be used because collected data would be compromised by the cadaver’s previous injuries. Therefore, it is extremely difficult to achieve reliable data. However, their use in experimental tests helps to generate experimental impact corridors.

As alternative test subjects, baboons, pigs, chimpanzees and other animals have been employed as occupants in vehicles. A series of 22 pregnant baboons were subjected to impact by Crosby *et al.,* (1968, 1972). Pregnant baboons were restrained by either a lap belt or a three-point seat belt. Robbins *et al.,* (1976) predicted thoracic impact injuries quantifying the thoracic impact response of baboons and cadaver subjects in experiments. The most commonly used animal subjects in experimental test studies were pigs, because they have similar internal structure to humans and can be placed in a vehicle in a good approximation of a seated human. Verriest *et al.*, (1981) studied the mechanical response of the pig thorax using belt loading conditions. However, animals were very different in structure and their capability for internal instrumentation is limited to produce useful data. Translating the animal's anatomy and injuries into human injury criteria was a serious problem.

In order to collect data to analyse effects of an impact on the occupant, crash test dummies, Anthropomorphic Test Devices (ATDs) were created. They have contributed to make safer cars since the 1950s (Nyquist *et al.,* 1980; Melvin *et al.*, 1993). Humanlike dummies have been designed using response data obtained from crash impacts to animals and human cadavers. Early dummies approximated human kinematics and provided acceleration movements. In order to describe the proofing of design changes, the models are validated. Testing and retesting an interactive process may be necessary to achieve an appropriate level of human error control in occupant modelling. For instance, a crash test predicts the bio kinematic of a 50th percentile male, the head impact force vector, and uses pass-fail injury criterion. However, in a real life crash, a 97 percentile male's head did move forward but then rotate downward. Thus, the injury prediction did not include a full range of drivers in terms of anthropometry. The simulations have a tolerable level of injury and failed to predict appropriately the biomechanics of injury. In fact, properly conceived validation criteria are the keys for advanced occupant models and crash test simulations. Colleting accurate car accident data is essential since simulation should adequately predict the ultimate real life criteria, entail relevant correct assumptions.

Controlled crashes with advanced ATDs in crash tests and high speed filming provide complete observation of collisions. Several new advanced restraint systems have been improved using crash test dummies. Crash tests incorporating those

devices in turn led the motor manufacturers to develop more sophisticated crash test dummies. Experimental tests with crash test dummies assist to obtain consistent results. ATDs simulate the weight, dimensions and articulation of the human body and collect several data such as bending, folding of the body during a collision in crash tests. However, using ATDs in experimental tests has a number of limitations. Crash test dummies are designed for repeatable conditions to reproduce predefined load deformation corridors and meet the vehicle legislation requirements in specific crash events. Effects of many parameters need to be investigated in these complex events. Many tests that needed ATDs can soon become impractical due to the costs involved in testing. ATD's are very expensive devices. Experimental tests with dummies can be time consuming with limited in their biofidelity and their application area. They have limited capability for assessment of injury of the soft tissue such as ligaments, internal organs. In addition to that, the crash test dummies represent only the population through 3 sizes; 50th percentile male, 95th percentile male and 5th percentile female and some child dummies.

The accuracy of a finite element occupant model is dependent on the accuracy of the occupant geometry, anatomy, the type and number of elements used, and the material property model (linear elastic, viscoelastic, etc.). In order to develop an accurate model, the model is tested for convergence of results with increasing mesh density and validated against experimentally obtained results. Convergence of the model does not guarantee accurate and realistic results. The accuracy with regard to the real problem depends on how realistic the model is in an overall sense, how well the anatomy of the occupant model and the material properties represent the physical case.

2.2 Early Developments (1914-1964)

Collision avoidance was the main concern in safety for the motor manufacturers, government agencies, safety organizations and insurance companies after vehicle mass production started in 1914. At this early stage, developments were based on fundamental necessities to drive vehicles properly. For instance, rear mirrors, dual windscreen wipers, hydraulic brake control and indicators were integrated into

vehicles. Occupant safety in vehicles was not considered in those years. In the late 1930s, road incident fatalities and injuries increased significantly and created a major public health and safety problem. Automobiles became an important part of daily life. Therefore, designing safer vehicles for occupants became a crucial problem. In order to encourage design a safer steel vehicle body structure, the first barrier frontal crash test was conducted in 1934 (Figure 2.1). In the late 1930s, rollover tests were also conducted to improve crashworthiness of vehicles.

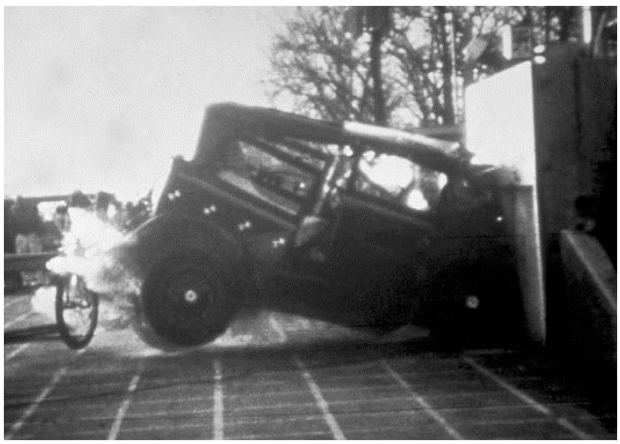

Figure 2.1 First car crash test, 1934 (taken by General Motors)

At the beginning of the 1940s, aircraft industry technology was implemented in the automotive industry. Crash tests were very simple and humans, animals, sandbags and even shop window mannequins were used to represent vehicle occupants in crash tests. Later, experimental crash tests with cadavers played a significant role in understanding and creating human responses to crash tests at high speed. However, complexity of the tests and durability of test subjects caused a decline in test repeatability which was a major problem. Durable and repeatable test devices having human like postures had to be designed. Therefore, dummies which are used in the aircraft industry were adapted into motor vehicle crash tests for better observations.

Dummies were designed obtaining human cadavers' response data from crash tests. The first crash test dummy, Sierra Sam (Figure 2.2), which was originally created for aircraft ejection seat testing, was used by car manufacturers for restraint system testing (Enever, 1999). Crash tests were intended to improve vehicle

stiffness. In 1949, the first car safety cage and re-enforced roof pillars were designed. In the same year, the first padded dashboard was introduced. Integrity of restraint systems were assessed by using the first version of dummies in frontal collisions. For instance, it was observed that two-point belt strapped across the body over the abdomen caused fatalities and serious internal injuries at high speeds.

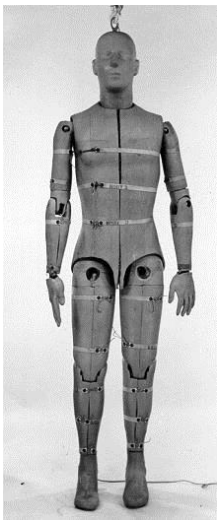

Figure 2.2 First crash test dummy, Sierra Sam, 1949 (Enever, 1999)

In the late 1950s, car manufacturers realised that the airbag might be a very effective supplemental restraint system in providing occupant protection in vehicle crashes. However, because of limited technology, it took the automotive industry another 20 years to reintroduce airbags. In the 1950s, a modular series of dummies were designed for vehicle collision tests. As a result of a number of crash tests, the most significant vehicle safety device of that era, three-point seat belt was invented by Nils Bohlin, a Volvo engineer, in 1958 (Invent, 2010). In 1959, three-point seat belt became standard safety equipment by Volvo in front seats in Sweden.

In the early 1960s, significant developments occurred in motor vehicle safety around the world. Governments promoted importance of occupant safety in motor vehicle accidents. The ADAC (Allgemeinen Deutschen Automobil-Club) (Germany Motorbike Association) an automobile club and break-down assistance service was launched in Germany. In 1974, the organization had 3.8 million members at a time when there were 19 million passenger cars registered in Germany. ADAC regularly

publish maps showing safety characteristics of German roads. Seat belt anchors in front seats were designed as standard equipment in US vehicles in 1962. Effectiveness of wearing seat belt in automobiles was investigated in Britain and survey results showed that seat belt would reduce the likelihood of death and serious injury by 0.6.

2.3 Further Developments (1965-1989)

Several significant improvements in crash test dummies and in automotive safety design were achieved from 1965-1989. In 1965, a requirement for the three-point seat belt anchorage points was introduced in Europe. The fitment of the three-point seat belts in the front seats became mandatory to fit in 1968 in Europe. In 1969, Thatcham Research Centre, the motor insurer's automotive research centre was established by the motor insurance industry. The main aim of this centre is to contain or reduce the cost of motor insurance claims whilst maintaining safety standards. It is the not for profit insurer funded research centre (Thatcham, 2013). In the same year, the National Highway Traffic Safety Administration (NHTSA) was established in the USA. A number of compulsory safety standards known as Federal Motor Vehicle Safety Standards (FMVSS) were introduced (NHTSA, 1973). The design and manufacture of vehicles became a regulated and standardized industry. In addition to that, demands on vehicle safety increased enormously. Car manufacturers discussed the credibility of crash tests with governments and started intensive research in occupant safety in motor vehicles. Anatomical design of dummies was part of this investigation. Previous dummies were designed to meet the standards of aircrafts and contained no pelvic structures, spinal articulation or realistic range of motion. Hence, they were not effective devices to evaluate the impact of road accidents on the human body.

Throughout the 1970s, dummy models were developed with improved joints, range of motion and spine segments to make them more realistic. Effectiveness of airbags on human safety was also tested in motor vehicle collisions. Designing airbags in vehicles became popular in the same years. In 1971, the Hybrid I dummy was designed to produce more repeatable data in crash tests. Variety of different size

dummies such as child dummies, small-stature female dummies were created in the 1970s. After these improvements, occupant safety in motor vehicles gained momentum. In 1970, wearing seat belt became compulsory for drivers and frontal seat passengers in Australia. Child dummies are used to develop child safety seats, booster seats and special restraint systems. However, there were still a number of limitations regarding child anthropometry data.

In 1972, the Hybrid II was designed and the same year became the standard for frontal crash testing to comply with the US automotive regulations for restraint systems. More repeatable lap/shoulder harness tests were conducted with this dummy. Car manufacturers developed and installed their own airbag restraint systems in vehicles and tested with Hybrid II. However, unacceptable sound levels when the airbag was inflated and re-designing car interiors to accommodate the airbags were only some of the problems for this restraint system.

Until 1976, existing crash test dummies represented humans poorly. As a third-generation, Hybrid III, 50th percentile male ATD, whose response was closer to human response than the Hybrid II dummy was developed (Foster *et al.*, 1977) (Figure 2.3). The Hybrid III test dummy is a 50th percentile dummy based on the height and weight of the US adult male population. Internal devices, such as rib cage were added and a more biofidelic head than the Hybrid II for forehead impacts to airbag or windscreen interaction was designed. Hybrid III was more durable and repeatable than the Hybrid II and was developed for a particular need in test measurement and to improve safety design.

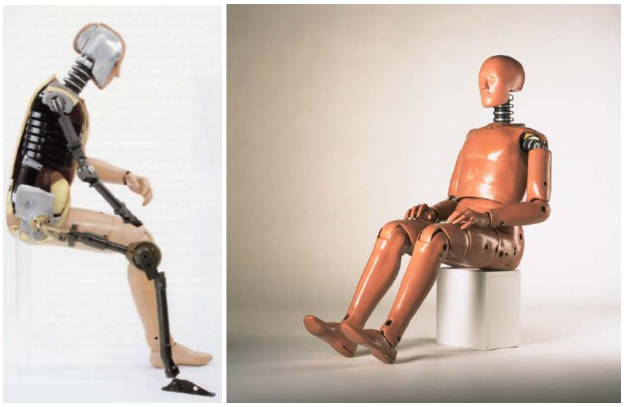

Figure 2.3 The Hybrid III dummy, 1976 (FTSS, 2012)

The Hybrid III dummy became a standard anthropomorphic test device around the world for impact restraint compliance testing in 1976. More research in airbag interaction with occupants in frontal collusions was conducted by a number of car manufacturers.

In 1979, side impact dummy (SID) was designed to measure injury severity on the ribs, spine and internal organs at side impact collisions. Although the Hybrid III was the most advanced dummy developed so far, it was designed for frontal crash testing. In 1982, side impact tests were performed by NHTSA, (1982). As a result of these tests, side beams to vehicles were installed.

In 1984, pretensioners were introduced to tighten the seat belt at early stages of a collision. In 1985, airbags were installed in many cars as optional safety systems. A more advanced side impact dummy, the EuroSID (a modified version of the Hybrid III) was designed. Side airbag was introduced in 1986. In 1987, the Hybrid III dummy was scaled to represent 5th percentile small female, 6 years old child and 95th percentile large male with the same level of biofidelity and measurements capacity. The Hybrid III 6 year old child crash test dummy was developed in cooperation with SAE Biomechanics Committees and the NHTSA. Originally designed in 1993, the dummy went through a complete upgrade in 1997. Weight, sitting height and stature were considered to scale the Hybrid III dummy.

2.4 Advancements in the Last Decade of the 20th Century (1990-2000)

At the beginning of 1990s, airbags were installed in vehicles as a part of the standard safety equipment. However, airbag inflation became a serious problem for children and small-stature occupants. There were a number of head, neck injuries and fatal accidents related to airbag deployments. In 1991, CRABI (Child Restraint Air Bag Interaction) dummies including 6, 12 and 18-month were designed to evaluate airbag interactions with rear facing infant restraints. Special child restraint seats, more effective airbags were developed as a result of a series of crash tests with the CRABI dummies.

THOR (Test Device for Human Occupant Restraint) dummy was designed to assist the evaluation of advanced vehicle occupant safety systems. The THOR dummy offered numerous functional benefits as compared with previously existing crash test dummies (Martinez *et al.,* 1999). Its biofidelity was better and injury assessment capabilities were expanded in all body regions. Its enhanced design such as face, neck, shoulder, thorax, spine, abdomen, pelvis, and femurs had been redesigned to achieve more humanlike responses in crash test simulations. As a result of these developments, airbag deployment thresholds were set and assessment of seat belt and airbag interactions were improved. In 1994, the first dual threshold airbags systems were introduced. Same year the idea for a (NCAP) New Car Assessment Programme was born. The UK Department of Transport considered the set up of an NCAP in the UK. It expanded across Europe later. For comparative vehicle safety testing, the testing was conducted to a higher standard than was necessary for legislation. Because of this, a detailed test protocol was developed. The load limiters for seat belts were introduced to keep the belt force at a predefined, controlled level. In 1992, The Insurance Institute for Highway Safety (IIHS) opened the vehicle research centre. The IIHS began crash tests in 1995. Vehicles are rated for safety based on performance in several tests.

In order to reduce the risk of neck injuries (whiplash) during vehicle collisions specifically rear impacts, reactive head restraint system for seats was developed in 1996 (SAAB, 1996). Side impact head protection airbags were installed in some of the vehicles in 1996 as well. In the same year, detection of airbag, belt and child seat interaction were introduced in the airbag system. In 1997, EuroNCAP (European New Car Assessment Programme) was founded and vehicles were tested using dummies in full scale frontal and side impacts (EuroNCAP, 2013). Safety features are standardised throughout the European Union. As a result of these tests, for the first time in Europe, crash performance details of automobiles were introduced to the public. Car manufacturers responded promptly to improve vehicle safety.

A pedestrian dummy (POLAR I) representing a 50^{th} percentile male pedestrian, was designed and tested to assess the external front sections of the vehicles for pedestrian safety in road accidents in 1998. The height of the Polar

dummy is 1775 mm and the weight is 770 N. External design of vehicles for human safety also started to become an important issue in these years. The POLAR I and THOR dummies have similar anthropometry, however, POLAR I had more advanced knee design. Mass, centre of gravity, and moments of inertia measurements were made on all the principal THOR segments. The THOR dummy is based on the anthropometry given by the UMTRI 50th percentile adult male (Schneider, *et al.*, 1983). An In 1998, pedestrian safety was also represented with separate star rates in the EuroNCAP tests.

In 1998, the SID/HIII dummy, which is a combination of the SID and the Hybrid III 50^{th} percentile male dummy, was designed for side impact pole tests. In the same year, side impact tests were conducted intensively by a number of car manufacturers. The Hybrid III dummy became the official crash test device for frontal collision restraint regulation compliance in Europe. A unique Whiplash Protection System (WHIPS) was introduced by Volvo to reduce neck injuries in specifically rear collisions. Installation of driver and passenger airbags in all new vehicles was targeted in 1998 in US. In the same year, airbags to protect knees were installed in vehicles for the first time. Curtain airbags were also introduced to protect front and rear passengers from side impact collisions.

Whiplash injuries were still a serious problem in non-severe rear impact accidents. In 1999, the BioRID dummy was designed to investigate and reduce neck injuries in specifically rear impact crash tests (Davidsson et. al, 1999). This dummy has a spinal column with separate vertebrae and linked to the human skeleton. It is used for the evaluation of body motion in rear impacts. Two years later, the RID (Rear Impact Devices) dummy series were introduced to measure the risk of neck injury in low speed, rear-end crashes. In 2001, the RID was upgraded to the RID II and the RID3D dummies. The neck assembly of the RID3D was redesigned and series of low speed, oblique rear tests were conducted with this dummy. The RID3D was more durable, repeatable and reproducible than previous models. It sustained higher severity test conditions both in rear impact and frontal impact collision tests. The interaction of the RID3D with the test seat compared to human subjects and improved head restraint systems were designed.

2.5 Recent Developments

Improving occupant and pedestrian safety in motor vehicles have continued significantly in the 21th century. More advanced and different types of ATDs have been designed. Communications of restraint systems which are called smart restraint systems have been developed.

In 2001, in order to keep the load on the occupant's chest constant during the road accidents, more advanced load limiters were introduced. The knee airbag was used by a number of car manufacturers and anti-submarining airbag was introduced in 2001 as well. In 2003, frontal airbags that were controlled according to the weight of the frontal passengers were designed. Airbag controller sensors have played significant role at vehicle occupant safety.

Several car manufacturer companies have focused on safety of vulnerable road users. In 2001, as a special anthropomorphic test device, MAMA2B dummy with pregnant abdomen and torso was created to represent a pregnant occupant dummy in crash tests. Standard Hybrid III 5th percentile female dummy was modified and 30-week pregnant uterus was represented with a fluid-filled silicone rubber bladder. MAMA2B had no foetus in uterus.

Child occupant safety has also been investigated by a number of car manufacturers in detail. In 2003, child safety performance of vehicles was rated to provide clear information for public by EuroNCAP. The first multi-directional child dummies, Q dummies, were designed to investigate frontal and side impact child restraint systems, out of position tests and EuroNCAP tests (Figure 2.4) (Q child dummies, 2010). Q dummies were more biofidelic than previous child dummies. The Q1.5 and the Q3 child dummies, representing a 1.5 and 3 year-old child, have been used to assess dynamic performance of child restraint systems by EuroNCAP. However, child safety in vehicle for out of position is still unsolved problem.

Figure 2.4 The Q series child dummy family :(from left to right) Q1.5, Q3, Q6, Q1 and Q1 without suit (Jager *et al.*, 2005)

The WorldSID, 50th percentile male side impact dummy was designed to assess vehicle occupant injury risk in lateral impact with a biofidelity rated 7.6 out of 10 in 2004. The dummy was developed to allow a single test procedure to be used for side impact in any regulation around the world. Several anthropometry of different populations around the world were used for the WorldSID. In 1999, the AMVO dataset for a 50th percentile male (Robbins, et al.,) were accepted. The WorldSID 50th percentile adult male has a mass of 77.3 kg, a theoretical standing height of 1753 mm and a seated height of 911 mm. The automotive posture as represented by the AMVO dataset was defined as the design reference posture for the dummy. Approximately 212 sensors capture data and help to measure head acceleration, pelvis forces and many other responses. The twin chamber airbag for the front occupants was introduced in 2004. In these years, rollover tests with crash test dummies were also improved.

The RID3D was upgraded in 2006 and in the same year active powered head restraint systems in car seats were installed in some vehicles. The WorldSID 5th percentile female side impact dummy was also introduced in 2007. Mass, seated height and standing height of the WorldSID 50th percentile adult male are used to be the basis for the development of a harmonized side impact dummy family. The 5th WorldSID anthropometry is based on the UMTRI dataset. This dataset describes a 3D surface description and almost 150 anatomical reference points, definitions of segments. For the first time, rear curtain airbags were introduced to prevent

specifically head injuries of rear seat passengers in 2008. In 2007, an active bonnet reversible system, which enlarges the deformation area and reduces the risk of injury to pedestrians, was installed on some vehicles (Figure 2.5) (Nissan Global, 2007). In 2009, the pedestrian score involved as part of the overall rating scheme in EuroNCAP tests. Vehicle designers and car manufacturers have focused on developing safer frontal vehicle design that reduces injuries to pedestrians in the frontal collisions.

Figure 2.5 Active bonnet system (Nissan, 2009)

Airbag safety systems for children and small-stature occupants have been investigated in recent years. In 2009, Q10, 10 year-old child dummy, the last in the series of Q dummies was developed to test child restraint systems and airbag interactions for out of position. Adaptive restraint systems which are adjusted automatically according to weight, size and anthropometry of occupant in vehicle have become more effective safety devices in recent years.

In 2010, an airbag which deploys in between rear seats to protect passengers from side impacts were introduced. Similar to this airbag, front centre airbag deploys between driver's and passenger's seats has also introduced and installed in some vehicle models manufactured in 2013 (Figure 2.6). These airbags are expected to protect the occupants in rollover crashes.

Figure 2.6 Front seat centre airbag (GM, 2011)

The Seat beltPlus system which is specifically designed for all however with particular emphasis on the needs of pregnant women, is introduced by Acar and Esat, (2010). The belt is applied to the conventional, three-point seat belt and holds the lap portion in the correct position.

Pedestrian dummy head forms were developed in 2010 and implemented EuroNCAP. In order to provide pedestrian and cyclist safety and protect them from serious head and neck injuries, external airbags which are located under the hood and inflate at the base of the windscreen have been designed and installed in vehicles in 2013 (Figure 2.7).

Figure 2.7 External airbag performing during crash test with pedestrian dummy on cycle (TNO, 2012)

Q10 child dummy has updated regarding handling and durability in 2013. Additional design improvements have been made based on tests conducted around

the world. EuroNCAP decided on the application of Q6 and Q10 dummies. Q1.5, Q3, Q6 and Q10 are implemented in EuroNCAP protocol in 2013.

Research and development in motor vehicle occupant safety still continues increasingly using Anthropomorphic Test Devices. Historical development of automotive safety design and its relations with physical crash test dummies are examined so far. Chronological successive development of ATDs and automotive safety is illustrated in Table 2.1.

Computational crash test simulations have also played important role in vehicle safety and their evolution is the subject of the next section.

Table 2.1 Chronological development of anthropomorphic test devices and automotive safety design

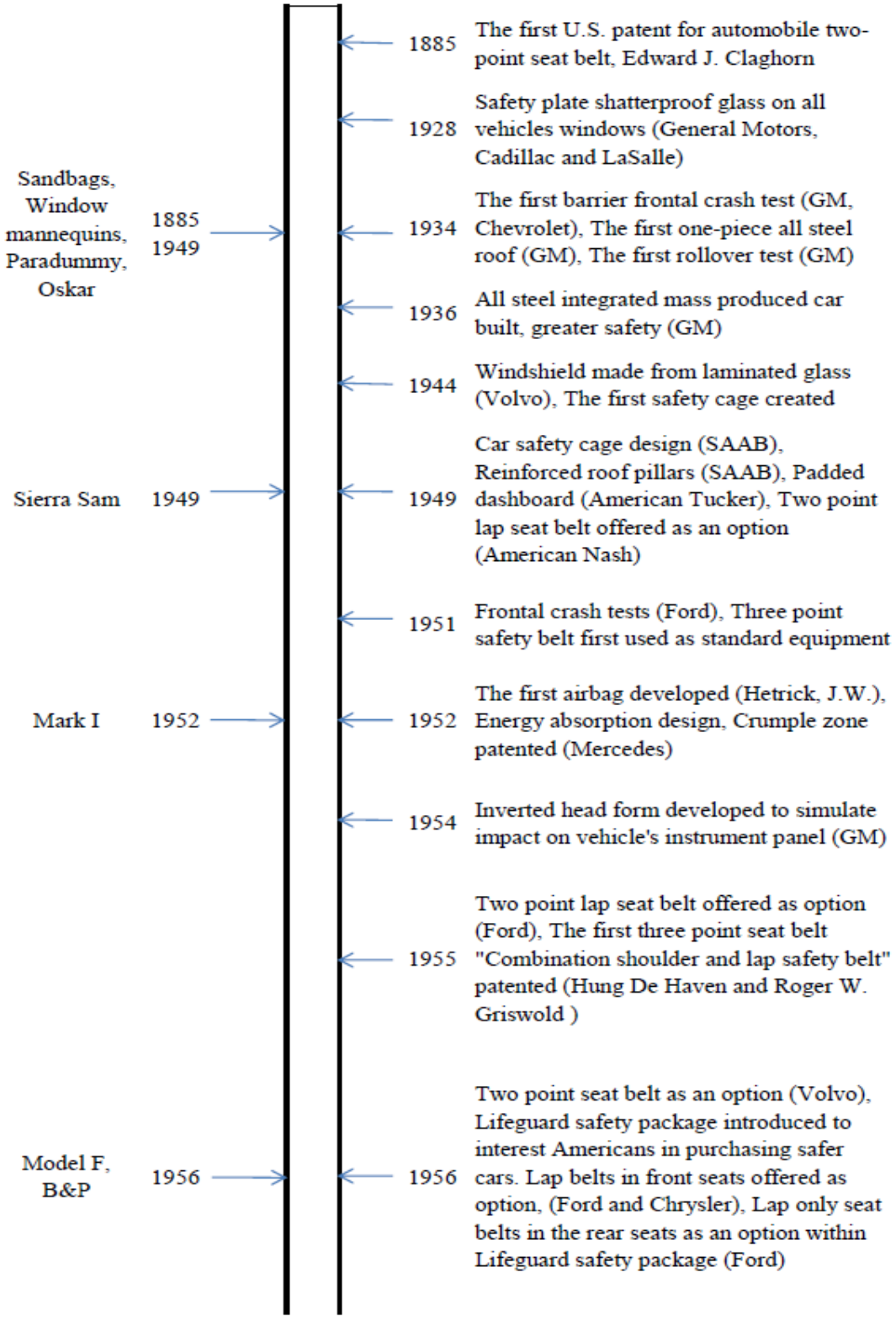
1885
The first U.S. patent for automobile two-point seat belt, Edward J. Claghorn
1928
Safety plate shatterproof glass on all vehicles windows (General Motors, Cadillac and LaSalle)
Sandbags, Window mannequins, Paradummy, Oskar
1885 1949
1934
The first barrier frontal crash test (GM, Chevrolet), The first one-piece all steel roof (GM), The first rollover test (GM)
1936
All steel integrated mass produced car built, greater safety (GM)
1944
Windshield made from laminated glass (Volvo), The first safety cage created
Sierra Sam
1949
1949
Car safety cage design (SAAB), Reinforced roof pillars (SAAB), Padded dashboard (American Tucker), Two point lap seat belt offered as an option (American Nash)
1951
Frontal crash tests (Ford), Three point safety belt first used as standard equipment
Mark I
1952
1952
The first airbag developed (Hetrick, J.W.), Energy absorption design, Crumple zone patented (Mercedes)
1954
Inverted head form developed to simulate impact on vehicle's instrument panel (GM)
1955
Two point lap seat belt offered as option (Ford), The first three point seat belt "Combination shoulder and lap safety belt" patented (Hung De Haven and Roger W. Griswold)
Model F, B&P
1956
1956
Two point seat belt as an option (Volvo), Lifeguard safety package introduced to interest Americans in purchasing safer cars. Lap belts in front seats offered as option, (Ford and Chrysler), Lap only seat belts in the rear seats as an option within Lifeguard safety package (Ford)

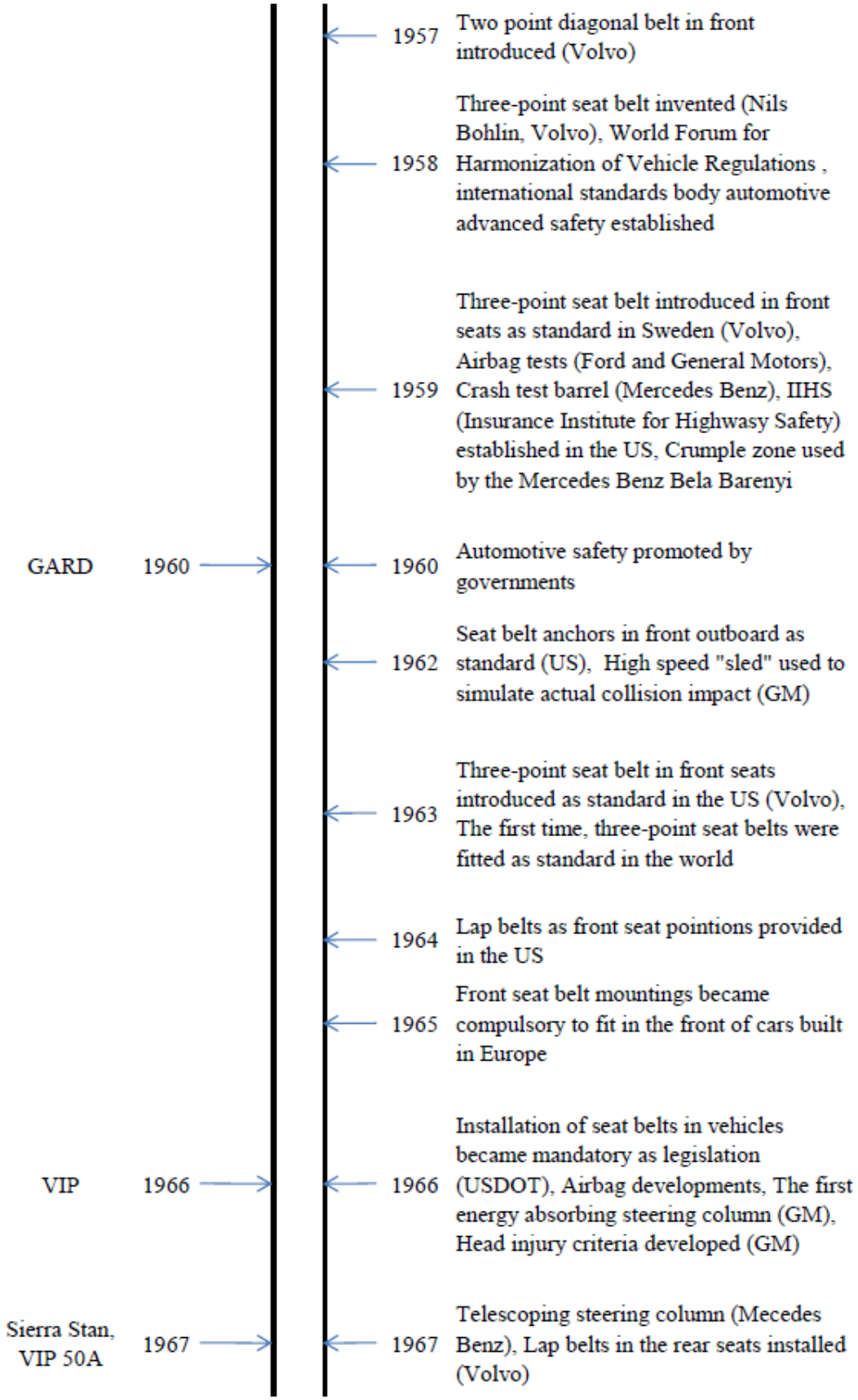
1957
Two point diagonal belt in front introduced (Volvo)
1958
Three-point seat belt invented (Nils Bohlin, Volvo), World Forum for Harmonization of Vehicle Regulations , international standards body automotive advanced safety established
1959
Three-point seat belt introduced in front seats as standard in Sweden (Volvo), Airbag tests (Ford and General Motors), Crash test barrel (Mercedes Benz), IIHS (Insurance Institute for Highwasy Safety) established in the US, Crumple zone used by the Mercedes Benz Bela Barenyi
GARD
1960
1960
Automotive safety promoted by governments
1962
Seat belt anchors in front outboard as standard (US), High speed "sled" used to simulate actual collision impact (GM)
1963
Three-point seat belt in front seats introduced as standard in the US (Volvo), The first time, three-point seat belts were fitted as standard in the world
1964
Lap belts as front seat pointions provided in the US
1965
Front seat belt mountings became compulsory to fit in the front of cars built in Europe
VIP
1966
1966
Installation of seat belts in vehicles became mandatory as legislation (USDOT), Airbag developments, The first energy absorbing steering column (GM), Head injury criteria developed (GM)
Sierra Stan, VIP 50A
1967
1967
Telescoping steering column (Mecedes Benz), Lap belts in the rear seats installed (Volvo)

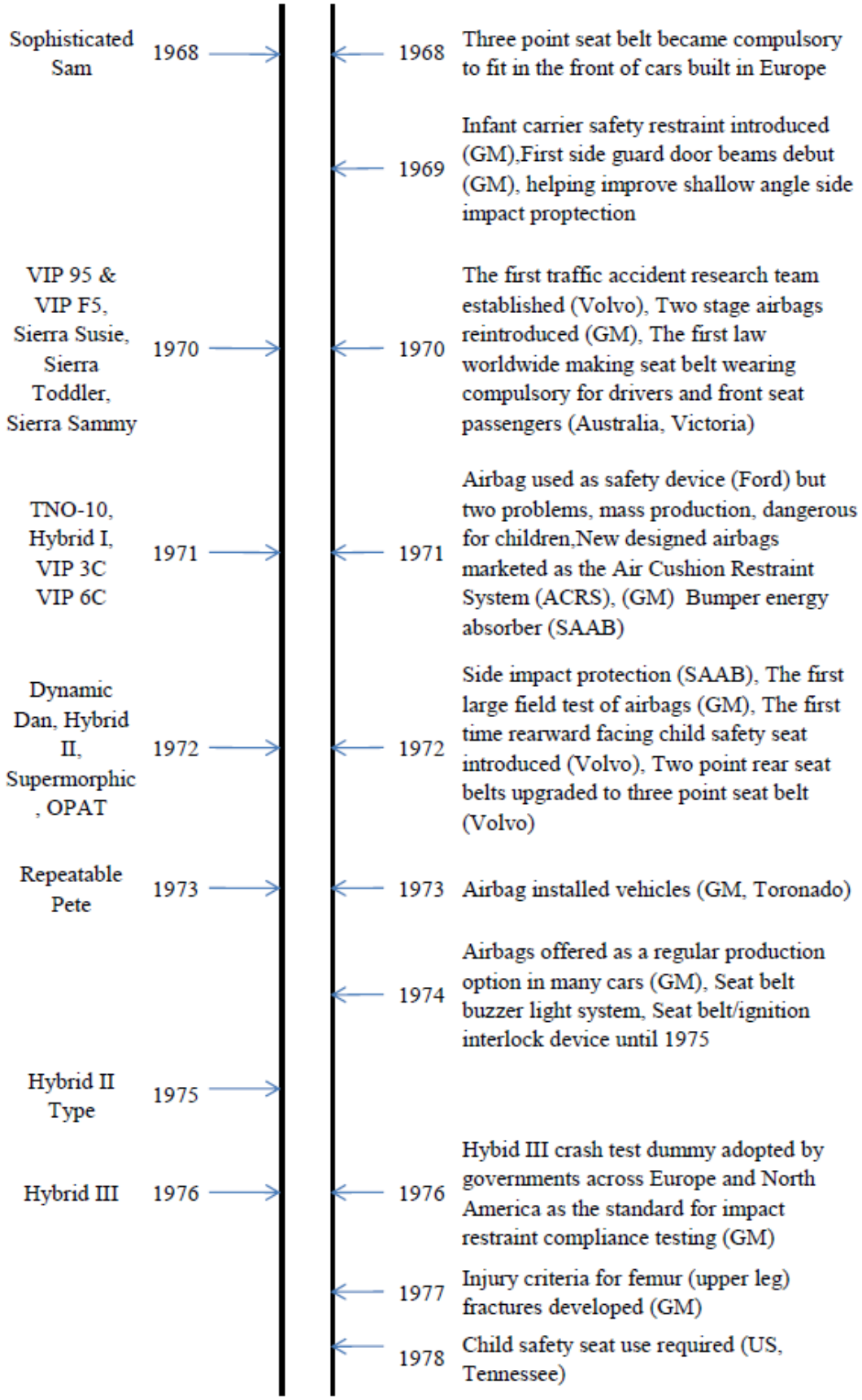
Sophisticated Sam
1968
1968
Three point seat belt became compulsory to fit in the front of cars built in Europe
1969
Infant carrier safety restraint introduced (GM),First side guard door beams debut (GM), helping improve shallow angle side impact proptection
VIP 95 & VIP F5, Sierra Susie, Sierra Toddler, Sierra Sammy
1970
1970
The first traffic accident research team established (Volvo), Two stage airbags reintroduced (GM), The first law worldwide making seat belt wearing compulsory for drivers and front seat passengers (Australia, Victoria)
TNO-10, Hybrid I, VIP 3C VIP 6C
1971
1971
Airbag used as safety device (Ford) but two problems, mass production, dangerous for children,New designed airbags marketed as the Air Cushion Restraint System (ACRS), (GM) Bumper energy absorber (SAAB)
Dynamic Dan, Hybrid II, Supermorphic , OPAT
1972
1972
Side impact protection (SAAB), The first large field test of airbags (GM), The first time rearward facing child safety seat introduced (Volvo), Two point rear seat belts upgraded to three point seat belt (Volvo)
Repeatable Pete
1973
1973
Airbag installed vehicles (GM, Toronado)
1974
Airbags offered as a regular production option in many cars (GM), Seat belt buzzer light system, Seat belt/ignition interlock device until 1975
Hybrid II Type
1975
Hybrid III
1976
1976
Hybid III crash test dummy adopted by governments across Europe and North America as the standard for impact restraint compliance testing (GM)
1977
Injury criteria for femur (upper leg) fractures developed (GM)
1978
Child safety seat use required (US, Tennessee)

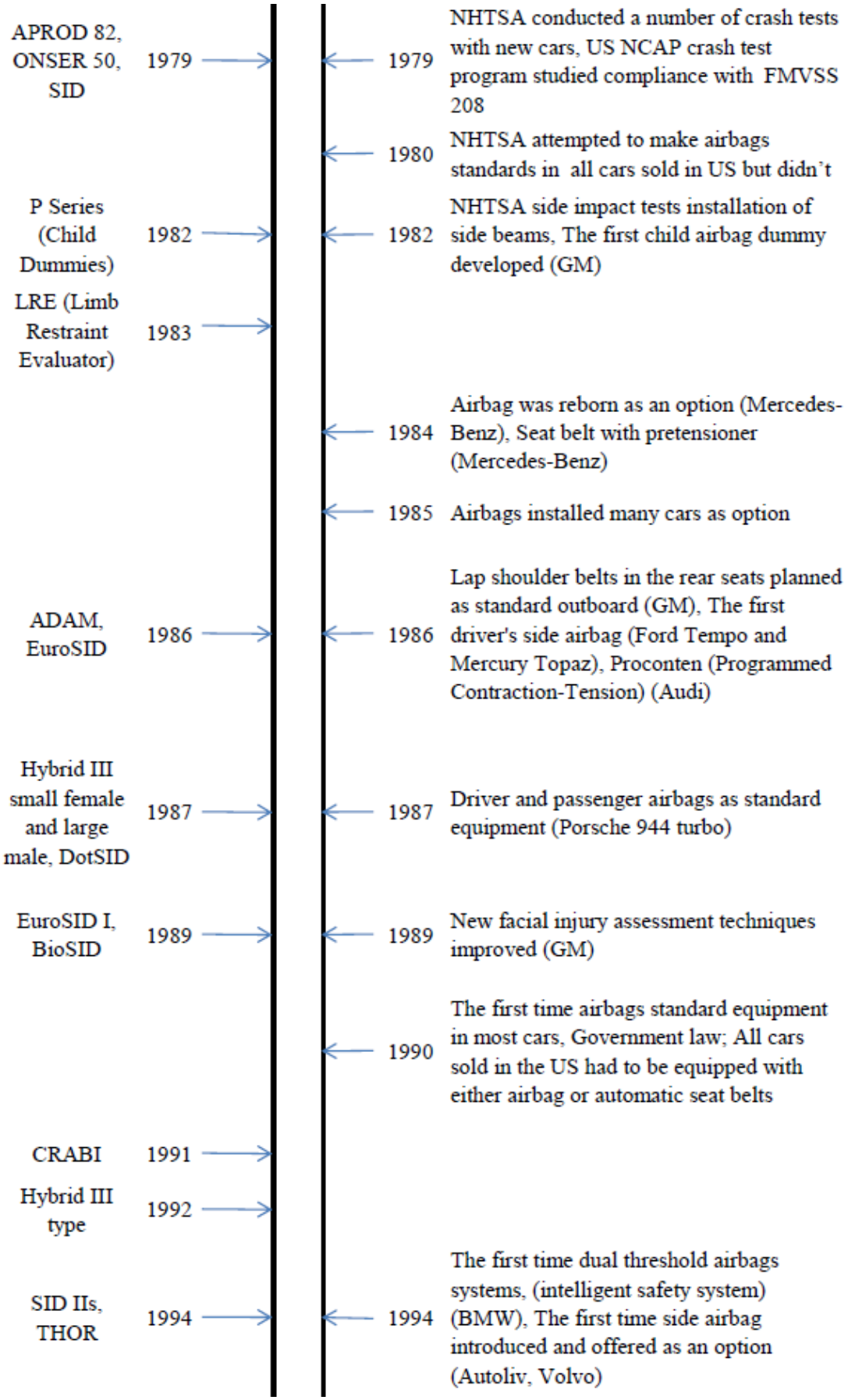
APROD 82, ONSER 50, SID
1979
1979
NHTSA conducted a number of crash tests with new cars, US NCAP crash test program studied compliance with FMVSS 208
1980
NHTSA attempted to make airbags standards in all cars sold in US but didn't
P Series (Child Dummies)
1982
1982
NHTSA side impact tests installation of side beams, The first child airbag dummy developed (GM)
LRE (Limb Restraint Evaluator)
1983
1984
Airbag was reborn as an option (Mercedes-Benz), Seat belt with pretensioner (Mercedes-Benz)
1985
Airbags installed many cars as option
ADAM, EuroSID
1986
1986
Lap shoulder belts in the rear seats planned as standard outboard (GM), The first driver's side airbag (Ford Tempo and Mercury Topaz), Proconten (Programmed Contraction-Tension) (Audi)
Hybrid III small female and large male, DotSID
1987
1987
Driver and passenger airbags as standard equipment (Porsche 944 turbo)
EuroSID I, BioSID
1989
1989
New facial injury assessment techniques improved (GM)
1990
The first time airbags standard equipment in most cars, Government law; All cars sold in the US had to be equipped with either airbag or automatic seat belts
CRABI
1991
Hybrid III type
1992
SID IIs, THOR
1994
1994
The first time dual threshold airbags systems, (intelligent safety system) (BMW), The first time side airbag introduced and offered as an option (Autoliv, Volvo)

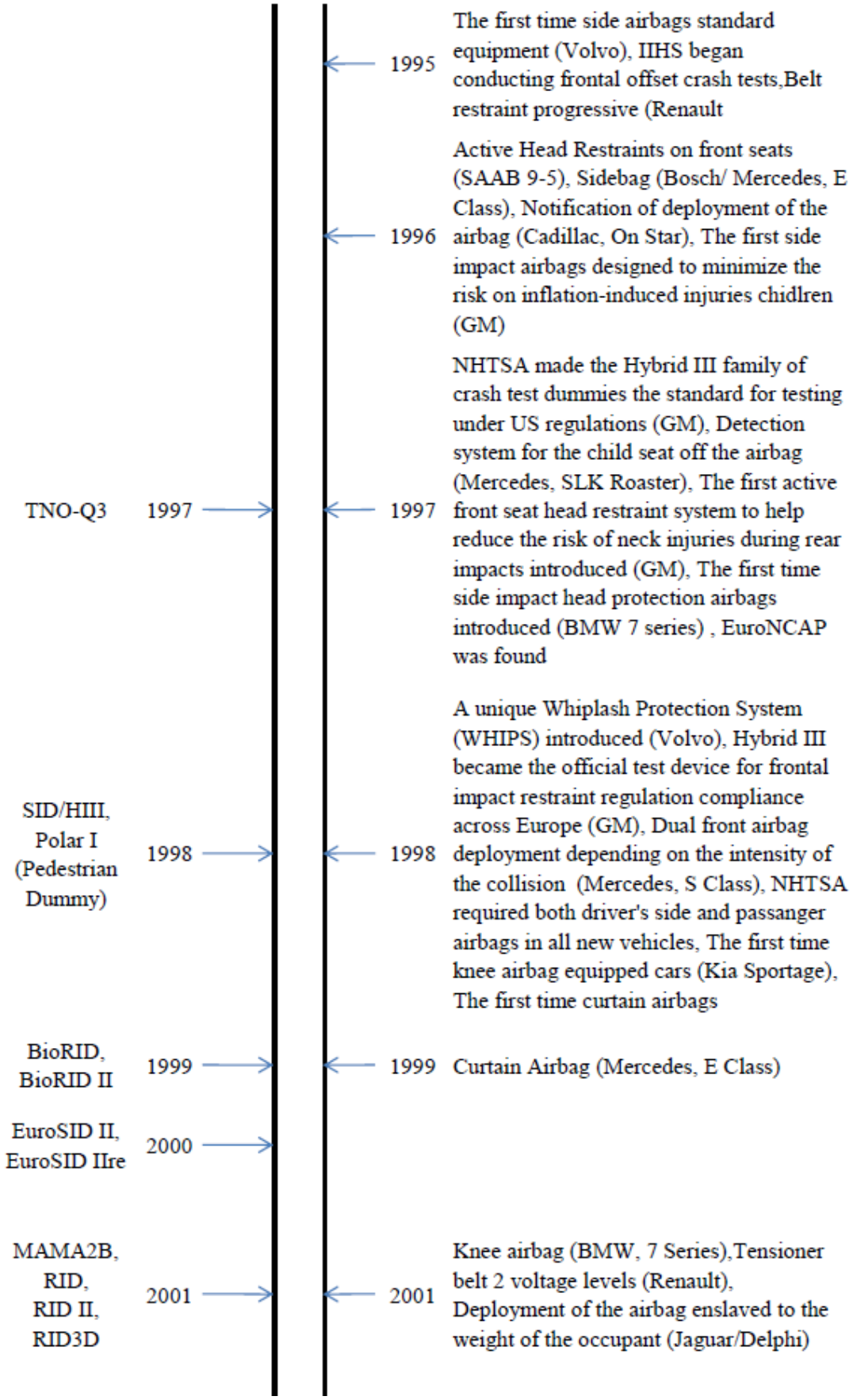
1995
The first time side airbags standard equipment (Volvo), IIHS began conducting frontal offset crash tests,Belt restraint progressive (Renault
1996
Active Head Restraints on front seats (SAAB 9-5), Sidebag (Bosch/ Mercedes, E Class), Notification of deployment of the airbag (Cadillac, On Star), The first side impact airbags designed to minimize the risk on inflation-induced injuries chidlren (GM)
TNO-Q3
1997
1997
NHTSA made the Hybrid III family of crash test dummies the standard for testing under US regulations (GM), Detection system for the child seat off the airbag (Mercedes, SLK Roaster), The first active front seat head restraint system to help reduce the risk of neck injuries during rear impacts introduced (GM), The first time side impact head protection airbags introduced (BMW 7 series) , EuroNCAP was found
SID/HIII, Polar I (Pedestrian Dummy)
1998
1998
A unique Whiplash Protection System (WHIPS) introduced (Volvo), Hybrid III became the official test device for frontal impact restraint regulation compliance across Europe (GM), Dual front airbag deployment depending on the intensity of the collision (Mercedes, S Class), NHTSA required both driver's side and passanger airbags in all new vehicles, The first time knee airbag equipped cars (Kia Sportage), The first time curtain airbags
BioRID, BioRID II
1999
1999
Curtain Airbag (Mercedes, E Class)
EuroSID II, EuroSID IIre
2000
MAMA2B, RID, RID II, RID3D
2001
2001
Knee airbag (BMW, 7 Series),Tensioner belt 2 voltage levels (Renault), Deployment of the airbag enslaved to the weight of the occupant (Jaguar/Delphi)

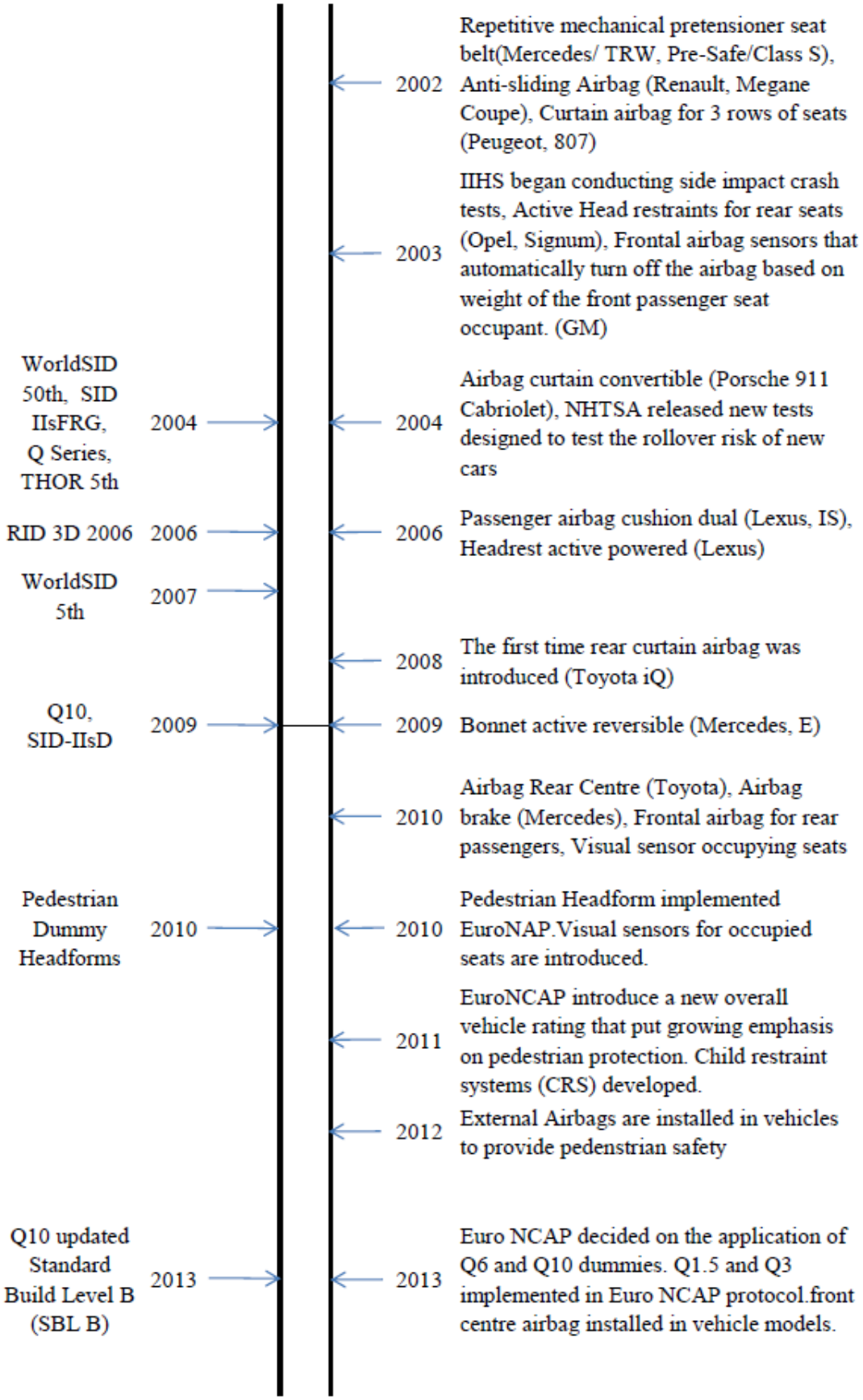
Repetitive mechanical pretensioner seat belt(Mercedes/ TRW, Pre-Safe/Class S), Anti-sliding Airbag (Renault, Megane Coupe), Curtain airbag for 3 rows of seats (Peugeot, 807)
2002
IIHS began conducting side impact crash tests, Active Head restraints for rear seats (Opel, Signum), Frontal airbag sensors that automatically turn off the airbag based on weight of the front passenger seat occupant. (GM)
2003
WorldSID 50th, SID IIsFRG, Q Series, THOR 5th
2004
Airbag curtain convertible (Porsche 911 Cabriolet), NHTSA released new tests designed to test the rollover risk of new cars
2004
RID 3D 2006
2006
Passenger airbag cushion dual (Lexus, IS), Headrest active powered (Lexus)
2006
WorldSID 5th
2007
The first time rear curtain airbag was introduced (Toyota iQ)
2008
Q10, SID-IIsD
2009
2009
Bonnet active reversible (Mercedes, E)
Airbag Rear Centre (Toyota), Airbag brake (Mercedes), Frontal airbag for rear passengers, Visual sensor occupying seats
2010
Pedestrian Dummy Headforms
2010
2010
Pedestrian Headform implemented EuroNAP.Visual sensors for occupied seats are introduced.
EuroNCAP introduce a new overall vehicle rating that put growing emphasis on pedestrian protection. Child restraint systems (CRS) developed.
2011
External Airbags are installed in vehicles to provide pedenstrian safety
2012
Q10 updated Standard Build Level B (SBL B)
2013
2013
Euro NCAP decided on the application of Q6 and Q10 dummies. Q1.5 and Q3 implemented in Euro NCAP protocol.front centre airbag installed in vehicle models.

2.6 Evolution of Computational Occupant Modelling

Computational occupant models and crash test simulations have become important tools and useful alternative to physical models in analysing biomechanical response and understanding injury mechanisms of occupants. With an advanced computational occupant model, stresses, strains on deformed shapes of bodies and internal organs can be predicted, details of injuries to the head, neck, thorax and extremities can be analysed. Non-standard vehicle occupants such as a pregnant woman and a fetus can be represented to investigate possible fetus fatalities in road accidents.

Computational crash test simulations can provide additional information that is not available in experimental physical tests. Several crash scenarios can be analysed quickly and inexpensively with computational modelling. A number of different parameters that cannot be measured on experimental testing can be calculated before designing physical models. Repeatable and controlled tests are very useful for car manufacturers.

Biofidelity of computational occupant model depends on how well each mechanism is defined and modelled. Accurate and detailed representation of occupant geometry and material properties are very important factors to characterize the model.

Three basic types of computational model have been developed to represent the occupant body in road accidents; lumped mass models, multibody models and finite element models. Lumped mass models represent the human body as one or several masses connected to a structure with springs and dampers. The most widely used type for simulating occupant dynamics are multibody models.

Technical specifications such as instrumentation, dimensions, and assembly weights of physical crash test dummies are important to develop computational dummy models. Several databases about specifications of ATDs have been collected since 1980s. One of the most popular computational dummy models is the Hybrid III crash dummy. A series of sled test simulations using the computational model of Hybrid III dummy has been conducted since 1985s (Prasad, 1990). As result of the tests, a number of recommendations were made for further improvements of the

Hybrid III dummy model (Obergefell *et al.*, 1988; Wismans and Hermans, 1988; Khatua *et al.*, 1988). Figure 2.8 illustrates some of the validated standard multibody dummy models currently available with the MADYMO software. The anthropometry of the adult occupant models are obtained from the database of the RAMSIS software package (RAMSIS, 1997). The Western European population aged 18 to 70 years of 1984 is used. For the mid-size male occupant model simply medium typologies are selected for height, weight and sitting height. For the small female a very short and very slim model is selected in RAMSIS. The resulting body mass and sitting height are considered to be somewhat extreme also in comparison to the small female Hybrid III crash dummy.

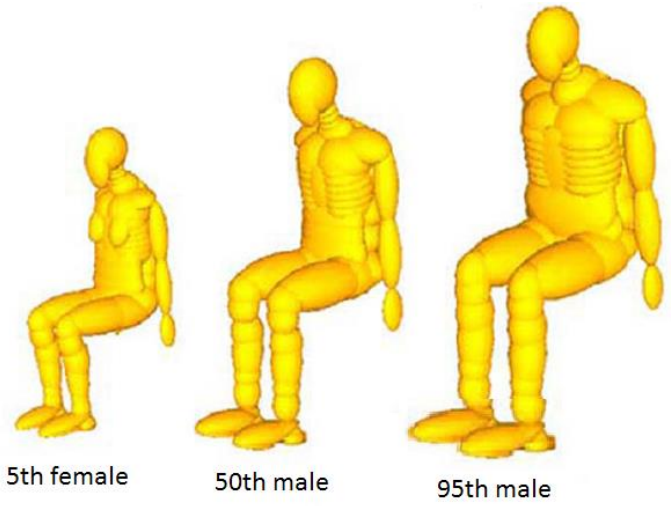

Figure 2.8 Multibody crash test dummy models, Hybrid III dummy family (MADYMO databases, 2010)

With the development of computer technology, finite element modelling of occupant body became very popular. This method provides deformations and can define the state of stress on occupant. Full occupant body models were designed in order to study the full body behaviour in a road accident and to improve vehicle safety systems. Lizee *et al.*, (1998) developed a 3D finite element model of seated 50th percentile adult male occupant body (Figure 2.9). Weight and inertial parameters were adjusted. The external surface of the model was based on Robbins' study for the 50th percentile US male in the driving position (Robbins, *et al.*, 1983). However, the model was not fully validated to predict the injuries. According to

Lizee *et al.*, this human body model is believed much more biofidelic tool compared to mechanical dummies or to their models.

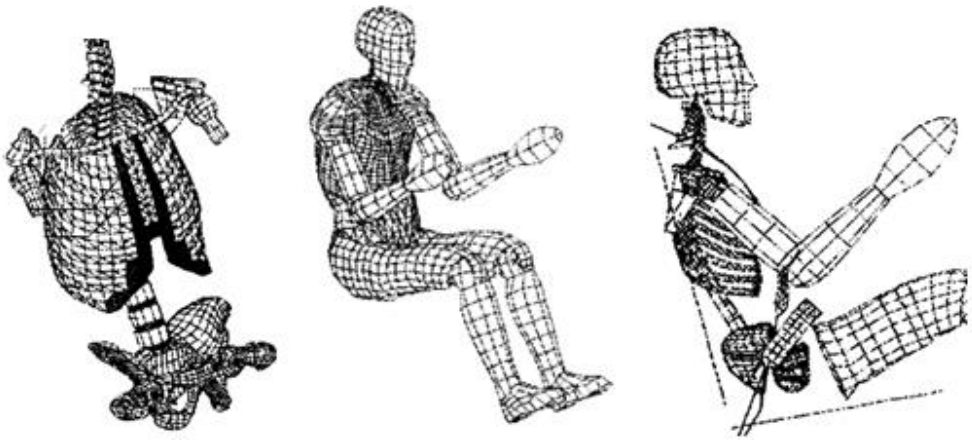

Figure 2.9 Finite element model of full occupant body, internal and external anatomy (Lizee *et al.*, 1998)

There are specific advantages and disadvantages working with the multibody method or the finite element method. With multibody method, complex kinematic connections in the human body or in the vehicle structure can be simulated very efficiently. However, with the finite element method, local structural stress distributions and deformations can be predicted. Injury mechanisms in the human body parts can be studied. Finite element model simulations require large CPU times than multibody crash simulation. Finite element method accuracy and reliability are also limited because it is difficult to develop highly detailed human body model and its material properties realistically.

2.6.1 Computational Dummy Modelling

Anthropomorphic test devices can be numerically modelled and designed with limited accuracy and usually represent an average stature of the human body. Computational dummy models have become the standard tool to represent the human body in occupant safety simulations. ATDs are used to validate the computer models.

The use of computational dummy models instead of using physical crash test dummies is a time and money saving method. Various test conditions can be reproduced accurately in a number of different crash scenarios.

Validated crash test dummy design specifications are important requirements for the effective computational dummy modelling. Model databases have been developed for many of the physical crash test dummies. For instance, Hybrid III dummy model data sets were developed and validated by Kaleps *et al.*, (1988); Whitestone and Kaleps (1988) as a first computational dummy model. Computational Hybrid III dummy model is widely used in crash environment. MADYMO, ATB (Articulated Total Body) and many model databases have been developed with Hybrid III dummy. In order to validate the computational dummy model designed at ATB, simulation results were compared with frontal impact sled test data of Hybrid III physical dummy (Obergefell *et al.*, 1988; Prasad 1988).

Several different finite element models of ATDs have been developed with varying degree of biofidelity. For instance, models of SID (Side Impact Dummy) have been developed and applied for different crash scenarios (Midoun *et al.*, 1993; Motojima *et al.*, 1997). Kirkpatrick *et al.*, (1993) developed a finite element SID model to understand how details of physical dummy design affect the measurement of injury criteria in a complex crash test (Figure 2.10). The SID model was validated with comparing pendulum side impact experimental tests results on the ribs and lower spine. However, more expansive comparisons between simulation and experiment tests were necessary. The effect of material properties and dummy design had to be improved.

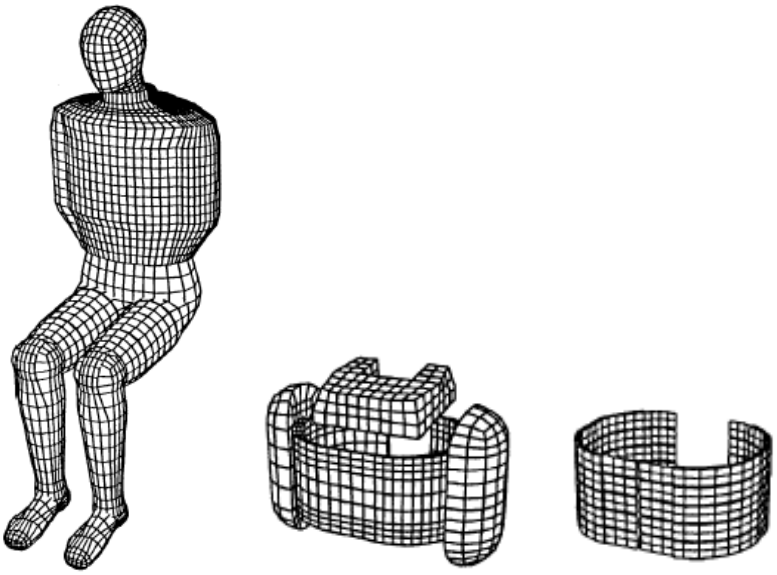

Figure 2.10 Mesh for the SID finite element model, (Overall mesh, Foam arm inserts, rib wrap, and shoulder pads, Ribs and damping material) (Kirkpatrick *et al.*, 1993)

In 1995, variety of 2D and 3D dummy models were created using MADYMO software. In addition to the Hybrid III family, Hybrid II, EuroSID I, SID, BioSID, child dummy models, TNO P3/4, TNO P3 and TNOP6 and other computational dummy models have been developed (TNO, 1995).

Hybrid III 5th percentile female dummy is the standard device to represent small adult occupants for frontal crash impacts. When the accuracy requirements have increased, a new model for this physical dummy has been developed using more powerful multibody techniques such as facet surfaces and deformable bodies (Figure 2.11) (Made *et al.*, 2001). The deformable thorax is described more precisely, dummy geometry is more accurate and load transfer through contacts is handled more realistically. However, the model is slower than ellipsoid models and a higher level of modelling detail is necessary to increase confidence in results obtained from experimental tests.

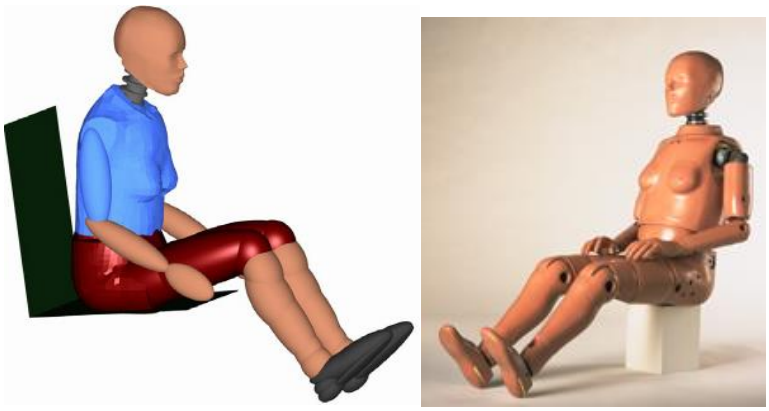

Figure 2.11 Facet Hybrid III 5th percentile model and physical Hybrid III 5th (FTSS, 2012)

In order to develop and validate an NCAP simulation using LS-DYNA3D, in 1996, a finite element model of a Ford Taurus vehicle in full scale, a Hybrid III dummy, and a driver side airbag were designed and combined to make accurate simulation tests (Figure 2.12) (Marzougui *et al.*, 1996). While the components of the thorax and neck assemblies were modelled with flexible parts, rest of the dummy parts were modelled with rigid body parts.

The geometry of the Hybrid III dummy model was obtained from design drawings of the physical Hybrid III dummy. The joints at the ankles, hips, elbows, shoulders, knees, and wrists are modelled with spherical or cylindrical rigid body joints. Properties of each rigid body joint are defined with simulation of the actual dummy. Table inlaid in Figure 2.12 shows the model information of the dummy model. However, more developments at several areas of the model are necessary to be used for accurate injury assessment such as HIC (Head Injury Criteria), head and chest accelerations. More detailed dummy mesh, contact algorithms and advanced material models were necessary for better prediction and assessment of occupant injury.

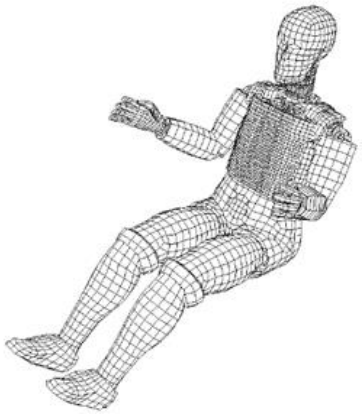

.

Item	Total Number
Parts	50
Nodes	14 200
Shell Elements	7,576
Brick elements	4, 479

Figure 2.12 Hybrid III 50th percentile LS-DYNA3D FE model (Marzougui *et al.*, 1996)

In 2005, Hybrid III 50th percentile Dummy LS-DYNA finite element model was developed to represent physical dummy more accurately (Figure 2.13) (FT-Arup, 2005). The Hybrid III 50th percentile dummy represents an average 50th percentile adult US male occupant in mass and inertia. Highly accurate strain and stress data can be obtained from this dummy model. However, the model has very high CPU time consumption. Modification of the model is very difficult to perform, because modification affects validity of the model. Table 2.2 shows details of the Hybrid III dummy model 2005. Number of elements that used at 2005 Hybrid III dummy model is approximately 9 times higher than 1996 Hybrid III dummy model.

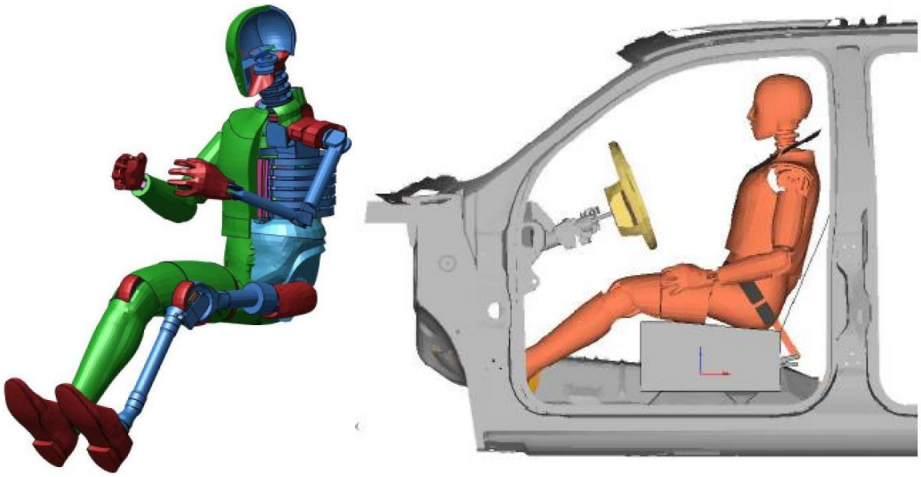

Figure 2.13 Hybrid III 50th Percentile Dummy LS-DYNA Finite Element Model (FT-Arup, 2005)

Table 2.2 Hybrid III dummy model details (FT-Arup, 2005)

Item	Total Number
Part, Section and Material	331
Nodes	64802
Elements: total	89978
Beam	370
Shell	43018
Solid	46574
Joint	32

The EuroSID-2 finite element model has been developed to represent behaviour of EuroSID-2 dummy (Schuster *et al.*, 2004) used to assess side impact injuries of occupants (Figure 2.14). The EuroSID-2 dummy model has very fine mesh. Strain and stress data can be obtained from the FE model. The model has high CPU consumption and modification of it is very difficult.

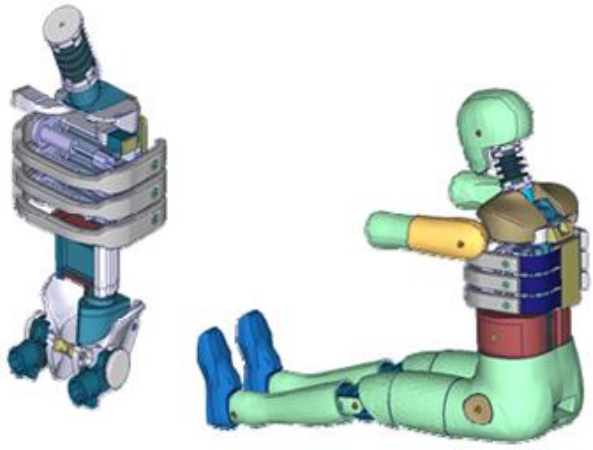

Item	Total N
Nodes	80 041
Hexahedron elem	24942
Tetrahedron elem	97114
Beam elem	218
Shell elem	64724
Discrete elem	12

Figure 2.14 EuroSID-2 Finite Element Model and details (Schuster *et al.*, 2004)

Sankar, *et al.* (2008) developed the BioRID-2 (Bio Rear Impact Dummy) finite element model at Abaqus software (Figure 2.15). The model contains fully articulated spine in the sagittal plane composed of 24 vertebrae connected with joints. In order to study BioRID-2 flexion/extension and retraction whiplash modes, numerous connector elements and advanced material models were used. Although the model represents the BioRID-2 physical dummy, a number of improvements were necessary such as the definition of neck forces and moments.

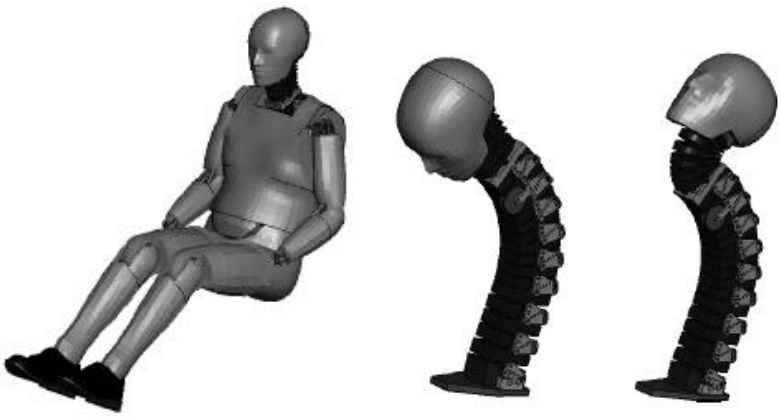

Figure 2.15 Abaqus BioRID-2 crash dummy model and flexion/extension and retraction whiplash modes (Sankar *et al.*, 2008)

Working with numerical dummies has a number of disadvantages. In an accident, assessment and prediction of injury risk on human body are important. Computational dummy model anatomy is very different than real human anatomy. Therefore, assessment and prediction of injuries are often limited and not accurate enough. Moreover, representation of large deformations of the internal organs in an accident is difficult. Vehicles tested with dummies can pass the requirements and can be safe for dummies but cannot be safe for vulnerable human occupants.

2.6.2 Computational Human Modelling

Computational human body models are used for vehicle safety design and play important role to simulate motor vehicle accidents within the last decade. While computational physical dummy models simulate their metallic, plastic and rubber parts, computational human models simulate the response of internal organs, soft tissues, and bones that humans are made of. Using of computational human models can have a number of advantages over computational dummy models.

Simulation models of the human body are usually based on multibody methods and/or on finite element techniques. With multibody modelling approach, complex dynamic systems with kinematic connections such as in the human body can be simulated efficiently. Computational modelling of the real human body allows the study of different aspects including body posture, muscular, body size, and internal organs activities, and post fracture response. They also offer significant advantages such as the prediction of injury criteria. Especially, finite element human modelling method plays an important role in improving our understanding of the injury mechanisms involved during crash events. With this method, local deformations and stresses can be described in a more biofidelic way. When injury mechanisms of human body are understood, more biofidelic injury criteria can be developed and more reliable injury tolerance level can be identified. If validated computational human body models can be created, establishment of injury criteria will depend more on finite element model and it is expected that the need for tests with human cadavers, animals and physical dummies will be reduced.

Development of a computational human body model is much more difficult than developing a computational dummy model, because of the lack of body tissue material data and the lack of reliable joint properties. Furthermore, creation of a finite element human model is time consuming, and biological tissue response are often non-linear. Because of large CPU time consumption, changing design parameters for optimization studies is difficult to perform.

A number of studies have been performed in the computational human body modelling since 1960s. The first of rigid multibody models that contained eight masses was proposed by McHenry (1963). McHenry developed one of the early human CVS (Crash Victim Simulator) models (Figure 2.16). Human body and restraint system are represented in this simulation. Vehicle is two-dimensional. The human or physical dummy is treated as an articulated assembly of rigid-mass segments consisting of head, torso, and extremities for purpose of determining vehicle clearances and body acceleration vectors. The model illustrated in Figure 2.16 includes the effects of some system nonlinearities, such as varying belt angularity, seat cushion deflection and friction, slack, and variations in the effective inertia of the articulated body. A more sophisticated 2D model was later developed by McHenry and Naab (1966).

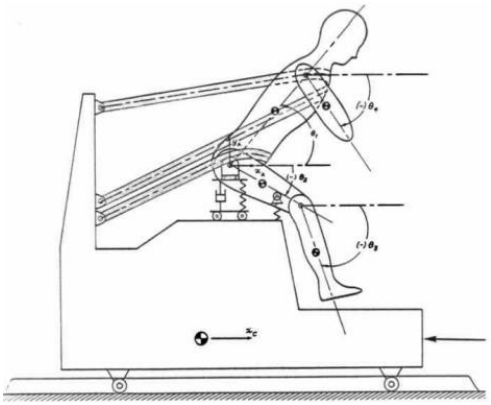

Figure 2.16 Multibody model, for frontal collisions (McHenry, 1963)

In many crash environments and especially for oblique impacts, two-dimensional human models were inadequate to simulate these crashes. For instance,

three-point seat belt is asymmetric. Therefore, more comprehensive human body and its environment simulation were necessary for more realistic crash simulations.

In 1970, a three-dimensional occupant model, named HSRI-3D, with three mass-segments was generated by Robbins (1970). It was a simple model with three bodies. However, only the forces that were generated by impact of the bodies could be simulated. Two years later, the model was expanded to include six rigid bodies (Robbins *et al.*, 1972).

Robbins *et al.*, (1974) developed a two-dimensional crash victim simulation model which was called MVMA-2D. Figure 2.17 illustrates MVMA-2D occupant simulation linkage system. There were eight rigid, two flexible segments and nine masses. The neck and shoulder were modelled by elements. These two features of the MVMA-2D model are different than other CVSs.

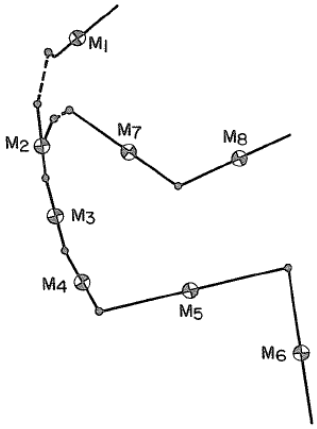

Figure 2.17 MVMA-2D occupant simulation linkage system (Robbins *et al.*, 1974)

These initial developments were followed by several more general occupant simulation tools. One of the best known three-dimensional models is, named Calspan, CAL-3D occupant simulation model or CVS model developed by Bartz (1971). The Calspan model had 15 bodies to simulate the human body frame. The bodies were described with ellipsoids connected by spherical and pin joints. Articulated Total Body (ATB) simulation model was created with some modifications of CVS by Fleck and Butler (1975).

The TNO transportation research institute developed MADAMO two-dimensional of three-dimensional occupant model respectively (Wismans and Maltha, 1981). 3D model consisted of a number of ellipsoids connected with spherical and hinge joints to represent the human frame. Vehicle interior was also described with surfaces. In 1983, the first version of MADYMO program for external use, version 3, was released. In MADYMO, the equations of motion for human body structure composed of rigid bodies connected by joints such as hinge or ball-socket type. MADYMO3D could also describe the motion in three dimensions.

Table 2.3 shows a summary of the computational human models developed until 1981 and some of their features. Although computational human models especially three-dimensional were very sophisticated for their time, most of them were not validated with experimental test data. The modelling of the joint properties and the soft tissues were very crude and inaccurate. Therefore, prediction of injury severity and mechanisms were almost impossible. In addition to that, modelling programs were not user friendly.

Table 2.3 Computational human models until 1981

Model Name	Degree of Freedom	Body segment shape	Analytical formulation	Developer
CAL 2D	7	Rods	Lagrangian	McHenry (1963) Calspan
CAL 2D	11	Spheres	Lagrangian	McHenry and Naab (1966) Calspan
HSRI 3D	12	Ellipsoids, cylinders	Lagrangian	Robbins (1970)
HSRI 3D	14	Ellipsoids, cylinders	Lagrangian	Robbins *et al.* (1972)
CAL 3D	40	Ellipsoids	Newtonian	Bartz *et al.* (1972) Calspan
MVMA 2D	10	Spheres	Lagrangian	Robbins *et al.* (1974)
CAL 3D	N	Ellipsoids	Newtonian	Fleck and Butler (1975) ATB
MADAMO 2D/3D	N	Ellipsoids	Lagrangian	Wismans, Maltha *et al.*, (1979, 1981)

Extensive data is necessary to describe human body geometry and inertial properties. Dealing with the large variations in human body geometries is challenge issue. Therefore, a number of multibody approach methods have been developed to generate various human body models. In 1983, GEBOD (Generator of BODy Data) was developed to generate geometric and inertia properties for 15 or 17 segments ATB or MADYMO multibody model (Baughman, 1983). Although 32 body measurements were specified by user or generated by GEBOD for set of geometrical parameters of occupant, body segments were approximated by simple geometrical volumes. Furthermore, correlation between body dimensions was disregarded at the GEBOD. The RAMSIS (1994) software has particularly been developed for ergonomic analyses. The RAMSIS model describes the human body with rigid bodies connected by kinematic joints and the human skin is described as triangular surfaces. RAMSIS models can also be translated into MADYMO models (Figure 2.18) (Happee *et al.,* 1998).

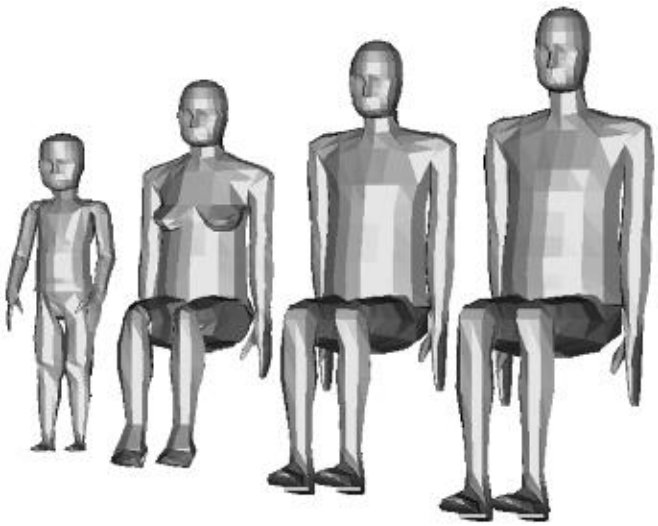

Figure 2.18 MADYMO human models of various body sizes generated from the RAMSIS model, from left to right:3 year old child, 5th percentile small female, 50th percentile male, 95th percentile large male (Happee *et al.,* 1998)

The RAMSIS models were to represent a human body for forward and rearward loading. However, abdomen area of the model was not biofidelic enough. Shoulder model had also lack of dynamic and detailed data. Furthermore, the model was not validated with seat belt and airbags interactions.

50th percentile finite element 3D human body model was developed by Lizee *et al.*, (1998) in the RADIOSS program package. The geometry of the seated 50th percentile US male was chosen for the model. The model was created by comparing anatomical data and test results. The neck, shoulder, thorax and pelvis were represented in detail. According to authors, this model could reproduce cadaver responses in frontal, oblique, lateral and some types of rear impact. However, the model was very simple to predict injury mechanisms directly.

In order to simulate injury mechanisms of occupant during vehicle side impact, a finite element model of the human body was created with ABAQUS FE codes by Jost and Nurick (1999) (Figure 2.19). The FE model consists of the skeleton bones, soft tissues representing skin, fat, muscles and internal organs. While pelvic and shoulder joints were modelled using solid elements, ligaments and muscles were represented with membrane elements. However, the finite element model shoulder impact prediction and experimental corridor test results were not satisfactory.

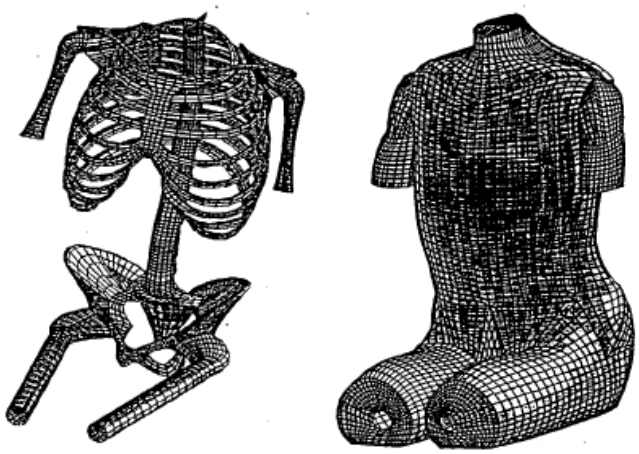

Figure 2.19 Finite Element of skeleton and overall shape of human body (Jost and Nurick, 1999)

Happee *et al.*, (1999) improved a mathematical human body model for lateral loading. The anthropometry of the human model presented was based on the RAMSIS database (Flugel, 1986; Geus, 1994). Since 1995, RAMSIS was distributed worldwide. More than 50% of all car manufacturers worldwide use RAMSIS to

design their cars. A 50th percentile male model using RAMSIS anthropomorphic database was converted to MADYMO. RAMSIS models have been developed for several population including Germany, USA/Canada, Japan/Korea. The German population age ranges from 18 to 59 was surveyed period between 1982 to 1984. Standing height, body mass, seating height and gender were the main stratification variables. The spine and thorax model was enhanced with additional degree of freedom and joint resistance models were added. In order to obtain omni-directional biofidelity, the torso and the head-neck systems were improved in more detail. While most of skeletal structures were modelled as rigid bodies, rib cage was modelled using flexible elements to define deformation. However, detailed human body model was necessary for analysis of injury mechanisms on material level. Figure 2.20 shows 50th percentile male MADYMO human body model.

A 5th percentile small female human body model was also developed by Happee *et al.*, (2000) with the same combination of modelling technique that uses rigid bodies for most segments and describes the thorax as a deformable structure.

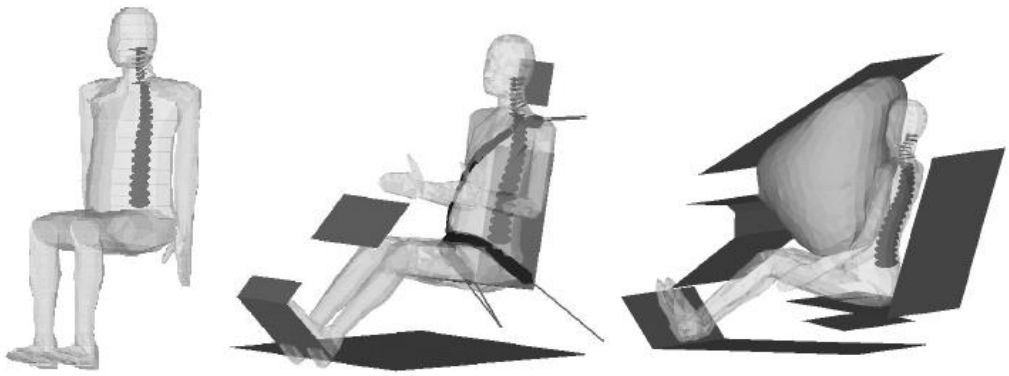

Figure 2.20 MADYMO human body model representing a 50th percentile male, spine, neck rigid bodies, restrained by finite element belts, with a passenger airbag (Happee *et al.*, 2000)

With the rapid improvement in both computational power and non-linear finite element technology, a number of finite element body parts and whole human body models were developed between 2000 and 2003. However, there were only three whole human body models available; ESI's H-Model (Choi *et al.*, 1999),

Toyota's THUMS (Total Human Model for Safety) (Oshita *et al.*, 2002) and TNO's HUMOS (Robin, 2001).

H-model is a finite element PamCrash code for 50th percentile male human body and it was conceived primarily to study injury mechanisms and to assess injuries of the human skeleton and organs during road accidents (Figure 2.21) (Choi *et al.*, 1999). Anthropometric data set from Robbin's work (Robbin, 1983) were used to determine each segment, dynamic properties such as mass, location of centre of masses, and joint resistance. The H-model can adopt itself with a modular modelling approach that is multibody H-ARB (Human Articulated Rigid Body) model. In a crash simulation scenario, the H-ARB model assures a correct overall kinematic behaviour for omni-directional impacts.

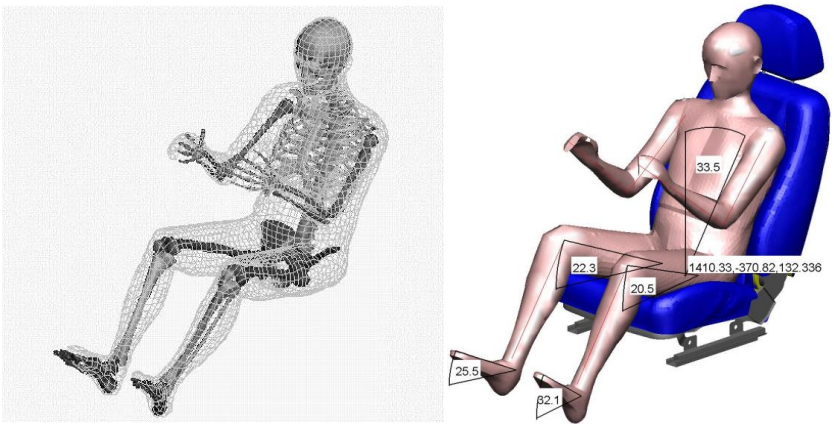

Figure 2.21 H-Model with skeleton and skin, 50th percentile male (Choi *et al.*, 1999)

The H-ARB versions of the H-Models consist of articulated rigid body segments with flexible joints. In order to study the injury mechanisms during the impact load, internal body components were modelled separately and can be selectively added into the whole-body model.

HUMOS-1 project was developed between 1999 and 2001 in the European institutes (Robin, 2001). In the project, physical slicing of PMHS (Post Mortem Human Subject) in a sitting driver position technique was applied and slices were photographed and digitised. The main human body structures of the HUMOS-1

model were reconstructed using CAD software. The model includes skin, bones, muscles, and main organs such as lungs, heart, liver, kidneys, and intestine. The model was implemented with three commercially available dynamic crash codes (MADYMO, Pam-Crash and Radioss). Figure 2.22 illustrates HUMOS-1 model.

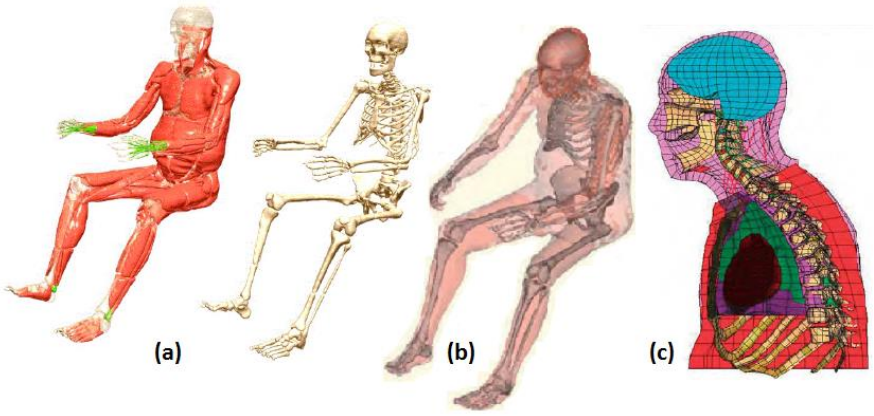

Figure 2.22 Geometry acquisition result of the (a) whole body and the skeleton, (b) TNO HUMOS-1 full body FE model (c) HUMOS-1 thorax FE model, mid-sagittal section (Robin, 2001)

The HUMOS-1 model is very detailed; the geometrical definition of the model comes from a unique human cadaver subject that was not generic. While different segments of the model were validated, the whole body model was not validated. Muscle contribution needed to be investigated for the low speed impact conditions. In addition to that, injury prediction capabilities of the model were limited due to the lack of knowledge of the injury mechanisms and the models limited complex internal organs such as kidneys, intestine and heart.

Finite element THUMS model was developed in LS-DYNA codes to simulate responses of the human body sustaining impact loads and to study injury mechanisms (Oshita *et al.*, 2002) (Figure 2.23). The whole body can be deformable and represents 50th percentile American male (AM50) in a seating posture based on pedestrian and passenger since 1997. The THUMS model has a very detailed skeletal structure with detailed representation of the cortical and the spongy bones using shell

and volume elements. The joints, ligaments, and tendons are modelled by using shell elements. The lung and heart are modelled as a single continuum body with solid elements. Skin and muscles that cover the bones are modelled with solid elements. The spine including the vertebrae, the intervertebral discs and muscles are also modelled using beam or discrete elements. In order to realize a practical level of computational time, only the sections expected to receive damage were selected for detailed modelling for analysis. The rest of the human body is modelled in a rough mode.

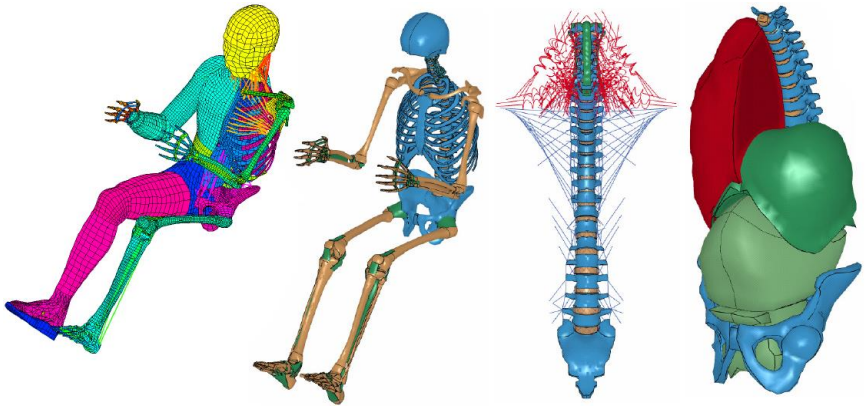

Figure 2.23 Details of the THUMS model; skin, skeletal structure, spinal and muscular system and internal organs (Oshita *et al.*, 2002)

The overall force-deflection response of the THUMS model showed a good agreement with the experimental corridors. However, the unloading path of the model response deviated from some of the experimental corridors (Oshita *et al.*, 2002). No active muscles were considered within the model. The responses of the internal organs cannot be predicted accurately with the THUMS model.

HUMOS-2 models were developed to represent a large range of the European population (Vezin and Verriest, 2005). Scaling software was developed to define 5th and 95th percentile occupant models from 50th percentile model (Figure 2.24). Scaling tool was established from geometric data collected on standing and sitting human volunteers. European databases of anthropometry measurements were analyzed in order to define the external geometry of the human body corresponding

to these percentiles. In order to represent the user population from the 5th percentile female to the 95th percentile male, three dimensional external and internal measurements data of human body are necessary. Data collected includes age, sex, weight, lengths, heights and circumferences. In addition to that, pedestrian models were also developed. In HUMOS-2, effect of muscle tone, mechanical properties of soft tissues and the whole body response for realistic impact conditions were investigated. It was identified that the abdomen area and muscle tone needed to be improved.

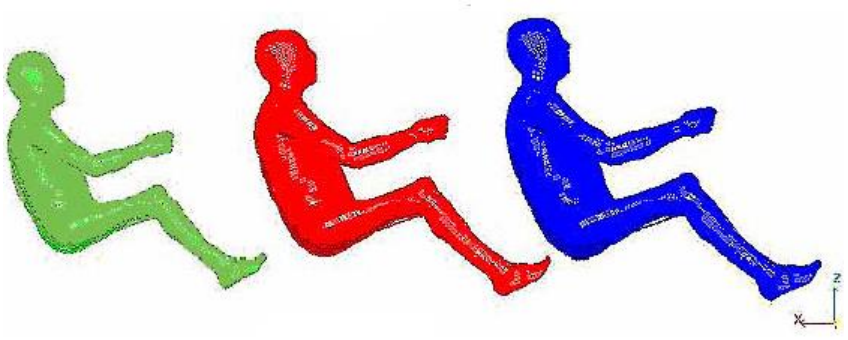

Figure 2.24 From left to right; 5th, 50th, and 95th percentile HUMOS-2 models obtained with scaling tool (Vezin *et al.*, 2005)

JAMA (Japan Automotive Manufacturers Association) human body models were developed using Pam-Crash and LS-DYNA codes to investigate pedestrian and occupants during road accidents (Figure 2.25) (Sugimoto *et al.*, 2005). The pedestrian model was designed based on both the THUMS and the H-model. While upper half of the body was THUMS model, the H-model was used for the lower half of the body. Posture of the occupant model was changed to develop pedestrian model.

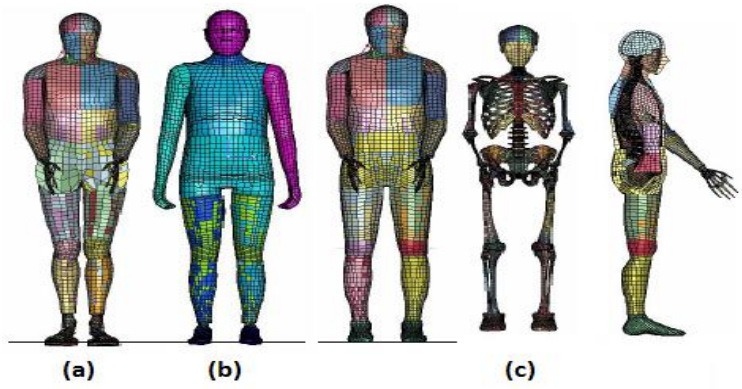

Figure 2.25 Existing human body models in Japan, (a)THUMS, (b) Pedestrian model based on H-model, (c) JAMA pedestrian model (external and internal) (Sugimoto *et al.*, 2005)

In 2005, Zhijijan and Gopal developed a finite element human body model to investigate restraint systems and develop applications (Figure 2.26) (Zhao and Narwani, 2005). The 50th percentile finite element male model consists of details of the major tissues and human skeleton such as skull, pelvis, clavicle, ribs, and shoulder bones, spinal column, neck muscles, joint ligaments, and joints, lungs, heart, aorta, liver, and kidneys. The human body represents an average adult male with weight of 75kg. However, lower and upper extremities were integrated as rigid bodies from Hybrid III. Injury prediction of the soft tissues was not possible at this model.

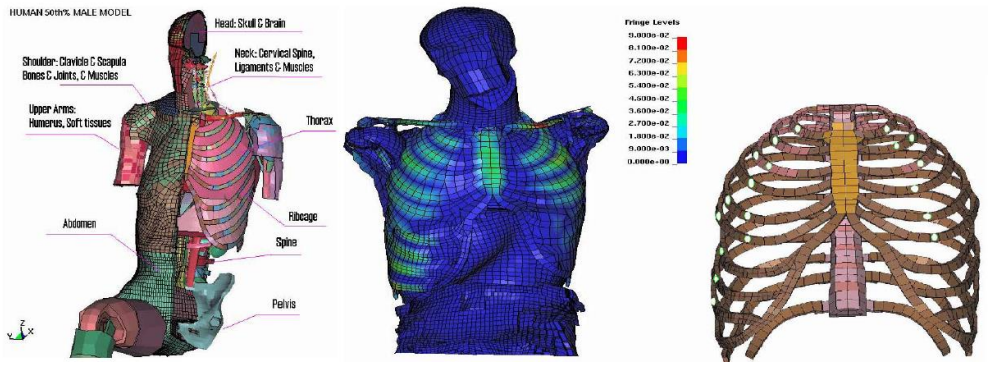

Figure 2.26 50th percentile male finite element human model and its simulated chest shapes at 96ms (Zhao and Narwani, 2005)

Developments in the finite element human body modelling have shown that in order to investigate injury mechanisms and severity of injuries in the material level on the occupants during road accidents, well defined and detailed interior and exterior human body model is necessary. Furthermore, it is also understood that muscle bracing influences the results of an impact crash test simulations.

In 2006, Behr *et al.* developed a computational lower limb model, including muscle structure and bracing capability on a European 50th percentile single human anthropometry. MRI image analysis method was used to extract the three-dimensional geometry of the musculoskeletal system. The coxal bone was taken from the HUMOS database. The muscles were modelled with 3-D viscoelastic solids, guided in the direction of fibres with a set of springs (Figure 2.27). The volunteer was 178 cm height and 78 kg weight, and was very close to the European 50th percentile. However, the model is only limited to lower limb modelling. The frontal impact simulations were performed using computational 50th percentile Hybrid III dummy model.

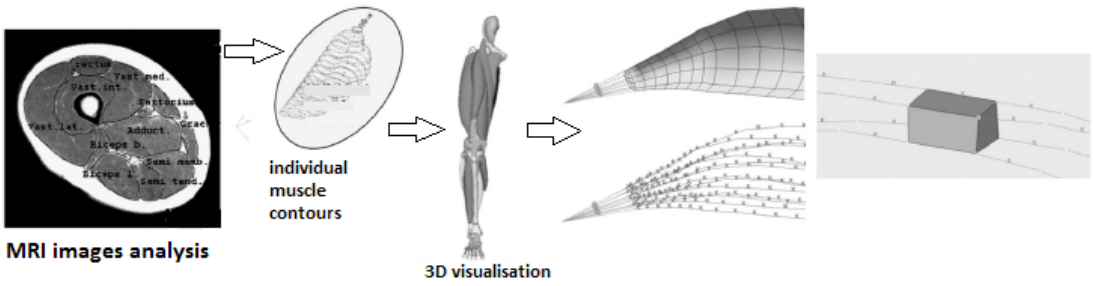

Figure 2.27 Geometry acquisition process and meshing of skeletal muscles. The muscle passive mass component is modelled with viscoelastic solids merged to a set of action lines (Behr *et al.*, 2006)

In order to create computational dummy, human and their environment models, some of the most popular software packages are; MADYMO, CAL3D/ATB, MVMA-2D, RAMSIS, LS-DYNA, RADIOSS, PAM CRASH. Each of these software packages uses some combination of rigid bodies, deformable elements, springs, and dampers to represent the human or dummy body. The equations of

motion are solved for system analysis by these software packages. MADYMO software offers two categories of models; human and ATD models. These two categories each have three types of model: Ellipsoid models, Facet models and Finite Element models (Figure 2.28). The characteristics of each type are given in the following Table 2.4.

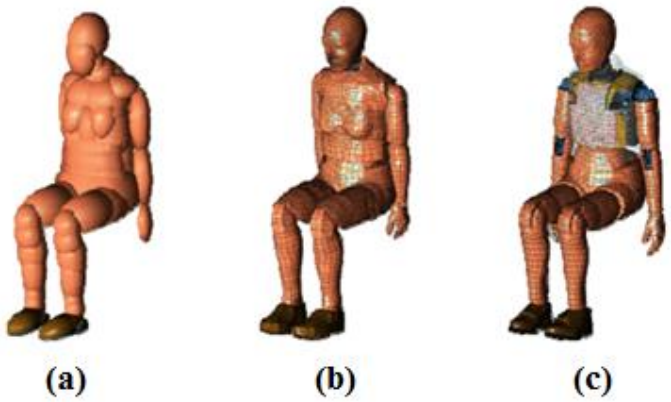

Figure 2.28 Hybrid III 5th percentile female, three model types; (a) Ellipsoid, (b) Facet, (c) Finite element (MADYMO database, 2010)

Table 2.4 Characteristics of MADYMO Human and Dummy Models

ELLIPSOID MODELS	FACET MODELS	FE MODELS
Geometry is represented with ellipsoids, cylinders and planes	Geometry is represented by rigid mesh, some deformable bodies	The most detailed and deformable bodies. Local effects of interaction and local material deformations are of interest
Only rigid bodies	The outer surfaces of the model are described with meshes of shell–type	Deformable bodies modelled with finite elements
Inertial proper. incorporated in the rigid bodies	The facets are fully connected to rigid and/or deformable bodies	Finite elements are created with nodes and material properties are defined
Particularly suitable for concept, optimization and extensive parameter sensitivity studies	More realistic and detailed than ellipsoid models	Less suitable for concept studies but more suitable method to study biofidelic and detailed modelling
Less CPU time, can be used in a facet or FE environment	Very efficient CPU time compared to FE models.	Longer CPU time than ellipsoid and facet models

A number of different crash test dummy numerical models have been created and fully integrated into the crash test simulation procedures since 1990s. Figure 2.29 illustrates the finite element Hybrid III family dummy models. They have become standard tools for occupant safety simulations. However, anatomy of crash test dummies is not exactly the same as the human body. Computer models of crash test dummies are also much more limited and simple than ATDs in terms of representing biofidelic human body. Computational modelling of the real human body offers improved biofidelity, because human anatomy, anthropomorphic variations and posture can be taken into account more accurately. Injury mechanisms of the skeleton and soft tissues and internal organs can be studied with a well-developed numerical human body model. However, this modelling process is considerably more complex. Defining soft tissue material properties and structures present difficulties in computational human body modelling. Figure 2.30 shows facet real human body models.

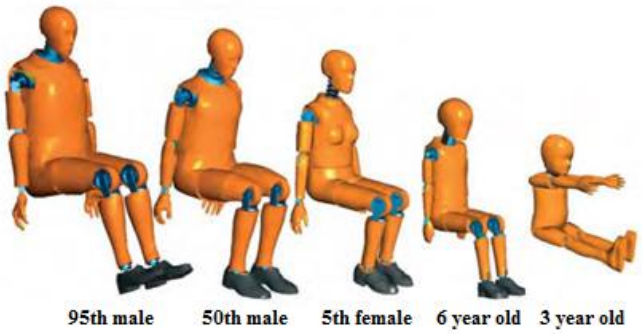

Figure 2.29 Hybrid III dummy family FE models (MADYMO Model Manual, 2010)

Figure 2.30 Human body facet models (MADYMO Model Manual, 2010)

2.7 Conclusions

Car manufacturers, research institutes and governments have been working to improve vehicle safety for more than 80 years. Development history of physical crash test dummies and their relations to vehicle safety design were reviewed critically. In the last 60 years, vehicle safety has been developed significantly. Evolution of computational crash test modelling using virtual dummy and human models was investigated.

Research and investigations are continuously directed to understand the injuries to human body in motor vehicle accidents. Car manufacturers, researchers and investigators have found new techniques to understand the mechanics involved in accidents resulting in injuries. In the field of vehicle safety research, simulating vehicle crash tests to study the effects on the human body is vital in order to evaluate and improve safety devices and occupant environment.

Experimental crash tests can anticipate safety problems and respond to a problem as an early warning to users. For instance, crash tests with ATDs showed that airbags in vehicles can be dangerous for some occupants such as children and small size passengers. As a result, children sit in the rear child car seats and special airbag systems are developed. Crash test dummies are standardized data collection devices to physically test deformations on the vehicles and injuries on occupants.

Current restraint and vehicle safety system designs consider small percentage of the variation. Versatility and efficiency of computational modelling establish a new alternative method for automotive safety designers.

This study is also closely related to investigate computational and physical pregnant occupant models and understand their development methods to design more realistic 'Expecting', which will be explained in the next chapter.

CHAPTER 3

PREGNANT OCCUPANT MODELS

3.1 Introduction

Understanding how pregnant occupant and their fetuses are injured in motor vehicle accidents may assist designers to improve protection for pregnant women and their fetuses. Several researchers investigated seat belt effectiveness on pregnant baboons and monkeys, conducted in the late 1960's and early 1970's women (Crosby *et al.,* 1968, 1972). The use of seat belts during pregnancy is a major safety concern (Eurostat, 2011). On the other hand, in the experimental crash tests, the 50th percentile male dummy is often defined as the standard and used as the main test object of investigations. Lack of representation of different shapes and sizes of occupants may result in unintended injuries and problems. In order to minimize pregnant occupant and fetus injuries or fatalities, new assessment tools, such as anthropomorphic test devices are developed in the mid 90's and early 2000. Two types of pregnant dummies were developed by Pearlman and Viano (1996) and Rupp *et al.,* (2001). Both crash test dummies were tested utilizing several restraint

conditions. Their findings agree with results from animal testing regarding the use of a three-point belt. Tests with the crash test dummies are costly and do not show the biofidelity of a human occupant. On the other hand, for a pregnant occupant and her fetus safety, real collision data is very limited and experimental tests with pregnant cadavers or volunteers are not viable. In the last decade, computational pregnant occupant modelling has become a very effective method for vehicle safety tests. Computational modelling of pregnant occupants provides a broad basis for studying factors that could prevent fetal fatalities from motor vehicle accidents.

3.2 Anatomy of the Pregnant Women

A number of changes occur a female body during pregnancy. The fetus starts to develop at around the ninth week of gestation. Pregnancy lasts approximately 9-10 months, around 40 weeks. This period is divided into tree trimester periods for convenience and simplify the different stages of prenatal development. These periods are defined with the physiology of fetal growth.

The first trimester represents the first twelve weeks of fetus' fetal life. In this period, primary fetal development occurs. The second trimester ends at 28 weeks. Pregnant women gains approximately 6kg and the fetus increases in mass about 0.64 kg. Uterus enlarges above pelvis and produces alteration in pregnant woman's centre of gravity because of carrying an increasing amount of weight in front. Height of the fetus from crown to rump is approximately 82-100 mm. At term about 38 weeks of gestation, pregnant women gains approximately 5 kg and weight of the fetus reaches about 3.2 kg and rest contains amniotic fluid and placenta (Klossner, 2005; S Standing, 2005).

The anatomy of the pregnant abdomen is illustrated in Figure 3.1. In 95% of pregnancies, the fetus is shown in an upside-down position with its head downwards nestled within the confines of the pelvis bone (Acar and Lopik, 2012). The uterus is a muscular organ and grows dramatically during pregnancy to accommodate the fetus. The uterus increases in weight significantly and displaces other abdominal organs upward. By the 36th week of gestation, uterine fundus reaches level of the

xiphisternum and uterine wall thickness becomes approximately 10 mm (Acar and Lopik, 2012). Anthony *et al.*, (2008) states that thickness measurements vary regional for uterine wall and placenta. Size of the uterus in the 3rd trimester of pregnancy is determined by the size of the fetus. The uterus also contains the amniotic fluid and placenta. The fetus is surrounded by amniotic fluid which allows physically cushions and free movement to the fetus. Approximately 98-99% of amniotic fluid is water (Fried, 1978).

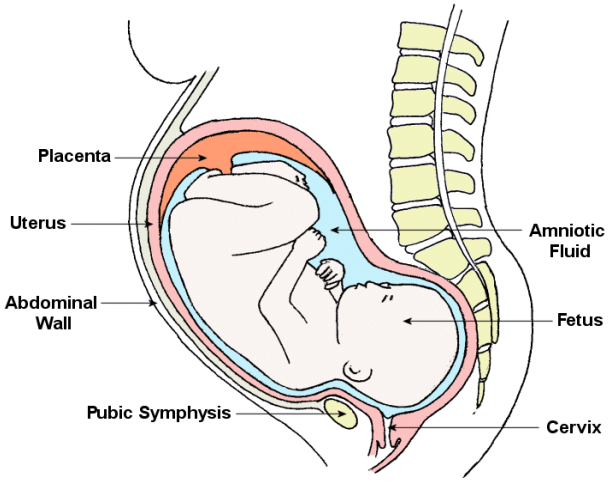

Figure 3.1 Anatomy of the pregnant abdomen (Acar and Lopik, 2009)

The placenta is essentially a large vascular fetal organ and represents the link between the developing fetus and the mother. It covers around a quarter of the inner surface of the uterus. In generally, it is located at the fundus (top) of the uterus in around 80% of pregnancies (Pepperell *et al.*, 1977 cited in Acar and Lopik, 2009). The placenta has its final thickness and shape after 16 weeks of pregnancy. However, growth of placenta continues by the meaning of circumferential enlargements throughout second and third trimester (Chervenak and Kurjak, 2003). The placenta has a discoidal circular shape. The placenta attaches to the internal surface of the uterus and connects the fetus to the mother. This interface is named uteroplacental interface (UPI). The uteroplacental interface is thought to be weaker than either the uterine or placental tissue.

3.3 Anthropometry of Seated Pregnant Occupant

A series of physical changes effect pregnant women safety. During pregnancy several changes occur such as at the abdominal region and throughout the body (Acar and Weekes, 2005). In order to fit and position to the seat belt properly during pregnancy, changes in the hip, abdomen and chest regions are particularly important (Acar and Weekes, 2005). The analysis of the anthropometry of pregnant women throughout the entire body, specifically for the car manufacturing industry, is presented by Acar and Weekes (2006). Weight, stature, trunk region, head and shoulders regions and limbs are classified in this study (Figure 3.2).

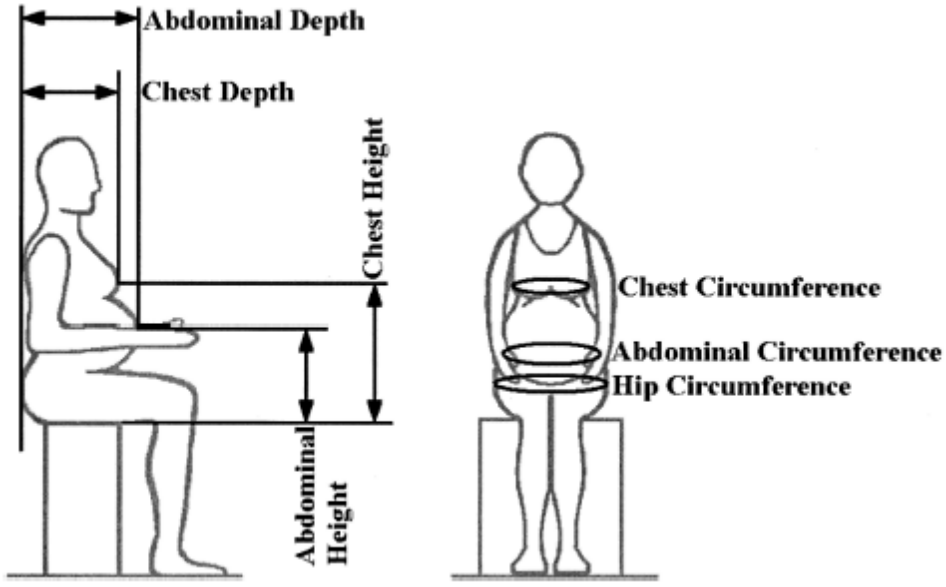

Figure 3.2 Anthropomorphic measurements recorded from pregnant women with particular relevance to safety aspects of vehicle travel (Acar and Weekes, 2005)

Culver and Viano, (1990) developed an anthropomorphic description using ellipses for the abdominal region of women at three, six, and nine months of pregnancy. The data were developed for women of 5th, 50th, and 95th percentile size. However, ellipses were produced scaling based on stature and the assumption that the abdominal size was proportional to stature. The correct position of the seat belt for pregnant women is defined by the NHTSA (2002), DfT (2003), 'Think road safety' (2013) guidelines and Acar and Weekes (2013), which briefly states that "The

lap belt should go across the hips, fitting comfortably under the bump, while the diagonal strap should be placed between the breasts and around the bump." (Figure 3.3).

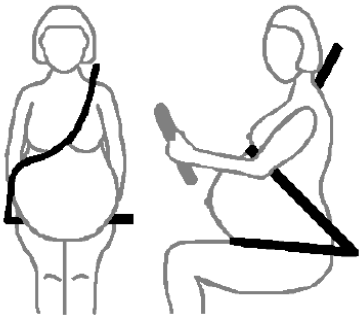

Figure 3.3 Correct seat belt position during pregnancy as advised by DfT and NHTSA (Acar *et al.*, 2004)

During pregnancy, the most obvious area of change is the abdomen. The mean abdominal depth is 359.5 mm for pregnant women measured in the third trimester (DTI, 1998). The fetus does not have a major effect on abdominal shape prior to the trimester of pregnancy. However, after this period, the fetus does have significant effect on abdominal size and causes to close to steering wheel (Figure 3.4) (Culver and Viano, 1990). Acar and Weekes (2005) found that 11% of pregnant occupants were seated with less than 2.5 cm between the abdomen and the steering wheel. Closeness to the steering wheel may cause fetus injuries and fatalities.

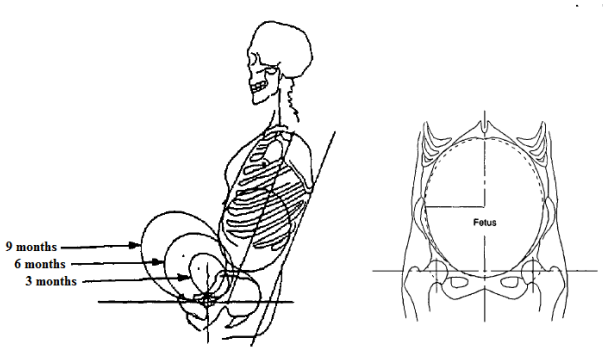

Figure 3.4 Lateral view of 5th percentile female seated women with 3-, 6-, and 9-month fetal ellipses, and frontal view of fetal ellipse at term (adopted from Culver and Viano, 1990)

The hips and breasts are two other main areas of change during pregnancy. For the women measured in the third trimester the mean standing hip circumference is 1155.1 mm, and the mean standing chest circumference is 1046.5 mm. These are 118.1 mm and 38.7 mm larger respectively than for non-pregnant women's anthropomorphic data (DTI, 1998). Acar and Lopik, (2009) stated that for pregnant women in the third trimester, it is important to use anthropomorphic data measurements taken from the seated posture in designs. The chest and abdominal sizes are also greater in seated position than in standing.

3.4 Injuries Unique to Pregnant Occupants in Vehicle Crashes

In the case of an crash impact, the risks to the fetus have been explained in medical studies as being; uterine injury (Pearlman 1990), placental abruption (Pepperell *et al.*, 1977; Bunai *et al.*, 2000), maternal death (Crosby and Costille, 1971), direct fetal injury (Agran *et al.*, 1987), fetomaternal transfusion (Goodwin and Breen, 1990), and preterm delivery (Pearlman *et al.*, 1996; Hammond and Edmonds 1990). It has been estimated that placental abruption accounts for around 50 to 70% of all fetal deaths in motor vehicle accidents (Pearlman *et al.*, 1990). Even relatively minor deformation forces can shear a placenta from the uterus (Pearlman *et al.*, 1990). Placental abruption is where the placenta becomes partially or completely detached from the inner surface of the uterus due to failure of the uteroplacental interface. It is thought that, due to the different material properties between the uterus and placenta, large deformation of the uterus creates a shearing effect at the UPI (Uteroplacental Interface) and leads to separation of the uterus and placenta. The potential for large deformation of the uterus during an automobile impact is high due to the likelihood of impact with the steering wheel or direct loading from the vehicle safety systems such as the seat belt of airbag. It is also possible that inertial effects during an acceleration impact could cause the fetus to strike the placenta causing large strains that could lead to placental separation. Quasi-static testing of uterus-placenta tissue samples has found that the UPI fails when a strain of around 0.6 is reached in the uterus (Rupp *et al.*, 2001).

Direct fetal injuries are less common, occurring in less than 10% of automobile crashes involving pregnant occupants (Klinich *et al.*, 1999a). The fetus sometimes sustains injury from direct loading of the abdomen as the protective cavity of the pregnant occupant abdominal-pelvic region is compromised by pelvic fracture or uterine rupture. It is also hypothesized that the most frequently injured fetal body region is the head, because it is the largest part of the fetus body. It is also thought that skull fracture most often occurs (Klinich *et al.*, 1999a).

Klinich et al., (1999) provided information on 120 automotive crashes involving pregnant occupants. Of the 120 cases, nine involve both maternal and fetal death. The fetus did not survive in 74 cases. The distribution of crash types of pregnant women was reported. While the majority of crashes were frontal impacts (61%, n=74), side impacts were 25%, (n=30). Rollover crashes were only 3%. Pregnant occupant was a driver at 55%, n=66 of all crashes. The distribution of restraint use of the pregnant occupants were reported. Approximately half of pregnant occupants (49%, n=59) were unrestrained. However, the cases date back to the 1960's. In this investigation, the most frequent outcome is placenta injury only and none of the fetuses in these cases survived. 69 cases involved some injury to the placenta or the placenta/uterine interface. Of these 69 cases, most of the impacts were frontal (n=46), 12 were side impacts, 3 were rollovers, 2 each were rear or multiple impacts and 4 impact types were not reported.

Klinich et al., (1999) reported in their investigation the majority of cases with placental abruption, the pregnant occupant was unrestrained (n=48 out of 69). Only one pregnant occupant sustaining a placental abruption was restrained by both a 3-point belt and a deploying frontal airbag. Cases with positive outcomes have the highest percentage of 3-point belt use and 3-point belt plus airbag use.

Weiss et al., (2011) did investigation on motor vehicle crashes during pregnancy. Motor vehicle police crash reports were linked to four years of birth and fetal death data. 5929 registered births and fetal deaths from 2002-2004 linking to a female driver crash report. Collision angles were mostly either frontal 35% or a rear-end collision 34%. Rollover occurred in 2.6%. The mean travel speed upon impact was reported as 27.5 miles per hour. Police reported 10% unrestrained and 16.6%

unknown belt use status. Airbags were reported by the police to have deployed in 17.1% of all crashes.

3.5 Pregnant Occupant Modelling

3.5.1 1st Generation Pregnancy Insert

In terms of crash test dummies, two pregnancy inserts are improved for use with the Hybrid III 5th percentile (height and weight) female dummy (First Technology, Farminghton, MI). The dummy represents the adult female population based on USA anthropometry studies. The biomechanical impact responses are derived from scaling functions applied to the Hybrid III 50th dummy. Originally developed in 1988. In 1996, the 1st generation pregnancy insert was placed in the pelvic region of the Hybrid III 5th percentile female dummy to represent uterus at 28 weeks (Pearlman and Viano, 1996) (Figure 3.5). The insert was composed of vinyl covered foam casting, with a silicone gel representing the amniotic fluid. In order to determine abdominal geometry, it was assumed that abdominal dimensions are proportional to maternal stature and weight. The fetus was a 50th percentile 28-week-size and composed of a separate head, neck, thorax and abdomen, and four extremities. Although placental abruption is one of the most common injuries seen in pregnant women (Pearlman, 1997), there was no placenta in this anthropomorphic test device. The fetus was instrumented with two triaxial accelerometers within the fetal head and thorax. The Hybrid III female, lap and shoulder belt were also instrumented to measure responses over range of crash severity and restraint placement. In addition, a force transducer (reaction plate) was placed behind the uterus to measure the loads transmitted through the uterus. HIC, force on abdomen, belt loads, fetal head and torso measurements were taken. However, although acceleration of the fetal component and forces transmitted through the abdomen could be measured, the relationships between these measures and the likelihood of fetal injury and loss were unknown.

Experimental tests included proper and improper belt placement, unbelted, airbags deployed with driver in normal or out of position for all at different speeds or

stationary. It was concluded that placing the seat belt over the uterus, increases force transmissions as much as four times. Therefore, Pearlman and Viano (1996) suggested that pregnant women should wear seat belts properly to reduce risk of directing loads onto the uterus. Physical crash tests also showed that while airbag deployment distributes loads and increases safety at higher speeds, the risk of detachment of placenta increase at lower speeds due to direct impact on the uterus (Pearlman *et al.,* 1996). It was also assumed that out of position condition would increase HIC. The experimental tests and the Hybrid III pregnant dummy had a number of limitations and lack of data. Real world data on pregnancy complications during accidents was not only limited but also based on animal experiments. Figure 3.5 illustrated 1st generation Hybrid III pregnant dummy.

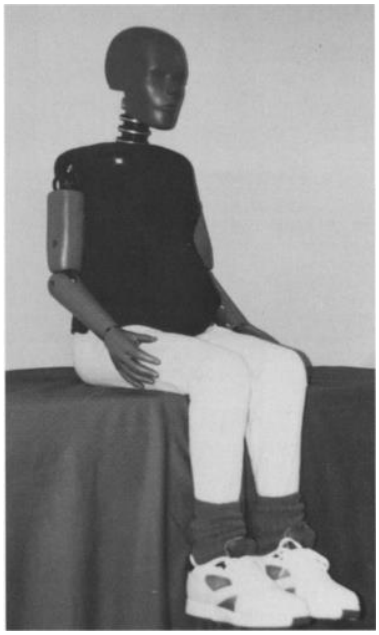

Figure 3.5 Urethane pregnancy insert and chest skin for the 5th percentile pregnant Hybrid III dummy (Pearlman *et al.,* 1996)

3.5.2 MAMA2B, 2nd Generation Pregnancy Insert

The second generation insert, or the 'MAMA2B', was developed in response to the limitations of the first generation pregnancy insert (Figure 3.6) (Rupp *et al.,* 2001). It was also based on the Hybrid III 5th percentile female dummy. The dummy represents the smallest segment of the adult USA population and derived from scaled

data from the Hybrid III 50th dummy. Originally developed in 1988, and was upgraded in 1991 and 1997. The MAMA2B consists of a water filled bladder to represent 30 weeks pregnant uterus, and neoprene 'skin' jacket (Figure 3.6). Its size, shape and force-deflection responses were more realistic. The water-filled silicon/rubber bladder for uterine insert provides internal pressure measurement to assess for the likelihood of fetal loss and the effectiveness of restraint systems. The geometry of pregnant abdomen was estimated by scaling abdominal depth measurements from 5th percentile Japanese pregnant women to their 5th percentile American counterparts assuming that abdominal dimensions are proportional to maternal stature and weight (Culver and Viano, 1990).

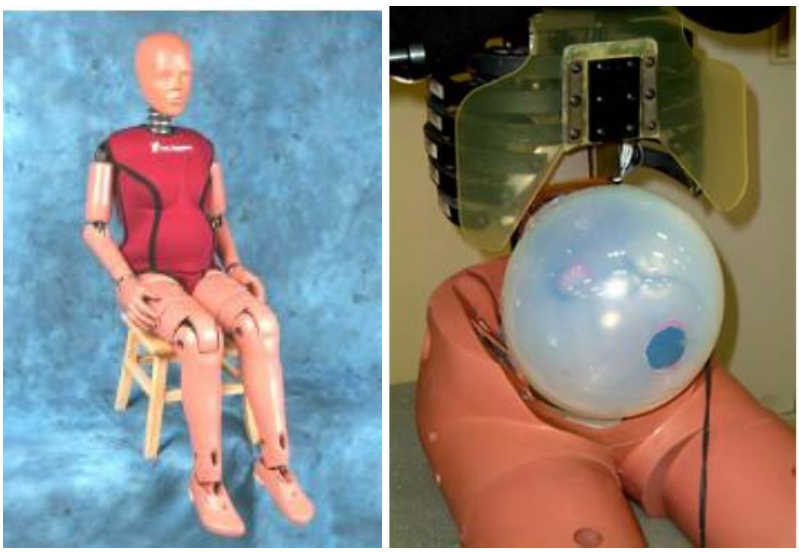

Figure 3.6 MAMA2B 5th percentile dummy and water filled silicon rubber bladder to represent uterus (FTSS, 2012; Motozawa *et al.*, 2009)

No placenta and fetus were included in the ATD. The Hybrid III lumbar load cell and chest deflection instruments removed and pelvis modified as with the first pregnant dummy. Pregnant abdomen was inserted in the 5th percentile female Hybrid III with minimal modifications to standard dummy components and with no significant changes in any of the non-abdominal response characteristics. In order to define geometry of the pregnant abdomen, Klinich *et al.,* collected anthropomorphic data of twenty-two pregnant women (Klinich *et al.*, 1999b). With very limited

pregnant women data, their research indicated that size and shape of the pregnant abdomen are relatively independent of maternal stature. In terms of pregnant women anatomy, there has been a lack of anthropomorphic data measured from pregnant women. In order not to redesign of the ribs and sternum of the small female Hybrid III, thirty weeks abdominal was selected as the largest abdominal component.

In order to develop and validate the MAMA2B, cadaveric abdominal response corridors were used. Force-deflection response of MAMA2B abdomen with and without the chest jacket, to belt loading compared to scaled belt loading corridors. It was found that the effect of the chest jacket on the belt loading response was small but the reason was not explained. Rupp *et al.* was also assumed that the response of the pregnant abdomen is the same as that of a cadaver of identical mass, and that pregnant and non-pregnant abdomens are geometrically similar (Klinich *et al.,* 1999b). However, dynamic response of the pregnant abdomen is different from that of the non-pregnant abdomen.

The abdominal insert was designed to predict the occurrence of placental abruption in motor vehicle accidents. However, water filled silicon rubber bladder does not assist to understand placental abruption. Rupp *et al.* investigated two hypothesized mechanisms of UPI (uteroplacental interface) failure using computer modelling and engineering principles (Rupp *et al.,* 2001) (Figure 3.7). These were:

1. Shear strains in the UPI caused by changes in the curvature of the uterus due to direct loading of the abdomen.

2. Tensile strain at the UPI from the pressure gradients generated by the inertia of the amniotic fluid

Considering these two hypothesized mechanisms for placental abruption, negative pressure in the posterior of the fluid-filled MAMA2B abdomen and deformation of the midline contour of the bladder were measured (Rupp *et al.,* 2001).

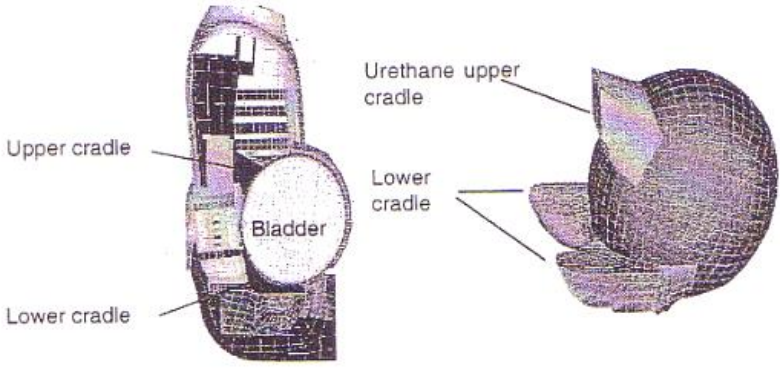

Figure 3.7 Finite element model of prototype uterus bladder installed dummy, showing urethane attachments (Rupp *et al.*, 2001)

In order to confidently assess vehicle and restraint system performance with reducing the likelihood of fetal injury outcome in vehicle accidents, additional instrumentation development and more detailed tests are necessary. MAMA2B was focused on only one type of injury without a fetus. However, results from this work suggest that the addition of a frontal airbag offers further protection to the pregnant occupant.

3.5.3 Working Model 2D Model

A number of computational human body models were developed in the late 1990s. However, there was no any computational pregnant women model. In order to investigate the movement of the fetus within the uterus during road accident, a simple kinematic Working Model 2D model of a pregnant occupant was developed by Thackray and Blackketter (2002) (Figure 3.8). Two multibody systems were used to represent the pregnant woman and the fetus. The geometry of the pregnant women and the fetus were based on approximations of the actual pregnant anthropometry. The model was validated by comparing output torso acceleration values with experimental data from sled test with Hybrid II dummy. Amniotic fluid was not included in the model. The fetus was simulated with four rigid bodies including the head, body, arms and legs interconnected with pin joints, which is then restrained within a rigid cavity representing uterus.

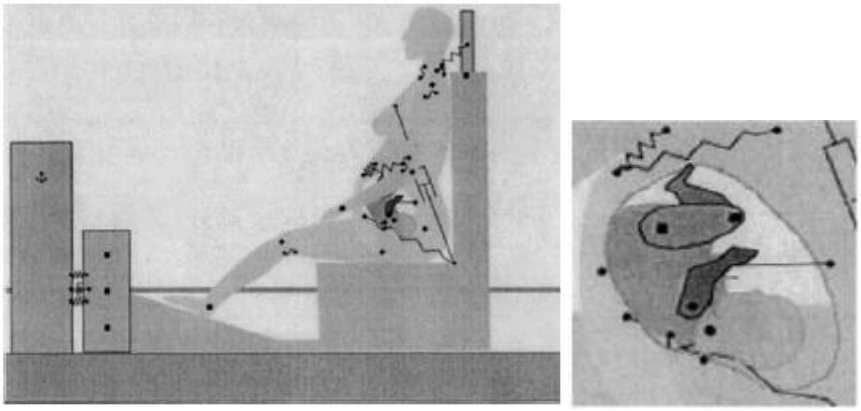

Figure 3.8 Working Model 2D model of the pregnant occupant and the fetus (Thackray and Blackketter, 2002)

With the Working Model 2D pregnant model, evaluating seat belt safety for the fetus was performed. It was found from simulations that fetal acceleration was nearly 3 times higher than pregnant occupant acceleration. This result shows the existing fetus in the pregnant abdomen may play important role on fetus injuries and fatalities. It was also concluded that there is significant comfort problems with current seat belts for the pregnant women and their fetuses.

3.5.4 'Linda', Finite Element Pregnant Dummy Model

In 2002, finite element model of a pregnant crash test dummy was created by Volvo (2002) (Figure 3.9).The model is called as Linda and as a computer model; it is a combination of a real human body and a Hybrid III (FTSS) crash test dummy. Since no technical papers about this pregnant woman finite element model have been released, it is difficult to comment about accuracy of the model; however a small amount of information has been given in press releases (Volvo, 2004). Her abdomen, pelvic bones, gravid uterus, placenta, amniotic fluid and a 36 week-old fetus represents pregnant women and their fetuses.

The rest of the model is same to physical Hybrid III crash test dummy, modelled of synthetic and steel materials. The fetus was represented as a lump body

without extremities. Crash simulations with this model have been performed to study effectiveness of seat belt and airbag on the uterus, placenta and fetus. It is stated that wearing seat belt is the best way of protection for pregnant women and their fetuses. It is also stated that the model has given promising results to simulate frontal impact crash tests. With scaling techniques, the model can represent different sized women. However, it is limited with physical Hybrid III dummy anatomy and material properties, whereas human body anatomy and tissue characteristics are completely different.

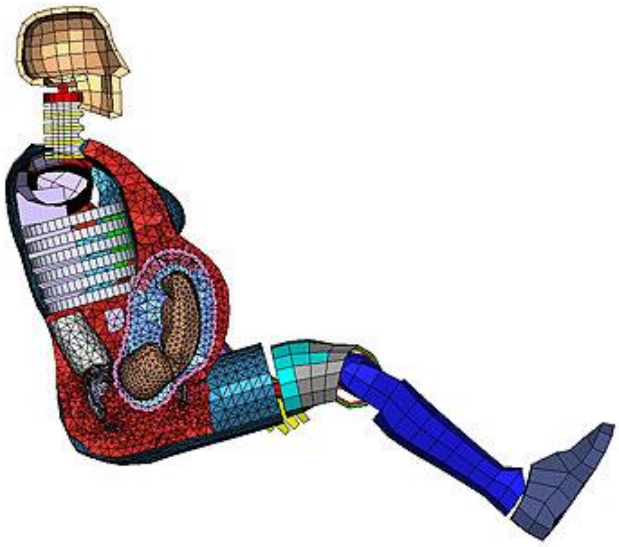

Figure 3.9 Linda', 5th percentile Hybrid III dummy finite element pregnant women (Volvo, 2002)

3.5.5 FE and Multibody Model of the Pregnant Occupant

Moorcroft *et al.,* (2003) have developed a computational pregnant occupant model with using dynamic modelling software MADYMO (Figure 3.10). An existing 5th percentile female facet occupant model was combined with a finite element model of a 7 month pregnant uterus that represents 30th week of gestation. The human model is a 5th percentile female (152 cm tall and 50 kg). For the small female a very short and very slim model was selected in RAMSIS. The Western European population aged 18 to 70 years of 1984 was used. The dummy model was upgraded in 1997. The model has been used to investigate injury mechanisms in unrestrained, 3-point belt

and 3-point belt with airbag crash tests in various crash speeds ranging from 13 km/h to 55 km/h. The vertical position of the lap portion of the seat belt was also varied over three predetermined configurations. However, no fetus was included in the pregnant occupant model was based on the findings of Rupp *et al.* in their design and development of the pregnant abdomen for the Hybrid III small female crash test dummy. According to Rupp *et al.*, the mechanism of injury that ultimately leads to fetal loss is independent of the fetus itself (Rupp *et al.*, 2001).

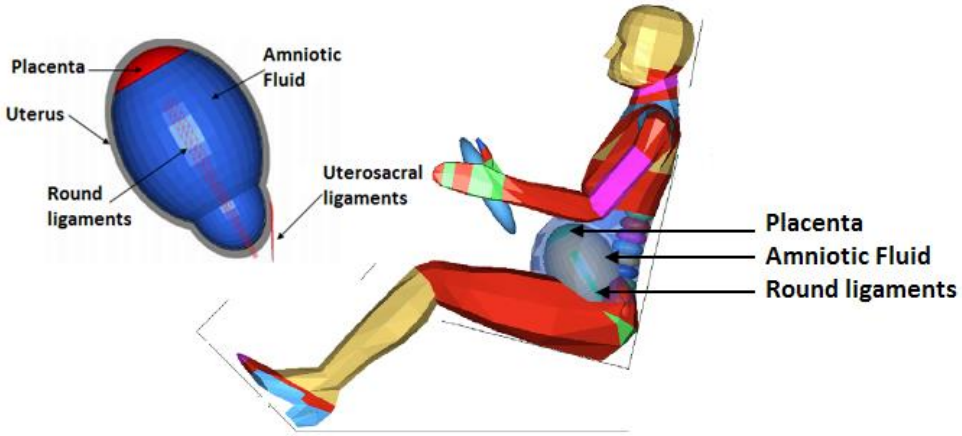

Figure 3.10 Multibody female model with finite element pregnant abdomen developed by Moorcroft *et al.* (2003)

The existing MADYMO 5th percentile female model weights 110 lbs with the body mass distributed over the rigid bodies of the model. The weight of the pregnant occupant model is stated 135 lbs, but there is no information about how this extra weight is distributed to the model. The abdominal contour of the pregnant occupant model was made to closely match the MAMA2B, second generation pregnancy insert for the 5th percentile female Hybrid III crash dummy. When the FE uterus model is placed in the abdomen, flexible bodies of the abdomen of the standard model have been disabled. It is also not clear how the interaction of the uterus with the spine is modelled.

Several assumptions have been made in order to model the finite element uterine. The uterus, placenta, and amniotic fluid were assumed to be linear, elastic,

isotropic solid. However, the uterus is known to be anisotropic and viscoelastic, but there is not currently enough data to apply these material properties to the model (Moorcroft *et al.,* 2003).

3.5.6 HUMOS to Pregnant Woman Model

In order to improve safety of the pregnant woman and her fetus, Delotte *et al.* (2006) developed a computational model of the human body with uterus from HUMOS model (Figure 3.11). The anthropometry of the HUMOS model was chosen as close as possible to the anthropometry of the 50th European adult male driver. A frozen cadaver was sliced physically. Main characteristics of the HUMOS subject are sitting height (920 mm), standing height (1730 mm) and weight (80 kg). The sitting height was considered as one of the most important factor for securing the choice of the subject. The geometries of the third-trimester uterus and the fetus were obtained from MRI data of pregnant woman. The 3D construction was created and meshed using the HyperMesh commercial software. This pregnant uterus was integrated in the HUMOS model (Serre *et al.,* 2002) which was a computational 3D model of a male whole human body in driving position.

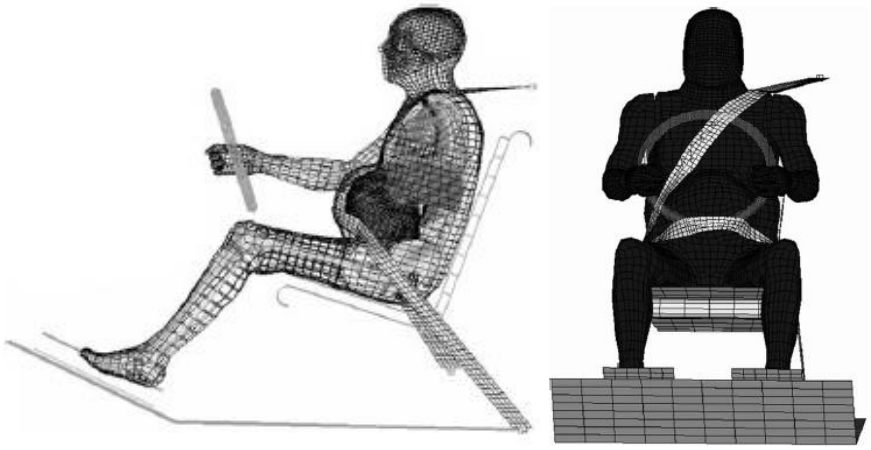

Figure 3.11Side and frontal view of the uterus model inserted in HUMOS (Delotte *et al.*, 2006)

In order to insert the uterus model, geometry and anatomy of the HUMOS model was modified. The abdominal wall was removed and replaced by the one of

the pregnant woman. Relations of internal organs were also changed. The pregnant uterus thickness was determined with slices of the MRI analysis from male cadaver. However, male and female pelvises are different. Very specific and only one pregnant woman geometry was designed. Female version of the HUMOS needs to be developed to obtain better final outcome of the model.

3.5.7 Scaling to 50th percentile female

The geometry of the HUMOS 50th percentile male model was scaled to the anatomy of a 50th percentile female (162 cm, 62 kg) by Peres *et al.*, (2011) with particular focus on the anatomy of the pelvis. The Humos model is a complete human body model resulting from a seated 50th percentile European male human body and was obtained from a frozen cadaver in driving position. HUMOS model is translated from FE software to LS-DYNA. Due to the direct contact with the uterus, anatomy of pelvis is considered as reference subject during scaling process. Anatomy of a 7 months uterus and fetus are represented with scaling method from MRI images. Therefore, the fetus has simplified geometry and its upper and lower extremities do not exist (Figure 3.12).

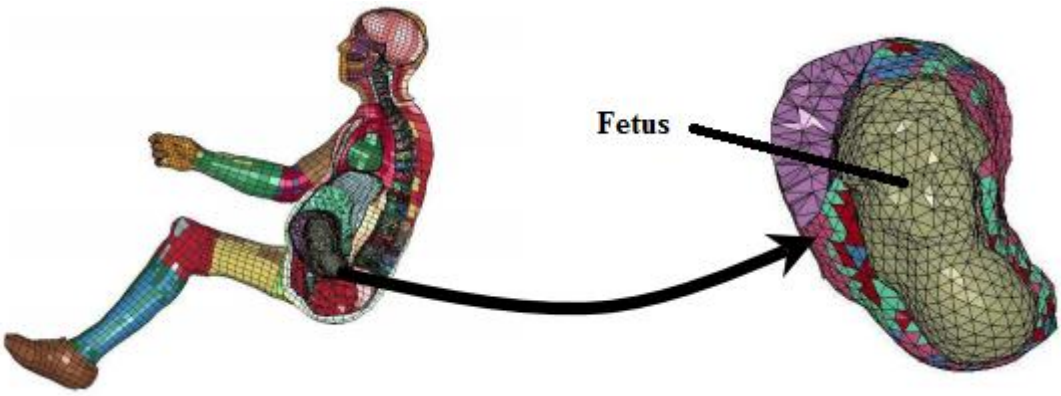

Figure 3.12 Scaled 50th percentile woman model and uterus detail (Peres *et al.*, 2011)

During the scaling process, anatomical target points were defined into a 50th percentile woman (Figure 3.13). The authors decided not to account for the anisotropic behaviour for the material model of the uterus. The fetus was modelled

uniform isotropic part with a material stiffness midrange between bones and soft tissues.

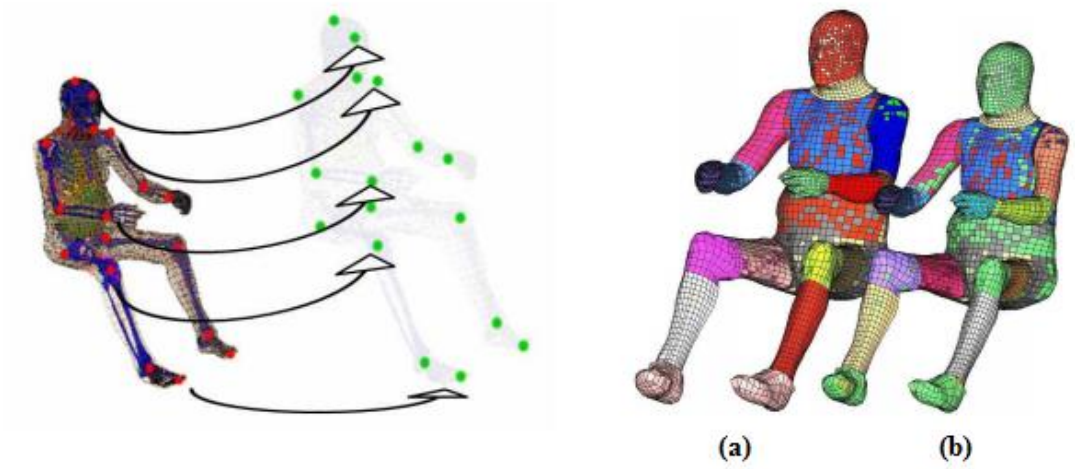

Figure 3.13 Scaling the HUMOS model into a 50th percentile woman, (a) 50th percentile male and (b) 50th percentile woman (Peres *et al.*, 2011)

A limitation of the method was that scaling based on some points was used to produce 50th percentile female which does not represent pregnant women. The HUMOS model was partially validated against post mortem human subject experimental tests. Artificial silicone uterus was inserted into a woman body. In this study, low impact speed (20 km/h) was used to validate the model.

3.5.8 'Expecting' Computational Pregnant Occupant Model

3.5.8.1 Introduction

During pregnancy women experiences a wide range of physical changes in size and shape. These changes may adversely affect the comfort and safety of pregnant women while driving. It was found that 99% of pregnant women experience some difficulty or problem with car travel (Acar and Weekes, 2003). A pregnancy and driving questionnaire is used to investigate how UK women's experiences of driving and using passive safety systems such as seat belt, airbags, and head restraints (Acar and Weekes, 2004). Over 100 sets of data have been collected spanning a wide range

of statures of women at different stages throughout pregnancy. Acar and Weekes (2005) presented analysis of comprehensive set of 48 anthropomorphic measurements of pregnant women body and created the Pregnant Women's Anthropometry Website (Pregnant driver, 2004) for automotive designers and engineers. They have stated that pregnant occupant should be considered as a separate user group to meet their specific needs.

3.5.8.2 Biomechanics of 'Expecting'

Previous pregnant occupant models have only focused on the abdominal region by inserting an expanded abdomen to an existing male and some female models. The anthropomorphic measurements from pregnant women based on MADYMO 5th occupant model are used to develop a parametric model of the pregnant female occupant which is called 'Expecting'. The model presented describes the changes throughout the entire body hence providing a more comprehensive depiction of the altered pregnant form.

The computational model of a realistic pregnant occupant with a fetus within uterus model could be used as a tool to predict the strains and stresses on the uterus and placenta (Figure 3.14) (Acar and Lopik, 2009, 2012). 38th week of pregnant woman is represented with a modified 5th percentile female. A multibody fetus and finite element uterus are integrated into an existing female model to incorporate pregnant female anthropometry.

3.5.8.3 MADYMO 5th percentile female facet occupant model

The MADYMO 5th percentile female facet occupant model is a multibody model with a complex surface representation. The anthropometry of the existing 5th percentile female facet MADYMO model were used from the Western European population aged 18 to 70 years of 1984. For the small female a very short and very slim model was selected in RAMSIS. The resulting body mass and sitting height were considered to be somewhat extreme also in comparison to the small female Hybrid III crash dummy A series of rigid bodies are defined representing the bony skeleton such as spine of the human body. Each rigid body is defined with mass,

centre of gravity position and moment of inertia. Rigid bodies are represented with ellipsoids. Each ellipsoid is positioned with respect to its parent rigid body relative to that body's local coordinate system. The positions of the kinematic joint centre represent actual joints in the human body and are positioned relative to the hip joint centre or 'H' point. Kinematic joints connect the rigid bodies. Spinal joints are represented with a single 'free' joint allowing relative movement in all directions with a 6 degree of freedom restraint. Rigid links are used to connect corresponding joint centres. The rigid bodies describing the upper and lower limbs are connected with spherical joints allowing movement in all rotational degrees of freedom (Acar and Lopik, 2012).

A series of cross sections that are positioned relative to their parent 'bone' linkage are used to construct the three-dimensional geometric surface of the model. Additional anthropomorphic data for 5th percentile UK females from the DTI's adult data handbook have been used to further define the 3D surface. The model has been developed in an upright standing position with arms horizontal, and out to the sides (Acar and Lopik, 2012).

Attached to the underlying multibody model is a complex surface representation of the 'skin'. This is actually an FE mesh comprising of about 1000 nodes resulting in around 2000 triangular elements. The skin is divided into 45 sections with the corresponding nodes of each section being attached relative to their closest rigid body. This FE mesh defined as a NULL material so no actual FE calculations are required; the nodal points are merely used to define contact with the environment and to transfer these contact forces to the multibody model. Local deformation of this skin surface is not possible i.e. any given node will always remain at fixed position relative to its parent rigid body. However, for the thorax and abdomen, where local deformation of the skin with respect to the spine is essential, deformable elements are defined.

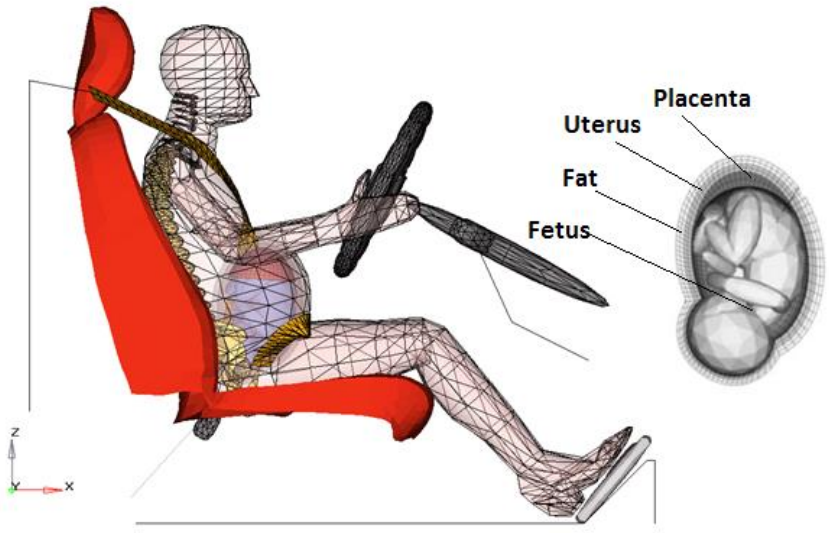

Figure 3.14 'Expecting', pregnant occupant and the multibody fetus within the finite element uterus (Acar and Lopik, 2009)

3.5.8.4 Finite Element Uterus Model

The finite element uterus model was developed in conjunction with the multibody fetus model. Geometry of the uterus model was determined with the fetal dimensions and configuration based on data reported in Acar and Weekes, (2006), (Acar and Lopik 2012) (Figure 3.15). The finite element placenta and uterus were meshed using HyperMesh (Altair) by first meshing the inner surface of the uterus using quad elements then mapping the elements to the outer surface to create the uterus, and mapping the corresponding elements of the placental outer surface to the inner surface of the placenta to create the placental elements. The element configurations and nodal coordinates were then exported into MADYMO where 8-noded solid elements were used for both FE components (Acar and Lopik, 2009) (Table 3.1).

Table 3.1 Element types used for 'Expecting'

Structure	Element Type	Number of Elements	Number of Nodes
Uterus	8-noded Brick	3388	5089
Placenta	8-noded Brick	884	1393
Fat	8-noded Brick	3388	5089

The material properties of the uterus and placenta are based on uterus and placental tissue tests and on decisions made by other researchers. The uterus has a Young's modulus of 566 kPa, poisons ratio of 0.4 and a density of 1052 kg/m^3. The placenta has a Young's modulus of 63 kPa, Poisson's ratio of 0.45 and a density of 995 kg/m^3. The total mass of the placenta and uterus is 1.29 kg (Table 3.2).

Table 3.2 Material properties used in the 'Expecting' pregnant model

Structure	Material Model	Density (kg/m^3)	Young's Modulus (kPa)	Poisson's Ratio	Thickness (mm)
Uterus	Linear Elastic	1052	566	0.4	10~
Placenta		995	63	0.45	20*
Fat		993	47	0.49	10~

~ The thickness is almost uniform all around the uterus and fat tissues

* The thickness of the placenta at its thickest cross-section, i.e. in the middle.

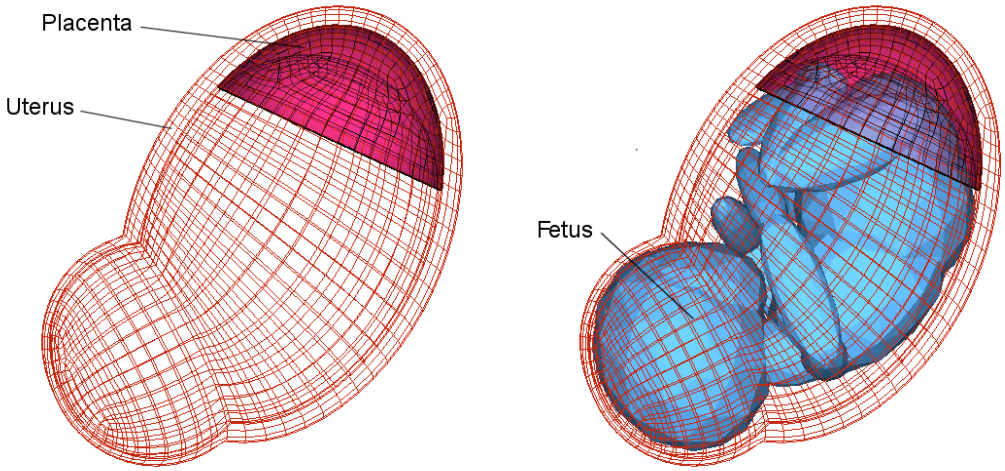

Figure 3.15 Side views of the FE uterus and placenta with and without the multibody fetus in position (Acar and Lopik, 2009)

3.5.8.5 Pregnant Occupant Model

The finite element uterus and the multibody fetus were integrated into an existing multibody female model to complete the computational pregnant women model. The

facet occupant model available within the MADYMO library represents a 5th percentile female, 1.52m in height and 49.8 kg in weight.

In 'Expecting', the cushion effect of amniotic fluid is created with defining springs and dampers between pelvis of female and pelvis of the fetus. The fetus damping characteristic has been defined with MADYMO codes with restraint cardan element. Cardan restraint consists of three torsional parallel springs and dampers that connect two bodies. The torques depends on the cardan angles that describe the relative orientation of the corresponding restraint coordinate systems. Point restraint, three mutually perpendicular springs and dampers that connects two bodies, has been also added to model the frontal and lateral stiffness and damping of the flexible bodies.

3.5.8.6 Validation

Numerous tests have been conducted to determine the response of the human abdomen to impact loading. Generally, physical or computational models of the human body are validated against experimental tests on soft tissues, isolated anatomical segments, whole cadavers or live human volunteers. The 5th percentile female facet occupant model used in the development of the pregnant occupant model has been previously validated against impactor tests and small female PMHS tests (MADYMO Human Models Manual, 2005). Accurate response of the pregnant abdomen is important to be able to predict risk of fetus fatalities for the pregnant occupant model.

Rigid-bar impact and belt loading tests performed by Hardy *et al.,* (2001) are used to validate the pregnant occupant model, 'Expecting'. In order to investigate difference in force-deflection response among previous test data, Hardy *et al.,* (2001) performed rigid bar impact tests into nine 50th percentile male cadavers and created new force-deflection abdominal corridors. The nine tests involved nine cadavers with an average age, stature, and mass of 78 kg, 170 cm, and 68 years old, respectively. As the reference mass, the mass of a Hybrid III 50th percentile male dummy were used. These corridors were scaled to a 5^{th} percentile female by Rupp *et al.,* (2001) in their development and validation of the MAMA2B ATD. These corridors have been

used to validate the response of the computational pregnant occupant model. Prior to the General Motor sponsored projects, the only information on pregnant anthropometry in the literature was contours that were estimated by scaling abdominal depth measurements from 5th percentile Japanese pregnant women to their larger 5th percentile American counterparts assuming that abdominal dimensions are proportional to maternal stature and weight (Culver and Viano, 1990). The anthropometry for the new pregnant abdomen was based on data collected from seated US pregnant occupants.

Nine rigid-bar impacts into nine pressurized cadavers using a 48 kg ballistic pendulum were applied. The impactor was a 2.54 cm diameter, 45.7 cm long rod. The effect of impact location was studied with impacting both mid-and-lower abdomens. The rigid-bar force deflection responses measured by Hardy et al., at 6 m/s (21.6 km/h) and 10 m/s (36 km/h) was constructed and impacted into the abdominal region of the model. 'Expecting' was validated using 6 m/s (21.6 km/h) rigid bar impact loading and force-displacement response of the model is calculated.

Hardy *et al.*, (2001) also performed several seat belt loading tests on human cadavers. The belt was positioned at mid-abdominal region and curved around abdomen. The belt was fastened to a driving mechanism (ram) behind the cadaver. The ram was used to pull the webbing into the cadaver abdomens from behind. Peak loading rate of approximately 3 m/s (10.8 km/h) was provided with the design. Penetration of the belt into the abdomen was calculated from the difference between the motion of the seat belt and the displacement of the spine. Finite element belt was curved around the pregnant abdomen at mid-abdomen level and was pulled across the pregnant abdomen at 3m/s (10.8 km/h). The force-displacement response of the model to the 3m/s (10.8 km/h) belt-loading case is shown in Figure 3.16 plotted against the response corridor.

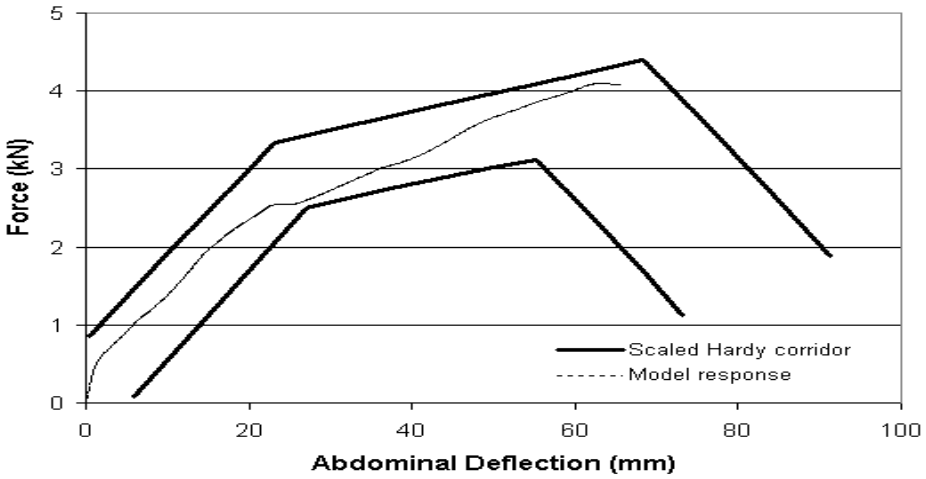

Figure 3.16 Abdominal response of the pregnant abdomen model to 3m/s (10.8 km/h) belt loading compared against the response corridor (Hardy *et al.*, 2001)

3.5.8.7 Around 'Expecting'

The 'Expecting' is placed within a typical vehicle interior consisting of a seat, vehicle floor, pedals, and steering wheel, as shown in Figure 3.17.

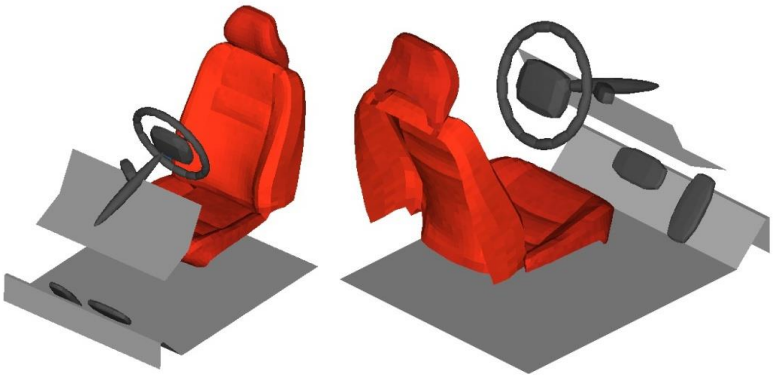

Figure 3.17 Vehicle interior for 'Expecting' model, isometric view

The seat height from floor is set at 270 mm. Seat pan angle is 10 to the horizontal. The horizontal distance from the H point (sagittal plane hip joint centre) to the ball of foot is 708 mm which defined the initial position of the vehicle pedals with respect to the seated occupant. The steering wheel tilt is 30 degree from vertical. No intrusion condition has been utilised between the occupant and restraint systems,

vehicle environment. The occupant compartment intrusion is not considered. Depending upon seating position and restraint condition of the occupant, intrusion may have beneficial, detrimental, neutral effects upon injury (Strother el a., 1984).

3.6 Conclusions

Although the road accidents are the leading cause of accidental fetal death, there are only a few researchers studying the impact of vehicle crashes on fetus fatalities. Most of the research performed on the development of physical and computational pregnant occupant modelling aim to provide enhanced safety of the pregnant occupant and her fetus in motor vehicle accidents. Furthermore, due to the lack of representation of complex shapes and sizes of pregnant occupants and their fetuses, most pregnant occupant models did not represent pregnant women realistically and had a number of significant omissions such as lack of a fetus in the uterus. The anatomy of pregnant women was not considered and a realistic fetus was not included in earlier models.

A pregnant occupant including a fetus is represented with the 'Expecting' computational model. In this thesis, 'Expecting' will be used in and further detailed.

CHAPTER 4

EFFECTIVENESS OF AIRBAG FIRING TIME

4.1 Introduction

Airbags are designed as inflatable restraint systems in automobiles and collectively they help decrease the severity of a vast amount of potential injuries during an impact. Airbag deployment initiates as the sensing system triggers the ignition of a gas generator following the onset of the collision. Generated inert gas inflates the airbag in approximately 20 to 30 milliseconds. When the occupant in the vehicle hits the airbag, the gas escapes from small vent holes in a controlled manner.

The objective of this chapter is to investigate the effects of airbag deployment time during full-frontal impacts and the interaction of the pregnant driver with the frontal driver airbag using 'Expecting', computational pregnant occupant model. This investigation involves simulations of crashes with varying impact severities for full-

frontal collisions with different airbag firing times. Strains and displacements in the uterus are calculated to predict the injury risk due to abdominal loadings.

4.2 Effect of Airbag in Vehicle Collisions

Real life crash data and laboratory crash tests illustrate that airbag technology helps decreasing the severity of a range of possible injuries (Huelke and Moore, 1993; Walter and James, 1996; D'Elia, 2012). For instance; steering wheel mounted frontal airbags facilitate enhanced driver protection in a number of different ways; by allowing for a more controlled deceleration of the head, by reducing and usually eliminating the head and facial contact with the steering wheel and other rigid vehicle interior elements, and by further distributing the inertial loads (Lau *et al.*, 1993; Richardson and O'Connell, 2000).

The inflation of an airbag under some circumstances also has the potential to cause serious injuries and even death at road accidents. Concerns have been raised for children, infants, elderly, pregnant, and short stature people (NHTSA, 1997). For instance, when the pregnancy develops, the fetus grows inside the pregnant abdomen and the uterus gets closer to the steering wheel. The proximity of the uterus to the deploying airbag creates an increased risk of fetal death. During the deployment, gas pressure in the cushion generates high forces on the occupant. In their case report, the possibility of an association between airbag deployment and traumas such as placental abruption, uterine rupture are investigated (Schultze *et al.,* 1998; Fusco *et al.,* 2001). Sims *et al.,* (1996) described three cases of minor injuries of pregnant occupants associated with airbag deployment. However, the authors of these studies suggest further research on the subject to determine effect of airbags on pregnant women safety. Metz and Abbott *et al.,* (2006) concluded that placental abruption does not appear to occur frequently in motor vehicle accidents with airbag deployment. The authors also revealed that it is unclear if fetal risk is higher than that without airbags.

At the time of airbag inflation, occupant position also plays an important role. Airbag induced injuries are caused when an occupant is in Out of position (OoP)

who sit relatively closer to the steering wheel (thus airbag) during collision (Richardson and O'Connell, 2000; Marklund and Nilsson, 2003; Richert *et al.*, 2007). 175 fatalities caused by airbags in the USA between 1990 and 2000 (NHTSA, 2008).

4.3 Airbag Working System

A typical airbag system consists of an airbag module containing an inflator and an airbag, a steering wheel connecting coil, collision sensors, a diagnostic monitoring unit, and an indicator lamp (Figure 4.1).

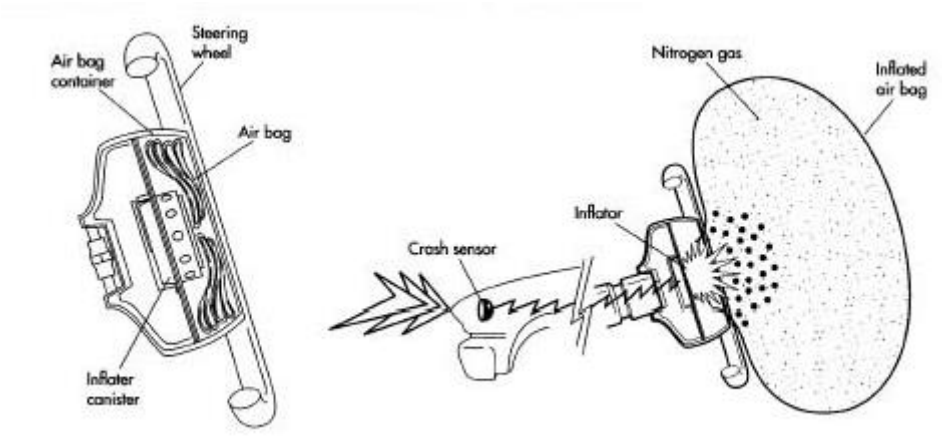

Figure 4.1 Airbag working system (Madehow, 2012)

There are a number of parameters which exist in an airbag including volume and shape of airbag, deployment timing, size of vents, material of airbag, and inflation system changes from one car manufacturer to another. Changing characteristics of airbag especially airbag deployment time plays an important role in occupant safety.

The time of deployment of an airbag system is usually programmed to occur within the first 60 milliseconds of the moment of impact and commonly referred to as *Time to Fire* (Walter and James, 1996; Mon, 2007; Miller and Allen, 2007; Welsh

et al., 2008) (Figure 4.2). In some airbag systems, the sensing system may be set to trigger at a different *TtF* depending on the severity of the collision, typically around 10-60 milliseconds (Mon, 2007). Airbag manufacturers and automotive companies consider *Time to Fire* as a confidential matter due to complexity of the airbag systems and impacts, and competitive advantages. If an airbag inflates too late or too early, airbag induced injuries on occupant increase. Therefore, the setting of airbag deployment time is crucial for occupant safety.

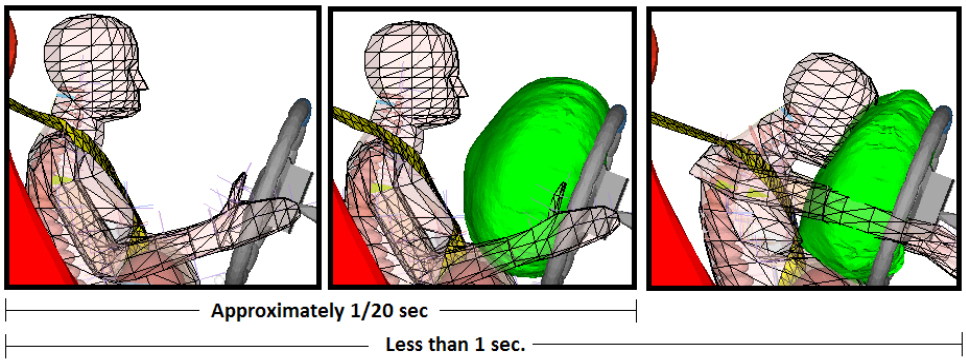

Figure 4.2 Deployment of an airbag and side view of the response of the 'Expecting' model

4.3.1 Airbag Model

In order to create realistic crash test simulations, designing of an accurate airbag model is very important. In MADYMO applications, finite element driver airbag model with Computational Fluid Dynamics (CFD) gas flow module is generated for in and out of position simulations (MADYMO Theory Manual, 2010) (Figure 4.3). 'Expecting' is based on the in position 5th percentile pregnant female driver, seated in an optimal seating position with the assumption of making a proper use of the seat belt (Acar and Lopik, 2009).

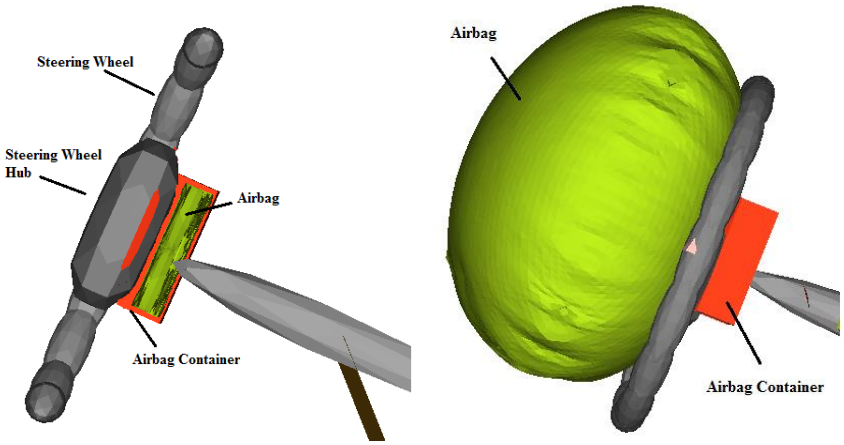

Figure 4.3 Steering wheel and driver airbag model (Acar and Lopik, 2009)

Figure 4.3 and Figure 4.4 illustrate a driver airbag model designed principally for occupants in position applications. The driver airbag is a two-dimensional European airbag model and when it is deployed it has a volume of 60 litres. Diameter of the airbag is 600 mm and totally symmetrical. When the airbag is fully deployed, crash test simulations requires a good level of accuracy at the moment of impact. Parameters such as deployment timing, final airbag volume and internal pressure are thus crucial to obtain a realistic model. Airbag model in crash test simulations with 'Expecting' is a driver airbag folded and placed in an open box at the bottom of which it is supported. The airbag is deployed from the centre of the supported part which is the centre of the steering wheel.

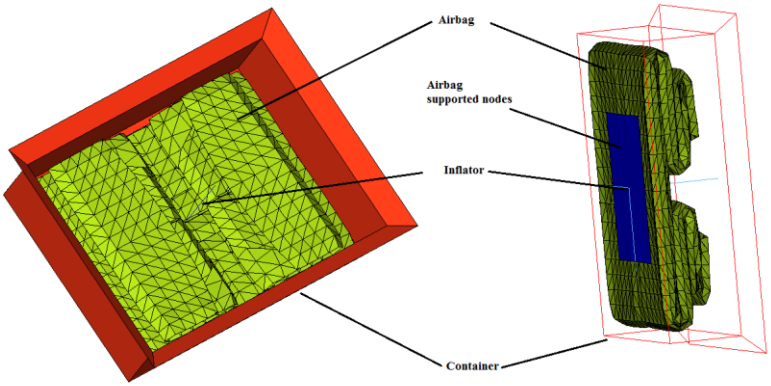

Figure 4.4 Driver airbag model in container (MADYMO Theory Manual, 2010)

The airbag model in MADYMO is meshed with linear triangular 3-node membrane (MEM3) elements, which do not possess hourglass modes and potentially describe the geometry of the components better (Figure 4.4). The element strains and stresses are calculated with the GREEN formulation in order to handle large deformations. Another reason to use GREEN formulation is its objective nature, meaning that the results do not depend on the node orientation within an element, which results in more accurate output. GREEN strain formulation utilises the left Green strain tensor and the 2nd Piola-Kirchhoff stress tensor, and is highly recommended for airbag modelling. In terms of material characteristics, the airbag is modelled with a linear orthotropic material (ORTHOLIN). It is assumed that the airbag fabric presents two orthogonal principal directions. The contact definitions in the airbag system are carried out in two major groups; the first one containing all the airbag elements and the second one all the box elements (MADYMO Applications Manual, 2010).

The driver airbag module incorporated into 'Expecting' is a uniform pressure mode single chamber unit with gas jet effect. *Uniform Pressure* mode is usually preferred in in-position analyses as it saves computation time compared to a *Gas Flow* calculation. The gas flowing in the airbag chamber is defined in terms of mass flow rate, temperature as a function of time, composition of the gas mixture and the location and dimensions of the orifice the gas is injected through. In this model, gas mainly flows out through vent holes. Outflow from the airbag through elements that are in contact is partially blocked with a value of 0.7, which means that there is only 30% of outflow through airbag elements making contact. The airbag inflator in the model supplies gas, mass flow rate and heat into the chamber (MADYMO Applications Manual, 2010).

4.3.2 Overview of the Crash Test Simulations

The computational pregnant occupant model 'Expecting', which incorporates the anthropomorphic and anatomical changes of pregnancy is used in this study to predict the optimum airbag firing times to minimise injuries to the fetus. Pregnant occupant constitute a vulnerable group in occupant safety in motor vehicles. Their

anatomies and dynamic characteristics are totally different than non-pregnant and any other occupants. Furthermore, experimental and analytical research show that an airbag unit designed to restrain a 50th percentile male occupant can be less effective on a person who is not classed as a 50th percentile male (Butler *et al.,* 1993).

Use of computational human and dummy models to investigate effectiveness of airbag restraint systems have been continually increasing. Computational human models have proved to be highly effective tools providing opportunities for cost and time-effective crash simulations and analysis, and related design processes.

A set of simulations were chosen to explore the effect of airbag and crash severity on the response of the pregnant occupant as a vehicle driver to a frontal impact. Thirty two simulations were conducted with crash speeds ranging from 15-30 km/h in 5 km/h steps. The acceleration pulse applied to the model was half-sine waves with 120 milliseconds duration. The crash pulses used for the 4 speeds simulated are shown in Figure 4.5. 'No restraint', 'seat belt and airbag', 'seat belt only', and 'airbag only' cases, which are simulated with airbag firing times range from 10, 30, and 60 ms.

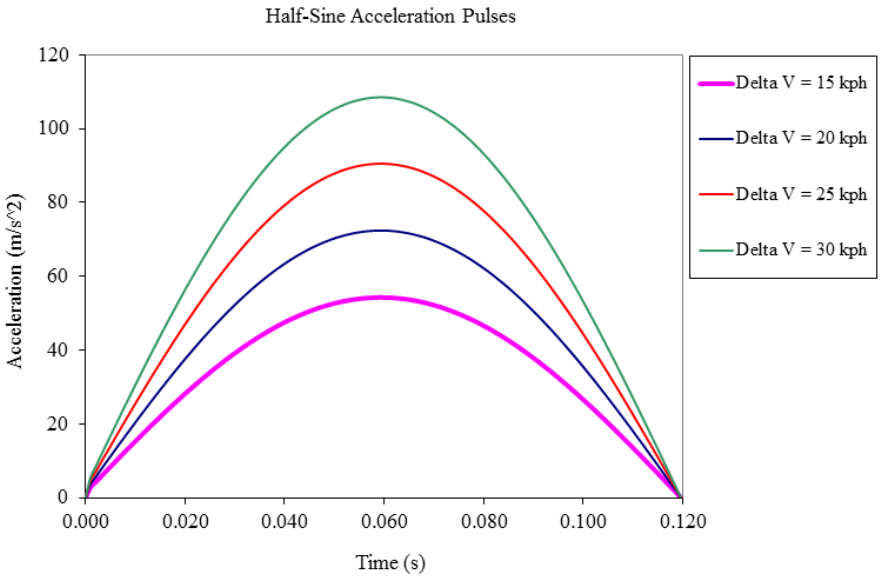

Figure 4.5 Half-sine wave acceleration pulses

The model was placed within a vehicle interior including of a seat, vehicle floor, pedals, and steering wheel. The positing and posture of the occupant in the driving seat was based on the study by Acar and Weekes, (2006). Parameters corresponding to the small female group in their final trimester of pregnancies were used to define the initial occupant position. Seat height was set at 270 mm with a seat pan angle 10 to the horizontal. Seat back angle was set at 14,8 past vertical-point (sagittal plane hip joint centre) to ball of foot horizontal distance was 708 mm which defined the initial position of the vehicle pedals with respect to the seated occupant. The horizontal distance between the steering wheel and the uterus was set at 45 mm. Steering wheel tilt was 30 degree from vertical (Acar and Lopik, 2009).

The restraint modelled consisted of a three-point seat belt and driver airbag. The seat belt was made up of a lap and shoulder portion modelled with width and thickness of the belt equal to 50 mm and 1 mm respectively. The sections of the belts that contact the occupant are modelled with non-linear 3-node triangular membrane elements with belt properties provided within MADYMO. The seat belt system incorporates a pretensioner and a load limiter. The pretensioner model in the frontal application is a spring-driven unlocking/locking type. It uses a separate stalk body that is connected to the seat frame with a revolute joint. The initial displacement causes the pre-loading of the pretensioner spring and positions the buckle body. During collision, the pretensioner restrains occupant instantly. The load limiter reduces load applied to the chest. Pretensioner prevent the occupant from jerking forward in a crash. As a result of this, maximum protection is obtained from the front airbags. Load limiter is located at the same place with the pretensioner. A load limiter limits the load level in the connected belt segment. A load limiter is activated when at least one of its load levels is active. If more than one load level is active at a time, the minimum of the active load levels is used. When the minimum active load level is reached, the load limiter starts to give out belt material. The belt system contains the load limiter of 3.5 kN. Pretensioner and load limiter reduce the seat belt impact loading on pregnant occupant's abdomen. Zellmer et al.,(2005) reported that with double pretensioning and tuned load limiter level, chest deflection and acceleration in crash tests can be reduced by about 20-25% compared to single pretensioning. Two pretensioners are located one for the retractor and one on the

anchor bracket. Double pretensioner reduces the action time of the seat belt systems and enables a modulation of forces applied to the pregnant occupant.

4.4 Simulations with 'Expecting' and Results

A typical simulation for the 'seat belt and airbag' case showing the whole model kinematics and the airbag deployment for the 30 km/h impact with airbag firing time of 30 ms is illustrated in Figure 4.6. The global and local kinematics of the pregnant occupant and stresses and strains occurring on the abdomen were investigated. Results from the simulations were used to investigate well-being of the fetus. The threshold strain value for the occurrence of placental abruption is widely accepted to be 0.6 at the UPI (Rupp *et al.*, 2001). 'Expecting' is in the driving position, because this is the most dangerous position for a pregnant occupant. Steering wheel impact to the pregnant abdomen and the uterus plays significant role on fetus fatalities. Crash test simulations are conducted crash speed ranging from 15 to 35 km/h. Simulation results show that after 35 km/h crash speed, the fetus dies instantly even pregnant occupant fully restrained.

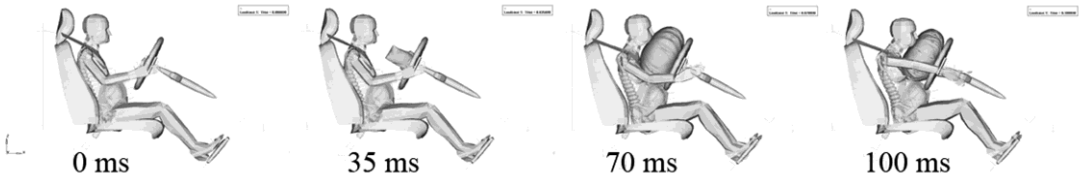

Figure 4.6 A typical full-frontal impact situation (30 km/h, Time to Fire: 30 ms)

The effects of the impact on the uterus such as maximum strains at uteroplacental interface (UPI), maximum overall strains and maximum displacements are studied. These results are tabulated for four impact severity and four restraint cases are listed in Table 4.1 and Table 4.2 respectively. The results for the three groups of analyses cases ('No restraint', 'seat belt only', and 'seat belt and airbag' cases) with three different Time to Fire ranging 10 ms, 30 ms, and 60 ms are provided in Table 4.1, whereas three 'airbag only' cases are tabulated in Table 4.2.

Table 4.1 Injury criteria and loading results for 'no restraint', 'seat belt only', 'seat belt and airbag' cases, crash speed ranging from 15-30 km/h, Airbag Time to Fire: 10 ms, 30 ms and 60 ms

	Delta V (km/h)	Max strain at UPI	Max strain in uterus	Max uterus displacement (mm)
No Restraint	**15**	0.63	0.79	122
	20	0.78	0.84	168
	25	0.89	1.05	180
	30	0.95	1.12	202
SB Only	**15**	0.13	0.34	83
	20	0.37	0.42	100
	25	0.5	0.62	117
	30	0.53	0.7	131
(SB + AB) 10 ms	**15**	0.13	0.41	78
	20	0.18	0.44	95
	25	0.22	0.52	107
	30	0.32	0.66	119
(SB + AB) 30 ms	**15**	0.12	0.5	77
	20	0.15	0.58	93
	25	0.22	0.63	110
	30	0.36	0.72	119
(SB + AB) 60 ms	**15**	0.15	0.44	81
	20	0.2	0.49	101
	25	0.31	0.63	114
	30	0.37	0.83	125

Table 4.2 Injury criteria and loading results for 'airbag only', crash speed ranging from 15-30 km/h, Airbag Time to Fire: 10 ms, 30 ms and 60 ms.

	Delta V (km/h)	Max strain at UPI	Max strain in uterus	Max uterus displacement (mm)
Airbag Only, 10 ms	**15**	0.45	0.48	106
	20	0.66	0.75	129
	25	0.94	0.98	159
	30	1.3	1.32	182
Airbag Only, 30 ms	**15**	0.56	0.67	107
	20	0.81	0.84	132
	25	1.12	1.16	161
	30	1.39	1.63	178
Airbag Only, 60 ms	**15**	0.57	0.91	108
	20	0.89	1.2	134
	25	1.14	1.12	164
	30	1.43	1.43	175

4.5 Investigation of Effectiveness of Airbag Deployment Time

Maximum von Mises strains in the whole uterus are presented in Figure 4.7. Maximum von Mises stress is considered to investigate the simulations withstand the load condition. If maximum value of von Mises stress induced in the material is more than strength of the material, design fails. The von Mises yield criterion also known as the maximum distortion energy criterion, states that the yielding of materials begins when the energy of distortion reaches the same energy for yield/failure in uniaxial tension. The von Mises stress is used to predict yielding of materials under any loading condition from results of simple uniaxial tensile tests. The von Mises stress satisfies the property that two stress states with equal distortion energy have equal von Mises stress (von Mises R.E., 1913).

'No restraint' case yields the highest strain results as expected. The 'seat belt only' case and the 'seat belt and airbag' cases form a similar set of results, again increasing from 15 km/h to 30 km/h. It is noted that the 'seat belt only' case results are amongst the low values within this group, meaning that airbag presence during impact may slightly increase the strains in the overall uterus at some particular speeds and airbag firing times. These results highlight the fact that airbag inclusion in the automobile restraint system contributing to strain development at overall uterus; however it decreases the strains at the UPI at all speeds (15-30 km/h) and airbag firing times (10-60 ms) investigated.

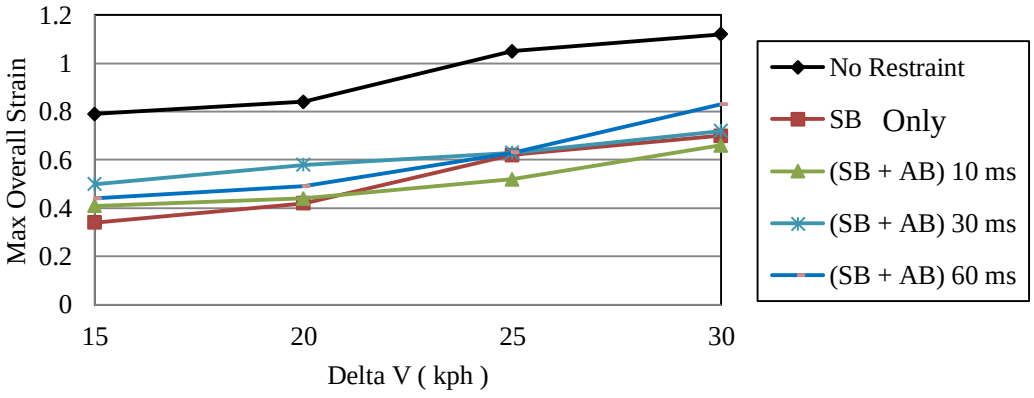

Figure 4.7 Maximum von Mises strains in overall uterus with respect to change in impact velocity

Maximum von Mises strains occurring in uterus at the UPI are presented in Figure 4.8. Any value above 0.6 indicates risk of placental abruption leading to fetus mortality. Figure 4.8 shows that the strains at the UPI for the 'no restraint' case are always above the injury threshold even at the 15 km/h simulation. For the 'seat belt only' case, the strain values approach the threshold at 30 km/h impact speed. When the three 'seat belt and airbag' case simulations (Time to Fire: 10, 30 and 60 ms) are examined, all results show a similar tendency, max strains at UPI are increasing from 15 km/h to 30 km/h as in Figure 4.8.

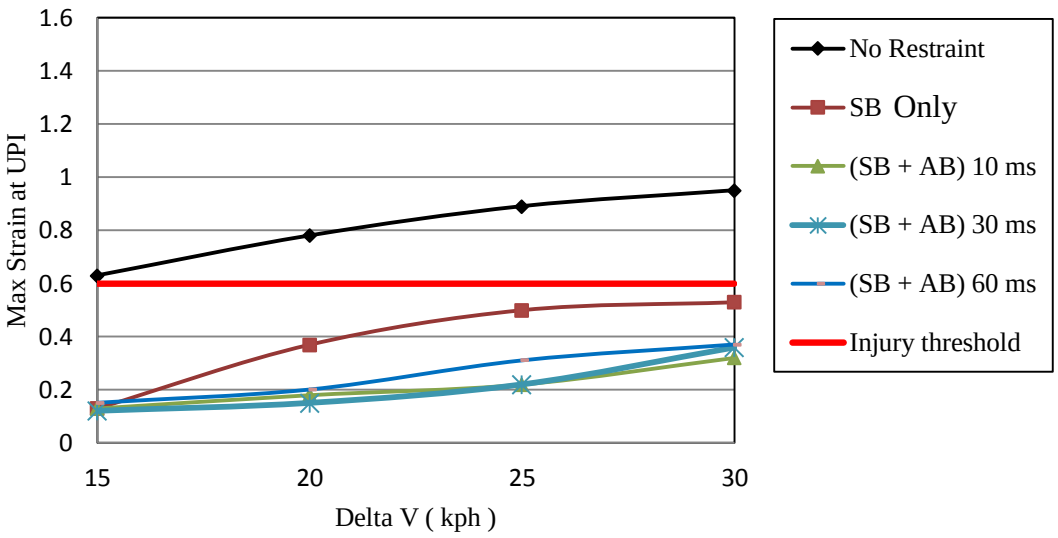

Figure 4.8 Maximum von Mises strains at the uteroplacental interface with respect to change in impact velocity

When the kinematics of the pregnant occupant and the fetus are observed, the simulation results show that forward motion of the upper region of pregnant body is reduced by airbag whereas the forward motion of the lower region of body remains constrained by the lap belt (Figure 4.9). In 'no restraint' case, the displacements are significantly higher, indicating an increased risk of injury during pregnant driver's impact with internal features of the automobile such as the steering wheel and the dashboard. Amongst all results, 'seat belt and airbag' cases for airbag firing times of 10ms and 30ms present lower displacement values than 60 ms values.

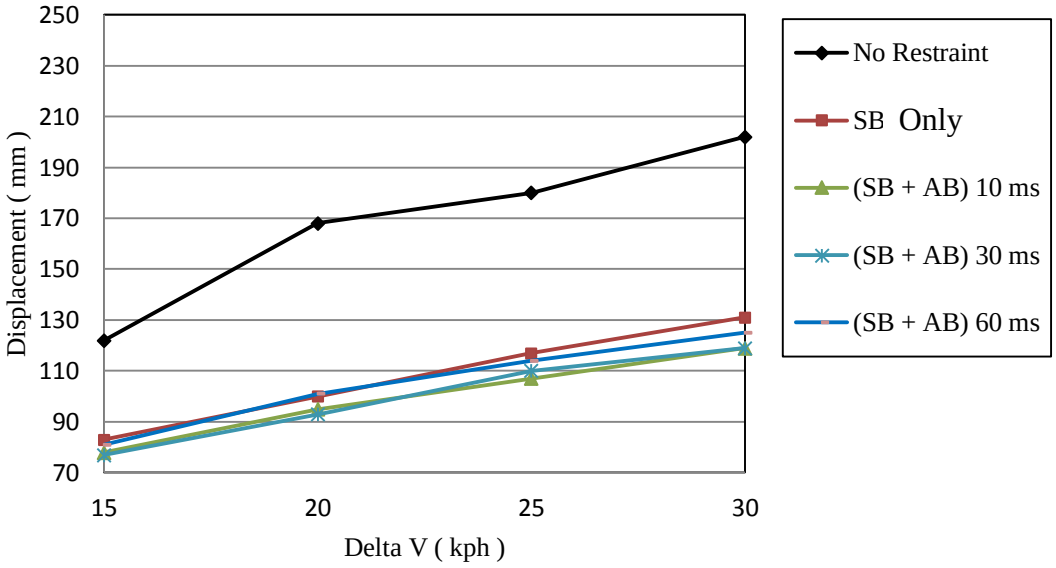

Figure 4.9 Maximum uterus displacements with respect to change in impact velocity

'No restraint', 'seat belt and airbag', and 'seat belt only' cases show that airbag inclusion cases have lower strains and displacements than cases without an airbag. While seat belt plays a significant role to protect the fetus and pregnant occupant in the road accidents, and Figure 4.8 demonstrates that the use of airbags with seat belts provides even better protection. Firing times of airbags seem to be making very small difference to the strains at the UPI. It is clear that airbags when used in conjunction with the seat belt, they reduce the strain at UPI. However, these results show that there is very little difference between the three firing times to decide which one is the best. In order to investigate if there is a significant role of airbag firing times, further investigation is needed. Therefore, 'airbag only' case is investigated for airbag firing times of 10 ms, 30 ms, and 60 ms. Maximum strains at the UPI for 'airbag only' case are presented in Figure 4.10. Simulation results show that airbag firing time of 10 ms cause lower UPI strain than airbag firing times of 30 ms and 60 ms for all impact speeds.

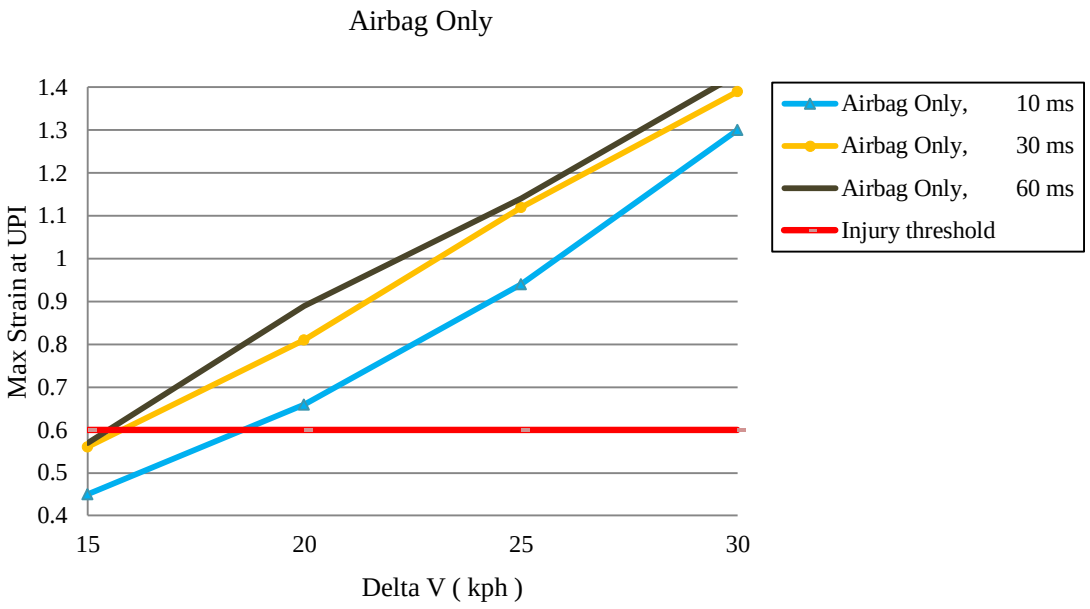

Figure 4.10 'Airbag only' case, Maximum von Mises strains at the uteroplacental interface with respect to change in impact velocity

4.6 Conclusions

The study investigates the dynamics of the fetus within the uterus in a typical automobile setting. Pregnant occupant initially sitting upright while crash severities and airbag firing timings vary.

Airbag firing times of 10, 30, and 60 ms appeared to make very little difference to UPI strains and displacements, when airbag only was considered 10 ms firing time appear to result was slightly lower strain levels than firing at 30 and 60 ms. When airbag firing time was reduced, predicted strain at UPI was reduced as well. However, it was clearly shown that when airbag was used without the seat belt, strain levels reached and exceeded the threshold level at crash speeds between 15-20 km/h. Whereas when the airbag was used together with the seat belt, the strain levels remained below the threshold level. Having no restraint system at all was shown to be the worst case for pregnant women.

It can be concluded from this study that, the airbags on its own cause high levels of strain and it must be used in conjunction with the seat belt to be effective in reducing the strains below the threshold level. The firing time of the airbag appear to make a small difference, not significant.

CHAPTER 5

EFFECT OF FETUS IN UTERUS

5.1 Introduction

During pregnancy, the anatomy of pregnant women change significantly. As the size and mass of the fetus increase, the uterus expands to create space for it. The mass of the fetus reaches about 3.3 kg at approximately 38 weeks of pregnancy. This significant mass in uterus is free to move and has potential to affect the entire dynamic response of pregnant women. The implications of including the fetus model in the uterus as opposed to an amniotic fluid filled the uterus with no fetus are investigated. Vertical drop tests onto a rigid-flat-horizontal surface at angle of orientations of 0°, 30°, 90°, and 180° have been simulated for the uterus model with and without the fetus for comparison to previously reported tests. The contribution of the presence of a fetus on the maximum Von Mises strains at the uteroplacental interface as well as anywhere in the uterine wall have been determined.

5.2 Pregnant Occupant Model without a Fetus

A computational pregnant occupant model was designed to include a finite element uterus and placenta without a fetus model (Moorcroft *et al.*, 2003). Existing 5th percentile female occupant model from MADYMO library was integrated with these two finite element components. According to findings of Rupp *et al.*, (2001) in their dummy designs, computational pregnant occupant model developed by Moorcroft et al., (2003) did not have a fetus.

Fetus-placenta interaction was investigated by Rupp *et al.*, (2001) to predict the occurrence of placental abruption in vehicle collisions. For this mechanism, a FE model of the pregnant uterus, placenta and fetus was developed (Figure 5.1).

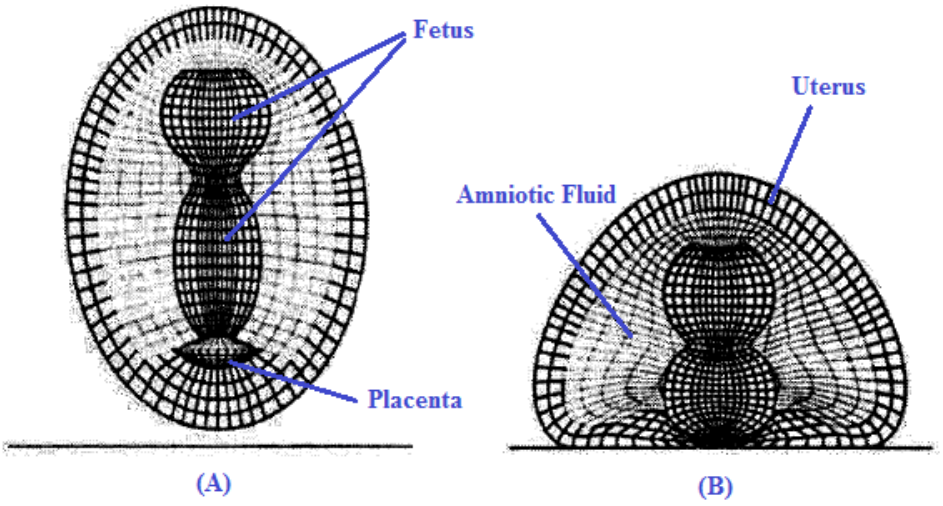

Figure 5.1 FE model of the ellipsoid pregnant uterus for investigation of fetal-placental loading (Rupp *et al.*, 2001)

The fetus was represented with two ellipsoids constructed from solid elements. This is a very simplistic representation of the fetus. The amniotic fluid was also represented as solid elements with zero shear modulus. However, no information on the material and element properties of this model was given. The model was used to simulate vertical drops on to a rigid-flat-horizontal surface at angle of orientation 0°, 30° and 90°. From the results of this test, Rupp *et al.*, (2001) concluded that contribution of the fetus to the stress and strain in the UPI is probably small relative

to the strain caused by deformation of the uterine wall. They added that in approximately 80% of pregnancies, the placenta is located in the fundal (top) region of the uterus (Fried, 1978) and therefore anterior-posterior compression, as seen in a frontal impact or inertial loading of the uterus, would not lead to cause fetal loading of the placenta. As a result of these findings, the computational pregnant model designed by Moorcroft *et al.,* (2003), did not include a fetus in the uterus.

Placental abruption is the primary cause of fetal death after motor vehicle accidents. It was investigated by Pearlman *et al.,* (1990) and found that it accounts for 50% to 70% of fetal deaths in road accidents involving pregnant women. The injury occurs where the placenta becomes partially or completely detached from the inner surface of the uterus wall, disrupting the supply of oxygen and nutrients to the fetus and causes fatalities. Depending on the degree of placental separation from the uterus, partial abruptions can occur. It is considered that placental abruption occurs during trauma because the placenta is stiffer than the uterus, interface between the placenta and the uterus is to be weaker than either the uterus or the placenta, therefore UPI usually fails before either the uterus or placenta fails.

Placental abruption may occur due to inertial and direct loading by the fetus. Overall body of the pregnant woman changes in the last trimester. The weight of most newborn babies carried to full term is generally 2.7 to 3.6 kg. This significant mass of the considerably solid fetus can move freely during crash impact but it is only constrained by uterus layer. Dynamic response to impact is affected by the fetus. Therefore, Acar and Lopik, (2009) included a fetus model in their computational pregnant occupant model, 'Expecting'.

Rupp *et al.,* (2001) concluded that fetal loss is independent of the fetus itself. In their study, the fetus model appears to be far from being realistic. Their conclusion is questionable and therefore, the same computational drop test as used by Rupp *et al.,* (2001) simulations are conducted with and without a fetus and then crash test simulations are performed and implications of including a fetus model in the uterus are investigated.

5.3 Development Phase of the Fetus in Utero

In Pregnancy, the first trimester is the primary fetal development; fetal phase starts at the beginning of the 9th week of pregnancy. Mass of the fetus is approximately 8 grams and length is typically about 30 millimetres from crown to rump (Klossner, 2005) (Figure 5.2). At the end of the 12th week of pregnancy, the height of fetus will be 75 mm in length. Size of the head reaches almost half of the fetus' size. The fetus makes uncontrolled movements and twitches. During the second trimester, which is between 14 to 26 weeks of pregnancy, the development process of the fetus organs is completed. Skeleton of the fetus starts to harden from rubbery cartilage to bone. Neck of the fetus becomes more defined. 15 weeks into the pregnancy, the fetus grows rapidly. Skeleton of the fetus becomes visible on ultrasound images. End of 16 weeks of pregnancy, length of the fetus becomes more than 120 millimetres from crown to rump. Fat stores begin to develop under fetus' skin. The fetus is about 16 cm in long from head to bottom and 25 cm from head to heel at the end of 20 weeks of pregnancy. Mass of the fetus is about 460 grams in week 22. At the end of second trimester, crown-to-rump length of the fetus might have tripled since the 12 week of pregnancy. The fetus weighs roughly 820 grams and is long 230 millimetres from crown to rump by the end of 27th week (Figure 5.3).

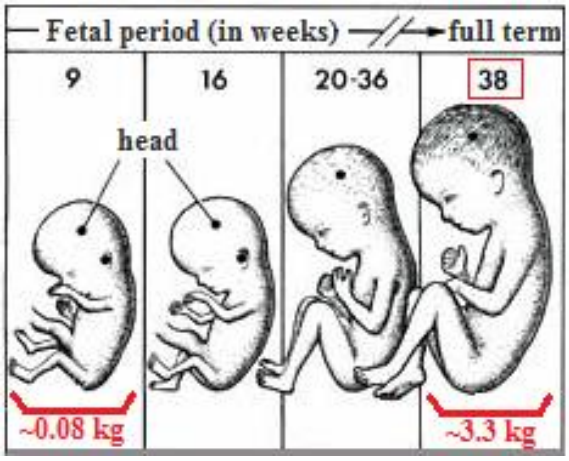

Figure 5.2 Weight of a fetus according to pregnancy period in weeks

Over the last trimester, fast development in size and weight of the fetus is seen. The volume of amniotic fluid decreases. The amount of body fat in the fetus also increases rapidly. At the end of the 28th week of gestation the fetus will be around 250 millimetres in length with a mass of around 1000 grams. Bones and skeleton system of the fetus are fully developed, but are still soft. 34 weeks into the pregnancy, fetus is 300 millimetres long from crown to rump and weighs 2100 grams. Rapid weight gain in fetus begins after 36 weeks into the pregnancy.

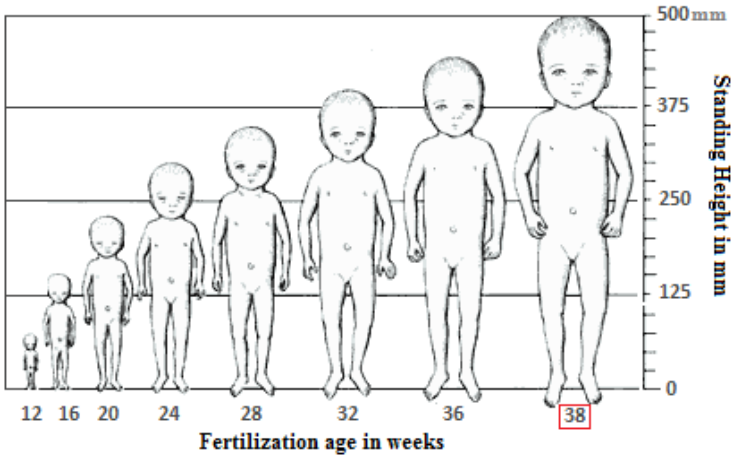

Figure 5.3 Standing height of a fetus during gestation age

The later stage of gestation fetus weighs about 2.7 to 3.6 kg and is about 450 to 500 millimetres long (Figure 5.2 and Figure 5.3). Romero *et al.*, (1988) based on the fetus' head measurements, 3.3 kg estimated fetal weight was found for a 38th week-old fetus. Fetus occupies the majority of uterine volume and amount of amniotic fluid in uterus is at minimum. Acar and Lopik (2009) designed a 38 week pregnant small women, 5th percentile model which represents a final trimester pregnancy with a large fetus and abdomen.

5.4 Multibody Fetus Model

5.4.1 Anatomy of the Fetus

By the end of the 38th week of pregnancy, anatomy of the fetus will become same as anatomy of newborn baby. Therefore, anthropometric specifications of the fetus are based on newborns, fetal MRI and ultrasound scanning (Figure 5.4).

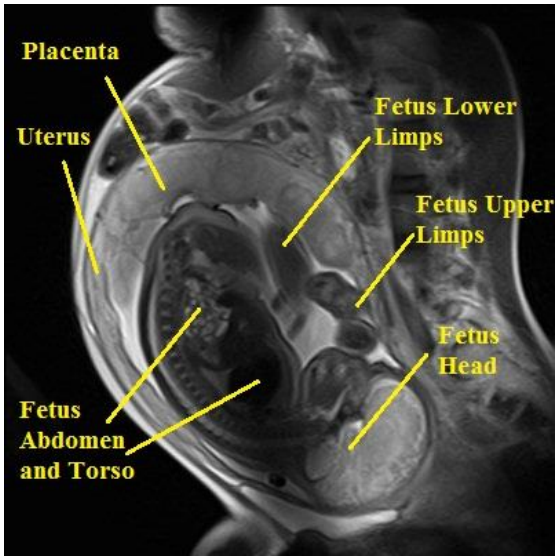

Figure 5.4 Anatomy of the fetus, MR scan (adapted from CRIC)

Ultrasound measurements of the fetus' head and body play significant role to assess gestational age. Snijders and Nicolaides, (1994) measured 1040 pregnancies and established fetal biometry. According to their ultrasound fetal measurements, fetal biparietal diameter (BPD) for median range in 38th weeks of pregnancy is 96 mm and occipito-frontal diameter (OPD) is 116 mm (Figure 5.5). Head circumference was 332 mm for the fetus of 38th week pregnant. So, the fetus' head were defined. Abdominal circumference of the fetus for median range is found 339 mm. They also measured femur length and found 72 mm for median range pregnant in her 38th week gestation.

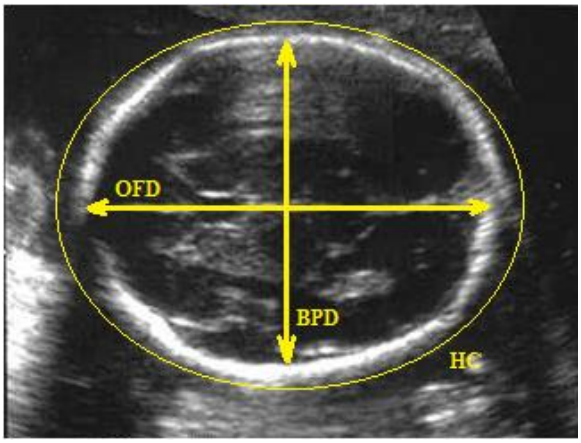

Figure 5.5 Top view of the fetus' head, Measurements of biparietal diameter (BPD), occipito-frontal diameter (OFD), head circumference (HC) (Novakov, 2002)

Jeanty *et al.,* (1984) measured upper and lower limps of a fetus. Arm bone length was measured 66 mm for a 38th week fetus humerus and ulna were measured 61 mm. Overall, 79.8% of all pregnancies, the fetus were born in the occiput anterior position, head of the fetus is down and back against the anterior uterine wall (Lieberman, *et al.,* 2005).

5.4.2 Model Geometry

Hyper ellipsoids are used to represent the anatomy of the 38th week fetus in MADYMO. Lengths of the three semi-axes of ellipsoids, their orientations and positions are necessary to define them. Previous researchers' ultrasound fetal measurements, scaling of anthropometric measurements from newborns and existing infant and child models in MADYMO dummy database are used to define the multibody fetus geometry (Figure 5.6) (Acar and Lopik, 2009, 2012).

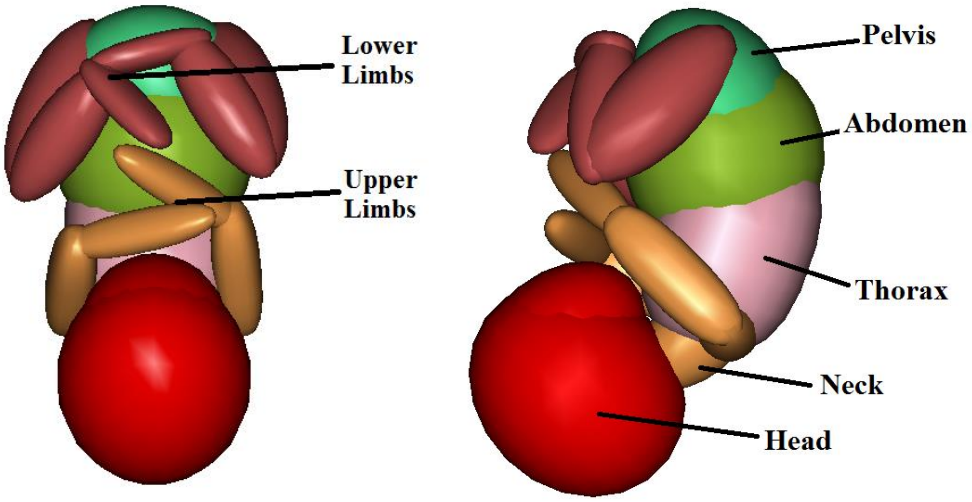

Figure 5.6 The multibody fetus model (adapted from Acar and Lopik, 2009)

The optimum fetus position in the pregnant model was estimated from MRI scans of pregnant abdomen and previous researchers' findings (Sutton, J., 2007; Lieberman, *et al.*, 2005). In this position, the back of the fetus is curved, the head is bowed and limbs are bent and drawn up to the abdomen and thorax. The fetus snug fits in the uterus with this position.

Head dimensions of the fetus were defined with using ultrasound fetal measurements of Snijders and Nicolaides, (1994), which were the mean BPD was 96 mm and OFD was 115 mm for a 38th week fetus. Pheasant, (1998) also measured similar values, the mean head length was 120 mm and head breadth was 95 mm, for a 38th week of pregnancy. Foot length of the fetus for the mean value was 77 mm was obtained from Chervenak *et al.*, (1992). Ultrasound fetal measurements of Jeanty *et al.*, (1984) such as legs and arms were also used to define the multibody fetus model in the uterus. Hands in the fetus model are not represented but the lower arms incorporate the added length of the hands. Abdominal circumference of the fetus, 339 mm for the 38th week were obtained from fetal biometry data of Snijders and Nicolaides, (1994) (Acar and Lopik, 2012).

5.4.3 Modelling in MADYMO

The multibody fetus model is composed of 15 hyper ellipsoids representing different body regions of the fetus. These 15 articulations of the fetus are connected by kinematic joints. Joint and contact characteristics such as damping, hysteresis, friction and stiffness, are scaled from existing multibody models of infants and children in MADYMO database. In order to adapt model geometry to the desired anthropometry parameters, MADYMO/scaler command is used for specified x-, y-, and z-dimensions of scaler factors. All other model parameters such as mass and moment of inertia, ellipsoids and penetration characteristics are also scaled from existing multibody models of infants (Acar and Lopik, 2012).

Weight of each rigid bodies and their position of the centre of gravity are scaled from the TNO 9 month-old child dummy. According to biparietal diameter and abdominal circumference (AC) measurements for the 38th week fetus, an estimated fetal weight of 3.3 kg is used from Romero *et al.,* (1988).

A number of different types of joints with different type of properties are used to connect rigid bodies of the fetus model. For instance, joint properties for the spine of the fetus model are scaled from adult values found in the literature (Prasad and King, 1974). Spherical joints to permit three-rotational degree of freedom are used to define spine, hip, ankle and shoulder joints of the fetus model. Revolute joints are used to represent elbow and knee joints to provide one degree of freedom in the rotational plane (Figure 5.7). A local coordinate system of the ellipsoidal pelvis forms the reference coordinate system of the model. Hip joint is located in the origin of the pelvis in the sagittal plane. Joint restraints are used to limit the range of motion of each anatomical joint to stay within the physiological range of motion.

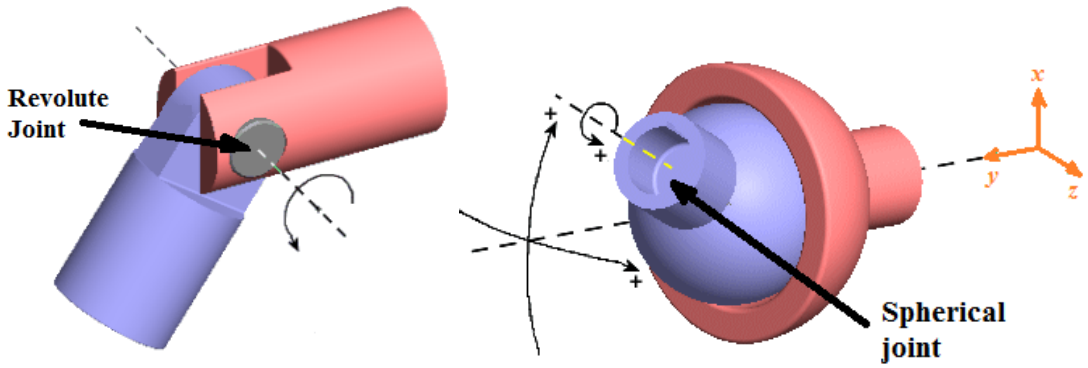

Figure 5.7 Revolute and Spherical Joints (adapted from MADYMO Theory, 2010)

5.4.4 Contact Penetration of Rigid Bodies

Contacts of various rigid bodies of the fetus are represented with body-to-body contact. Force-penetration characteristics are defined to use in the calculation the elastic contact force for each ellipsoid surface separately. Contact interaction is defined by a master surface against a slave surface. In order to define body-to-body contact, CONTACT.MB_MB command is used to select groups of multibody surfaces to be used as master ellipsoid and slave ellipsoid in a contact calculation. Contact detection parameters, damping, friction are also defined with this command (Figure 5.8).

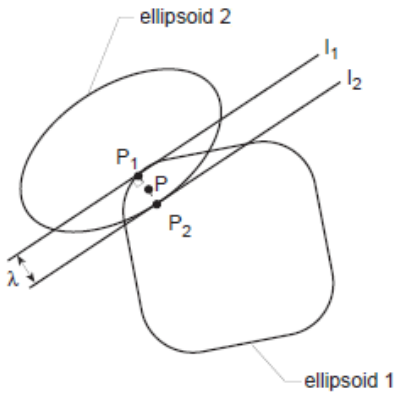

Figure 5.8 Penetration in ellipsoid-ellipsoid contacts (MADYMO Theory, 2010).

5.5 Drop Test Modelling

5.5.1 Design Approach of Test Parameters

In order to investigate the fetus-placenta interactions, simulation tests of Rupp *et al.*, (2001) which are vertical drops of the fetus within the uterus model onto a rigid-flat-horizontal-surface at angle of orientation 0˚, 30˚, 90˚, and 180˚ tests are conducted. Drop angles of orientation of the model are defined according to orientation of the placenta model with placenta axis (Figure 5.9).

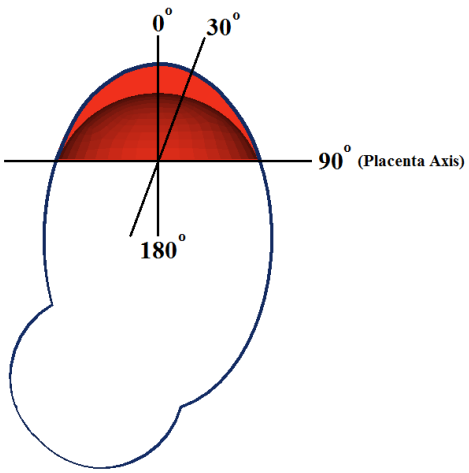

Figure 5.9 Uterus drop angles of orientation according to placenta disc axis

The multibody fetus and the finite element uterus and placenta model have been extracted from the 'Expecting' pregnant occupant model. In addition, uterus drop tests without the fetus model are designed to investigate the effect of the fetus in the uterus. The uterus is filled with the amniotic fluid model to represent the 'without-fetus' investigations. Angle of 180º drop tests are also simulated. Drop impact simulations involve dropping the model onto a rigid plate from a height of 0.5 m. The dimensions of the surface are 1m × 1m × 0.01 m represented as rigid plane in MADYMO software package (Figure 5.10). Square plane is attached to reference space of the ground system.

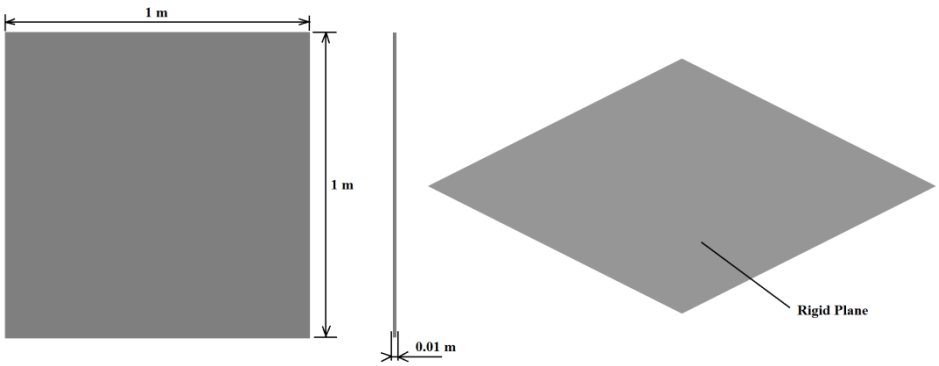

Figure 5.10 Rigid surface for drop test simulations

5.5.2 Multibody Fetus and Finite Element Uterus Model

The uterus model in Acar and Lopik, (2009) is represented with two ellipsoidal shapes and gives a snug fit around the fetus. Two layers of elements with each element size are 5 mm is designed for the uterus model. A 10 mm thick fat layer is also meshed to cover the uterus. At the upper interior region of the uterus, finite element placenta is located with discoid circular shape. Diameter of the placenta is approximately 185 mm. The placenta model has also two layers of elements. However, sizes of elements vary. Finite element uterus placenta and fat tissues are modelled as linear elastic solids (Figure 5.11)

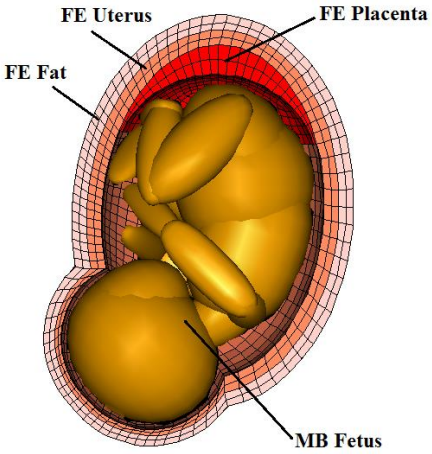

Figure 5.11 The uterus model with the fetus used for drop test

5.5.3 Finite Element Amniotic Fluid Model

Finite element amniotic fluid filled model without a fetus is designed to represent drop test simulations. The multibody fetus and its Cardan restraints which are dampers and springs are between uterus and fetus are removed from the uterus model. Amniotic fluid in the uterus model is modelled in HyperMesh using 4-noded tetrahedral elements (Figure 5.12).

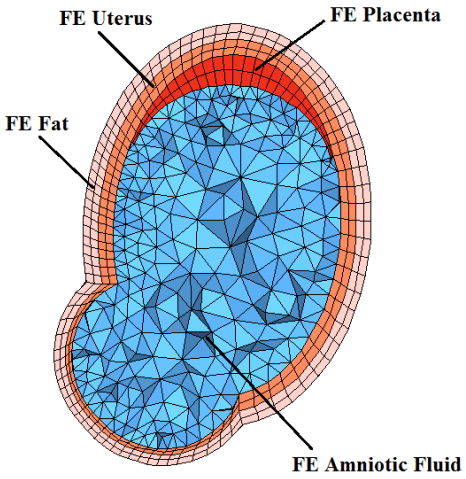

Figure 5.12 Uterus model with amniotic fluid used for drop test

5.5.4 Material Properties

The material properties of fat, uterus, placenta, and amniotic fluid are based on data published in open literature (Pearsall and Roberts, 1978; Rupp *et al.*, 2001) and previous researchers' estimates (Moorcroft *et al.*, 2003). Placenta is vascular organ therefore it is assumed to be softer than uterus but stiffer that fat (Table 5.1).

Table 5.1 Material properties used for uterus model

Structure	Material Model	Young's Modulus (kPa)	Density (kg/m^3)	Poisson's Ratio
Uterus	Linear elastic	566	1052	0.4
Placenta		63	995	0.45
Fat		47	993	0.49
Amniotic Fluid		20	993	0.49

The amniotic fluid is modelled as a solid with fluid properties because MADYMO does not utilize fluid elements. In MADYMO, MATERIAL.ISOLIN code is used to define material density, Young's modulus and Poisson's ratio of the amniotic fluid properties. The Young's modulus ranged from 20.3 kPa to 1379 kPa, with average of 566 kPa. 98-99% of amniotic fluid is water and therefore it is assumed incompressible and has a negligible Young's modulus and a Poisson's ratio of 0.49.

5.5.5 Contact Characteristics between Rigid Surface and Uterus Model

Contact between the multibody surface, which is a rigid plane, and finite element surfaces used in the uterus model, are defined with using the CONTACT.MB_FE command in MADYMO software package. The rigid surface is treated as master surface while the uterus model is treated as slave surface which is defined by the nodes of the finite element surface (Figure 5.13).

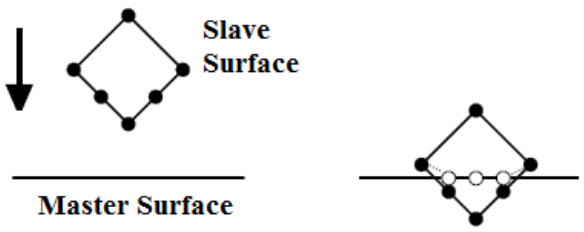

Figure 5.13 Contact Type, slave surface deformed

Contact force is calculated by using the kinematic contact model which does not allow a finite element node to penetrate the master contact plane surface (Figure 5.14). The contact force is based on an inelastic impact between the nodes and the surface. Friction coefficient between the rigid plane and the finite element uterus model is taken as 0.3.

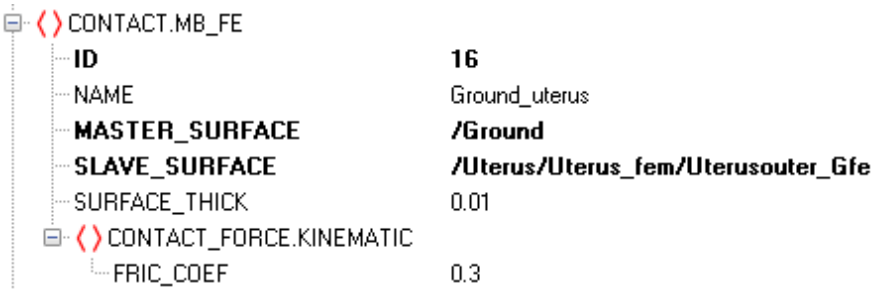

Figure 5.14 Contact definitions in MADYMO

5.6 Drop Test Simulation Results

Eight impact simulations are conducted. The uterus with and without the fetus is dropped onto a rigid plate from a height of 0.5 m (Figure 5.15). During the drop test simulations, it is observed that the leading end of the uterus is stopped by the rigid flat impact surface when the uterus hits rigid plate. However, the fetus within the uterus still continues to move due to momentum gained until it is also stopped by the impact surface or bounce back begins to occur. Finite element uterus model including fat and placenta are compressed between the impact surface and the fetus leading to high stresses. Effect of inertial moment of amniotic fluid model on the uteroplacental interface (UPI) is also observed during drop test simulations.

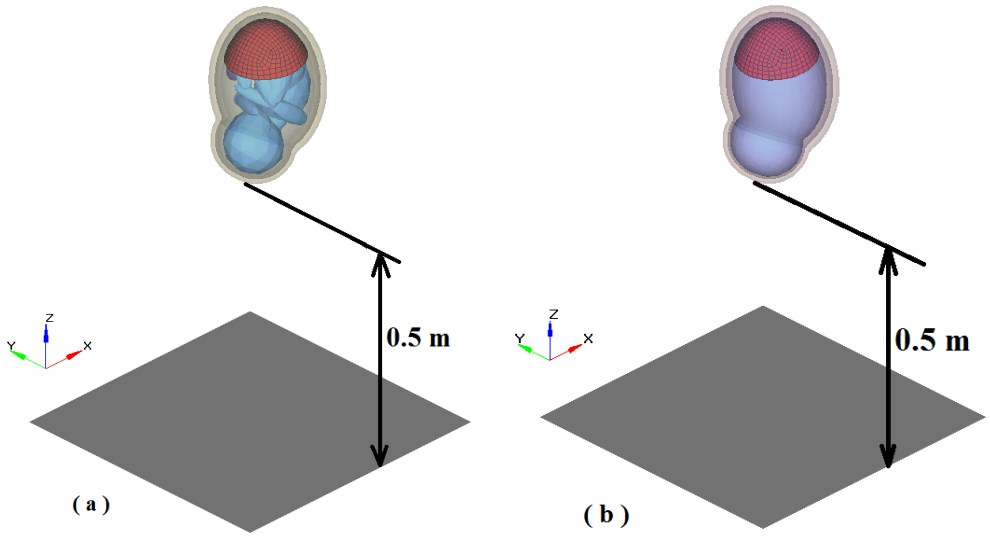

Figure 5.15 Drop tests (a) with fetus and (b) without fetus

5.6.1 Vertical Drop Tests at angle of 0 degree

The placenta axis angle of 0 degree represents the uterus and fetus position in pregnant occupant. The head of the fetus is down and disc of the placenta is horizontal to the ground (Figure 5.16). For the 0° contact angle, it is observed that the model becomes unstable when the finite element uterus model contacts the rigid surface. The fetus model hits the floor and the uterus wall is squeezed between the rigid surface and fetus head rupturing the uterus model. With the no-fetus model, highest strains are observed around contact surface of the uterus with rigid floor. However, strain at UPI is below the threshold level.

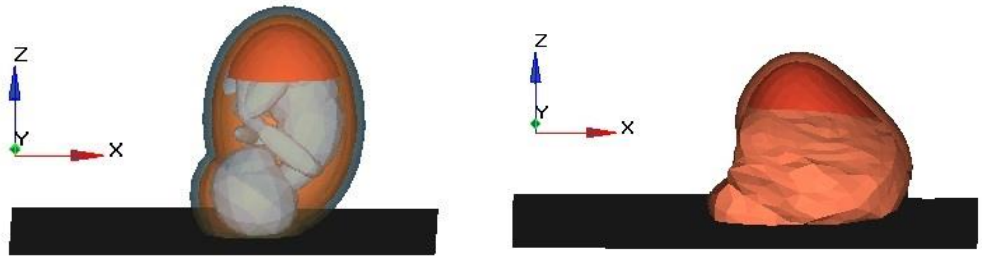

Figure 5.16 Vertical drop tests at angle of 0°

5.6.2 Vertical Drop Tests at angle of 30 degree

The finite element uterus with and without the fetus model is dropped from 0.5m at angle of 30° (Figure 5.17). In the drop test simulations, maximum Von Mises strain at UPI and at full uterus has been investigated. For the 30 degree contact angle with fetus drop test simulations, the maximum strain in the full uterus model consistently higher than without the fetus model. Similar results were also obtained when the maximum strain at UPI was investigated. For instance, 30° contact angle drop test without the fetus, the maximum strain at UPI is 0.02, whereas, with the fetus, the maximum strain at UPI is 0.17.

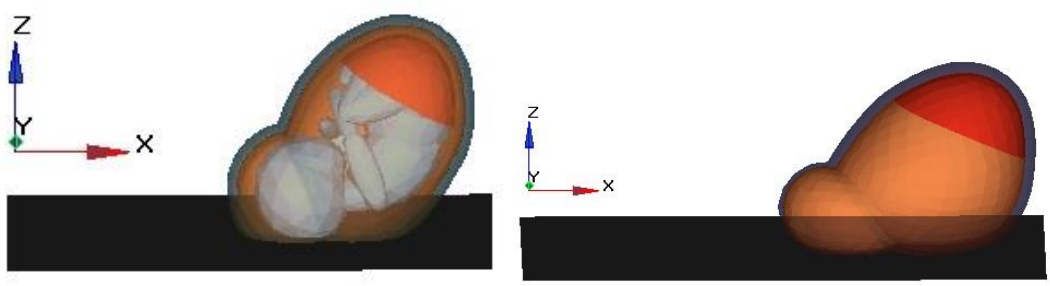

Figure 5.17 Vertical drop tests at angle of 30°

5.6.3 Vertical Drop Tests at angle of 90°

For the 90° orientation angle (Figure 5.18), the maximum strain values at anywhere in the UPI are similar for both with and without the fetus simulations, but maximum strain at the UPI with the fetus is still greater than the one without the fetus.

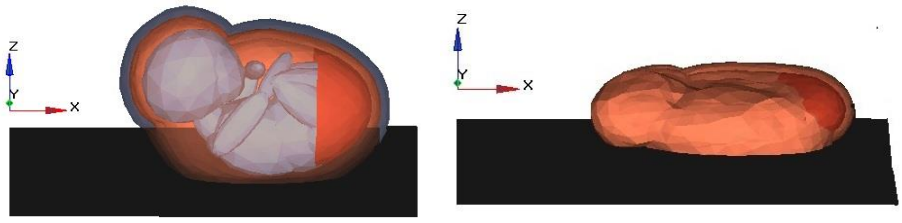

Figure 5.18 Vertical drop tests at angle of 90°

5.6.4 Vertical Drop Tests at angle of 180°

In the 180 orientation, the placenta is at the leading end of the uterus in the impact simulations (Figure 5.19); hence the placenta is compressed between the fetus and the impact surface. Therefore, a very high strain value of 2.57 is obtained at this simulation with the fetus. In the drop tests without the fetus the strain value is 0.66. The results clearly show that the fetus causes a sharp rise in the UPI strain due to the compression between the fetus and the impact surface. Even without the fetus, the strain at the UPI is high, higher than the threshold value, due to direct impact with the surface.

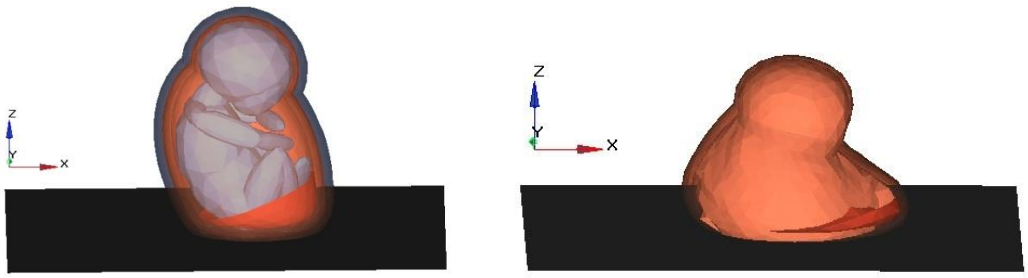

Figure 5.19 Uterus vertical drop tests at angle of 180°

Table 5.2 Von Mises strain levels with and without fetus drop tests

Drop Test	0°		30°		90°		180°	
	Whole Uterus	UPI	Whole Uterus	UPI	Whole Uterus	UPI	Whole Uterus	UPI
With Fetus	1.37	0.07	2.02	0.17	0.89	0.3	2.57	2.57
Without Fetus	0.72	0.01	0.66	0.02	0.86	0.24	0.66	0.66

5.6.5 Conclusions

In this section, implications of including the fetus model in the uterus were investigated. Vertical drops onto a rigid flat horizontal surface at angle of orientation of 0°, 30°, 90°, and 180° have been simulated for the uterus model with and without the fetus. Contribution of the presence of a fetus on the maximum von Mises strains at the uteroplacental interface as well as anywhere in the uterine wall have been determined. Drop test simulation results shows that the existence of a fetus have a significant effect on the strain levels both in the uterus in general and of the UPI, with the exception of 90° orientation, where the difference is small. In all cases, the maximum strain level are higher with the fetus than the without fetus model. It is therefore crucial to the simulations of pregnant occupant model to include a fetus in the uterus.

5.7 Expecting' with and without fetus model

5.7.1 Design Approach

Drop test simulations clearly demonstrates that the fetus changes the dynamics of the simulation of the uterus and therefore the fetus should be included in the uterus in all pregnant woman models for realistic results in crash test simulations. In this study,

implications of including the fetus in the uterus are investigated with the 'Expecting' model at crash test simulations.

The pregnant occupant model with and without the fetus is used to simulate four frontal impact speeds, 15, 20, 25 30 km/h with varying levels of restraint system including 'unrestrained', 'seat belt only', 'seat belt and airbag', 'airbag only' to explore the effectiveness of the existing fetus in the uterus (Figure 5.20). Strains developed in the uterus due to loading from the seat belt and steering wheel are presented. Contribution of the presence of a fetus on the stresses and strains generated at the uteroplacental interface are discussed.

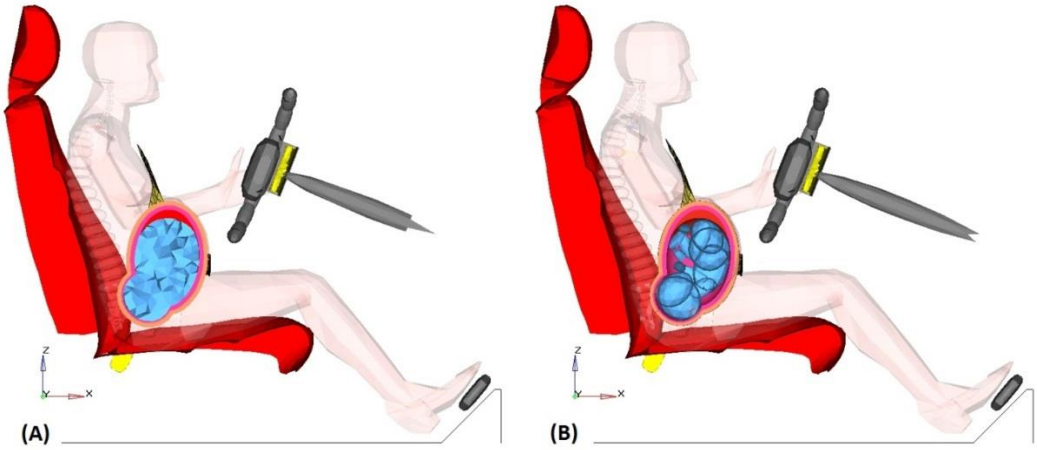

Figure 5.20 (A) Side view of 'Expecting' computational pregnant occupant model without the fetus; (B) 'Expecting' (with the fetus)

The research strategy adopted in this study was to use the 'Expecting' pregnant occupant model which has a fetus in crash test simulations and create another 'Expecting' model by removing the fetus and filling the uterus with amniotic fluid only. These two uterus models with and without the fetus are already used at vertical drop test simulations in section 5.6.

5.7.2 Simulation Parameters and Applications

'Expecting', the pregnant occupant model and its "without fetus" version are used at four sets of simulations; the 'seat belt and airbag' case group which is also termed full

restraint, incorporates the seat belt and airbag, representing a properly restrained pregnant driver, the 'seat belt only' case group excludes the airbag, 'airbag only' case group excludes the seat belt, and yet the airbag is active, whereas 'no restraint' case group excludes all restraints, in other words neither the seat belt is worn nor the airbag is deployed. For each group, tests are run with crash speeds of 15, 20, 25, 30 and 35 km/h, and the half-sine wave is used to represent acceleration pulses with 120 ms duration. The seat belt system has a pretensioner and a load limiter same as used in Chapter 4. While the load limiter protects pregnant occupant from seat belt-inflicted injury, pretensioner restrains occupant instantly and reduces the amount they are thrown forward in frontal crash. The system reduces steering wheel and airbag impacts on pregnant abdomen. Standard MADYMO European driver airbag model is used in crash test simulations. It has 60 litres volume.

5.7.3 Injury Criteria

Maximum von Mises equivalent strain levels in uterus at placental location (uteroplacental interface) and in overall uterus are investigated for with and without fetus models to assess the possibility of placental abruption, which leads to fetal, and occasionally maternal death. The threshold strain value for the occurrence of placental abruption is widely accepted to be 0.6 at the UPI (Rupp *et al.*, 2001).

5.7.4 Crash Test Results

Figure 5.21 depicts a typical impact response for the 'seat belt and airbag' with and without fetus cases. Figure 5.21 (a) shows the excessive deformations on the uterus due to the fetus loading, whereas Figure 5.21 (b) shows minimal deformations at 30 km/h impact.

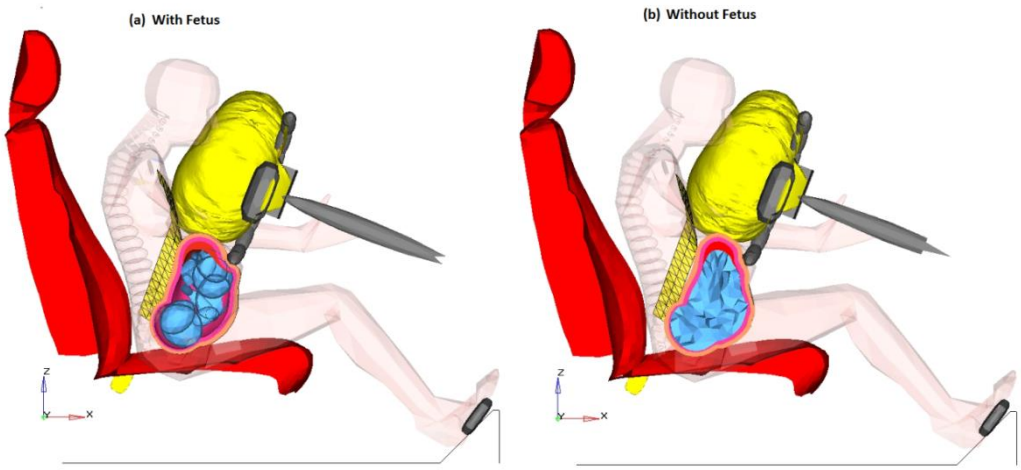

Figure 5.21 Typical frontal impact responses for 30 km/h at 105 ms of impact

The maximum strains at the uteroplacental interface are compared in Figure 5.22 in order to demonstrate the differences between with and without the fetus model simulations for varying crash speeds for 'seat belt and airbag' case. It is clearly seen that strains increase with increasing speed as expected. Figure 5.22 shows that the strains at the UPI for with the fetus model changes from 0.24 to 0.42, whereas the strains at the UPI for without the fetus model increases from 0.18 to 0.42. It is also clearly seen that without the fetus, all strain values at the UPI are considerably below the injury threshold value of 0.60. At 35 km/h impact, strains at the UPI for with and without the fetus models are same, 0.42. Full restraint case shows that although there is no great difference between with and without the fetus models at high speeds, without the fetus model simulation results are always lower than with the fetus model simulations (Figure 5.22).

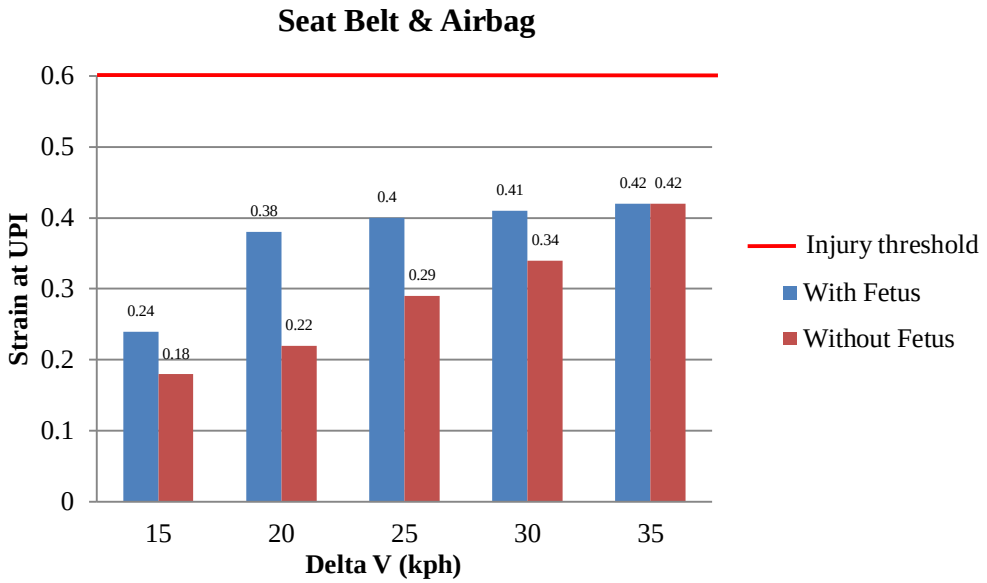

Figure 5.22 'Expecting' with and without the fetus for 'seat belt and airbag case'. Maximum Von Mises strains at the uteroplacental interface comparison for with and without the fetus cases

'Seat belt only' case results for the maximum strains at the UPI of with and without the fetus models are demonstrated in Figure 5.23. 'Seat belt only' case follows a similar pattern to the strains at the 'seat belt and airbag case'. Differences of strains at the UPI for with and without the fetus cases are higher than 'seat belt and airbag case'. At 35 km/h impact, placental abruption risk is the same for both cases and close to threshold of 0.60. Without airbag, especially at high speeds, it is clearly seen that effect of the fetus for 'seat belt only' is higher than 'seat belt and airbag case'. Following the impact, the fetus moves forward and restrained by the uterus within the restrained body. The steering wheel loads the uterus at the anterior edge of the placental location forcing the fetus downwards also compressing the placenta between the fetus and steering wheel. The motion generates considerably higher strains at the UPI than without the fetus model.

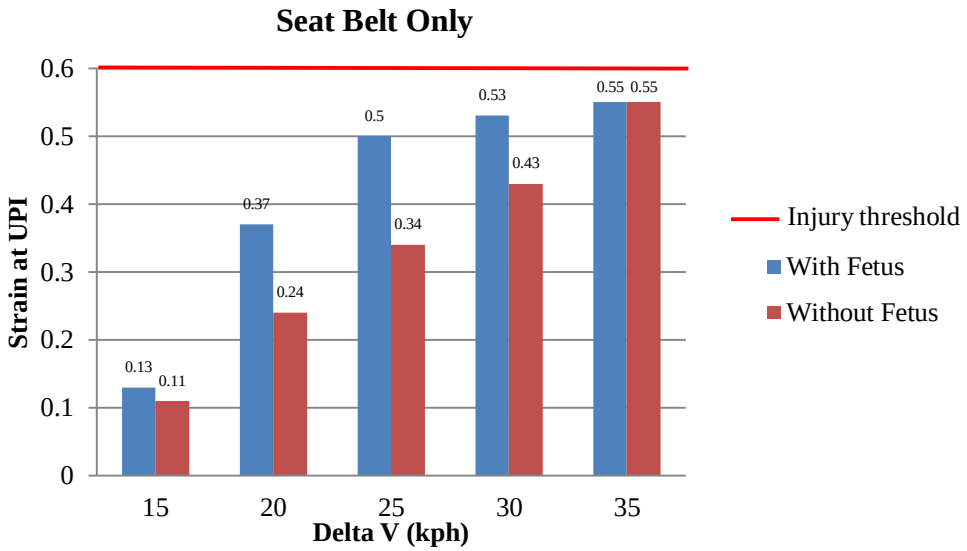

Figure 5.23 'Expecting' with and without the fetus for 'seat belt only' case. Maximum von Mises strains at the uteroplacental interface comparison for the with and without the fetus cases

Figure 5.24 shows the maximum von Mises strains at the UPI for the 'airbag only' case of 'Expecting' with and without the fetus. First of all, it is clearly seen that when the fetus is included, placental abruption risk emerges at all speeds but 15 km/h, whereas without the fetus model, placental abruption risk emerges at the speeds of 30-35 km/h. Even at 20 km/h impact, placental abruption risk is present for the with the fetus model with a strain of 0.70, exceeding the threshold of 0.60. However, strain at the UPI is only 0.43 for without the fetus model which below injury threshold value of 0.60. Without the seat belt, it is clear to see the contribution of presence of a fetus on the maximum von Mises strains at the UPI. This significant mass (3.3 kg) plays a significant role at the dynamics of the simulation of 'Expecting'. These results clearly demonstrate that the fetus changes the entire dynamic response to impact. Figure 5.24 shows that the strains at the UPI for the with the fetus model changes from 0.55 to 1.26, whereas the strains at the UPI for the without the fetus model increases from 0.43 to 0.73.

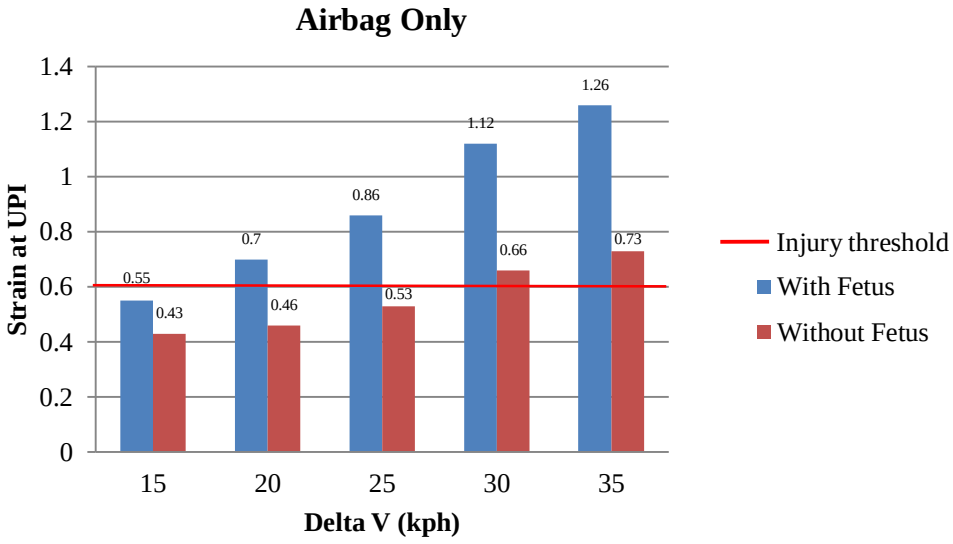

Figure 5.24 'Expecting' with and without the fetus for 'airbag only case'. Maximum von Mises strains at the uteroplacental interface comparison for the with and without the fetus cases.

For the 'no restraint' case in Figure 5.25, with the fetus model, placental abruption occurs at all speeds, 15-35 km/h, whereas without the fetus model at 15, 20, and 25 km/h strains at the UPI is below the injury threshold value of 0.60. As for with the fetus model, the strain at the UPI reaches a maximum of 1.08 at 35 km/h impact, which is considerably above threshold value of 0.60.

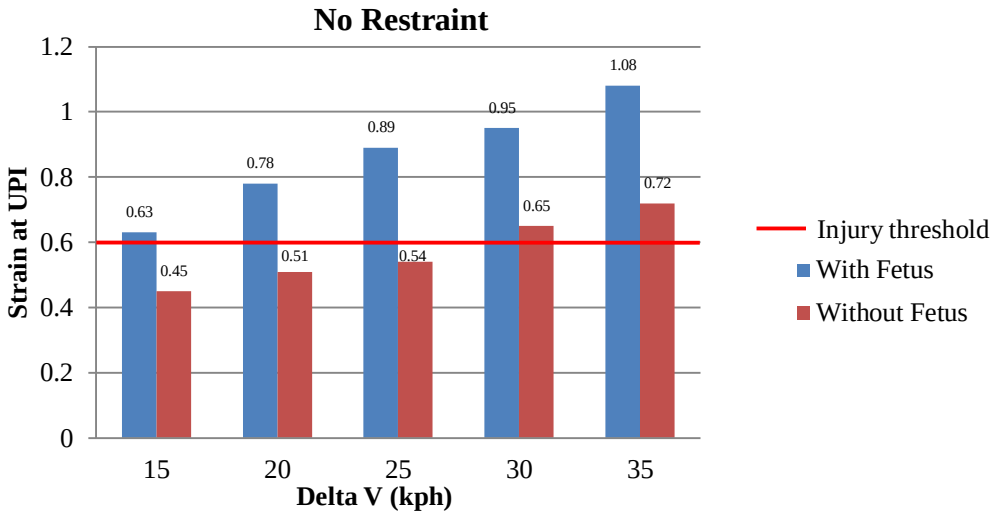

Figure 5.25 'Expecting' with and without the fetus for 'no restraint' case. Maximum von Mises strains at the uteroplacental interface comparison for the with and without the fetus cases.

5.8 Conclusions

The implications of including a fetus model in the uterus of the 'Expecting' were investigated. The 'Expecting' with and without the fetus model were used to simulate a range of frontal impacts of increasing severity from 15 km/h to 35 km/h. Four levels of occupant restraint, seat belt and airbag, seat belt only, airbag only and completely unrestraint were investigated. As a result of loading from the seat belt, steering wheel unit and airbag, the strains developed in the uterus. When the fetus existed, inertial loading of it on the uterus occurred as well.

In case of a crash, inertial effects on the fetus caused it to move forwards relative to the pregnant women. When the fetus model was included, the uterine wall

was effectively sandwiched between the fetus, lap belt, steering wheel and airbag. The fetus was forced against the uterus anterior wall. This dynamic motion of the fetus generated significantly higher strains at the UPI than without the fetus model.

Crash test simulation results with and without the fetus model clearly showed that the fetus changes the dynamics of the simulation of the uterus and therefore the fetus should be included in the uterus in all pregnant woman models for realistic results in crash test simulations.

CHAPTER 6

EFFECT OF PLACENTA LOCATIONS

6.1 Introduction

The placenta is normally located at the top (fundus) of the uterus and this is the location used in the models in this investigation. However, the placenta can be positioned at different locations in the uterus in real life. Different positions of the placenta in the uterus may affect the strain levels.

The work described in this chapter, different locations of the placenta in the uterus and their potential influences on the risk of placental abruption were investigated. These models were used as before, to simulate several collisions of increasing crash speed from 15 km/h to 35 km/h. The same type of occupant restraint; 'seat belt and airbag', 'seat belt only', 'airbag only' and 'unrestrained' cases were investigated. The strains developed at the uteroplacental interface were

determined and the influence of the placental position on the risk of placental abruption studied.

6.2 Placenta Locations in the Uterus

The anatomy of pregnant abdomen may be different from one pregnancy to another. For instance, the placenta in the uterus can be situated anywhere on the inner surface of the uterus wall. The locations of placenta in the uterus can be observed by ultrasonography measurements. Approximately six locations are defined to explain position of the placenta in the uterus. Placenta at the front wall of the uterus is known as the anterior placenta while placenta at back wall of the uterus is called the posterior placenta. In addition, the placenta attached to the side walls are defined as left lateral and right lateral placenta. The placenta situated at the top of the uterus is the fundal placenta and at the bottom of the uterus is the placenta praevia. Figure 6.1 shows few of these positions. Figure 6.2 shows posterior placenta in fetal MRI. In around 80 % of pregnancies, the placenta is located in the top of the uterus (Pepperell *et al.*, 1977).

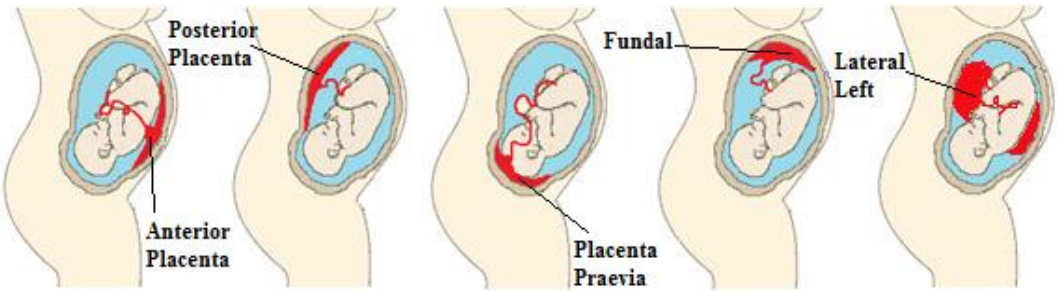

Figure 6.1 Placenta at different locations in the uterus

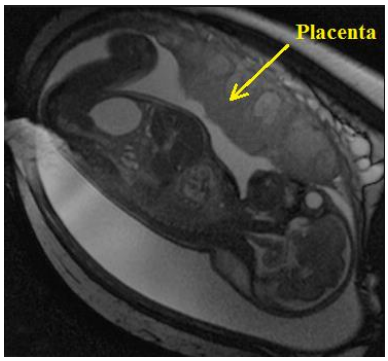

Figure 6.2 Posterior placenta in fetal MRI (adapted from CRIC)

The position of the placenta inside the uterus may potentially play a crucial role and hence influences the likelihood of placental abruption. Hence the work described in this chapter, investigates the effect of placenta at four further locations on the risk of placental abruption during a motor vehicle accident.

6.3 Finite Element Placenta Model

6.3.1 Anatomy of Placenta

The placenta is a highly vascular organ. Its primary function is to exchange oxygen, nutrients, and waste between the mother and the fetus. The placenta covers about a quarter of the inner surface of the uterus. Microvillus, which are small finger-like protrusions, attach the maternal side of the placenta to the decidual layer of the uterine wall. Two structures are connected together and this area is called the Uteroplacental Interface (UPI) (Figure 6.3). There is also a blood flow from the mother to the placenta and from the placenta to the fetus at UPI during pregnancy. The placenta receives approximately one sixth (800 ml) of the total amount of blood pumped from the heart of mother per minute. Therefore, partial or complete detachment of the placenta in the uteroplacental interface can cause fetus mortalities. Placental abruption, which is the separation of the placenta from the uterus, has been shown to account for 50-70% of fetal losses in motor vehicle collisions (Pearlman *et al.*, 1990).

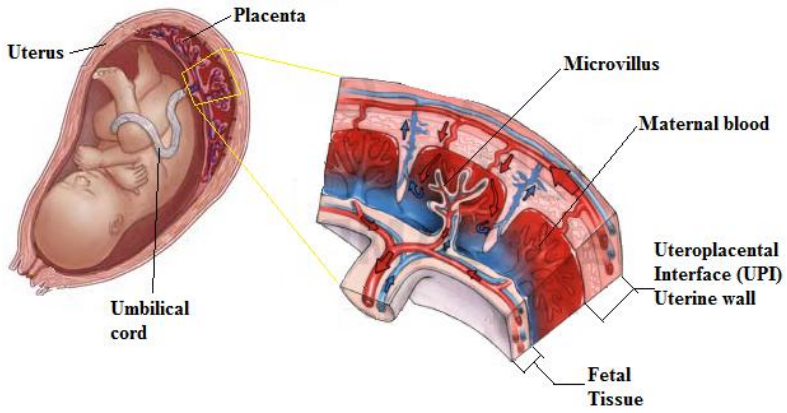

Figure 6.3 Section through uterus, placenta and fetal membranes, placenta in detail (adapted from Medivisuals)

The fetus is attached to the placenta via umbilical cord which is on average 50 cm but can vary from 20-120 cm in length. It is 1-2 cm in diameter.

The shape of the placenta is a flattened discoid. The centre of the placenta represents the thickest part of the placenta while thinning towards the periphery. Average thickness of the placenta at term is 23 mm and average diameter is 185 mm. The average weight of the placenta is 470 gram, average volume is 500 ml and inner surface area of on average 30000 mm^2 (Duck 1990 and Standing, S. 2005). Sivaraoa *et al.*, (2002), has also reported similar values about the anatomy of the placenta.

6.3.2 Model Geometry in 'Expecting'

The discoid shape of the placenta is designed with SolidEdge CAD software. The placenta's diameter is chosen to be 185 mm. While the placenta thickness is approximately 20 mm at centre, thickness at periphery is about 4 mm. The most common position, which is the upper region of the uterus, is chosen to position the placenta in the uterus. Surface area of the placenta is 26866 mm^2 at the uteroplacental interface (UPI).

6.3.3 Modelling in HyperMesh and in MADYMO

The placenta geometry is meshed using HyperMesh software package. In the meshing process, two layers of elements are designed and from placental outer surface to the inner surface of the uterus are mapped to create the placental elements (Acar and Lopik, 2009, 2012). Solid 8-noded brick elements are used to represent the placenta. Uteroplacental interface consists of mutual nodes. The 3D placenta model is represented with 884 elements (Figure 6.4).

Node coordinates and element configurations are exported into MADYMO. Cartesian coordinates, x, y, z of nodes are defined in the MADYMO table.

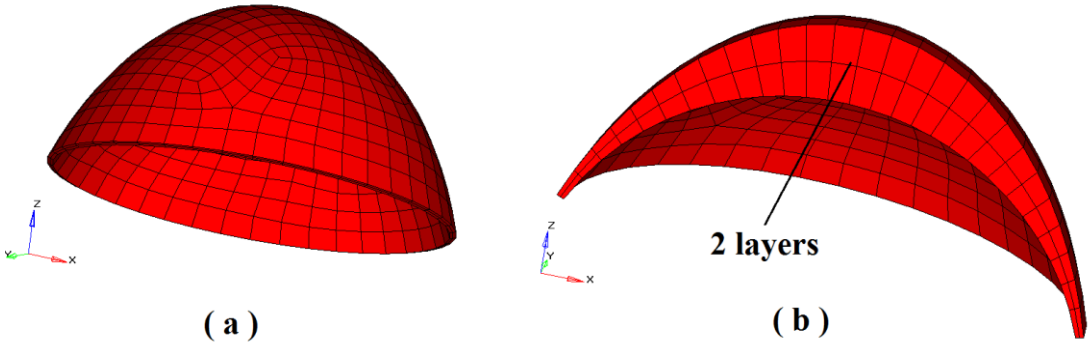

Figure 6.4 Meshed placenta; (a) Isometric view, (b) Sagittal plane view

6.3.4 Material Properties of the Placenta

There is lack of research about mechanical and material properties of the placenta. In addition, the placenta and its surrounding membranes change their physical properties when the pregnancy nears the final trimester. However, the placentas used in research are from pregnancies at or near to term in the most of the cases.

All uterine bodies including the placenta were modelled as linear elastic isotropic solid material. However, the uterus and placenta are considered viscoelastic and anisotropic (Mizrahi and Karni, 1975). This means material properties vary depending on the direction. Viscoelastic materials exhibit both viscous and elastic

characteristics when undergoing deformation. When stress is applied, viscous materials strain linearly and resists shear flow. Elastic materials strain instantaneously and stretched, but when the stress is removed, just as quickly return to their original. Because of insufficient data, these material modelling methods are not applied. The material properties for placenta, uterus and fat are taken from literature (Pearsall and Roberts, 1978 cited in Acar and Lopik, 2009). It was assumed that the placenta is stiffer than fat and therefore the higher Young's modulus is used for the placenta. However, the placenta is muscular tissue and the Poisson's ratio is lower than fat. The Poisson's ratio of the human placenta is reported as 0.49 (Manoogian *et al.*, 2008) (Table 6.1). These material properties of the placenta such as density, Poisson's ratio and the Young's modulus are defined in MADYMO.

Table 6.1 Placenta material properties

	Density	Young's Modulus	Poisson's Ratio
Material Properties	995 kg/m^3	47 kPa	0.49

6.4 Contact Characteristics of the Placenta in MADYMO

Finite element placenta model is defined in HyperMesh as one of the components of the uterus model. Element properties and Cartesian coordinates of nodes are exported into MADYMO. Model definition data of the placenta are written under the FE uterus model. GROUP_FE element is used to assemble selected set of finite element placenta within the FE uterus model. Contacts between the multibody fetus surfaces, which are chosen as the master surface, and finite element placenta surface, which is chosen as the slave surface, are defined with CONTACT.MB_FE (Figure 6.5).

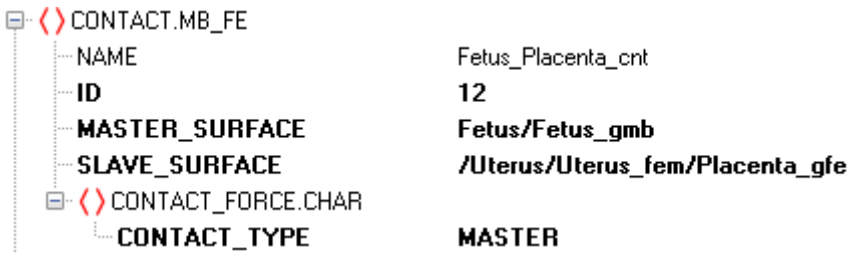

Figure 6.5 Contact definitions between the placenta and the fetus

6.5 Modelling the Placenta at Different Locations

Understanding of the design process of the uterus model in detail is very important to redesign a new placenta models. During the design process, model geometry, element type, supports, boundary conditions, contact definitions, and outputs are decided. Design criteria for the new placenta models are taken from the original placenta model of the 'Expecting'. Therefore, values for surface area of the UPI, placenta diameter or length, and placenta volume are designed as close to the values of the original placenta as possible. The most common locations of the placenta in the uterus are investigated and four additional regions are chosen in additional to the original fundal position. Placenta praevia is not modelled due to its rarity (0.5%) in real life and it brings many other complications to pregnancy and child birth.

6.5.1 FE Placenta Model at Anterior

The finite element placenta model is positioned on the frontal wall of the uterus (Figure 6.6). This is the nearest location to the abdomen muscles of the pregnant body. Finite element mesh pattern of the uterus model is kept unchanged and therefore the placenta model is designed to match the inner surface of the uterus elements. The anterior placenta has rectangular shape approximately 185 x 145 mm with thick centre, 17 mm and the thin peripheral, 3mm. Surface area of the new placenta is the similar as the original placenta, 26816 mm^2. In order to investigate the effect of different placental locations in the uterus, it is important to maintain the properties of the placenta models at different locations. Especially, surface of the

uteroplacental interface (UPI) plays significant role from this point of view. This model has also two layers which consist of 8-noded hexahedral elements. Anterior placenta is normal place for the placenta to implant and develop.

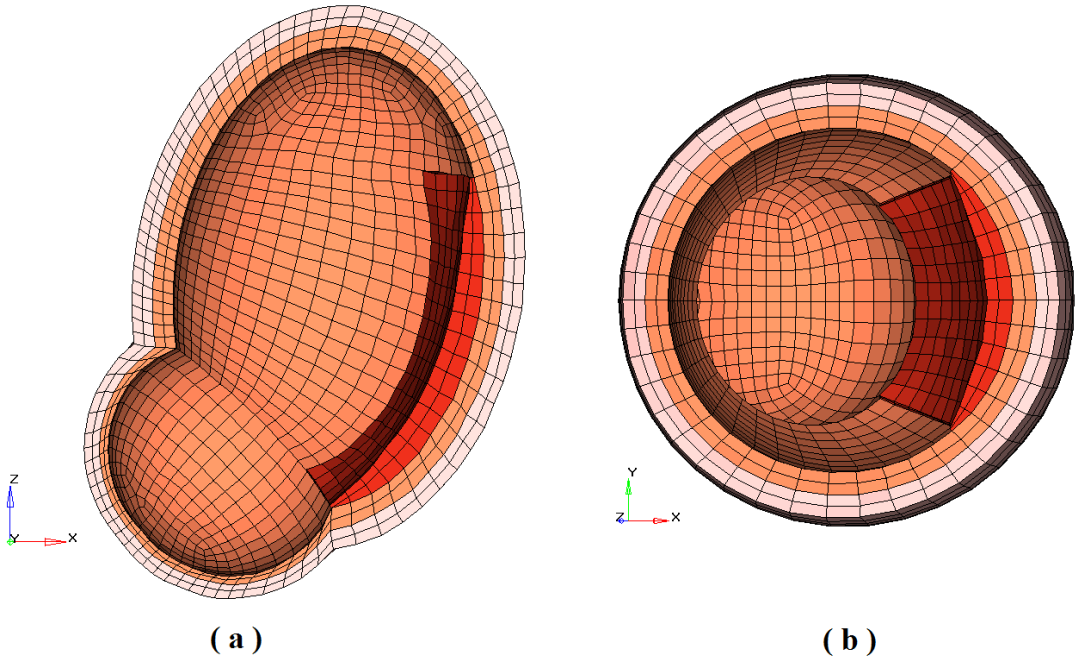

Figure 6.6 Anterior placenta in uterus; (a) Side view, (b) Top view

6.5.2 FE Placenta Model at Posterior

The computational placenta model is attached to the back wall of the uterus (Figure 6.7), posterior placenta. The back wall of the uterus is the closest to spine of the pregnant woman. Due to its position on the back wall of the uterus, posterior placenta forces the fetus forward and closer to the abdomen of the pregnant woman. The new placenta model is also meshed using HyperMesh. Due to the mesh pattern of the finite element uterus model, posterior placenta has also rectangular shape. Posterior placenta has approximately 188 x 135 mm with thick centre, 15 mm. Peripherals of the posterior placenta is thinned to about 3 mm. UPI area of the placenta at the back wall of uterus is about 25350 mm^2. Two layers of linear elastic 8-noded hexahedral elements are used to construct the new placenta. Posterior placenta is considered normal for the mother and the fetus during pregnancy.

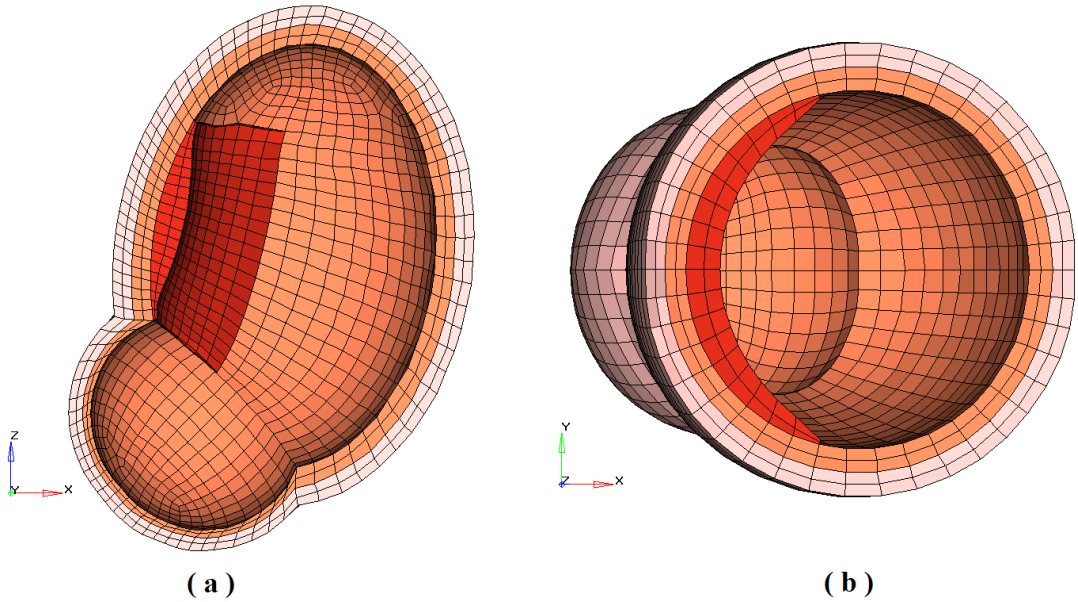

Figure 6.7 Posterior placenta; (a) Side view, (b) Top view

6.5.3 FE Placenta at Lateral Left and Lateral Right

The finite element placenta model is positioned on the lateral left and lateral right of the uterus (Figure 6.8 and Figure 6.9). Both of the placentas are designed to be symmetric to each other from sagittal plane to investigate external impacts from asymmetric loadings due to asymmetrical shoulder belt. Design criteria for the new placenta models on the lateral left and lateral right of the uterus are the same. Placenta covers almost a quarter of the inner surface of the uterus with its UPI area of about 26725 mm^2 for both. Due to the mesh pattern of the uterus model, rectangular shape placenta models are generated. Height of the placenta towards to the back wall of the uterus becomes shorter while it is the tallest near front wall of the uterus. Therefore, length of the placenta ranges from 110 mm to 188 mm. Width of the each placenta is approximately 135 mm. Placenta on the left or right side of the uterus is also considered normal for the pregnancy.

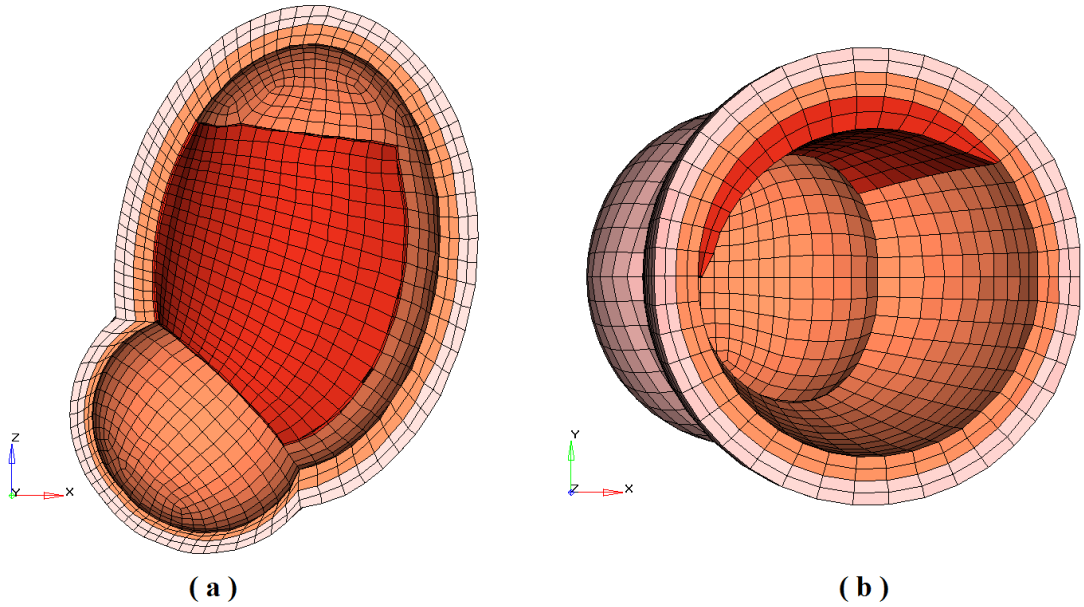

Figure 6.8 Placenta at lateral left; (a) Side view, (b) Top view

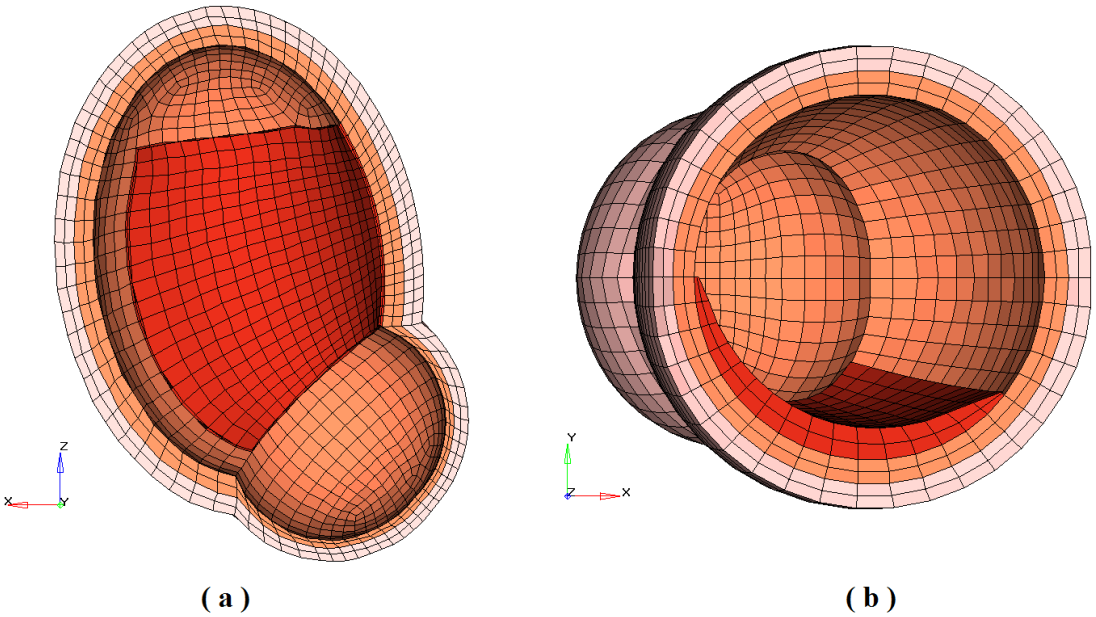

Figure 6.9 Placenta at lateral right; (a) Side view, (b) Top view

6.6 Crash Test Simulations with New Placenta Models

6.6.1 Simulation Set-up

Four sets of simulations, 'seat belt and airbag', 'airbag only', 'seat belt only', and finally 'no restraint' cases, are simulated with 'Expecting' pregnant occupant model with four different placental locations. Standard MADYMO European driver airbag model (60 litres) is used. Seat belt system has a pretensioner and a load limiter. Each group is used to simulate a frontal impact at speeds of 15, 20, 25, 30 and 35 km/h. Simulations at these crash speeds are repeated for anterior, posterior, lateral left and lateral right placental locations. The simulation results of 'Expecting' which has placenta at upper region of the uterus are taken from Acar and Lopik, (2009).

In order to investigate the potential influence of the placenta position on the risk of placental abruption, the maximum von Mises equivalent strain level in uteroplacental interface and in overall uterus are determined.

6.6.2 New Placenta Models with 'Expecting'

'Expecting' is used with a replaced uterus with four placenta locations in the crash test simulations. Every other feature such as vehicle interior, restraint systems are used as in 'Expecting' (Figure 6.10).

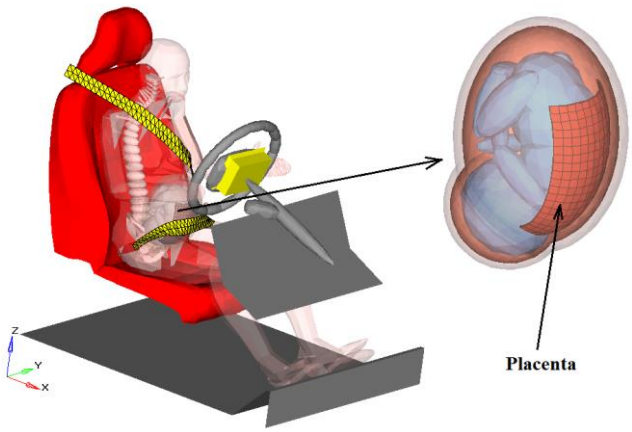

Figure 6.10 'Expecting' with anterior placenta model

6.6.3 Simulation Results

For the fully restrained pregnant occupant, the maximum strains at the UPI are presented in Figure 6.11, for the range of crash scenarios simulated. Figure 6.11 shows that the strain at the UPI for the placenta located at anterior in the uterus is always higher than all other placental locations. Especially, at a crash speed of 30 km/h, there is a significant maximum strain difference between placenta at other positions and anterior position, the latter exceeding the threshold level. Figure 6.11 also shows that the strains at the UPI for the placenta located at posterior, lateral right and left, all remain below the threshold levels, similar to the results from 'Expecting', at all speeds considered. Although placentas located at lateral left and right are designed symmetric from sagittal plane of 'Expecting', simulation results for these placenta models are not identical, because the three-point seat belt is not symmetrical. Furthermore, the multibody fetus in the uterus model is not symmetric either, due to the crossing of legs, where the left leg of the fetus interacts differently with placenta to right leg of the fetus. For all range of crash speed cases when pregnant occupant is fully restrained, strain values for placenta located at lateral right is always lower than placenta located at fundus (Figure 6.11). The only danger to fetus is at the crash speed of 30 km/h for the placenta located at anterior position in the uterus.

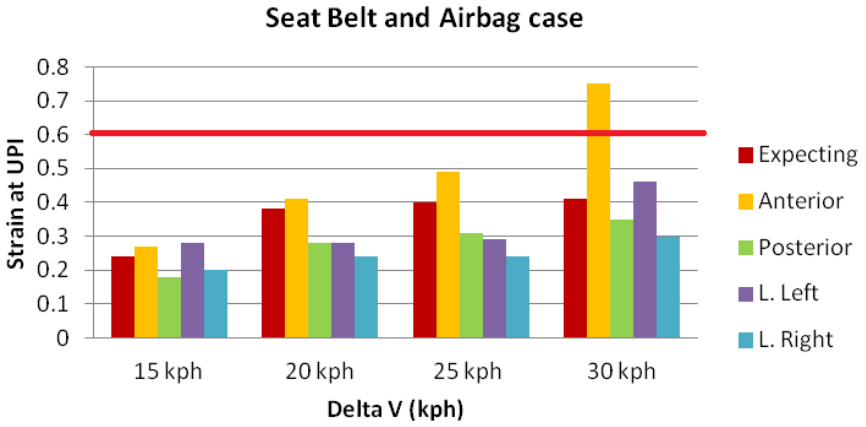

Figure 6.11 Occupant fully restrained, maximum von Mises strains at the uteroplacental interface comparison for the four different placental locations

'Seat belt only' case is investigated in detail to show the influence of different placenta locations on fetus injuries and mortality (Figure 6.12). Airbag is not activated in this case. For 'seat belt only' case, strain values at UPI for low crash speeds e.g., 15 and 20 km/h, are low in general whereas strains are higher at higher speeds compared to the fully restrained case. Similarly only a crash speed of 30 km/h, strain value at UPI exceeds threshold level when placenta located at anterior. Generally, posterior, lateral left and right placenta locations result in lower strain levels. These results shows that fetus of a pregnant driver who has a placenta which is located at fundus and at anterior in the uterus is more at risk than fetus of a pregnant driver who has placenta located at posterior, lateral left and lateral right.

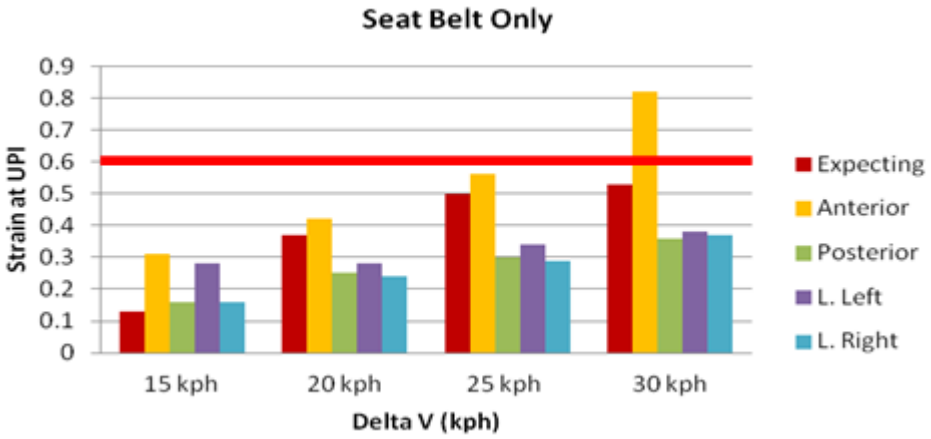

Figure 6.12 'Seat belt only' case, maximum von Mises strains at the uteroplacental interface comparison for the four different placental locations

Figure 6.13 depicts the fetus, placenta located at anterior in the uterus and the lap belt. It is clearly seen that strain is developed from the loading of lap belt with placenta located at anterior. The anterior placenta and uterus are sandwiched between the belt and the fetus. Peak von Mises strains for placenta located at anterior is always higher than placenta located at fundus.

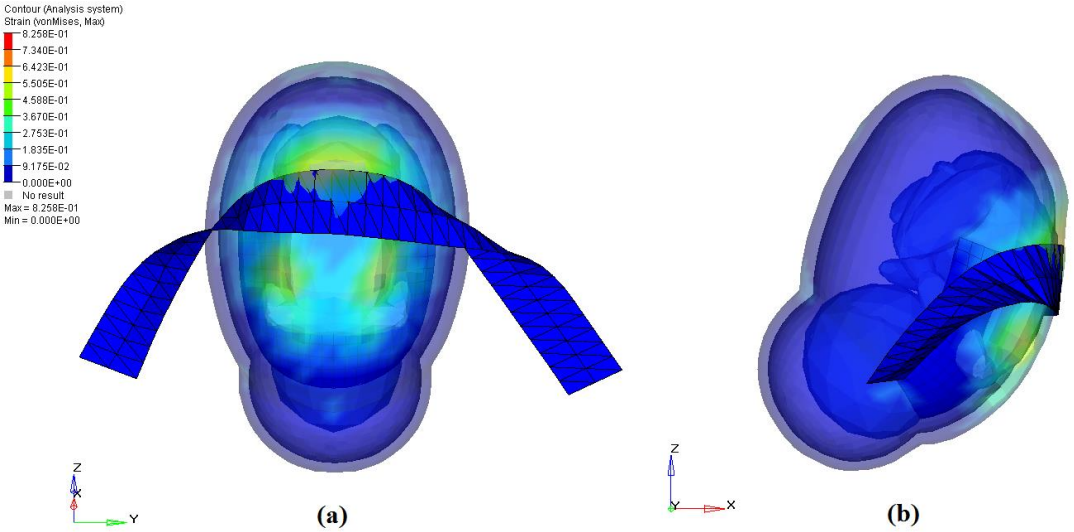

Figure 6.13 Anterior placenta and lap belt; (a) Front view, (b) Side view

Figure 6.14 shows the peak strains at the UPI for five different placenta locations when there is only airbag exist as a restraint system. Strain values for all placental locations at a crash speed of 15 km/h are under threshold value for placental abruption. However, at higher crash speeds, significantly different strain values are derived when placenta is located from fundus to other positions. Figure 6.15, clearly shows that airbag and steering wheel loading on uterus generates generally higher strain values at the UPI for all placenta locations but the highest strains occurring at anterior and fundus positions. These results show that the safest position for the fetus of pregnant driver is to have the placenta located at posterior region in the uterus. Comparison of Figure 6.11 and Figure 6.14 also shows that, not wearing the seat belt and relying on the airbag only appears to be hazardous for a pregnant driver.

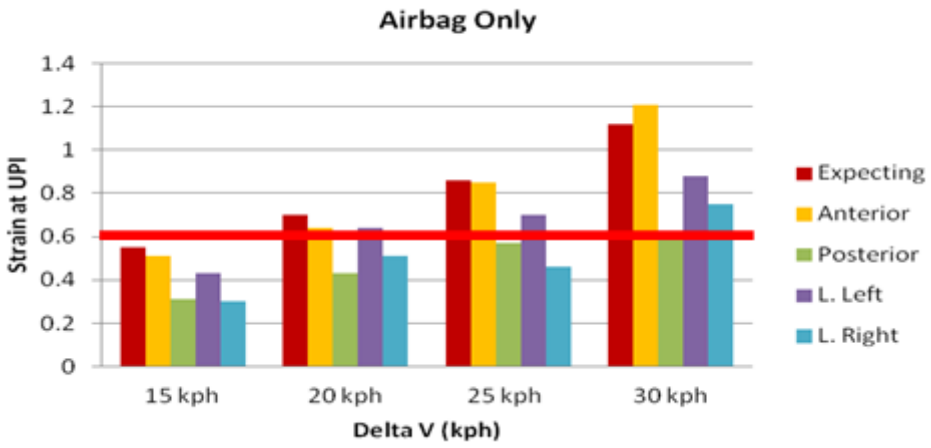

Figure 6.14 'Airbag only' case, maximum von Mises strains at the uteroplacental interface comparison for the four different placental locations

'No restraint' case is analysed in detail to express the influence of five different placenta locations on fetus injuries and fatality (Figure 6.15). Maximum von Mises strains at the UPI are investigated when there is no airbag and seat belt restraint systems. Strain values for 'Expecting' at all crash speeds are above threshold value for placental abruption, whereas strains at UPI when placenta is located at anterior is below and on the threshold value for 15 and 20 km/h crash speeds. For a crash speed of 30 km/h, different strain values are derived when placenta is located from fundus to other locations. These results shows that fetus of a pregnant driver who has placenta which is located at fundus and anterior in the uterus is more likely to be injured seriously than fetus of a pregnant driver who has placenta located at posterior.

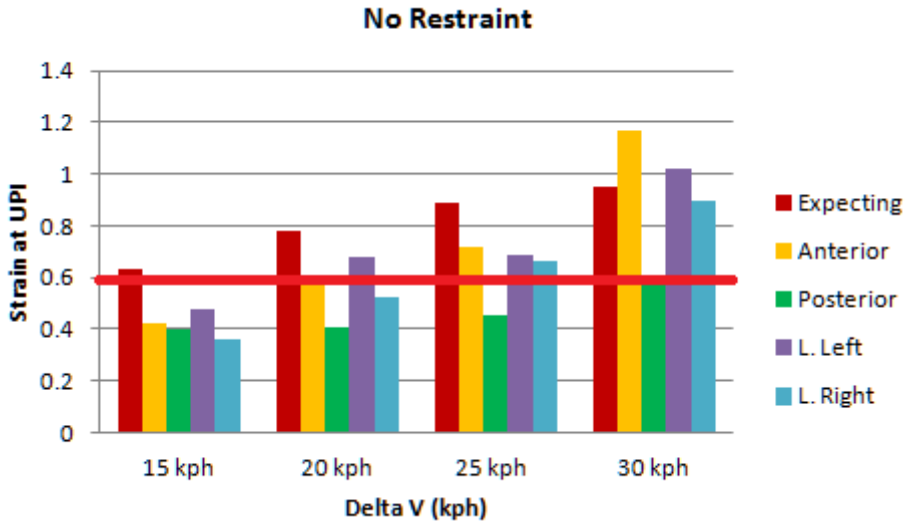

Figure 6.15 'No restraint' case, maximum von Mises strains at the uteroplacental interface comparison for the four different placental locations

6.7 Conclusions

The Chapter focused on the effects of placental locations on the fetus injuries and mortality. The impact of placenta position on the risk of placental abruption was investigated. It was found that the placenta position plays important role on the risk of fetus mortality. The highest peak strain value was generated at anterior placenta, whereas posterior placenta generated relatively low peak strain values. Results also

showed that the risk of placental abruption for the anterior placenta and the placenta positioned at fundus were high and the difference between the two was very little for the range of crash speeds at 'airbag only' case. It was found that wearing seat belt and activated airbag restrained systems protects the fetus well in all cases. This study has found that fetus of a pregnant driver who has a placenta located at anterior in the uterus is more likely to be injured than fetus of a pregnant driver who has a placenta located at original position (fundus) of 'Expecting'.

CHAPTER 7

FETUS IN AMNIOTIC FLUID

7.1 Introduction

Amniotic fluid is vital to the well-being of a fetus. From the beginning of the first trimester to the end of pregnancy, amniotic fluid always exists inside of the uterus. Accumulation of the amount of water-like liquid is important to support fetal growth and to allow for maternal physiological changes. The amniotic fluid cushions a fetus from injuries. It also surrounds the fetus and allows free movements for the fetus. Although the volume of amniotic fluid changes with the growth of the fetus during pregnancy, this circulation and interaction continues until the end of pregnancy. This protective liquid contained by the amniotic sac of pregnant women plays a significant role in fetus safety. Its interaction with the fetus needs to be investigated to create a realistic model.

In the original 'Expecting' model, the cushion effect of the amniotic fluid is obtained with defining damping characteristics between the multibody fetus and pregnant occupant in MADYMO (Acar and Lopik, 2009). In the literature review in

Chapter 3, it was explained that Moorcroft *et al.,* (2003) developed a finite element amniotic fluid model in the uterus without the fetus in their design. In this work, crash test simulations with pregnant occupant models are conducted with the fetus but the effect of the physical amniotic fluid is mimicked with cardan restraints. Finite element amniotic fluid model filling the uterus entirely, without the fetus is developed in Chapter 5 in order to investigate the effect of no-fetus in the uterus. The original 'Expecting' with the fetus and the modified model without the fetus, amniotic fluid only, are compared and shown that the fetus plays a significant role in the dynamic behaviour of the pregnant abdomen. Finite element amniotic fluid model surrounding the multibody fetus is developed to create a more realistic representation of the pregnant abdomen.

7.2 Anatomy of Amniotic Fluid with Fetus

Amniotic fluid in the uterus exists from the first trimester of pregnancy to the end of the pregnancy. In the first trimester of pregnancy, fluid is derived from the maternal circulation across placenta. It then circulates through the fetal membranes by osmotic and hydrostatic forces. After about 12-14 week of gestation, the liquid contains proteins, carbohydrates and urea, which aid in the growth of the fetus. Fried (1978) found that approximately 98-99% of amniotic fluid is water. By 25 weeks of pregnancy, the fetal lung and bladder contributes to amniotic fluid volume. Fetal urine becomes the major source of amniotic fluid in the second trimester of pregnancy.

Normal amniotic fluid volume changes steadily through pregnancy. Wide variation of these changes also exists. Figure 7.1 illustrates approximate volumes at various gestational ages, based on a compilation of 12 published studies of amniotic fluid volume (Brace and Wolf, 1989). Amniotic fluid volume is represented in millilitre while the gestation age is defined as weeks of pregnancy. The data summarizes covering 8 to 43 weeks' gestation. According to the diagram, amniotic fluid has a uniform variability from 8 to 43 weeks of pregnancy. Mean amniotic fluid volume does not change significantly between 22 and 39 weeks of pregnancy. Figure

7.1 also shows that amniotic fluid volume reaches a peak volume at 32 to 33 weeks of pregnancy.

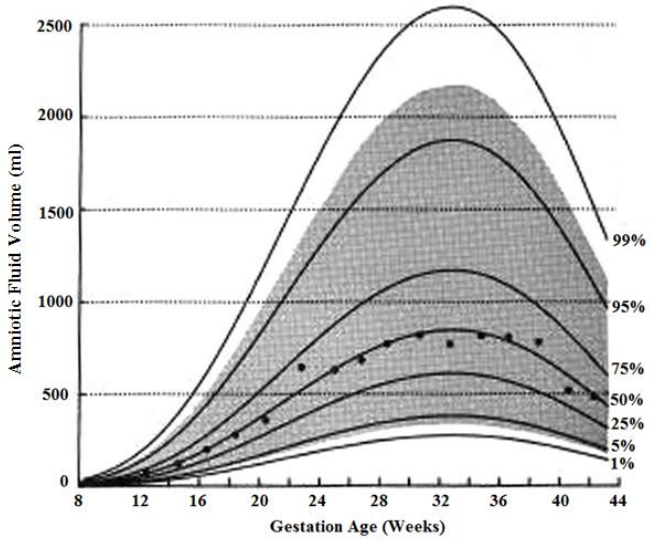

Figure 7.1 Amniotic fluid volume as a function of gestation age (Brace and Wolf, 1989)

Volume of amniotic fluid is an important indicator of fetal well-being. Therefore, amniotic fluid volume should be evaluated together with evaluation of the fetal growth. The ratio of amniotic fluid to fetal volume increases until approximately 30 weeks of pregnancy and then appears to decline. The volume of amniotic fluid is correlated with growth of the fetus until about 28 weeks of gestation. Anatomy of the amniotic fluid indicates that the amniotic fluid and the fetus should be always considered together in the uterus.

7.3 Computational Amniotic Fluid Model

The amniotic fluid is modelled with finite elements while the multibody fetus model still exist in its original position to create more realistic 'Expecting' model. This model allows investigating the cushioning effect of the amniotic fluid on the fetus and the uterus motion at the crash test simulations.

Representation of the cushion effect of amniotic fluid in the original 'Expecting' model is explained in Chapter 3. Parallel springs and dampers that connect the fetus and pregnant occupant bodies define cushioning effect of amniotic fluid in the 'Expecting'. Fetus damping characteristics has been defined by the MADYMO codes.

In order to model the amniotic fluid in the finite element uterus model, the multibody fetus model and its cardan restraints which are dampers and springs are extracted from the uterus model. Chapter 5 reports a model of the uterus which is completely filled with 4-noded tetrahedral elements to represent the amniotic fluid. The fetus is placed in its original position and the amniotic fluid elements which are replaced with the multibody fetus components are deleted one by one in order to represent the amniotic fluid and the fetus simultaneously inside of the uterus. Figure 7.2 illustrates this modelling process. Figure 7.2 (a) shows that entire volume of the uterus is filled with amniotic fluid (Chapter 5). Figure 7.2 (b) illustrates the uterus model with the fetus and the amniotic fluid simultaneously inside of the uterus. It is clearly seen that the 38th weeks of pregnancy, the fetus occupies significant volume in the uterus. The mass of the fetus is 3.3 kg, whereas the mass of the amniotic fluid is about 0.5 kg.

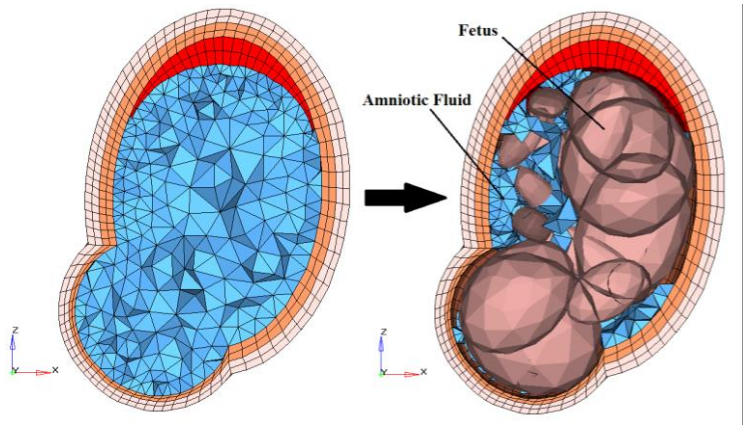

(a) (b)

Figure 7.2 The finite element amniotic fluid and the multibody fetus modelling process; (a) Only FE amniotic fluid model from Chapter 5, (b) FE amniotic fluid and the fetus model

The volume of the amniotic fluid in the uterus is reduced by deleting finite elements one by one according to the volume of the fetus. Due to the zero gap between the fetus body and the uterus at some points, amniotic fluid elements are deleted completely and direct interaction occurs between the fetus and the uterus. Specifically, the head of the fetus touches to the base of the uterus directly due to the gravitational force on the fetus body. Material properties for the amniotic fluid model are taken from Section 5.4.Table 7.1 shows material model and properties used to define the computational amniotic fluid model in MADYMO.

Table 7.1 Amniotic fluid material properties

	Material Model	Young's modulus (kPa)	Density (kg /m^3)	Poisson's ratio
Amniotic Fluid	Linear Elastic	20	993	0.49

7.4 Model Validation

The facet 5th percentile female occupant model has been validated as described in Happee *et al.* (2000) published small female impactor corridors for the SID2s dummy (Daniel *et al.,* 1995) and some other female PMHS tests. The MADYMO human facet occupant model has been previously validated against rigid bar impact, belt loading with cadaver tests for frontal, lateral, and rearward impact loading (Happee *et al.*, 2000), (MADYMO Human Models Manual, 2010).

The existing MADYMO human female model was modified to represent 'Expecting' pregnant occupant which is explained in Chapter 3. An accurate and realistic response of the pregnant abdomen is necessary to predict risk of fetal injuries and fatalities for the computational pregnant women model. Rigid bar impact and belt loading tests performed by Hardy *et al.* (2001) were used to validate 'Expecting', pregnant occupant model (Acar and Lopik, (2009). Same validation tests are conducted to validate the modified 'Expecting ' model.

7.4.1 Rigid Bar Impact Test

Force-deflection abdominal corridors for a 50th percentile male based on dynamic testing of human cadaver (175 cm, 88 kg, 80 years) have been developed by Hardy *et al.*, (2001). These corridors have been scaled to a 5th percentile female by Rupp *et al.*, (2001) in the development and validation of the MAMA2B ATD. Response of the computational pregnant occupant model to impacts is evaluated with these corridors. The impact test is conducted using a ballistic pendulum with a rigid bar impactor in the test set up (Acar and Lopik, 2009). The 'Expecting' model validation is explained in detail in Chapter 3. Figure 7.3 depicts a rigid bar impact test for the modified 'Expecting' model. The grey colour rigid bar in front of the pregnant occupant's abdomen illustrates the impactor.

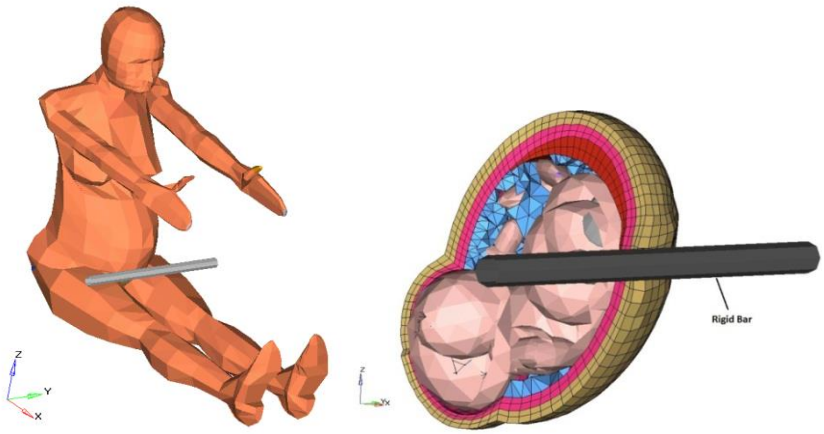

Figure 7.3 Modified 'Expecting' rigid bar impact test

The same test set up was described by Hardy *et al.*, (2001) to develop a 6 m/s (21.6 km/h) abdominal response corridor. The force-displacement response of the model and results of earlier researchers to the 6 m/s (21.6 km/h) rigid bar loading case are shown in Figure 7.4.

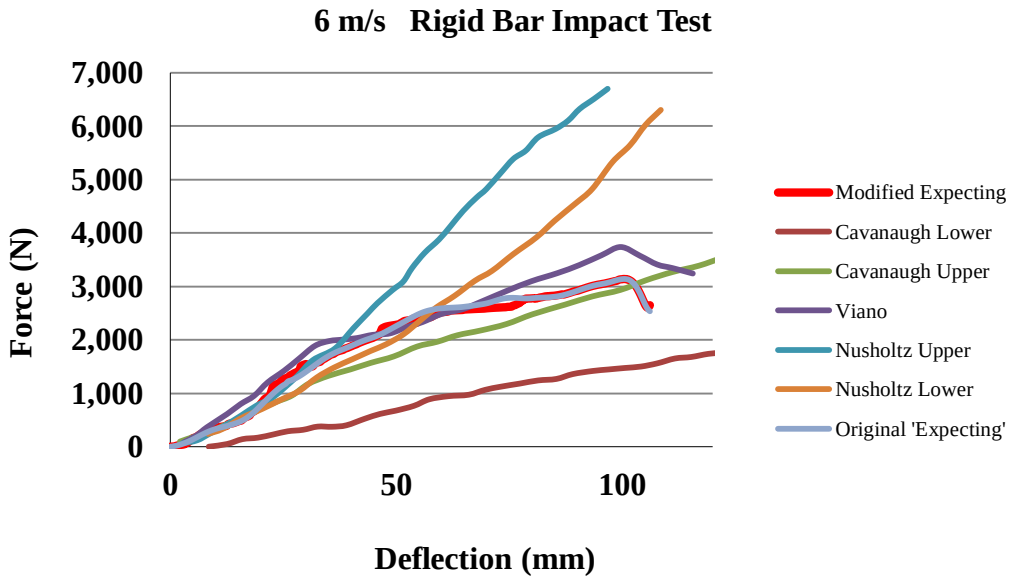

Figure 7.4 Abdominal response of the modified pregnant occupant model, 'Expecting', to 6 m/s (21.6 km/h) rigid bar impact test compared with the results of earlier researchers

Force-displacement of the pregnant abdomen was recorded and found to be in reasonably good agreement with the experimental data falling within the defined response corridors. Figure 7.4 also shows that there is significant similarity between 'Expecting' and modified 'Expecting' models.

7.4.2 Belt Loading Test

A dynamic belt loading test was conducted to validate 'Expecting' by Acar and Lopik, (2009) and explained in detail in Chapter 3. For belt-loading a finite element belt is initially wrapped around the pregnant abdomen at mid-umbilical region and is pulled across the pregnant abdomen at 3 m/s (10.8 km/h) (Figure 7.5). Belt penetration is calculated by determining the motion of the belt relative to the position of the lumbar spine.

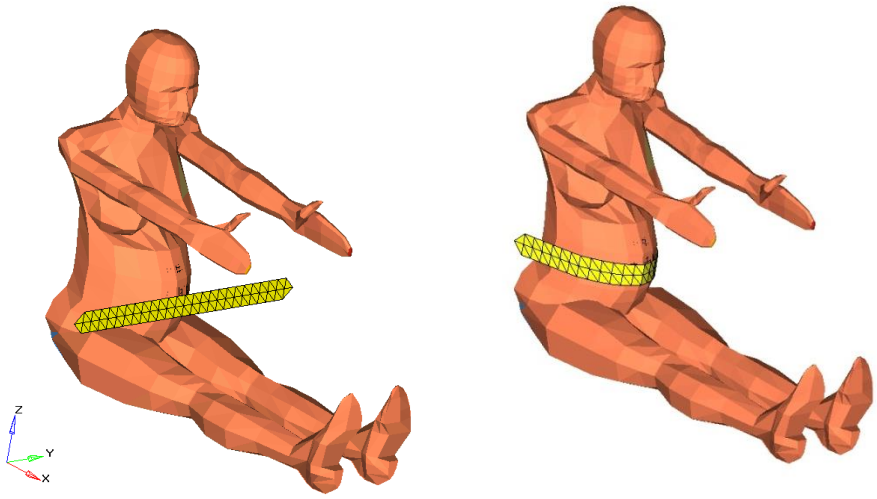

Figure 7.5 Belt loading test

Belt loading on the uterine wall generates high von Mises stresses around the uterine wall where the finite element belt and back of the fetus interact. Figure 7.6 shows the von Mises stress distribution in the uterus as a result of the belt loading test. Von Mises stress increases when the blue colour contour becomes lighter. Along the path of the lap belt line, the highest stress concentration is observed. Stress distribution is low at posterior wall of the uterus. Figure 7.6 illustrates that the fetus still play significant role in the uterus while the finite element amniotic fluid model exists in the model.

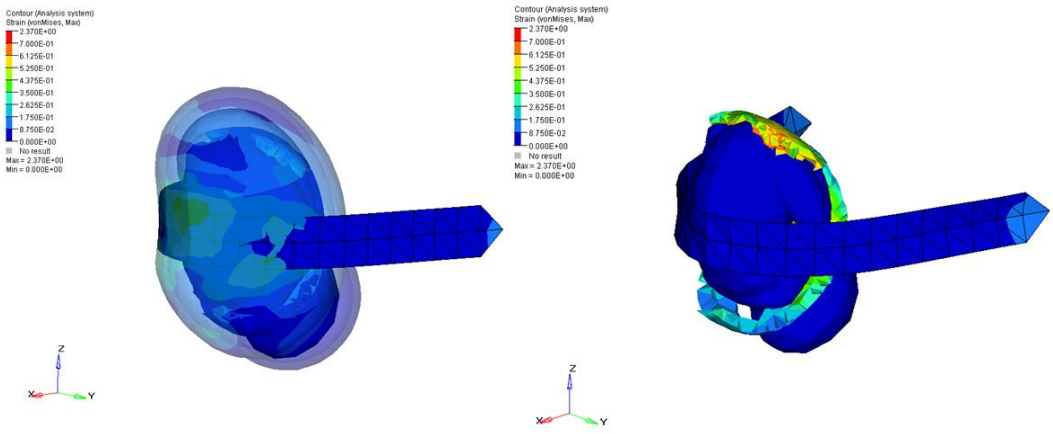

Figure 7.6 Modified 'Expecting' belt loading test

Figure 7.7 shows abdominal response of the pregnant occupant model to the 3 m/s (10.8 km/h) belt loading. Red colour lines illustrate scaled abdominal response corridors to belt loading performed by Hardy *et al.*, (2001). The blue line depicts abdominal responses of the modified 'Expecting' model and it shows that pregnant abdomen deflections are within the corridors (Figure 7.7). However, at about 30 mm abdominal deflection, response is on the lower corridor with approximately 2500 N loading.

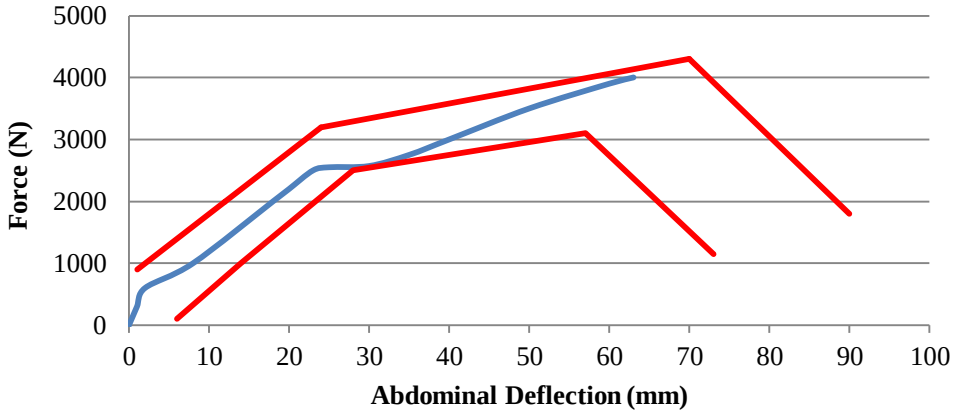

Figure 7.7 Abdominal response of the pregnant occupant model, to 3 m/s (10.8 km/h) belt loading compared against the response corridor

Rigid bar impact and belt loading tests results are within the response corridors and hence validate the modified 'Expecting' model. For both cases the force-deflection responses of the abdomen of the modified 'Expecting' model are recorded and found to be in reasonably good agreement with the experimental data.

7.5 Crash Test Investigations with Finite Element Amniotic Fluid and Multibody Fetus Model

The modified 'Expecting' model is used to simulate a range of frontal impacts of increasing crash severity from 15 km/h to 35 km/h. Totally, 20 tests are run with collision speeds increasing in 5 km/h steps. Several simulations are chosen to investigate the effect of the finite element amniotic fluid model on the dynamics of the abdomen. The modified 'Expecting' model is used in identical crash test

simulations of the original 'Expecting' model. These include (i) 'seat belt and airbag', incorporating a 3-point seat belt and a frontal airbag, in other words representing a properly restrained pregnant driver; (ii) 'seat belt only' excludes the airbag but includes a 3-point seat belt; (iii) 'airbag only' excludes the seat belt, but the airbag is still active; and finally (iv) 'no restraint' represents no restraint systems at all, in other words neither the 3-point seat belt is worn nor is the airbag deployed. Half-sine waves are used to represent the acceleration pulses with duration of 120 ms as shown in Chapter 4, Figure 4.5.

Maximum von Mises equivalent strain levels in the uterus at uteroplacental interface (UPI) and in the overall uterus are found for the modified 'Expecting' model. Crash test results of the modified 'Expecting model are compared with the original 'Expecting' model. Figure 7.8 shows a typical ‘seat belt and airbag' restrained pregnant driver model with the finite element amniotic fluid at impact speed of 30 km/h.

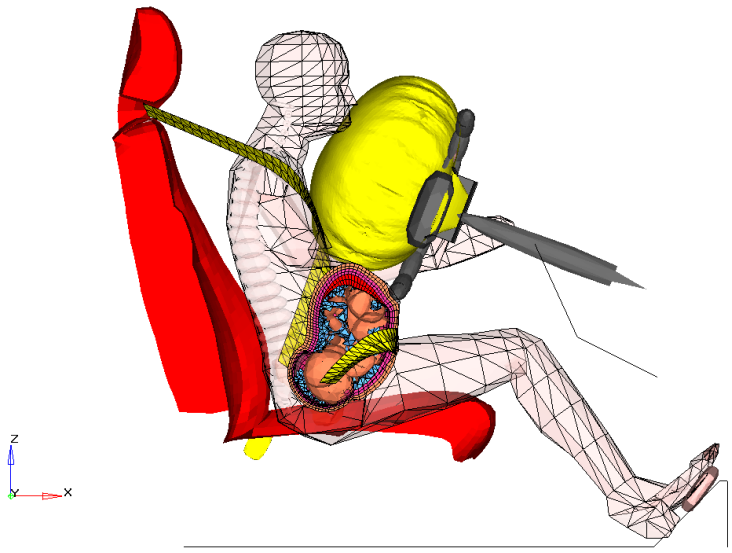

Figure 7.8 Typical frontal impact responses for 30 km/h

The peak strain values at the uteroplacental interface increase with crash speed for all crash scenarios as expected. In general, the maximum strain of the modified 'Expecting' model is typically higher than the strains of the original

'Expecting' model. This could be attributed to the removal of springs and dampers simulating the amniotic fluid cushioning in the absence of amniotic fluid in the original 'Expecting'. Furthermore, as the amount of amniotic fluid is only about 0.5 lt, it does not have a significant cushioning effect on 3.3 kg fetus.

The 'seat belt and airbag' case results for the maximum strains at the uteroplacental interface are shown in Figure 7.9. The original 'Expecting' model simulation results show lower strain levels than the modified 'Expecting' model simulations for all crash severities, but this is more pronounced at speeds of 30-35 km/h. At 30 km/h and 35 km/h impacts, strain values at the UPI for the modified model are above the injury threshold value of 0.60.

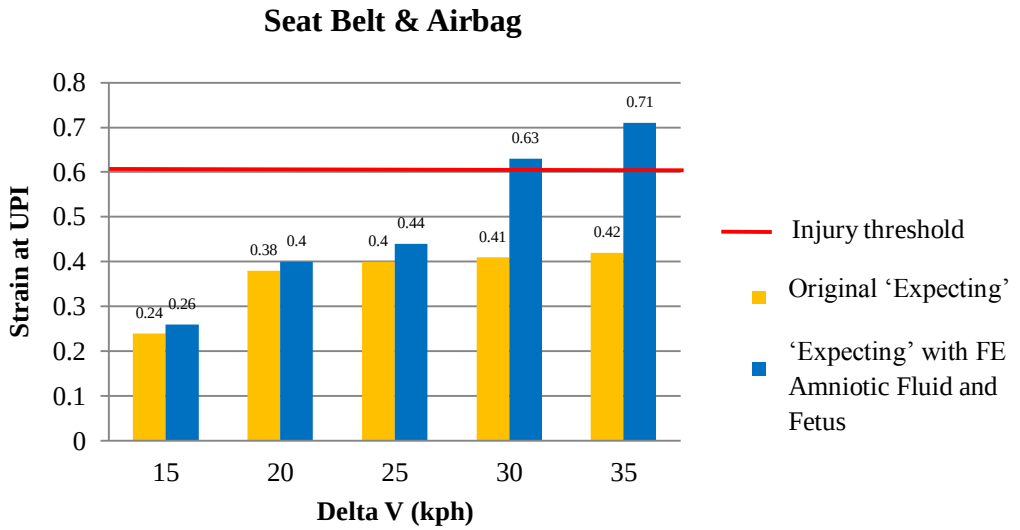

Figure 7.9 Modified 'Expecting' with and without the fetus for 'seat belt and airbag case'. Maximum von Mises strains at the uteroplacental interface comparison for the 'With and without the fetus' cases

Figure 7.10 compares the peak strain levels for the 'seat belt only' case for crash severities of 15 km/h to 35 km/h. At 15 km/h and 20 km/h impacts, the strain levels for the both models are very close to each other. However, after the crash speed of 25 km/h, there is considerable difference in strain between the two models. Placental abruption occurs at a crash speed range of 25-35 km/h for the model with the computational amniotic fluid model while the all strain values at the UPI are below the injury threshold value of 0.6 for the original 'Expecting'. With the finite element amniotic fluid model with the multibody fetus the maximum strains at UPI are much more pronounced at higher speeds and the placental abruption risk is found to be higher.

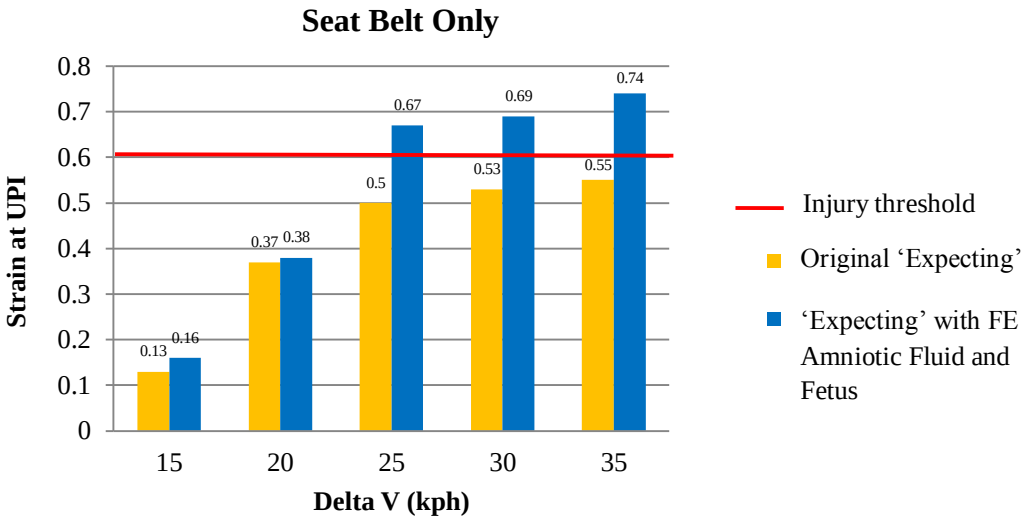

Figure 7.10 Modified 'Expecting' with and without the fetus for 'seat belt only case'. Maximum von Mises strains at the uteroplacental interface comparison for the with and without the fetus cases

The 'airbag only' case results for the maximum strains at the UPI of 'Expecting' and with finite element amniotic fluid models are shown in Figure 7.11. Almost all strain levels at the UPI for both models are above the threshold value of 0.6, so there is close agreement between the two models. Due to the high impact loading from deployment of airbag, placental abruption occurs even at 15 km/h. Maximum strains at the UPI for the 'Expecting' with the FE amniotic fluid and the original 'Expecting' models are very similar, the amniotic fluid model being slightly higher, except the 35 km/h case, where there is a considerable difference in strain at a crash speed of 35 km/h between the models. This is an indication of the dynamics of the pregnant abdomen including the fetus becoming more significant at higher speeds.

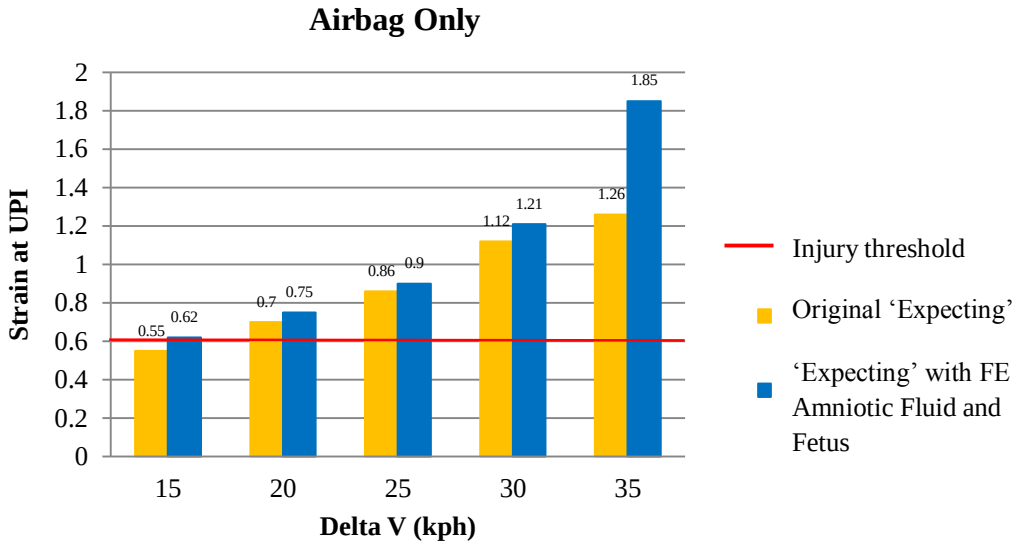

Figure 7.11 Modified 'Expecting' with and without the fetus for 'airbag only case'. Maximum von Mises strains at the uteroplacental interface comparison for the with and without the fetus cases.

Figure 7.12 shows the maximum strain levels at the UPI for the 'no restraint' case. The placental abruption risk emerges at a crash speed of 20 km/h when the amniotic fluid is represented as a finite element model, whereas at all crash speeds, placental abruption occurs for the original 'Expecting' model. There is a greater increase in strain from 25 km/h to 35 km/h for the modified model, whereas the increase for the original model is gradual and almost linear.

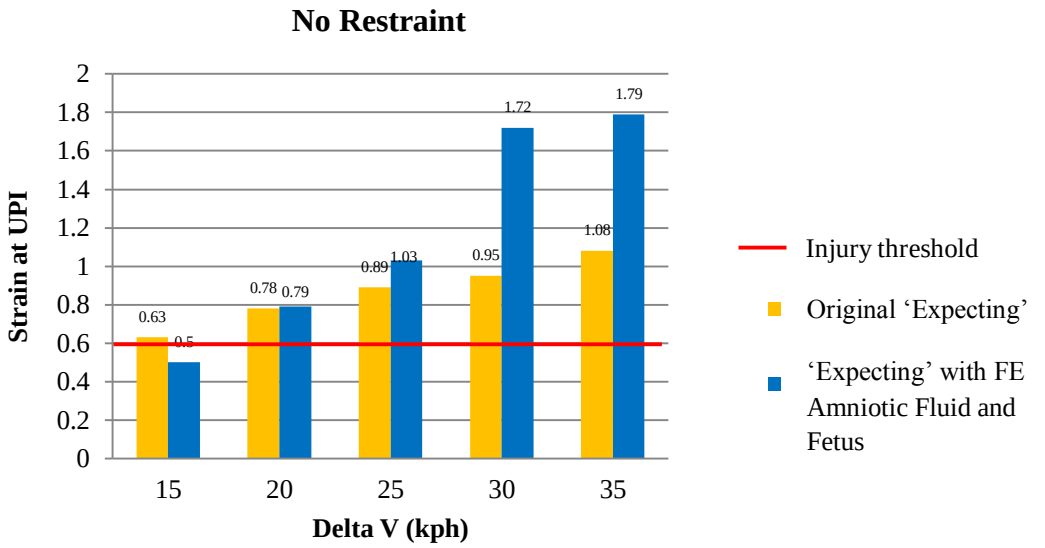

Figure 7.12 The modified 'Expecting' with and without the fetus for 'No restraint case'. Maximum Von Mises strains at the uteroplacental interface comparison for the with and without the fetus cases

7.6 Conclusions

The effect of including a finite element amniotic fluid model filling the voids in the uterus with the multibody fetus within the 'Expecting', the pregnant occupant model, were investigated. A computational amniotic fluid model while the multibody fetus still exists in the uterus was developed. In order to do that, the full amniotic fluid model in the uterus which was developed in Chapter 5 was used. Material properties for the water-like liquid model were taken from Chapter 5. Rigid bar impact and belt loading tests were used to validate the modified 'Expecting'. Force-deflection abdominal corridors were used and the 'Expecting' with the amniotic fluid and the

multibody fetus model results were found to be in reasonably good agreement with the experimental data. The validated model was used to simulate a range of frontal impacts of increasing severity from 15 km/h to 35 km/h. Four levels of occupant restraint, seat belt and airbag, seat belt only, airbag only, and completely unrestrained were investigated.

Maximum strain levels in the uterus at the placental location obtained from modified model were compared with the original 'Expecting'. At high crash speeds, it was observed that the increase in the UPI strain was greater for the modified model. For both models, the peak stress was observed on the anterior wall of the uterus. Fetal and amniotic fluid movement caused the high strain levels in the uterus when the amniotic fluid was represented physically between the fetus and the uterus.

For the 'unrestrained' and 'airbag only' cases, loading from the steering wheel and airbag significantly increased the maximum strain at the UPI for both models. However, higher velocity impacts for all restraint cases, maximum strain values at the UPI for the modified model were considerably greater than the original model. Although both models followed a similar pattern and close maximum strain results were seen at low crash speeds for all cases, the spring-damper characteristic representation of the amniotic fluid cushioning effect were stiffer at higher speeds resulting in lower strain levels than the finite element representation of the amniotic fluid.

CHAPTER 8

HYBRID FETUS MODEL

8.1 Introduction

During pregnancy, as the fetus grows and develops, a number of anatomical changes occur to the female body to accommodate the growing fetus, including placental development, amount of amniotic fluid, abdominal extension. In 'Expecting', a 38 week fetus is represented in the uterus. During this final trimester of pregnancy, the bones and skeleton system of the fetus develop rapidly. The head of the fetus undergoes structural and morphological developments. The skull of the fetus becomes stiffer and heavier. Over the final trimester, the head becomes the heaviest part of the unborn occupant. Approximately 1 kg mass of the solid fetus head and its large volume might play a significant role on dynamic motion of the pregnant abdomen. In addition, its position in the uterus is crucial. It may cause deformations to the uterus and may even play a role in causing placental abruption during an impact.

The whole fetus model in the original 'Expecting' is developed as multibody, hence the head does not deform. A deformable head may change the dynamics of the system and therefore can affect the stress and strain levels in the uterus. Hence a finite element fetus head model replaced the multibody fetus head.

In this study, the effect of further developments to 'Expecting', by incorporating a finite element fetus head model is investigated. In order to generate deformable fetus head model, further detailed anatomic head geometry is used. The hybrid fetus and finite element amniotic fluid model are validated with lap belt loading and the rigid bar impact tests. Interactions between the uterus and head of the fetus are studied. The effect of having a finite element head fetus on the strains at the uteroplacental interface is discussed. 'Expecting' model is used to simulate several crash test severities and risk of placental abruption is investigated.

8.2 Fetus Head Modelling

8.2.1 Anatomy of Fetus Head

Anatomy of human head is complicated. There are several layers of different tissues covers the brain. Their material, mechanical and anatomic properties are different. There have been many studies on biomechanics of adult human head as early as 1950s (Roche, 1953; Dekaban, 1977). Anatomical dimensions and properties of the adult human head are available. In order to investigate adult human head injuries, these anatomical data were used and a number of different finite element head models were developed (Sances and Yoganandan, 1986; Willinger, R., et al, 1999; Zhang, *et al.* 2001). However, in contrast to adult head studies, there are relatively few studies investigating the biomechanics of the fetus head. Modelling of the fetus head is limited due to lack of experimental and real world data.

Basically, the fetus head consists of scalp, skull, and brain layers from exterior to interior (Figure 8.1). The brain is protected by outer layers, mainly by the skull. There are four regions in the bony skull. The frontal bones, the parietal bones, the occipital bone, and face/base region (Figure 8.1). Displacements of these bones

are limited. From a structural point of view, there is significant difference between adult and fetus skull. The skull of the fetus consists of thin, flexible plates, soft bony tissue, while adult skull is very stiff. The skull of the fetus consists of a soft spot which are called fontanel. Its approximate dimensions are 3 cm by 3cm. This diamond shape space assists the bony regions of the skull to flex and allow the head of the fetus to pass through birth canal. Material properties of the soft spot are different than the fetus skull and the skull thickness of the fetus is less than that of the adult human skull.

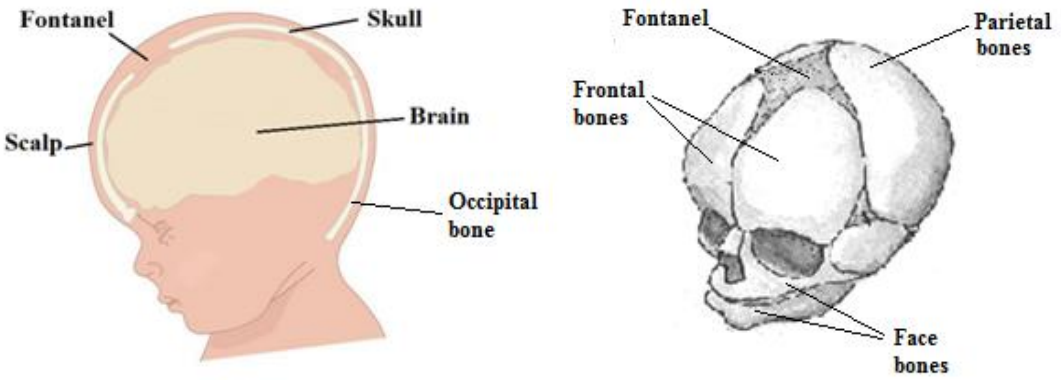

Figure 8.1 Anatomy of a fetus head (adapted from UTMS)

The fetal head is connected to the neck with articulation through occipital condyles, supporting ligaments. However, this connection is very weak. In order to have a correct finite element analysis, it is necessary to know precisely the anatomy of the head. Semi axes of the head were defined by using ultrasound measurements of the biparietal diameter (BPD) and occipito-frontal diameter (OFD) (Figure 8.2). Snijders and Nicolaides (1994) measured the head from the outer boundary of the skull. These two main measurements, the mean BPD (96mm) and OFD (115mm) for a 38th week old fetus head model are taken as reference in the original 'Expecting' model (Acar and Lopik, 2009, 2012). Pheasant (1998) investigated head of newborns and found the mean head breadth (95mm) and head length (120mm). Head breadth is defined as maximum breadth of the head above the level of the ears. Head length is

distance between the glabella (the most anterior point of the forehead between the brow ridges) and the occiput (back of the head) in the midline (Pheasant, 1998 cited in Acar and Lopik, 2012).

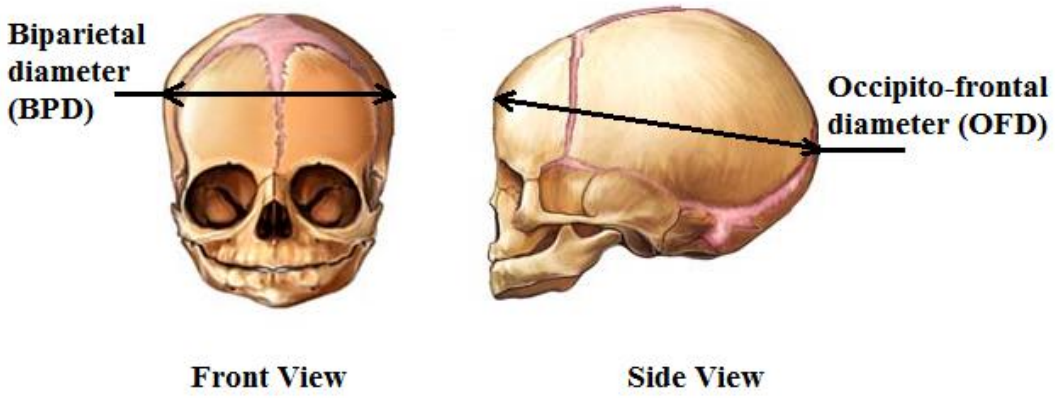

Figure 8.2 Fetus head diameters (adapted from MBBS Medicine)

8.2.2 Finite Element Modelling of the Fetus Head

Anatomic geometry of the fetus head is taken as the reference geometry to develop a finite element head model. Geometry of the ellipsoidal rigid structure is redefined to represent deformable head body. Face of the fetus which is also rigid ellipsoid component is considered as part of the skull geometry. The skull, fontanel, and brain, which are the main anatomical features of the head, are modelled. Meshing of the finite element head is performed using the HyperMesh (Altair HyperMesh 7.0 software). Nodes and elements are created in HyperMesh then exported to the MADYMO. The FE_MODEL attribute is defined under SYSTEM.MODEL file of fetus to write finite element codes of the head. Node coordinates are recorded in one table and elements are written in another. Two GROUP_FE files are created to define the finite element skull and brain with fontanel. The finite element skull model is composed of 4-noded tetrahedral elements. Each element has a single integration point. Unlike the eight-node hexahedral element, the one-point integration of the four-node tetrahedral element does not result in any zero energy or hourglass mode. The tetrahedral elements are also more suitable for modelling complex bodies and surfaces than the eight-node hexahedral elements.

Modelling complex bodies and surfaces including head models, when using eight-node solid elements, the shape of the element becomes often quite poor, resulting in a loss of accuracy or leading to numerical instability. This problem is avoided by using four-node tetrahedral elements. Two layers of these brick elements cover approximately 85 % of the head leaving fontanel at the top of the head (Figure 8.3). The fontanel is represented as a diamond shape using 4-noded tetrahedral elements as well.

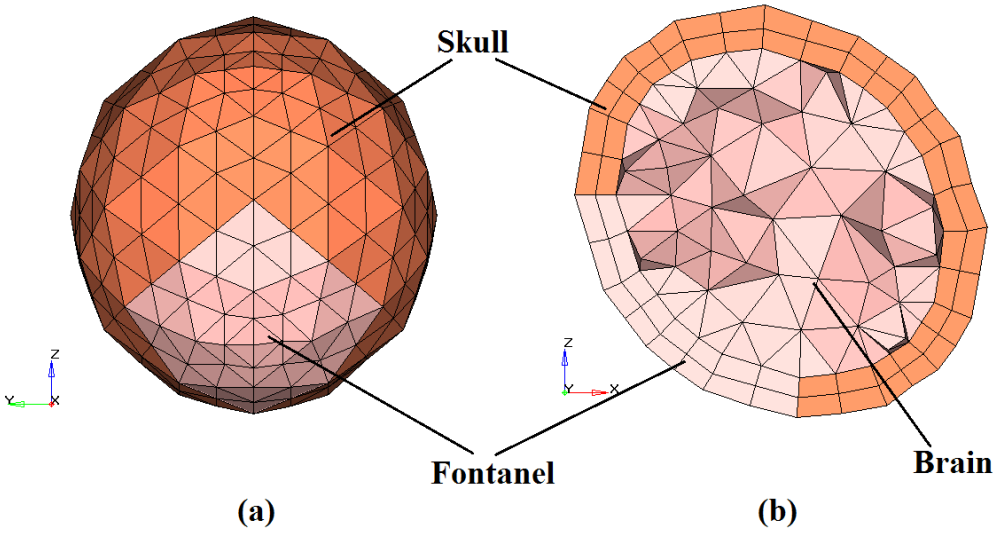

Figure 8.3 Finite element fetus head; (a) Front view, (b) Side view

The brain is also represented with tetrahedral brick elements inside of the skull. Globally, the model consists of brick elements. The brain is assumed homogeneous. The mass of the global head is approximately 1 kg.

In order to determine the density of the finite element mesh of the fetus head, a mesh convergence study is performed. In finite element modelling, more accurate results are generated if a finer mesh is used. However, mesh developed with finer elements increases computational time. It is important to have accurate interpolation inside each element when their mesh is defined. The number of elements is varied in this study to determine the mesh density of the model. In order to analyse the model, finite element head models are dropped from 0.5 m height onto the rigid plane and

maximum von Mises strains are compared (Figure 8.4). Drop position and orientation of the fetus head is taken same as in the uterus. Density of the finite element fetus head mesh model is chosen 1 at the beginning of this convergence study. The mesh of the head model is recreated with a denser element distribution and reanalysed. The results are compared with the previous mesh. The mesh density is kept increasing from 1 to 4 and the model is reanalysed until the results converge satisfactorily. It is observed that the strain results at the finite element head model converged upon a solution 0.72 as the mesh density increased. The model is consistent and stable when the mesh density is 2 (Figure 8.5). Although the mesh density is increased up to 4, there is no considerable change observed in maximum von Mises strains. Therefore, the fetus head model is meshed according mesh density of 2 as the run time would be much smaller compared to size 3 and 4 with no real gain in accuracy.

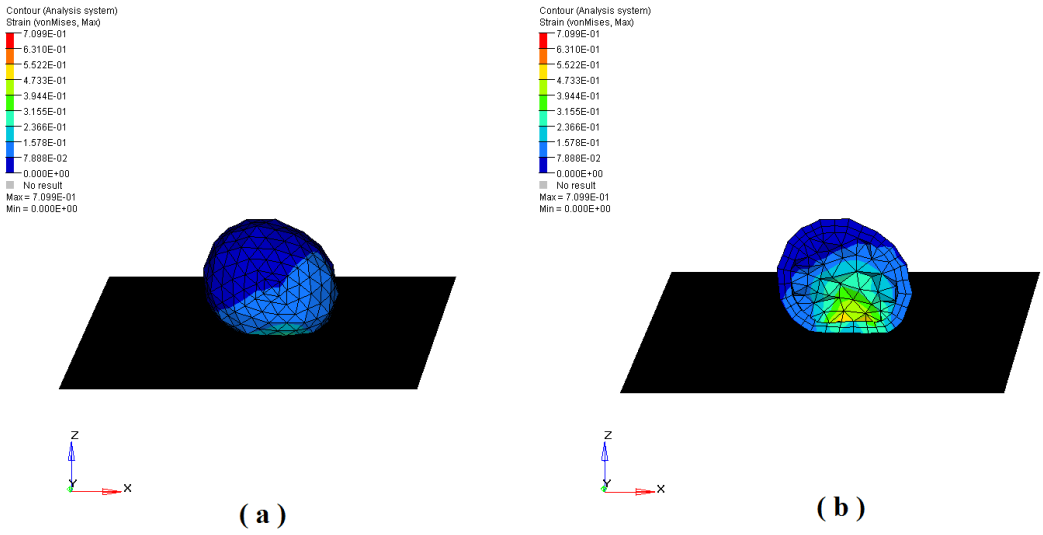

Figure 8.4 Finite element fetus head drop test with element density of 2; (a) Side view, (b) Sagittal plane view

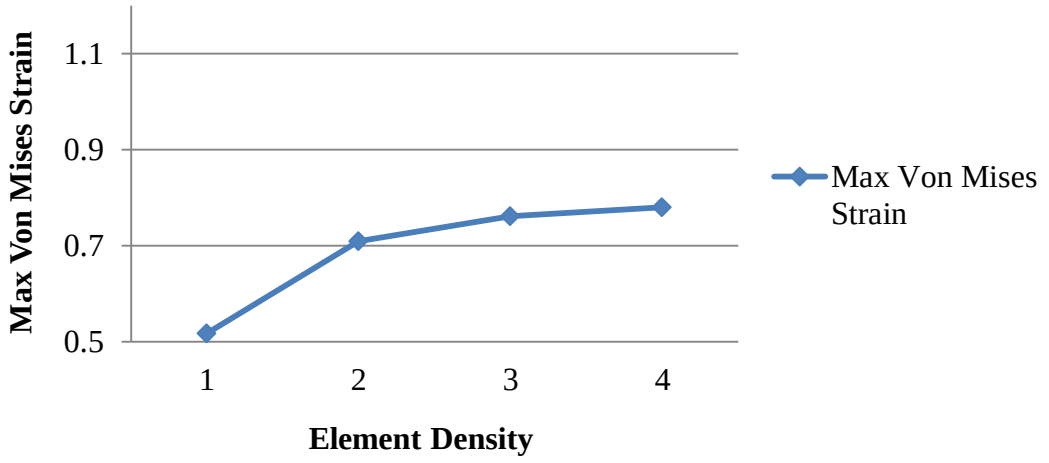

Figure 8.5 Convergence study; Element density and maximum Von Mises strain

The whole model is made of total of 2279 tetrahedral brick elements. The brain and the fontanel models have 1383 elements while the skull has only 896 brick elements. In MADYMO, the tied surface tool which does not allow relative displacement between the skull and brain is used to represent contact condition between the brain and skull models. Connections between nodes and elements of the skull and the brain are tied.

8.2.3 Material Properties

The material and mechanical properties of the adult human head are well represented (McElhaney *et al.*, 1970; Wood, 1971) but there are only a few studies that have investigated material and mechanical properties of child head (Roth *et al.*, 2008). However, detailed investigation of the material properties of the fetus head is the scarcest (Margulies and Thibault, 2000). Response of the fetus head to an impact differs from an adult skull. The fetus skull is capable of deformation under external loading easily, but adult head resists well to external loading. Material properties such as elastic modulus, Poisson's ratio, density of the fetus head affect the biomechanical behaviour. Therefore, material properties play significant role in determining the head injury risks. Due to the limited available data in literature, much estimation needs to be done to determine material properties.

The fetus skull bones are nonhomogeneous and have viscoelastic material properties. Information of both viscous and elastic behaviour of the material properties is necessary at simulations. However, no parameters exist in literature for the viscoelasticity and nonhomogeneous properties. Therefore, the fetus skull is simplified to be homogeneous and have only elastic properties.

McPherson and Kriewall (1980) derived the elastic modulus of fetal skull bone from three-point bending tests on 86 specimens. They indicated that elastic modulus and ultimate stress of the fetus bones increases with gestational age. Coats and Margulies (2006) tested the elastic modulus and ultimate stress of parietal and occipital bone specimens to failure in three-point bending tests as well. They also concluded that infant age plays significant role on the elastic modulus. Margulies and Thibault (2000) tested human and porcine infant cranial bone specimens from 25 weeks gestation to six months of age in three-point bending. The data from Margulies and Thibault (2000) was used as a basis to obtain age specific material properties for the 38 weeks fetus skull.

The brain and fontanelle are represented as linear viscoelastic solid and assumed incompressible with a bulk modulus of 2110 MPa. Material properties for the brain and fontanelle are based on experimentally determined mechanical response of infant porcine brain tissue (Thibault and Margulies, 1998). There are no slip at the interface between the brain and skull and they are assumed to be displacement compatible. Table 8.1 summarizes the material properties used in the model.

Table 8.1 Material properties found in the literature and used in simulations (Thibault and Margulies, 1998, 2000)

	Young's modulus (MPa)	Poisson's ratio	Density (kg/m^3)
Skull	820.9	0.28	2150
Brain and Fontanel	$G(t) = G_\infty + (G_0 - G_\infty) \times e^{-\beta \cdot t}$ $\beta = 0.09248$ s^{-1} with a bulk modulus $K = 2110$MPa $G_0 = 5.99 \times 10^{-3}$ MPa $G_\infty = 2.32 \times 10^{-3}$ MPa		

The finite element head is modelled with elements and nodes with MATERIAL.ISOLIN that describes material properties including material density, Young's modulus and Poisson's ratio. Linear elastic material properties are applied to the structure. Using these specifications, MADYMO calculates stress-strain contact deformations on the head. For the fontanel, the material property of the brain is used.

8.2.4 Hybrid Fetus; FE head and rigid body

The original fetus model in 'Expecting' is represented with 15 rigid bodies. These 15 ellipsoids are connected to each other with different kind of joints. Two spherical joints are defined at neck ellipsoid. One is at upper neck used to connect neck and head bodies. Another is at lower neck used to connect neck and thorax bodies. This type of joint permits three rotational degrees of freedom. Spherical joints are used to define the hip, ankle and shoulder joints. Head and face, form an integrated rigid body.

Kinematic joints can only be defined between two bodies. Therefore, head body is defined at its original position in 'Expecting' model. In this study, the fetus head is modified and the fetus is represented with 13 rigid bodies and 1 finite element head. In order to define connection between FE head and ellipsoid neck, SUPPORT attribute is used in MADYMO. Finite element head is attached to the neck. This code defines which degrees of freedom of nodes are constrained, by supporting them on rigid body or the reference space (Figure 8.6).

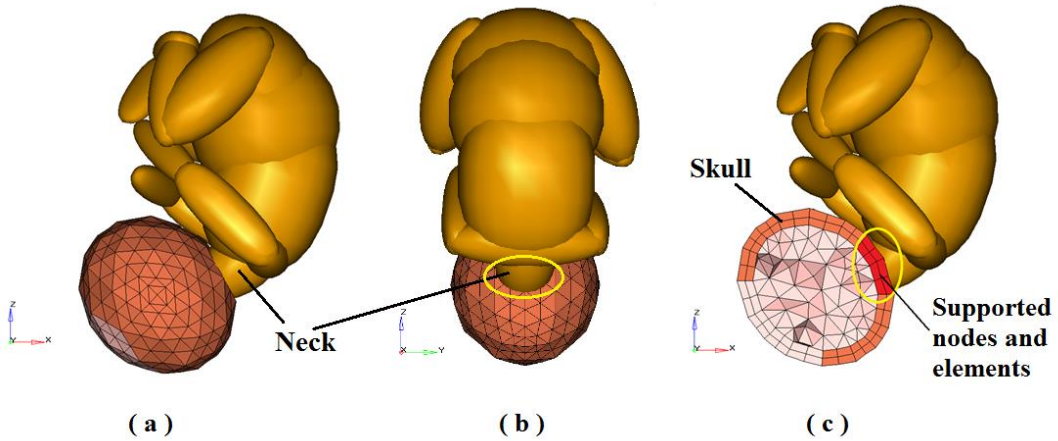

Figure 8.6 Head and neck connection of the hybrid fetus

In order to decide which and how many nodes to be selected and constrained, the full hybrid fetus models are dropped on to the rigid plane. Their motions are compared with the multibody fetus model and the most similar model is chosen. For this study, 21 nodes from finite element head model is constrained and supported on head body (Figure 8.7). During drop test simulations, both of the heads act similarly. Naturally, deformations are observed on finite element head. Connection nodes are chosen symmetrically.

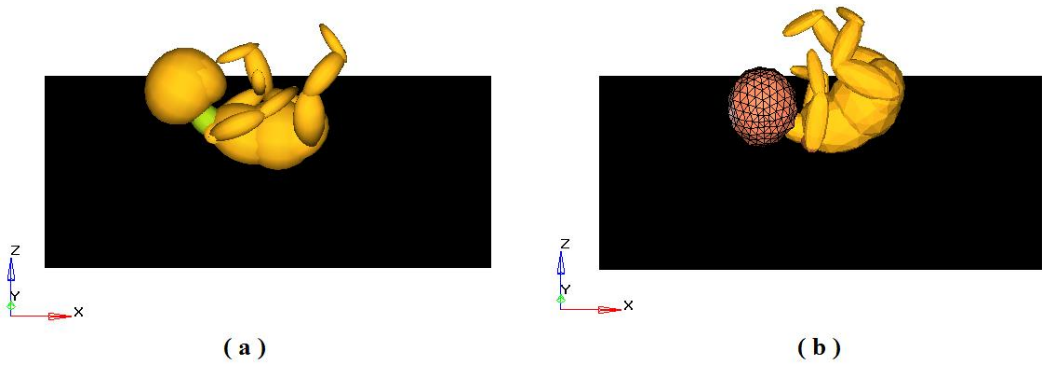

Figure 8.7 The multibody and the hybrid fetus drop test comparison

8.2.5 Contact Properties

During pregnancy, the fetus has a close relation with amniotic fluid, placenta, umbilical cord and uterus wall. Due to the position of the fetus in the uterus, a large degree of interaction can be observed with these body regions during an impact situation. The amniotic fluid surrounds the fetus while the uterus envelopes both of them. The amniotic fluid may generate pressure on the uterus wall and placenta. The placenta stays between the uterus and fetus.

A number of different body regions and tissues with different material properties contacts with each other in the pregnant abdomen. Therefore, definition of the contacts between these body regions and tissues play a significant role in the development of a realistic model. Since ellipsoid bodies and finite element head model are defined for the hybrid fetus, it is very important that the contacts between the ellipsoid bodies, finite element head of the fetus and the contact surface of the uterus are defined carefully.

Five contact interaction models are defined between these body regions and tissues. These are the contacts between the finite element fetus head and finite element amniotic fluid model, the finite element fetus head model and finite element uterus model, the finite element fetus head model and the multibody fetus model as explained in section 8.2.4, finite element uterus model and the multibody fetus model, finite element amniotic fluid model and the multibody fetus model. Contact interactions between the uterus, the placenta, the amniotic fluid, and the hybrid fetus are shown in Figure 8.8. Multibody to multibody contact between the fetus bodies are used same as in the original 'Expecting'.

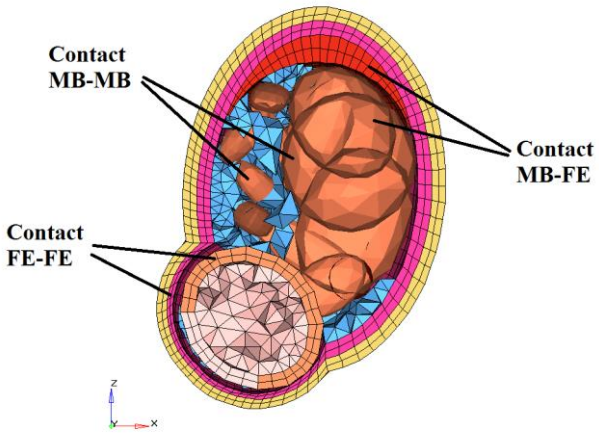

Figure 8.8 Typical contacts in the uterus; Contact MB-MB; Multibody surface to multibody surface. Contact MB-FE; Multibody surface to finite element surface. Contact FE-FE; Finite element surface to finite element surface.

Contact interaction can be defined with a master surface against a slave surface in the MADYMO. In these contacts, ellipsoids and finite element models are specified. For contacts between ellipsoid bodies of the fetus are defined body to body contact and a force-penetration characteristic is developed for each ellipsoid surface that contacts with another region of the body. The various ellipsoid body regions of the fetus model are penetrated based on the force-penetration characteristic values used in the TNO dummy models and engineering judgement (MADYMO Model Manual, 2010). Actual material properties and contact definitions for these body regions are not available in the literature.

For the contact between FE structures, master surfaces are defined as a group of contact segments that are formed by several finite element groups, slave surfaces are defined as a group of contact nodes that are formed by several finite element groups. Choice of which surface must be the master and which surface must be the slave surface depends on the coarseness of the mesh. The finer mesh is chosen as the slave surface.

Contacts between finite elements are defined with two algorithms in MADYMO; Intersection based contact and penetration based contact. In this study, penetration based contact is used because it is used for deformable FE structures

while the intersection based contact is mainly used for contact between rigid surfaces where the surface stiffness is defined in the contact force characteristic. CONTACT.FE_FE elements are used to define contacts between finite element structures. MASTER_SURFACE represented one finite element group and SLAVE_SURFACE represents another finite element group which has finer mesh than elements of master surface. These attributes are the standard contact definition of surfaces (Figure 8.9).

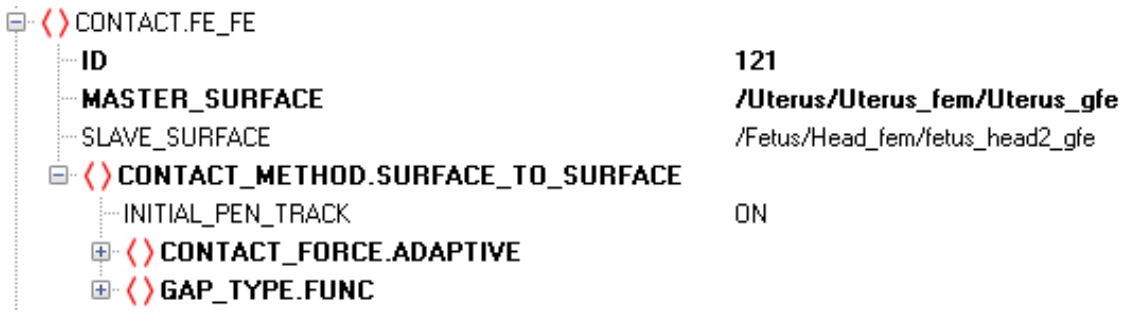

Figure 8.9 Contact definitions between finite element surfaces

Finite element contact algorithms based on penetrations, contact thickness of the contact segments are specified. All nodes of the finite element surfaces penetrate the gap of the contact segments. Nodes penetrating the gap are pushed away on the back of the contact segment. The gap is specified as a function of time and the same for the entire master/slave surfaces (Figure 8.10). Initial penetrations generate initial contact forces which can cause instabilities in the simulation. In order to avoid initial contact forces for initial penetrations, the INITIAL_PEN_TRACK option is used.

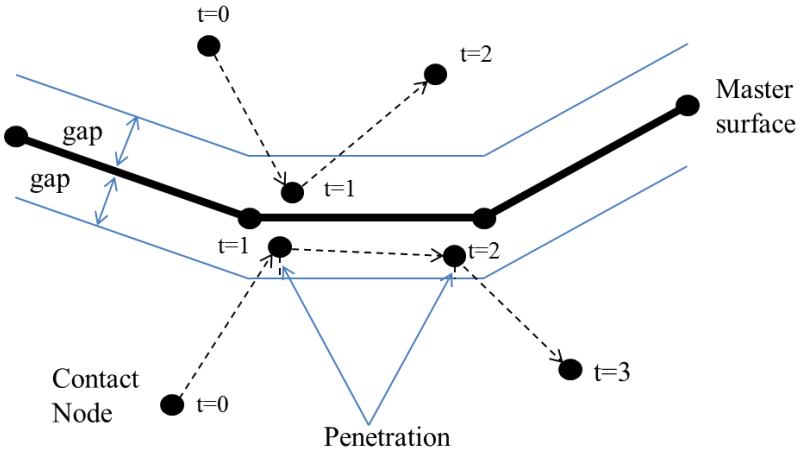

Figure 8.10 Penetration based contact

"Surface to surface" contact method is used to represent penetration based contact between finite element surfaces which are curved and complex. In the "surface to surface" contact method, the slave nodes are compared with the master contact segments and also the master nodes are compared with the slave contact segments.

There is a second phase which is contact force calculation phase in the penetration based contact algorithm. In the force calculation phase for all contacts, penetrations of contact nodes of the contact segments are calculated. Minimum distance between the node and the segment gives the penetrations (Figure 8.10). By using this penetration, the contact forces are calculated depending on which contact force model is used. The contact force has the same direction as the penetration and is applied to both the contact node and master surfaces.

In MADYMO, three contact force models are available; penalty based contact, adaptive based contact and elastic characteristic based contact. Elastic characteristic based contact is only available for the intersection based contact algorithm. Therefore, this model is not used. CONTACT_FORCE.ADAPTIVE attribute is used to generate good results for contacts between FE structures. For this model, contact force is calculated based on the TIME_STEP. For FE calculations, time step of 1.10^{-6} is used. This value is recommended by the MADYMO and results normally in a good working contact.

8.2.6 Hybrid Fetus Model Validation

The impact response of the hybrid fetus in the uterus is validated under two different conditions. These include corridors developed from rigid bar impacts and belt loading tests same as validation of the original 'Expecting' model (Acar and Lopik, 2009).

8.2.6.1 Rigid Bar Impact

Mathematical model of the hybrid fetus is developed in which maximum strain can be estimated from the measured change at uteroplacental interface displacement. The rigid bar loading response corridors developed by Hardy *et al.,* (2001). However, these corridors were developed using the 50th percentile male post mortem human subject. Rupp *et al.,* (2001) scaled these corridors to a 5th percentile female. Due to the lack of test data, there are no force-deflection corridors for pregnant women. Therefore, original 'Expecting' and in this study, 'Expecting' with the finite element fetus head are validated rigid bar impact tests performed by Hardy *et al.,* (2001).

The finite element head with the multibody fetus body and the uterus are integrated into the existing 'Expecting' model. The test configurations used by Hardy *et al.,* (2001) are constructed as a mathematical dynamic model. The rigid bar impactor is a 2.54 cm diameter and 48 kg ellipsoid (Figure 8.11). This is the same 48 kg ballistic pendulum used by Hardy *et al.,* to verify the 6 m/s (21.6 km/h) Cavanaugh corridor and to develop the average 3 m/s (10.8 km/h) abdomen response. The rigid impact bar is applied at the approximate height of the umbilicus at 6m/s (21.6 km/h). During a typical experimental test, the dummy was seated on Teflon skid-plate. The whole body of the 'Expecting' is also skidded when the rigid bar impacts on abdomen.

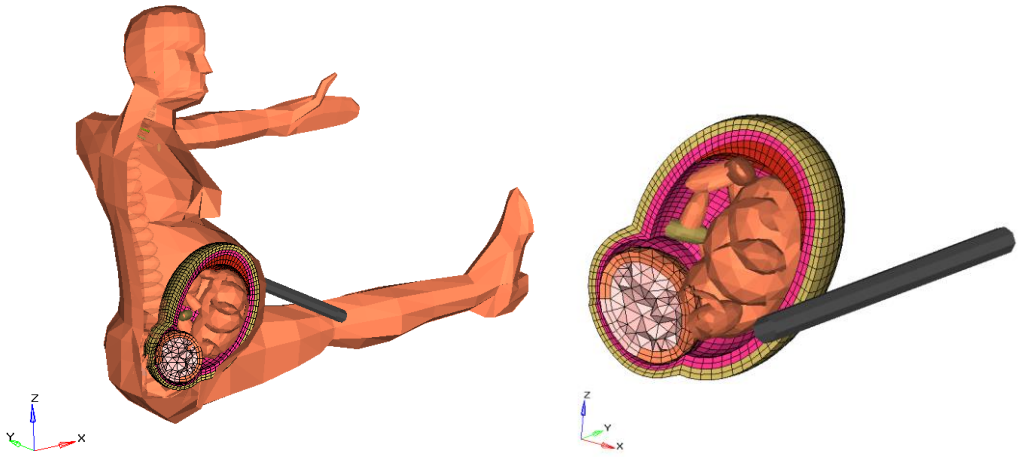

Figure 8.11 Rigid impact bar test for the 'Expecting' with the hybrid fetus

The force-displacement response of the model to the 6 m/s (21.6 km/h) rigid bar impact case is shown in Figure 8.12. Results are compared with the earlier researchers' findings. Response of the 'Expecting' with the finite element fetus head model is similar to the 6 m/s (21.6 km/h) Cavanaugh upper corridor.

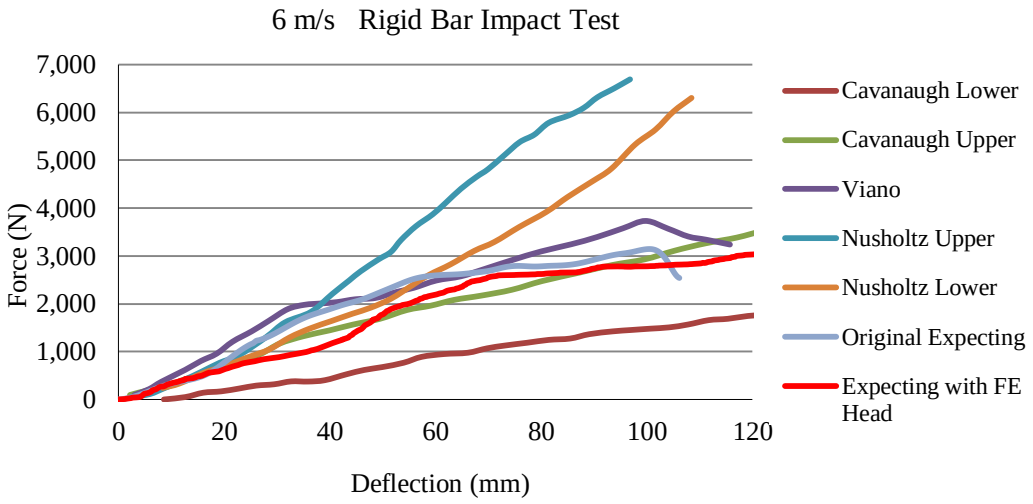

Figure 8.12 The hybrid fetus model rigid impact bar test

For comparison, Figure 8.13 shows the response of the original 'Expecting' model and the 'Expecting' with the hybrid fetus model. The dynamic force-deflection response of the original 'Expecting' abdomen is slightly stiffer than the 'Expecting' with the hybrid fetus model. The maximum force-displacement difference occurs

when the rigid bar impacts 40 mm onto the pregnant abdomen. For the original model, approximately 2 kN force is necessary while the model with the hybrid fetus 1 kN force is enough to generate 40 mm deflection. Because for the hybrid fetus model, there is deformable finite element head instead of rigid head, which allows further deformation.

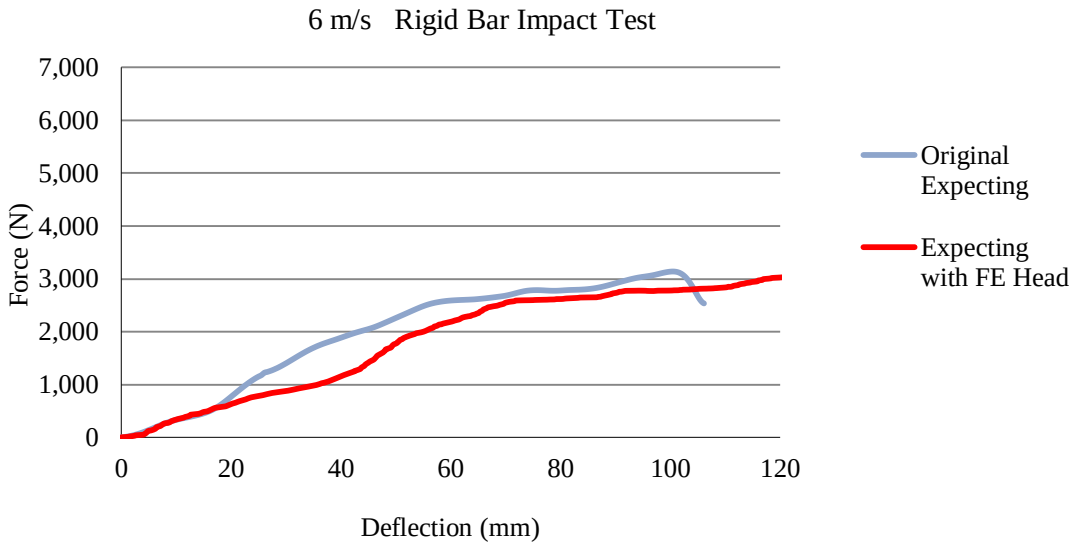

Figure 8.13 Rigid bar impact test; the original 'Expecting' and the 'Expecting' with FE head

8.2.6.2 Belt Loading

The belt-loading response corridor generated by Hardy *et al.*, (2001) is also used to develop and validate the 'Expecting' with the finite element fetus head model. This corridor is developed from force-deflection data collected during simulated belt-loading tests on the abdomens of the three cadavers. The corridor has been equal-stress, equal-velocity scaled from the reference mass used in pregnant dummy development and validation. The belt-loading simulation is shown in Figure 8.14. This is the same test configuration used by Hardy *et al.*, to develop the belt-loading corridor. During the simulation, the belt is used to apply a horizontal load to the abdomen of the seated pregnant occupant model through a length of belt webbing connected at both ends to a yoke-fixture.

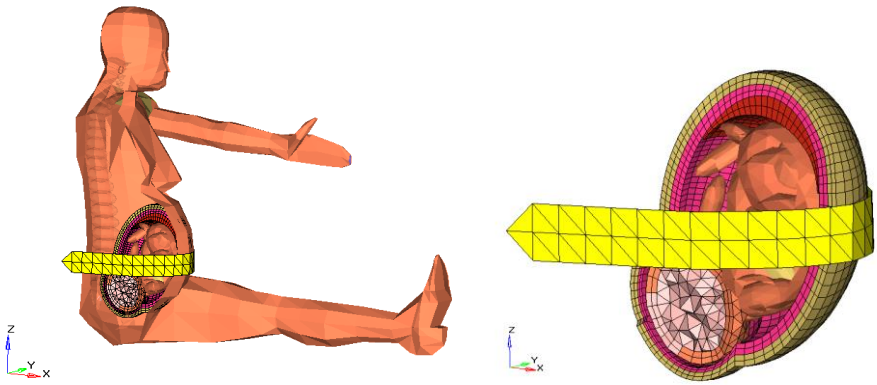

Figure 8.14 Belt loading test for the 'Expecting' with the hybrid fetus model

Prior to the simulation test, the belt is in contact with abdomen of the pregnant occupant. However, there is no loading to the abdomen. Finite element belt displacement at the centre of the abdomen is measured. The motion of the pregnant occupant is observed. Abdomen penetration is calculated with determining the motion of the belt at the centre of the abdomen relative to the position of the lumbar spine.

Force-deflection response of the pregnant abdomen is shown in Figure 8.15. The belt-loading response of the 'Expecting' with the hybrid fetus to the 3 m/s (10.8 km/h) belt-loading corridor is compared. The model response is within the 3 m/s (10.8 km/h) belt corridor.

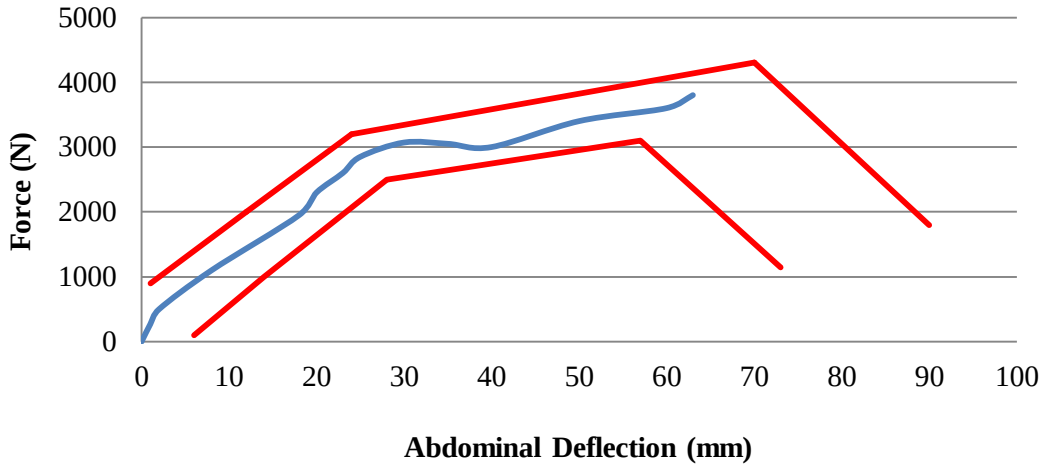

Figure 8.15 Force-deflection response of the 'Expecting' with the hybrid fetus model, to belt loading compared to scaled belt-loading corridors

8.3 Crash Test Simulations with Hybrid Fetus Model

Validated 'Expecting' with the hybrid fetus model, rigid body with FE head used to simulate; 'seat belt and airbag', 'seat belt only', 'airbag only' and completely 'unrestrained' conditions. 'Unrestrained' case excludes all restraints, which means there is no airbag and seat belt. Standard MADYMO European driver airbag is used. The volume of the airbag is 60 litres. The seat belt system has a pretensioner and a load limiter. The pretensioner is activated and de-activated by a switch. The load limiter is activated when at least one of its load levels is active. Typical crash test simulation with the 'Expecting' including the hybrid fetus is shown in Figure 8.16.

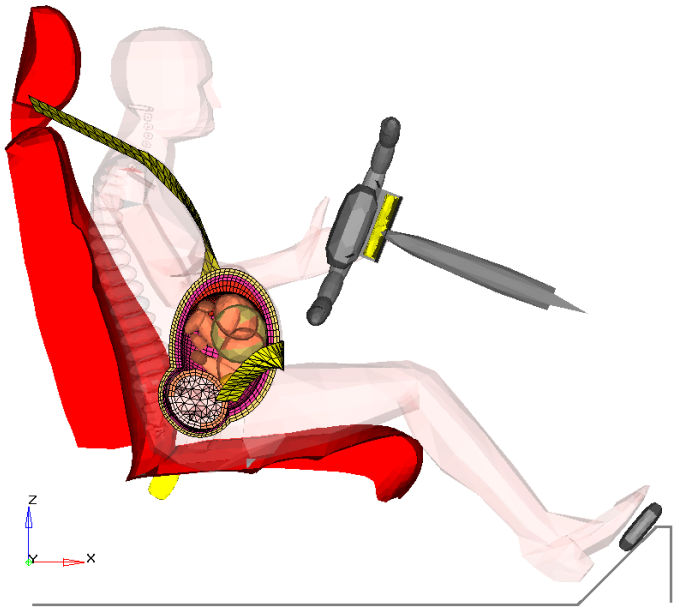

Figure 8.16 Typical frontal impact test configurations with the 'Expecting' including the hybrid fetus

Simulation tests with the hybrid fetus are run at the same conditions as used for the original 'Expecting', i.e. with crash speeds of 15, 20, 25, 30, and 35 km/h, and the acceleration pulse of half-sine waves. These crash speeds were chosen, because after the crash speed of 35 km/h, although the pregnant occupant was fully restrained, the fetus in the uterus dies instantly in the vehicle collision. In the MADYMO software, crash pulse values (half-sine wave) used in the frontal application model. This is a generic pulse representative for full frontal impact of a typical crash test simulations with the 'Expecting'. Although the crash pulse values are defined in the MADYMO model, crash speeds are named in order to make the model easier to understand. The maximum von Mises strains at the uteroplacental interface for the each group are compared with the original 'Expecting' results. The possibility of the placental abruption, which leads to fetal death, is investigated. The threshold strain value for the occurrence of placental abruption is widely accepted to be 0.6 at the UPI (Rupp *et al.*, 2001).The red line in Figure 8.17, 8.18, 8.19, 8.20 represents threshold strain value for the occurrence of placental abruption.

The maximum strains at the uteroplacental interface are compared in Figure 8.17 to demonstrate the effect of the finite element fetus head for varying crash

speeds. For the 'seat belt and airbag' case, maximum von Mises strains increase as expected when the crash speed increases. There is no great difference between the models. In addition to this, for both models, maximum strain at UPI is under the threshold value. For the speed of 15 and 20 km/h, maximum strain at UPI for the original 'Expecting' is slightly higher than the model with the finite element fetus head. However, after the speed of 25 km/h, the hybrid fetus model generates higher strains at UPI than the original model. This could be attributed to the deformation of the head which in turn allows further displacement of the abdomen.

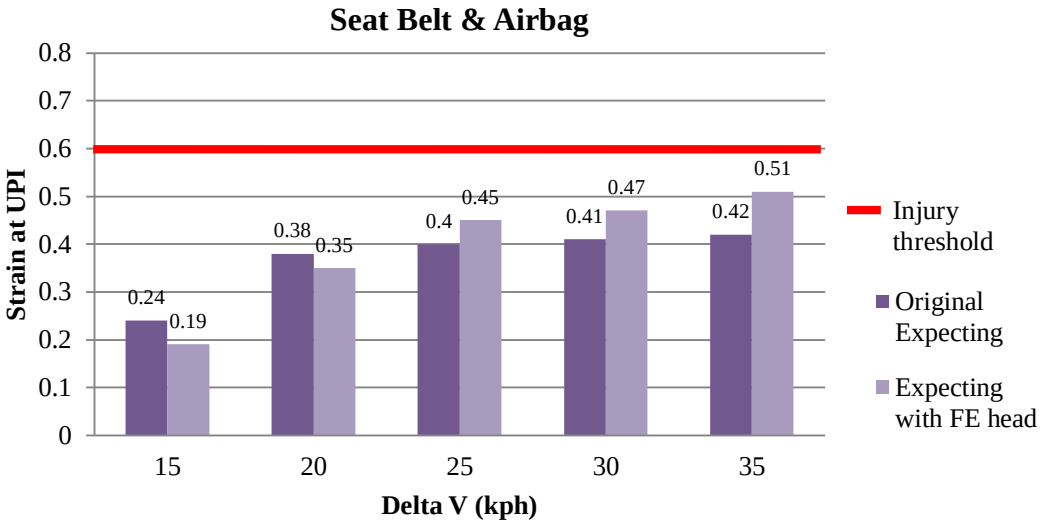

Figure 8.17 Comparison of the original 'Expecting' and 'Expecting' with the hybrid fetus model crash test simulation results for 'seat belt and airbag' case

The response of the 'Expecting' model with the finite element fetus head for 'seat belt only' case is demonstrated in Figure 8.18. The results for the maximum strain at the UPI for the both models are compared. Higher strains at UPI are generally higher than the fully restrained case. Maximum von Mises strains at UPI for both the original 'Expecting' and the 'Expecting' with finite element head model are similar; the finite element head model giving slightly higher strain levels at higher speeds. However, for the 'Expecting' with the hybrid fetus model, the strain level at the crash speed of 35 km/h exceeds the critical threshold level when there is only seat belt is worn and no airbag is activated.

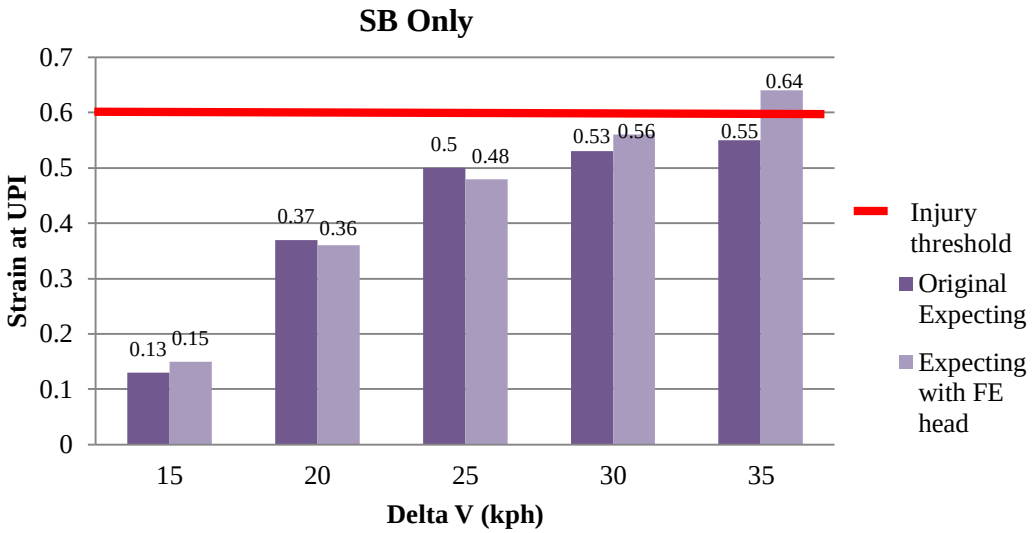

Figure 8.18 Comparison of the original 'Expecting' and 'Expecting' with the hybrid fetus model crash test simulation results for 'seat belt only' case

The two 'airbag only' test results from the original 'Expecting' and the 'Expecting' model with the finite element fetus head are compared in Figure 8.19. The difference in strain levels appear to be greater than those observed with the fully restrained and 'seat belt only' cases. It is clearly seen that for both models the risk of placental abruption is high at speeds between 25 to 35 km/h. 'Airbag only' case, the contribution of the deformable head is clearer than other cases. Maximum von Mises strains at the UPI for the 'Expecting' are higher than the model with the hybrid fetus at all speeds. Risk of placental abruption occurs at speeds between 20 to 35 km/h for the original model, whereas the hybrid fetus model, placental abruption risk occurs at the speed of between 25 to 35 km/h. Without the seat belt, the contribution of the multibody head fetus on the maximum strains at the UPI is much more pronounced and the placental abruption risk is found to be higher.

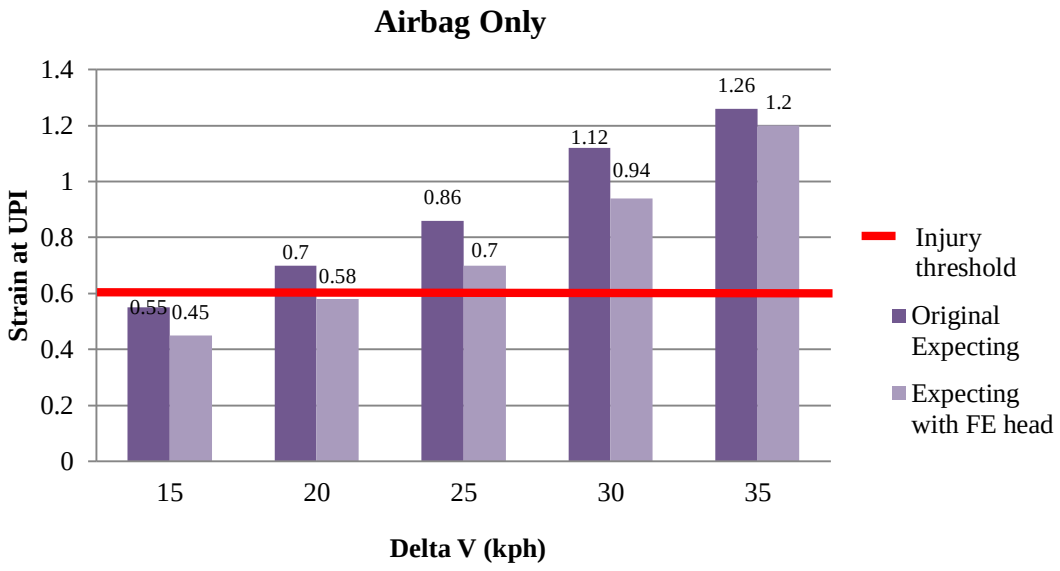

Figure 8.19 Comparison of the original 'Expecting' and 'Expecting' with the hybrid fetus model crash test simulation results for 'airbag only' case

For 'unrestrained' case shown in Figure 8.20, the strain levels at the UPI are consistently above the threshold at all speeds considered (15-35 km/h). Therefore, placental abruption occurs at all speeds for both models. The difference between the strain levels demonstrated by both models is small. Results confirm that the 'no restraint' case is the worst possible case amongst the four restraint conditions investigated.

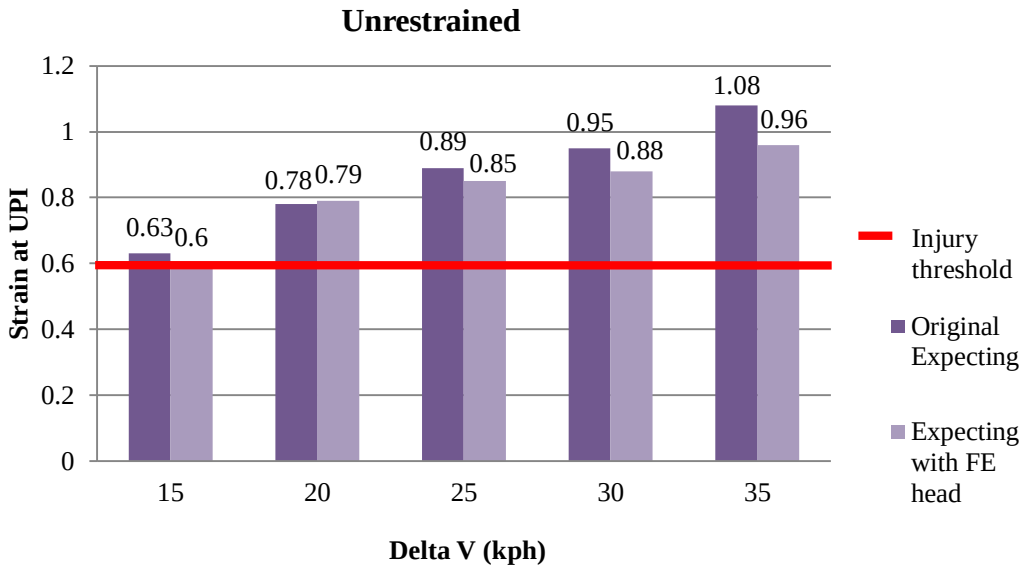

Figure 8.20 Comparison of the original 'Expecting' and 'Expecting' with the hybrid fetus model crash test simulation results for 'unrestrained' case

The original 'Expecting' and a modified Expecting with a FE-head fetus model are used to simulate a range of frontal impacts of increasing severity from 15 km/h to 35 km/h. In this study, it is observed that no matter which model is used, is that the correct use of seat belt in conjunction with the airbag is essential for the protection of the fetus in vehicle crashes. Crash test simulation results show that incorporating a FE-head fetus in the model slightly changes dynamics response of the model in crash simulations. Using a deformable fetus head model than a solid one, is more realistic. However, it increases the processing time significantly.

8.4 'Expecting' with the hybrid fetus and the FE amniotic fluid model validation

The original 'Expecting' did not have amniotic fluid representation as finite element model but the effect of the amniotic fluid was simulated by springs and dampers attaching the fetus from pelvis of female and pelvis of the fetus. The fetus damping characteristics has been defined by the MADYMO codes with restraint cardan element hence suspending the fetus in the uterus. This model was validated using same method as explained in section 8.2.6, rigid bar impact and belt loading tests.

In this section, springs and dampers were replaced with the finite element amniotic fluid model when the hybrid fetus model exist in the uterus. In Chapter 5, inner volume of the uterus was filled with finite elements to represent finite element amniotic fluid only. In this section, the hybrid fetus model is placed its original position and the amniotic fluid elements are deleted one by one in order to represent the amniotic fluid and the hybrid fetus models simultaneously inside of the uterus. Rigid bar impact test to validate the 'Expecting' with the finite element fetus head and finite element amniotic fluid model is illustrated in Figure 8.21.

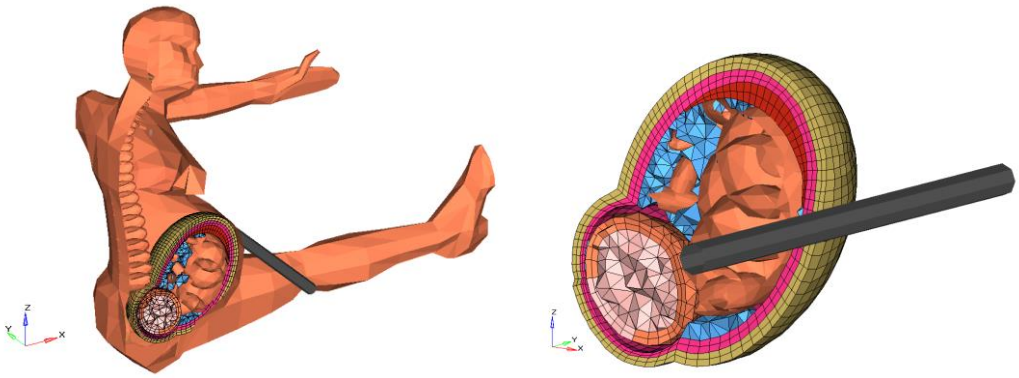

Figure 8.21 Rigid bar impact test, 'Expecting' model

The force-displacement responses of the 'Expecting' model with FE amniotic fluid and the finite element fetus head, and the original 'Expecting' model are shown in Figure 8.22 and Figure 8.23, plotted to compare the effect of finite element head

and amniotic fluid. Comparison of the both model under rigid bar impact loading conditions clearly shows that the finite element fetus head and the amniotic fluid model have very similar response, showing slightly higher force up to 55 mm displacement and reversing roles after this point.

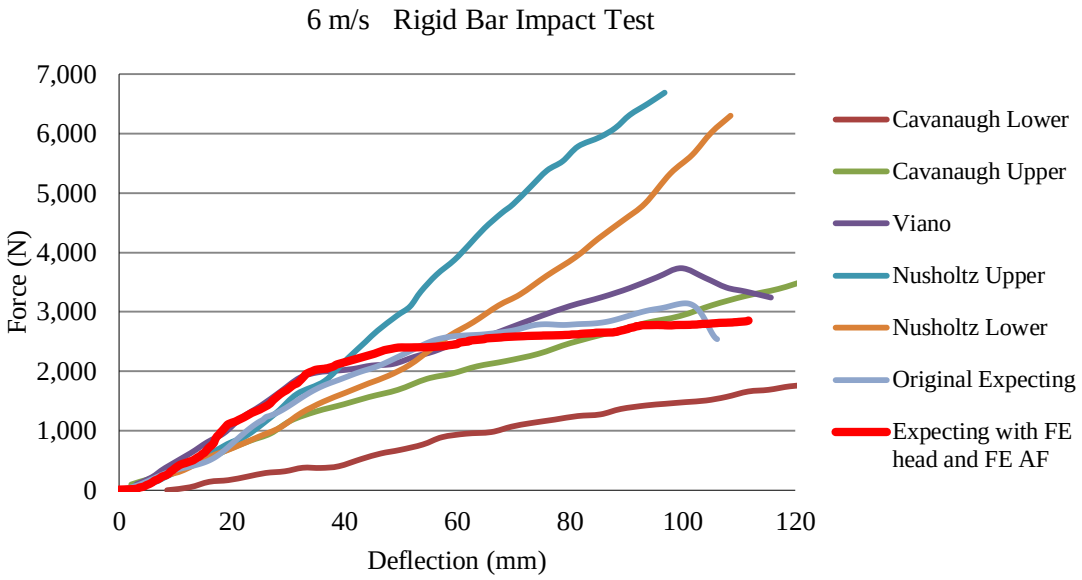

Figure 8.22 Comparison of the abdominal response of the advanced pregnant occupant model with the hybrid fetus, 6m/s (21.6 km/h) rigid bar impact test

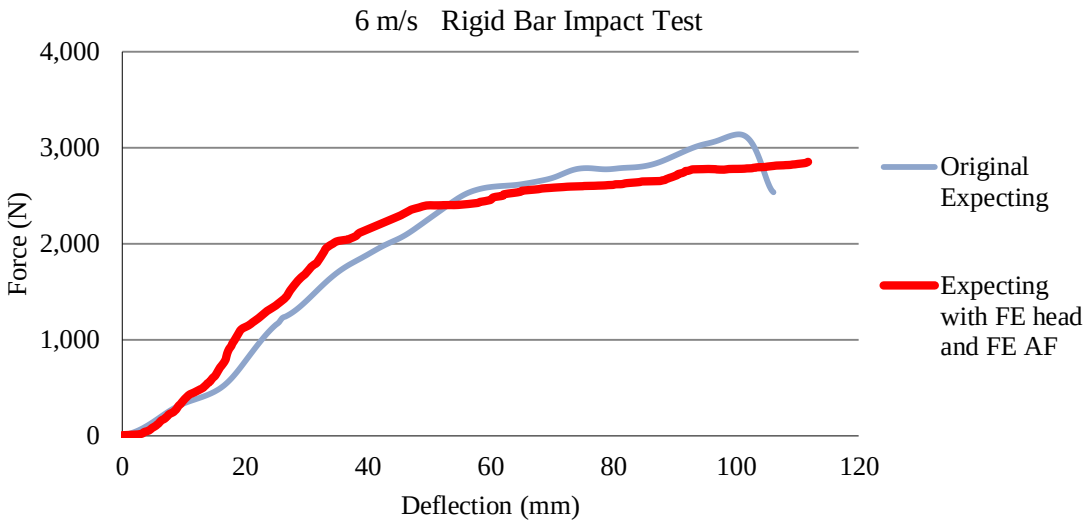

Figure 8.23 Comparison of abdominal response of the original 'Expecting' and 'Expecting' with the finite element fetus head and the finite element amniotic fluid model

Please refer to section 8.2.6.2 for further details of the belt loading test. The belt-loading corridor for the abdomen of the advanced 'Expecting' model is shown in Figure 8.24. Dynamic belt loading tests are performed on the 'Expecting' with the hybrid fetus and finite element amniotic fluid model. The force-deflection response from the tests lies between the belt-loading corridors. However, it passes from lower corridor at around 30 mm abdominal deflection closely.

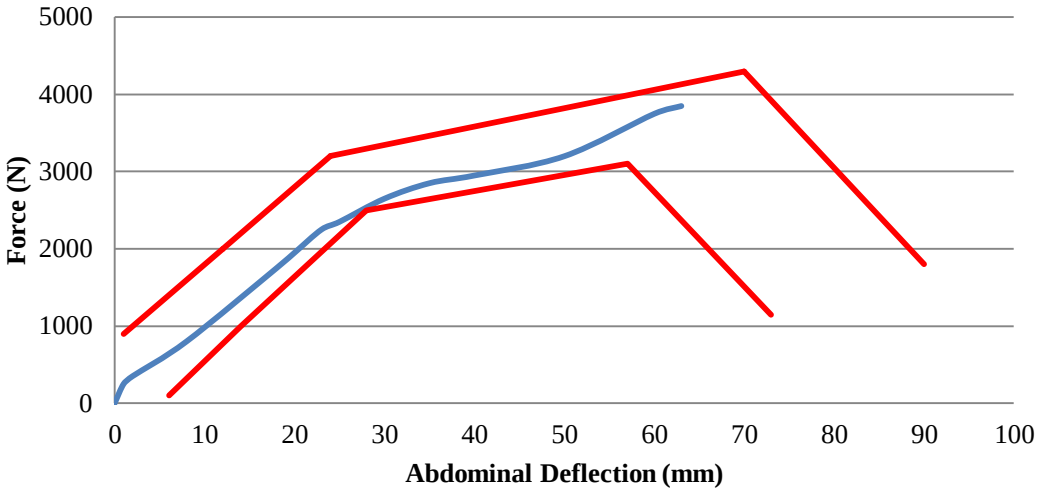

Figure 8.24 Abdominal response of the 'Expecting' with finite element amniotic fluid and finite element head, to 3 m/s (10.8 km/h) belt loading compared against the response corridor

8.5 Crash Test Simulations with the 'Expecting' Model with the hybrid fetus and the finite element amniotic fluid model

A set of simulations are chosen to investigate the effect of the finite element fetus head and the finite element amniotic fluid model on the response of the computational pregnant women model as a driver to a frontal impact. The simulations includes pregnant occupants with 'no restraint', 'seat belt only', 'airbag only', and 'seat belt and airbag' under at five different severity increasing from 15 km/h to 35 km/h, a total of 20 simulations.

During the crash test simulations, steering wheel, airbag, seat belt and inertial loadings on the pregnant uterus are identified. Simulations are run approximately 120 ms to ensure that the forward motion of the occupant has stopped. Acceleration pulses applied to the computational model are half-sine waves as shown in Chapter 4, Figure 4.5. In each simulation, the pregnant occupant is a driver in a frontal crash. Peak von Mises strain in the uterus at the uteroplacental interface is used to measure for predicting the risk of placental abruption. This maximum strain is compared to the threshold strain value for the occurrence of placental abruption, as defined by

Rupp *et al.*, (2001). 'Expecting' with the finite element fetus head and the finite element amniotic fluid model within vehicle interior is demonstrated in Figure 8.25.

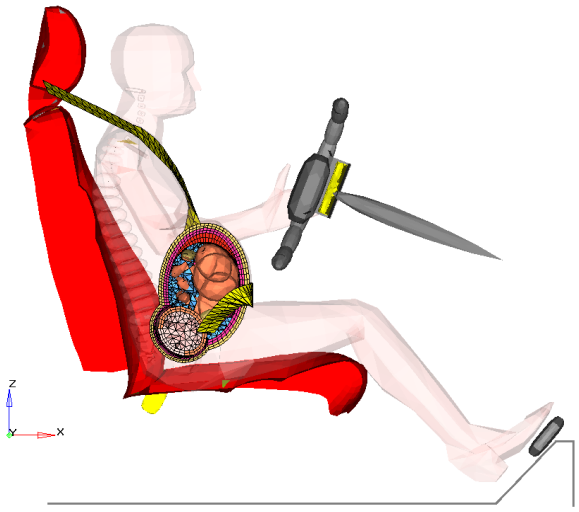

Figure 8.25 'Expecting' with finite element fetus head and finite element amniotic fluid model

Maximum strain levels in the uterus at uteroplacental interface responses are considered. Simulations in which the pregnant occupant is 'fully restrained' are resulted lower peak uterine strains then all other cases (Figure 8.26). When crash speed increases, substantial increase is seen at maximum strain for all cases.

Pregnant occupant model is compared with the original 'Expecting' model. The effect of steering wheel for 'seat belt and airbag' case, maximum von Mises strain values for both models are below threshold level. Therefore, there is no risk of placental abruption. For the 'Expecting' model with the finite element fetus head and the finite element amniotic fluid, lower peak strains are recorded in the 'seat belt and airbag' case at crash speeds of 15, 20, and 25 km/h (Figure 8.26). The abdomen does not contact the steering wheel at low speeds, due to the seat belts in this case. However, at speeds of 30 and 35 km/h, maximum strain at UPI for the advanced 'Expecting' model is higher than the original model. For 'seat belt and airbag' simulations, the peak strains are 0.12 and 0.14 higher at crash speeds of 30 and 35 km/h response for the 'Expecting' with the finite element fetus head and the finite element amniotic fluid model simulations compared to the original 'Expecting' model simulations.

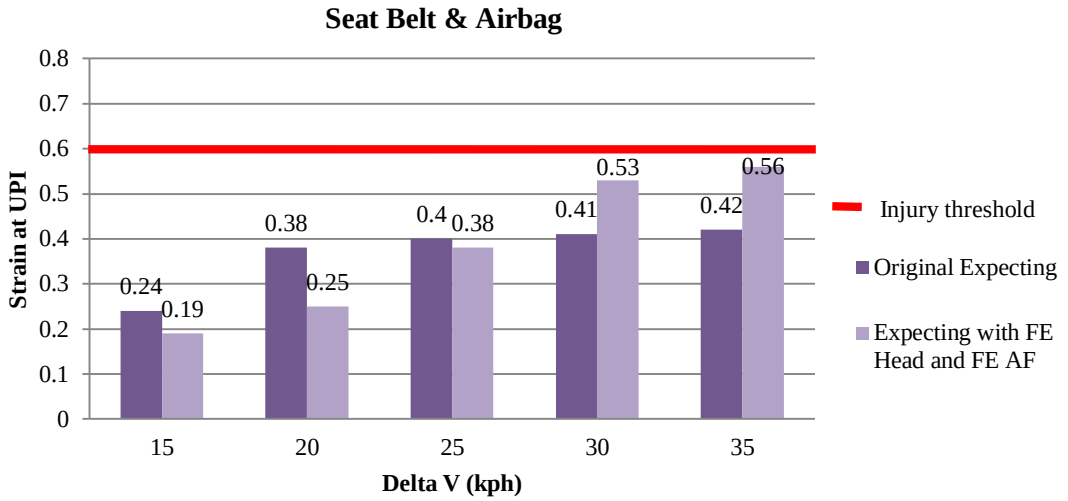

Figure 8.26 'Seat belt and airbag' case; Maximum von Mises strains at the UPI for the original 'Expecting' and 'Expecting' with the finite element fetus head and the finite element amniotic fluid model

Maximum strains occurring at the uteroplacental interface in the uterus are presented in Figure 8.27 for the 'seat belt only' case. Forward motion of the pregnant occupant is stopped with only seat belt, but due to the lack of airbag, the model contacts with the steering wheel. Lap belt compresses the pregnant abdomen. For this case, the effect of the steering wheel on strains at UPI is higher than the fully restrained cases.

Effect of finite element head and finite element amniotic fluid model developments in the uterus is investigated in the 'seat belt only' case. The strains at the UPI change from 0.16 to 0.72 for the 'Expecting' model with the finite element fetus head and finite element amniotic fluid while they increase from 0.13 to 0.55 for the original 'Expecting' model for the crash severities of 15 km/h to 35 km/h. These results highlight that the finite element fetus head and the finite element amniotic fluid model developments in the uterus predicts higher risks of placental abruption. However, for crash speeds of 20 km/h and 25 km/h, the strain values are less in the 'Expecting' with the finite element fetus head and the finite element amniotic fluid simulations by up to 0.10 compared to the original 'Expecting' model simulations. The model with the finite element fetus head and the finite element amniotic fluid shows the strain values exceed the threshold with 0.64 and 0.72 strains respectively, posing a risk of placental abruption at crash speeds of 30 and 35 km/h.

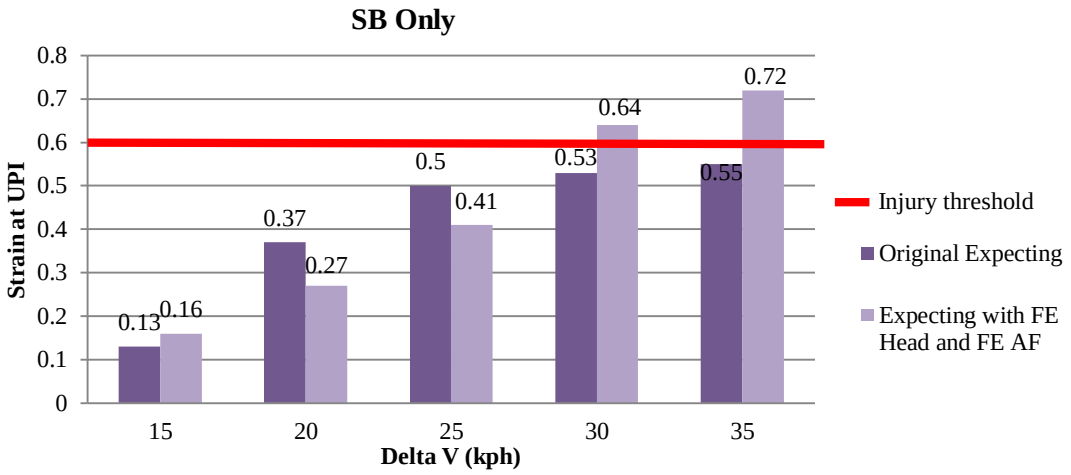

Figure 8.27 'Seat belt only' case; Maximum von Mises strains at the UPI for the original 'Expecting' and 'Expecting' with the finite element fetus head and the finite element amniotic fluid model

Simulation results for airbag only case are demonstrated in Figure 8.28for both models. The maximum strains at the uteroplacental interface are compared for varying crash speeds. Peak strains increase with increasing crash speed as usual. Figure 8.28 shows that the strains at the UPI for the 'Expecting' model with the finite element fetus head and the finite element amniotic fluid simulations increases from 0.61 to 1.34, whereas the strains at the UPI for the original 'Expecting' model changes from 0.55 to 1.26.

It is interesting that the both models give close strain values to each other. This results show that the effect of the finite element fetus head and the amniotic fluid on prediction of risk of placental abruption might be insignificant compared to the original model. However, the difference is significant for the cases including seat belts. The airbag decreases forward movement of the pregnant occupant and deformation impact on abdomen due to contact with the steering wheel.

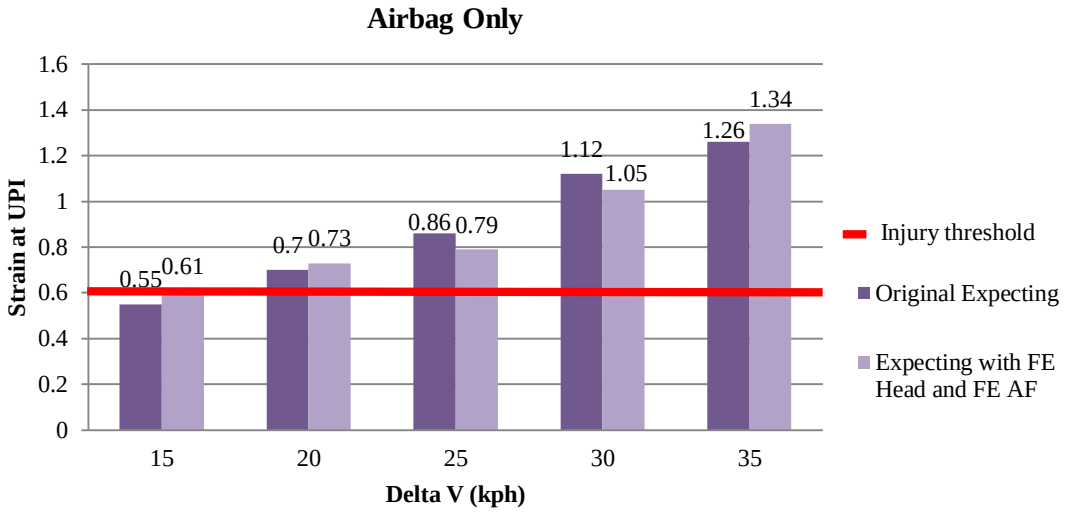

Figure 8.28 'Airbag only' case; Maximum von Mises strains at the UPI for original 'Expecting' and 'Expecting' with finite element fetus head and finite element amniotic fluid model

Figure 8.29 shows maximum von Mises strains at the UPI comparison between the 'Expecting' with the finite element fetus head and the finite element amniotic fluid model and original 'Expecting' model for 'unrestrained' case and varying crash speeds from 15 km/h to 35 km/h. The strains at all speeds are similar for both cases. For all crash severities, the peak strain at UPI exceeds 0.60 for the unrestrained case, indicating the likelihood of placental abruption. However, the 'Expecting' with finite element head and finite element amniotic fluid model gives slightly lower strains than the original 'Expecting' model at all speeds of 15 km/h to 30 km/h.

Due to the absence of the seat belt, the both models contact the steering wheel in all simulations, hence is exposed significantly high loading from the steering wheel. The uterus, including the placenta, is compressed downwards and the fetus moves forwards. There is no direct impact on the finite element fetus head.

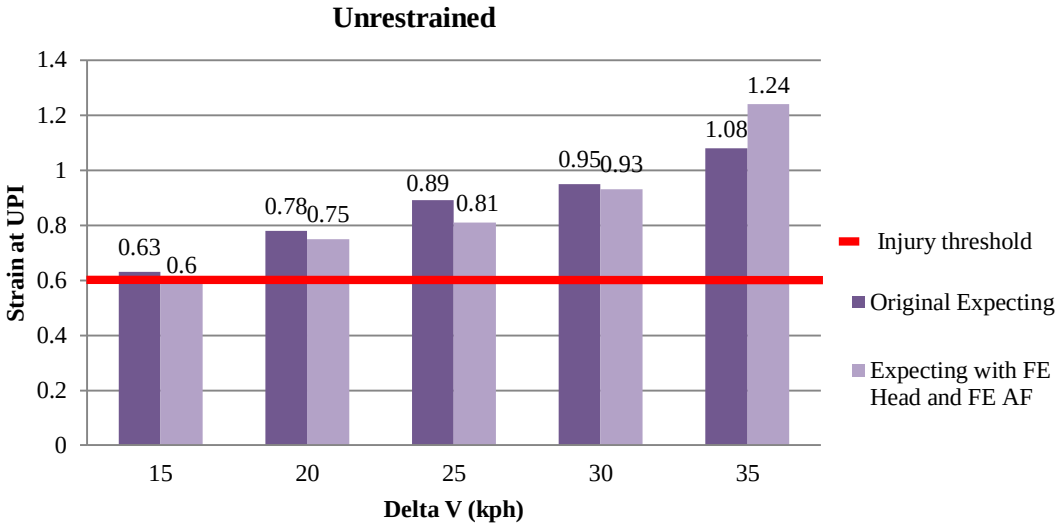

Figure 8.29 'Unrestrained' case; Maximum von Mises strains at the UPI for the original 'Expecting' and 'Expecting' with the finite element fetus head and the finite element amniotic fluid model

8.6 Conclusions

The finite element fetus head and the finite element amniotic fluid models were developed and integrated into the uterus. The deformable fetus head was designed, meshed, and connected with the multibody fetus neck. The hybrid fetus model was inserted into the pregnant abdomen and validation tests including rigid bar impact and belt loading were applied to the this model. New contacts between the hybrid fetus and the uterus were defined. Validated 'Expecting' model with the finite element fetus head was conducted at several crash test simulations. Maximum von Mises strains at the UPI were investigated. Results were compared with the original 'Expecting' model and found to be in reasonably good agreement with it. It was observed that the computational fetus head model changes dynamic motion of the pregnant abdomen. The rest of the body in the fetus model was rigid whereas head model was deformable. Therefore, the deformable fetus head plays a significant role in creating realistic computational pregnant occupant model.

Finite element amniotic fluid model was integrated into the 'Expecting' model which includes the hybrid fetus model. Instead of using the fetus damping and spring attributes to represent effect of amniotic fluid in the uterus in the original model, the computational amniotic fluid model was developed to fill the gap between the fetus and the uterus. This 'Expecting' model with the finite element fetus head and the finite element amniotic fluid was also validated against the abdominal response using the rigid bar impact and the belt loading tests. The same crash test simulations were conducted with the validated model.

Peak strains at the UPI for the 'Expecting' with the finite element fetus head model and the "Expecting' with the finite element fetus head and the amniotic fluid model are compared with the original 'Expecting' model for four crash test cases in Figure 8.30, Figure 8.31, Figure 8.32, and Figure 8.33. Crash test simulation results are found to be in reasonably good agreement with the original 'Expecting' model.

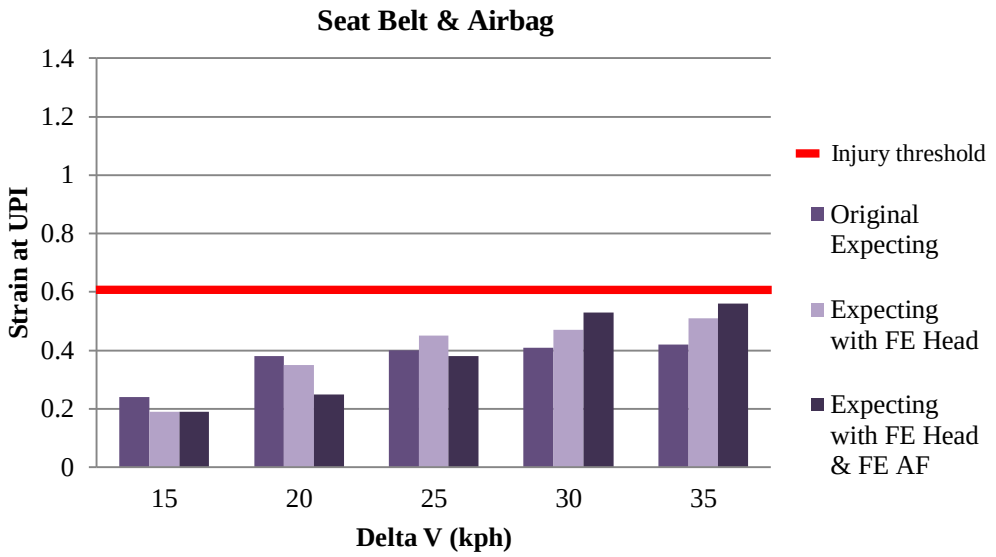

Figure 8.30 'Seat belt and airbag' case Maximum von Mises strains at the UPI for original 'Expecting' model, 'Expecting' with the finite element fetus head model, the 'Expecting' with the finite element fetus head and the finite element amniotic fluid model

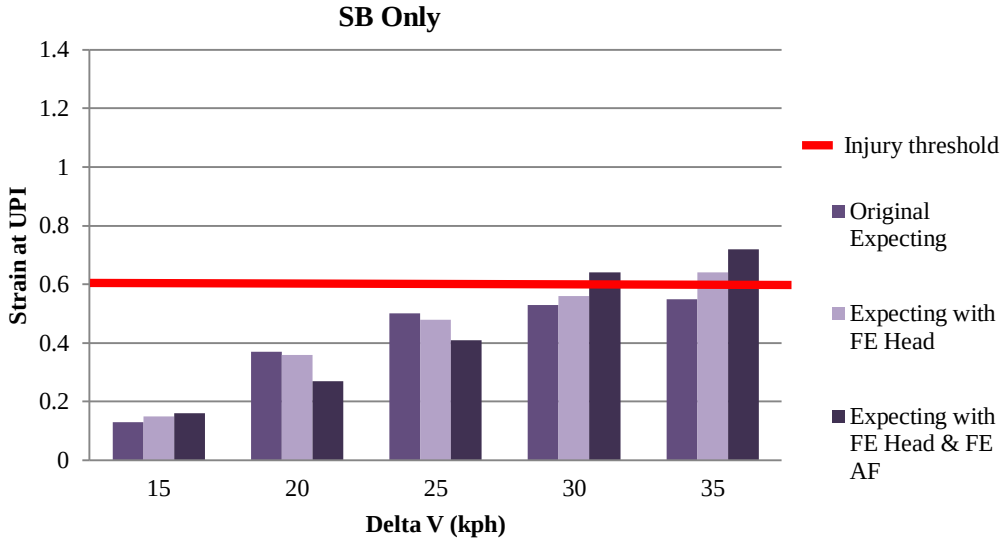

Figure 8.31 'Seat belt only' case; Maximum von Mises strains at the UPI for the original 'Expecting' model, 'Expecting' with the finite element fetus head model, the 'Expecting' with the finite element fetus head and the finite element amniotic fluid model

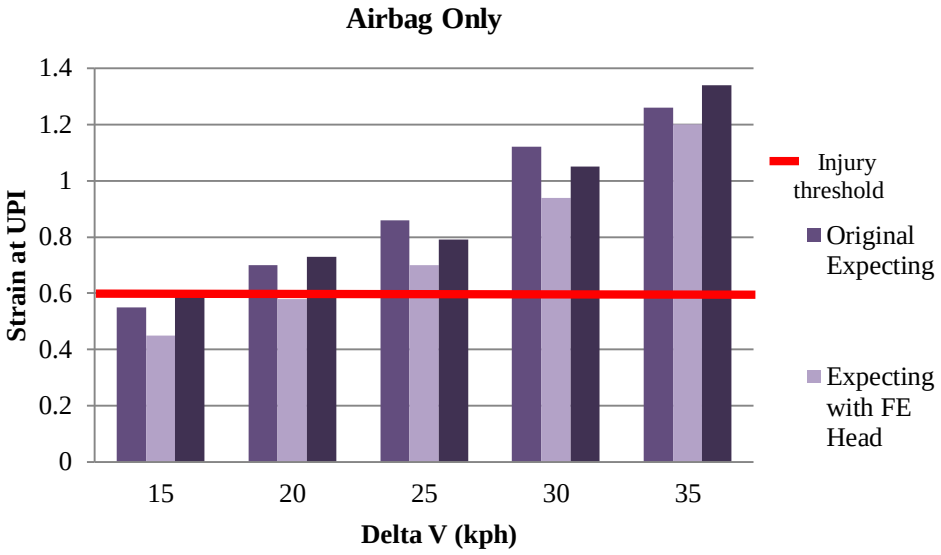

Figure 8.32 'Airbag only' case; Maximum von Mises strains at the UPI for original the 'Expecting' model, the 'Expecting' with the finite element fetus head model, the 'Expecting' with the finite element fetus head and the finite element amniotic fluid model

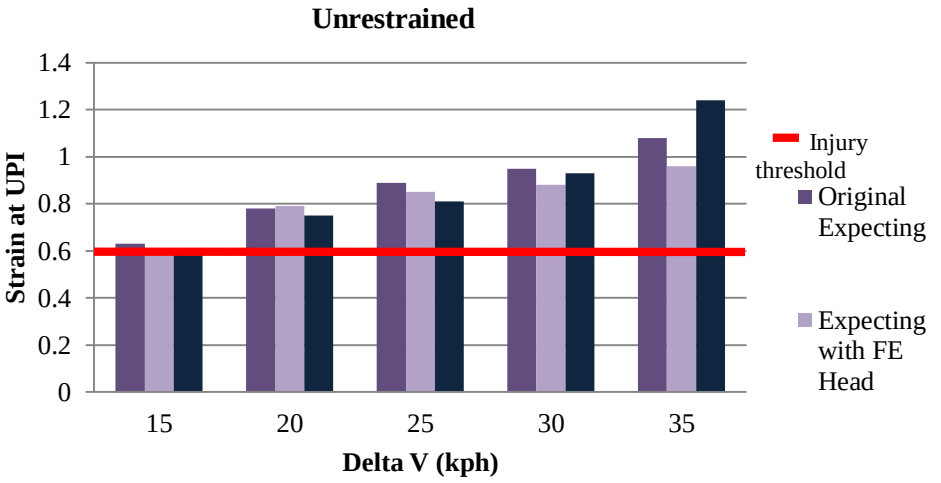

Figure 8.33 'Unrestrained' case; Maximum von Mises strains at the UPI for the original 'Expecting' model, the 'Expecting' with the finite element fetus head model, the 'Expecting' with the finite element fetus head and the finite element amniotic fluid model

These results also show that the fetus within the uterus makes some difference. It was observed that deformable bodies react more realistically than rigid bodies during the crash test simulations. For all models, the unrestrained occupant resulted in substantially higher risk of placental abruption compared to the fully restrained driver in a similar crash case. When there is the seat belt, the strain predicted by the original 'Expecting' poses no danger to the occupant at high speeds. However, for the same case, the 'Expecting' with the finite element fetus head and the amniotic fluid models predict high strains at placental location. This provides that the finite element fetus head with the finite element amniotic fluid causes different dynamic responses of the uterus. In addition, at high speed crashes, maximum strains at the UPI increases significantly for all models and airbag only case give higher strains than ‘no restraint’ case.

All three models show the same trend with small differences. The 'Expecting' with the finite element head and the finite element amniotic fluid model represent a more realistic representation of the pregnant occupant model.

Based on the discussions of simulation results and comparison with the original 'Expecting' model, the 'Expecting' with the finite element fetus head model and the 'Expecting' with the finite element fetus head and the finite element amniotic fluid model are capable of aiding parametric study to determine the sensitivity of the pregnant occupant and the fetus kinematics to the airbag system, three-point seat belt and vehicle interaction.

CHAPTER 9

DISCUSSION AND CONCLUSIONS

9.1 Discussion

Motor vehicle collisions are the leading cause of accidental fetal death but the developments in safety of pregnant women and their fetuses has not been a major concern and not received sufficient attention. Furthermore, modelling pregnant occupant has presented more challenges than modelling other occupants such as ethical issues, the complexity of having an occupant within an occupant and the size and shape changes during pregnancy. Hence, only a few pregnant occupant models have been developed but models have several omissions and do not represent pregnant women realistically. Pregnant occupant models are necessary for more realistic crash test simulations which should assist vehicle manufacturers and researchers to realistically investigate road accidents involving pregnant occupants and their unborn babies. Despite their limitations, physical crash test dummies still

play an important role in occupant safety for vehicle manufacturers. On the other hand, crash test simulations with computational human and dummy models became an alternative method to experimental ones. The objective of this thesis was to investigate effects of external and internal factors on fetus fatalities by understanding the risk of placental abruptions in motor vehicle accidents where a pregnant occupant is involved. The main goal of this investigation is to improve fetus safety in road accidents.

This study investigated fetus safety in motor vehicle accidents. Crash, rigid bar impact, belt loading, and drop tests were conducted. The research involved impact simulations of several impact severities for only frontal crash situations. In real life, drivers are exposed to several different motor vehicle accidents. Frontal collision is the most common type of crash resulting in fatalities. Simulations included a 5th percentile pregnant female model 'Expecting', which embodies a detailed representation of a fetus and a finite element uterus at around 38 weeks gestation. The kinematic output of the 'Expecting' with the hybrid fetus model around the finite element amniotic fluid in the uterus allows for a close-up view of the interior of the uterus. The motion and deformation of the uterine wall and placenta were investigated more realistically than in previous models. This also reveals an advantage over dummy testing. The location of tissue failure can be determined and used to design advanced restraint systems.

In Chapter 8, the effect of incorporating a finite element fetus head and amniotic fluid on the strains generated at the uteroplacental interface of the pregnant occupant model was investigated. Maximum strain in the uterus at the placenta location, maximum displacements and peak von Mises strains in the uterus were provided. Different crash pulses were applied to the model resulting in different crash speeds. The effect of safety systems such as seat belt and airbag during the impact were investigated. Simulation results were compared with the original 'Expecting' and found reasonably good agreement with it. Maximum strain at the uteroplacental interface was found to be a good predictor of fetal outcome. For the seat belt and airbag case, the 'Expecting' with the finite element fetus head and finite element amniotic fluid predicted slightly higher strains than the original 'Expecting' at the placenta location. Strain values at the UPI were below the injury threshold

value and the fetus was less likely to be injured because of possible placental abruption risk. A deformable fetus head and finite element amniotic fluid changed dynamic behaviour of the fetus and affected the dynamic response of the uterus. Due to external impacts such as seatbelt, airbag on the fetus during an accident, structural deformations on the fetus head were monitored. These deformations changed the fetus motion and affected the risk of placental abruption. It was observed that deformable bodies react more realistically than rigid bodies during the crash test simulations.

The test methods used in this research represented simulations and approximations of real world events. Rigid multibody modelling were used to predict the displacements and motion at the boundaries between the rigid bodies. In this research, finite element analysis was conducted at every numerical integration time to determine the reaction stress and strains at the boundaries and also the structural deformations. However, many challenges exist in human body modelling such as characterisation of material properties, complex anatomy of the human body, modelling of some internal organs, prediction of injury mechanisms and injury criteria. It was also difficult to handle with the large amount of data and elements. In order to create more realistic crash test simulations, a finite element method was used to develop the 'Expecting', computational pregnant occupant model with a hybrid fetus in a finite element amniotic fluid in the uterus. It is more realistic to use a deformable model than a solid one. Complex surfaces on occupant and fetus bodies were divided into a finite number of elements and the motion of these elements was determined over short periods of time. In Chapter 8, the 'Expecting' with finite element fetus head model was developed to investigate the implications of changing the fetus model partially, from a multibody head model to a more realistic deformable finite element head model. The interaction between fetus, uterus and placenta can be observed easily. Simulation results showed that incorporating a finite element fetus head in the model slightly changed the dynamic response of the model in crash test simulations and there was no great difference between the models for the seat belt and airbag case. However, after the crash speed of 25 km/h, the 'Expecting' with finite element fetus head model had higher strain levels than the original 'Expecting' model. Similar differences with higher strain levels between the

original and modified 'Expecting' were also observed for the seat belt only case. The strain levels approached the placental abruption risk threshold of 0.60 for both models and there was high risk of fetus loss. At the 35 km/h seat belt only case, strain at the 'Expecting' with finite element fetus head was seen to exceed the threshold value for placental abruption. These results showed that improved 'Expecting' demonstrates its ability to predict fetus outcome and multibody fetus head to finite element fetus head model increases placental abruption risk. This was due to deformation on the fetus head, changes on dynamic motion of the fetus and displacements of the fetus. Simulations increased the processing time. Both fetus models gave reliable results for the cases investigated in this study. The benefit of using the modified 'Expecting' model lies in its ability to provide a more realistic movement of the fetus within the uterus.

Human anthropometry varies significantly between individuals and across populations. Changes during pregnancy drastically alter the pregnant abdominal anatomy of the pregnant female. Pregnant occupants involved in motor vehicle accidents are at risk for pregnant-specific injuries, such as placental abruption. The placenta in the uterus can be situated anywhere on the inner surface of the uterus wall. Therefore, the effects of placental locations on the fetus injuries and mortality were investigated. The placenta position was varied alone and maximum uterine strain values were recorded. This study showed that the fetus of a pregnant driver who has a placenta located at the anterior in the uterus is more likely to be injured than the fetus of a pregnant driver who has a placenta located at the original position (fundus) of 'Expecting'. The results from the series of simulations suggest that a pregnant driver who has a placenta located at the anterior in the uterus should be more careful and drive less than a pregnant driver who has a placenta located at the original position (fundus) of 'Expecting'.

A 5th percentile female near the end of pregnancy represents the worst-case scenario in crash test simulations and real word accidents in terms of vulnerability while driving. The anthropometry of the existing 5th percentile female MADYMO model were created from the Western European population aged 18 to 70 years in 1984. This data was updated in 1997. Body mass and sitting height were considered to represent the small female anthropometry. The female model was altered to

represent the anatomy of a pregnant 5th percentile female using the anthropometric data collected from pregnant volunteers. Changes were only made to the chest depth, abdominal profile, abdominal height and depth, thigh depth and hip breadth. A pregnant occupant must position herself far forward in a car to reach the pedals due to her short limb length. Moreover, by the 38th week of pregnancy her abdominal size is at maximum, resulting in very close proximity to the steering wheel. Therefore, it is more appropriate to model and develop a pregnant female as close to term as possible to investigate the worst-case scenario.

The test methods were designed to provide simplified, easily controlled and measured tests containing key aspects of real-world impact inputs and injury outcomes. Placental abruption is the only criteria to investigate fetus safety in crash test simulations. The crash test results show that in road traffic accidents, even if the fetus itself does not directly cause placental abruption, its existence alone has the potential to affect the dynamic response of the pregnant occupant and strain levels at the UPI and overall uterus. The placental abruption risk was associated with the strains at the UPI and the threshold value for the occurrence of placental abruption is widely accepted to be 0.6 at the UPI. For crash speeds of 30 km/h and 35 km/h, the strain values exceed the threshold value, posing a risk of placental abruption. The fetus would have suffered fatal injuries at the crash speed of 35 km/h and then the simulation software became unstable. Therefore, in this research, a crash speed of 35 km/h was taken as the highest impact speed at crash test simulations. The results from the series simulations with and without restrained cases show that the use of a three-point seat belt with an airbag offers the greatest protection to the fetus for frontal crash impacts

The modified pregnant occupant model, 'Expecting' was validated in Chapter 7 and 8 against rigid bar impact and belt loading tests. Force-deflection abdominal corridors for a 50th percentile male cadaver were developed and scaled to a 5th percentile female. There are no real force-deflection corridors for pregnant women. Therefore, force-deflection corridors developed by Hardy et al. (2001) were used until new corridors specifically for pregnant women are available. The rigid bar impact tests illustrated the rate dependent nature of the pregnant occupant abdomen. The mass of the 48 kg impactor is significantly greater than the effective mass of a

typical pregnant abdomen. This helped to generate response corridors. The 6m/s corridors were plotted and compared with the original and modified 'Expecting'. Mid speed data (6 m/s) was chosen for rigid bar impact tests. The original 'Expecting' model was validated against rigid bar impact at 6 m/s. Modified 'Expecting' was also validated at 6m/s to compare the results with the original 'Expecting' and previous results. The results of modified 'Expecting' validation tests agreed well with the stiffness of the Hardy et al. (2001) corridors for rigid bar loading of the pregnant abdomen at 6m/s. Results appeared to be within the defined response corridors. The seat belt test was conducted to determine the response of the pregnant occupant abdomen to low-speed distributed loading. For the belt loading test, a finite element belt section was pulled across the pregnant abdomen at 3 m/s. In this research, belt penetration into the pregnant abdomen was calculated. Hardy performed a series of belt loading tests on human cadavers at a rate of 3 m/s. Pregnant abdomen response corridors for 3 m/s lap belt loading were developed and compared in Chapter 7 and 8. The peak seat belt loading rate in these tests was 3 m/s. However, these test standards were determined from 13.4 m/s sled tests conducted by FTSS using a lap and shoulder belt restrained Hybrid III dummy. For rigid bar impact and belt loading validation tests, force-displacement data of the abdomen were found to be in good agreement with the experimental data.

The actual mechanisms of placental abruption are not known. The placenta and uterus have different material properties. The uteroplacental interface also shows different material properties. Recorded strain value and actual injury risk are dependent on material properties. Inertial or directly applied forces can act on the fetus and the fetus may move within the uterus during an impact. This movement causes it to push directly on the placenta and thereby begin to dislodge the placenta from the uterus. Possible mechanisms of placental abruption and effect of the fetus were explored with drop test simulations in Chapter 5. The fetus-placenta interaction was investigated using the FE models of the uterus, placenta and the multibody fetus to simulate direct loading of the uterus with the fetus. Impact simulations involved dropping the uterus with and without the fetus onto a rigid plate from a height of 0.5 m. Vertical drops onto a rigid flat surface at angles of 0°, 30°, 90°, and 180° were simulated. Implications of including the fetus model in the uterus were investigated.

Drop test simulations assisted the investigation of different fetus-placenta interactions. The contribution of the fetus to the strains generated in the UPI was considerably high. Drop test simulation results showed that the existence of a fetus in the uterus plays an important role on the strain levels in the UPI and anywhere in the uterus. In all cases, the peak strain levels were higher with the fetus than without the fetus. This clearly demonstrated that the fetus changes the dynamics of the simulation of the uterus and fetus should be included in the uterus in all pregnant models to investigate crash test simulations realistically.

The airbag was positioned at the centre of the steering wheel in line with the steering wheel tilt angle. When the pregnant occupant was unrestrained, the airbag tilted up slightly from the steering wheel line in crash tests. This was due to high impact of the pregnant abdomen. The initial posture of the pregnant occupant in the driving seat was based on seated anthropometric measurements by Acar and Weekes (2004). The horizontal distance between the steering wheel rim and the uterus was set at 45 mm in the initial position. The steering wheel tilt was 30° from vertical. The clearance from the abdomen to the steering wheel decreased with increasing gestational age. Occupants generally do not adjust their fore-aft seat position to compensate for their increased abdomen depth (Klinich et *al.*, 1999). Close proximity to the steering wheel, increases impacts on pregnant abdomen. This study investigated the worst-case scenarios in terms of vulnerability for a pregnant occupant as a driver. Positions of the steering wheel and pregnant occupant were not changed in simulations. The inclusion of the three-point belt reduces the degree of steering wheel loading for each crash speed. In this study, the original initial position of the 'Expecting' in the vehicle and the initial position of the vehicle interior were not changed to compare the original 'Expecting' with the modified 'Expecting'. Different steering wheel tilt angle and close proximity to the steering wheel may affect fetus safety.

Airbags are essential safety devices in vehicles to prevent injuries during road accidents. However, the inflation of an airbag under some circumstances also has the potential to cause serious injuries and even death in motor vehicle accidents. Pregnant occupants constitute a vulnerable group in occupant safety in motor vehicle accidents. During pregnancy, the fetus grows inside the pregnant abdomen and the

uterus gets closer to the steering wheel. The proximity of the uterus to the steering wheel and deploying airbag creates an increased risk of fetal death and injuries. Airbag units designed to restrain a 50th percentile male occupant can be less effective on a person who is not classed as a 50th percentile male (Butler *et al.*, 1993). Airbag deployment systems and setting of deployment time are crucial elements for occupant safety in motor vehicle accidents. The roles of a range of airbag firing times for a typical driver airbag system that potentially reduces the risk for pregnant women and their fetuses were investigated in Chapter 4. Well-being of the fetus was investigated using the 'Expecting' pregnant model. The investigation involved simulations of crashes with varying impact severities for full-frontal collisions with different airbag firing times. In this study, airbag firing times ranging from 10, 30, and 60 ms were chosen to mitigate critical injury criteria values. Strains and displacements in the uterus were calculated to predict the risk of placental abruption and fetal fatalities. 'Seat belt and airbag', 'seat belt only', and 'no restraint' cases showed that airbag inclusion cases had lower strains and displacements than cases without an airbag. When an airbag was used without the seat belt, strain levels reached and exceeded the threshold level at crash speeds starting from 15 km/h. 'Seat belt and airbag' case simulations were examined for airbag firing times of 10, 30, and 60 ms. All results showed a similar tendency and maximum strains at UPI increased when crash speed increased. In order to understand the effect of airbag deployment time on fetus safety, the airbag only case was investigated for the first time with the 'Expecting'. Simulation results showed that an airbag firing time of 10 ms caused lower UPI strain than airbag firing times of 30 ms and 60 ms, for all impact speeds. When the airbag firing time was reduced, predicted strain at the UPI was reduced as well. The airbag on its own causes high levels of strain and it must be used in conjunction with the seat belt to be effective in reducing the strains below the threshold level. The firing time of the airbag appeared to make a small but not significant difference to fetus safety. The results from several simulations suggest that the use of a three-point seat belt with an airbag offers the greatest protection to the fetus for frontal impacts.

All measurements in the experimental crash tests are independent of the stretch of the belt webbing. Therefore, belt stretch is not included in any analyses in

crash test simulations. For the seat belt systems including lap belt, shoulder belt, retractor, pretensioner and load limiter, a moderate amount of stretch in a seat belt harness can be considered. According to the work-energy principle, a vehicle collision stops the vehicle and the occupants and removes their kinetic energy. A longer stopping distance decreases the impact force on the vehicle and on the occupants. A stretching seat belt can extend the stopping distance of an occupant and reduces the average impact force on the occupant compared to a non-stretching harness. For only lap belt loading, this effect was neglected in the experimental tests and consequently in crash test simulations.

The improved 'Expecting' model can be used for the evaluation of safety systems and vehicle interiors. The 'Expecting' was used in predicting fetus safety in real-world accident case studies. Previous pregnant models had only focussed on the abdominal region by simply adding an enlarged abdomen to a female model. The significant mass of the fetus and finite element amniotic fluid fill the entire volume of the uterus. In this research, movement of the fetus within the uterus and fetus interactions with its surroundings such as amniotic fluid and placenta were investigated more realistically than in previous models, with a finite element method. Simulation results with improved 'Expecting' are more realistic than the original 'Expecting', because not only displacement of the bodies were defined but also deformation on the bodies and their interactions were defined. A cushioning effect of the finite element amniotic fluid was observed from the simulation results. Stresses and strains induced in the uterus and placenta were more accurate. Different crash scenarios were investigated by changing and developing several different parameters as a step forward to more realistic accident recreation for fetus safety in motor vehicle accidents.

9.2 Limitations of the Research

Investigations on pregnant occupant safety in motor vehicles revealed that there is very little experimental and realistic crash test data about pregnant occupants. Furthermore, volunteer data are impossible to collect due to ethical issues. Hence, computational models play a significant role in safety investigations.

Creating a finite element or multibody computational model of a human body is also a challenging task. Human anthropometry changes according to ethnic composition of population, lifestyle, and nutrition. Every pregnancy and hence each uterus, placenta, fetus size and position are different. Hence a number of assumptions were made in the modelling of the pregnant occupant. The original 'Expecting', the pregnant occupant model, was developed at Loughborough University. For the modified versions of 'Expecting', the finite element fetus head and the amniotic fluid are assumed to be linear, elastic, isotropic solid materials. The uterus was also modelled with the same approach although it is known to be anisotropic and viscoelastic. However, currently there is not enough data to apply these material properties to the model. The amniotic fluid is defined as a solid with fluid properties because MADYMO does not allow fluids to be defined. Due to the complexity, fetus head geometry in the uterus is simplified. Material properties of the finite element fetus head were taken from new-born baby data as a basis to obtain age specific material properties for the 38 week old fetus skull. Over the final trimester, the head of the fetus becomes stiffer and heavier. Material properties of the fetus head play an important role in representing the fetus realistically. Response of the finite element fetus head to an impact differs with different head material properties. The whole fetus model in the original 'Expecting' is developed as a multibody, hence the head does not deform. The finite element fetus head is capable of deformation under external loading easily. A deformable head changed the dynamics of the system and affected the stress and strain levels in the uterus. It is also possible to measure local stress and strain values at the fetus head. But there is no injury criteria for the fetus head. Realistic representation of the fetus with finite element modelling and material properties generates more realistic and accurate results.

Crash test simulations were performed using a half-sine wave acceleration pulse with 120 ms duration. A real acceleration pulse could be different for each crash even for the same speed crashes. Some crashes may show much a longer acceleration pulse at even low speed whereas in some cases the pulse duration could be much shorter with high peak values. The vehicle compartment is modelled as multibody while the pregnant occupant uses a finite element model. Material properties of pregnant occupant skin and its interaction with restraint systems are not

considered. In order to investigate the effects of intrusion on the pregnant occupant, vehicle interior and compartments need to be modelled and defined with the finite element method. Depending on the restraint system of the pregnant occupant and vehicle interior properties, passenger compartment intrusion may have beneficial, detrimental or neutral effects upon injury to the pregnant abdomen. Intrusion with a deformable vehicle interior depending on its material properties and design may increase or decrease the strain levels around the uterus and at the UPI. Deformable bodies react more realistically and may give more accurate results than rigid bodies. Strain values from the simulations and consequently the actual absolute injury risk for the fetus safety are highly dependent on material properties of finite element bodies and should be investigated further.

The main difficulty in developing the 'Expecting' pregnant occupant model is its validation. The computational pregnant occupant model can only be validated with rigid bar impact and belt loading tests due to lack of experimental data and ethical issues. In the case of a human fetus, there is no force-deflection data based on cadaver or volunteer tests. The threshold strain value in the uterus for the occurrence of placental abruption is accepted as the reference value for the occurrence of fetus fatality. Placental abruption is the only quantifiable injury criterion for the fetus. This limits the investigation of fetus safety in motor vehicle accidents because there are also some other risks to the fetus in the case of an automobile impact. Fetal injuries may occur due to direct contact with the deploying airbag and seat belt loading. As a result of road traffic accident and trauma, feto-maternal transfusion, loss of fetal blood cells into the material circulation, and preterm delivery may occur. Causes of these injuries and fetal loss in motor vehicle accidents may not only be as a result of placental abruption. If more injury criteria about fetus safety could be defined, the fetus model and the accuracy of the simulation results would have improved.

9.3 Future Work

The finite element fetus head and the finite element amniotic fluid in the 'Expecting' model are significant improvements for a more realistic model of pregnant occupants. Creating a broader, more realistic model will also raise awareness of the issues surrounding pregnant women as drivers. Although 'Expecting' has been the most realistic pregnant occupant model with the finite element fetus head and the finite element amniotic fluid, there is still room for further developments. The next stage of the work could be the modelling of the full finite element fetus body. Since the fetus may have a direct contact with the placenta, it is possible that a deformable fetus body could affect the strain levels and the risk of placental abruption. A fully deformable fetus model would give a more realistic representation of the fetus but the material properties would be difficult to obtain.

Different restraints such as advanced "smart" systems, which could be tuned to the range of test conditions, booster seats, side airbags, retractable seats, integrated airbag on seat belt can be modelled and their impacts on modified 'Expecting' can be investigated. Different seating positions such as the pregnant occupant as a passenger in the front seat or rear seat could be investigated with crash test simulations. Different airbag and impact types could be compared with other computational and experimental occupant models. Simulations at higher crash speeds could be modelled and validated with the modified 'Expecting'.

Side and rear impact crash test simulations could be conducted when the placenta is located at different regions in the uterus in order to investigate the risk of placental abruption. For different seating positions of the pregnant occupant in the vehicle, higher crash speeds can be tested. The vehicle interior compartment including the steering wheel could be modelled as finite elements and the effect of intrusion on the pregnant abdomen could be investigated.

The modified 'Expecting' model can also be converted into a commercial software package. The next generation of 'Expecting' can be parametric to represent different stages of pregnancies.

9.4 Conclusions

The evolution of finite element occupant models was explained and computational pregnant models were examined. The most realistic pregnant occupant model 'Expecting' was used in conducting several crash scenarios. The implications of including a fetus in the uterus of 'Expecting', the pregnant occupant model, were investigated. First of all, the uterus with and without a fetus model was used to simulate a range of vertical drops onto a rigid flat horizontal surface at four different angles. Drop tests with a fetus in the uterus changed dynamic behaviour of the uterus and increased strain levels. Then, in order to explore the role of including a fetus in the uterus, 'Expecting' with and without a fetus were used in crash test simulations and the results were compared. It was observed that the loading from the seat belt, steering wheel and airbag, caused strains to develop in the uterus. Furthermore, due to the motion of the fetus, inertial loading on the uterus occurs. Crash test simulation results from the 'Expecting' model showed that the inclusion of the fetus in the model changes the dynamics of the occupant and generates significantly higher strains at the UPI than the without fetus model. Therefore, it was concluded that a fetus should be included in the uterus in pregnant occupant models, for realistic simulations.

The role of placenta position on the risk of placental abruption was investigated using different placental locations. In the design approach of the placenta models at different locations, limited space between the fetus and the uterus was considered. It was found that there is a significant role of placental position on the risk of fetus mortality. The highest strain value was predicted with the anterior placenta, whereas with the posterior placenta a relatively low strain value was predicted. This study found that the fetus of a pregnant driver with an anterior placenta has a higher risk than the fetus of a pregnant driver with the placenta located at the fundus.

The uterus with the multibody fetus was filled with finite element amniotic fluid to replace the spring suspended fetus of the original 'Expecting' model. The multibody fetus was also given a finite element head. The effect of external loadings such as seat belt, airbag, steering wheel as well as internal loadings such as fetus, amniotic fluid, and pregnant body were investigated. 'Unrestrained', 'seat belt only',

'airbag only', and 'seat belt and airbag' tests were simulated with the new amended model in frontal impacts. During crash test simulations with the modified model, peak strain at UPI was observed to be almost always higher than with the original model. It was observed that the dynamic response of the pregnant occupant changes considerably when the finite element fetus head and amniotic fluid models are integrated into the 'Expecting' model. The main observed difference in simulations is the deformation of the fetus head and changing shape of the uterus. During the forward motion of the pregnant abdomen, the fetus moves downwards and the head of the fetus compresses and presses on the uterus. This generates more space between the fetus and placenta than the space observed in simulations with a fully rigid fetus body. This may have led to the prediction of reduced risk of placental abruption with the deformable fetus head model.

Overall, there is high probability that placental abruption would occur in the unrestrained, frontal impact simulations. The use of a three-point seat belt and an airbag reduces the risk to the pregnant occupant and the fetus. The findings of this research lead to the recommendation that the use of a three-point seat belt with the airbag is crucial for the safety of a pregnant occupant and her fetus. The fully restrained case offers the greatest protection to the fetus and the mother in frontal crash impacts. More realistic modelling of the pregnant occupant leads to realistic responses to the impacts. It is particularly important for the car industry to work with more biofidelic and realistic crash test models in order to develop vehicle safety for vulnerable occupants, such as pregnant women. It is hoped models such as the realistic 'Expecting' could be used to improve pregnant occupant safety in motor vehicles.

REFERENCES

Acar, B.S. and Esat, V. (2010) Seat belt designs to protect pregnant vehicle occupants, *Recent Patents on Mechanical Engineering*, 2010, 3, 1-10

Acar, B.S. and van Lopik, D. (2009) Computational pregnant occupant model, 'Expecting', for crash simulations, *Proceedings of the Institution of Mechanical Engineers, Vol.223, Part D, Journal of Automotive Engineering*

Acar, B.S. and Weekes, A.M. (2003) Pregnant driver behaviour and safety. First International Conference on Driver Behaviour and Training, Stratford-upon-Avon, UK, 11 November, pp.125-133.ISBN:0754638359

Acar, B.S. and Weekes, A.M. (2004) Designing for safety during pregnancy through a system for automotive engineers, *International Journal of Crashworthiness*, 9, No. 6, 625-631

Acar, B. S. and Weekes, A. M. (2005) Design guidelines for pregnant occupant safety, *Proceedings of the Institution of Mechanical Engineers Part D - Journal of Automotive Engineering*, Vol.119

Acar, B.S., Weekes, A.M., van Lopik, D. (2004) Anthropomorphic modelling of the pregnant occupant, Proceedings of ESDA2004, *7th Biennial ASME Conference on Engineering System Design and Analysis*, July 19-22, 2004, Manchester, UK

Acar, B.S. and Weekes, A.M. (2006) Measurements for pregnant driver comfort and safety, *International Journal of Vehicle Design*, 42(1), 101-118, ISSN 1741-5314

Acar, B.S. and Weekes, A.M. (2013) Seat belt positioning during pregnancy

Agran, P.F., Dunkle, D.E., Winn, D.G., and Kent, D. (1987) Fetal death in motor vehicle accidents, *Annals of Emergency Medicine*, 16(12), 1355-1358

Baker, S. P., O'Neil, B., Karpf, R.S., The Injury Fact Book, Lexington Books, (1984)

Baughman, L. D. (1983) Development of an interactive computer program to produce body description data, Report No.AFAMRL-TR-83-058

Behr, M., Arnoux, P. J., Serre, T., Bidal, S., Kang, H. S., Thollon, L., Cavallero, C., Kayvantash, K., and Brunet, C. (2003) A human model for road safety: from geometrical acquisition to model validation with Radioss, *Computer Methods in Biomechanical and Biomedical Engineering*, 6, No.4, 263-273

Behr, M., Arnoux, P. J., Serre, T., Thollon, L. and Brunet, C. (2006) Tonic finite element model of the lower limb, *Journal of Biomechanical Engineering*, 128, 223

Brace, R.A. and Wolf, E.J. (1989) Normal amniotic fluid volume changes throughout pregnancy, *American Journal of Obstetrics and Gynecology*, 1989:161:382-288

Bunai, Y., Nagai, A., Nakamura, I., and Ohya, I. Fetal death from abruptio placentae associated with incorrect use of a seat belt. The American Journal of Forensic Medicine and Pathology, 2000, 21(3), 207-209

Butler, P.B., Kang, J., and Krier, H. (1993) Modelling and numerical simulation of the internal thermochemistry of an automotive airbag inflator, *Progress in Energy and Combustion Science*, Vol. 19, 1993, pp. 365-382

Chervenak, F.A., Isaacson, G., Campbell, S., (1993) Textbook of *Ultrasound in Obstetrics and Gynecology*, Little, Brown, and Company. Boston, 1993

Choi, H. Y., Eom, H. W., Kho, S. T., Lee, I. H. (1999) Finite element human model for crashworthiness simulation, *Society of Automotive Engineers*, Paper No. 1999-01-1906

Clinical Research Imaging Centre, (CRIC), University of Edinburgh, fetal image http://www.auntminnieeurope.com/index.aspx?sec=supandsub=mriandpag=disandItemID=605973 [Accessed 10 May 2013]

Coats, B. and Margulies, S.S. (2006) Material properties of human infant skull and suture at high rates, *Journal of Neurotrauma*, Volume 23, Number 8, 2006 Pp1222-1232

Crosby, W.M. and Costiloe, J.P. (1971) Safety of lap-belt restraint for pregnant victims of automobile collusions. New England Journal Medicine 1971, 284, 632-636

Crosby, W.M., King, A.I., Stout, L.C. (1972) Foetal survival following impact: Improvement with shoulder harness restraint, *American Journal of Obstetrics and Gynaecology*, 1101-1106

Crosby, W. M., Snyder, R. G., Snow, C. C., and Hanson, P. G. (1968) Impact injuries in pregnancy I: Experimental studies, *American Journal of Obstetrics and Gynaecology*, 101:100-110

Culver, C.C., and Viano, D.C., (1990) Anthropometry of seated women during pregnancy; defining a fetal region for crash protection research, *Human Factors* 1990; 32:625-636

Daniel, R. P., Irwin, A., Athey, J., Balser, J., Eichbrecht, P., Hultman, R. W., Kirkish, S., Kneisly, A., Mertz, H., Nusholtz, G., Rouhana, S. and Scherer, R. (1995) Technical Specifications of the SID-IIs Dummy, *Society of Automotive Engineers*, Paper No. 952735

Davidsson, J. (1999) BioRID II Final Report, *Crash Safety Division, Department of Machine and Vehicle Design, Chalmers University of Technology*, Gotenborg, Sweden

Dekaban, A. Tables of cranial and orbital measurements, cranial volume, and derived indexes in males and females from 7 days to 20 years of age, Annals of Neurology, 1977; 2/6:485-91

D'Elia, A., Scully, J., and Newstead, S. (2012) Evaluation of vehicle side airbag system effectiveness, *Monash University, Accident Research Centre,* July 2012, Report No.132

Delotte, J., Behr, M., Baque, P., Bourgeon, Andre, Peretti, F. and Brunet, C. (2006) Modelling the pregnant woman in driving position, *Surgical and Radiologic Anatomy*, 28:359-263

Delotte, J., Behr, M., Thollon, L., Arnoux, P.J., Baque, P., Bongain, A., and Brunet, C. (2008) Pregnant woman and road safety: experimental crash test with post mortem human subject, Surg Radiol Anat (2008) 30:185-189

Department for Transport (DfT) (2003) Seat belts and child restraints (Leaflet No. T/INF/251). London: Department for Transport UK; 2003 https://www.gov.uk/government/organisations /department-for-transport [Accessed 10 March 2013]

Department of Trade and Industry Adultdata (DTI) (1998): The Handbook of Adult Anthropomorphic and Strength measurements- Data for Design Safety, 1998, London

Duck, F.A. (1990) *Physical properties of tissue*: a comprehensive reference book, Academic Press, London, 1990

Enever G. (1999) The "Sierra Sam" Story. Available from: <http://research.ncl.ac.uk/nsa/sam.html> [Accessed 10 April 2010]

EuroNCAP, (2013) A history of the future of safety, http://www.euroncap.com/files/euroncap_history---d7e9ac87-c4bd-4a7f-90fd-88b2bcf4da8d.pdf, [Accessed 15 October 2013]

Eurostat (2011) Transport accident statistics, http://epp.eurostat.ec.europa.eu/statistics_explained/index.php/Transport_accident_statistics [Accessed 20 May 2013]

First Technology Safety Systems, (2006) History of Crash Test Dummies. Available from: <http://www.humaneticsatd.com/about-us/dummy-history> [Accessed 5 September 2010]

First Technology Safety Systems, (2010) Hybrid III 5th percentile female physical dummy. Available from: <http://www.humaneticsatd.com/crash-test-dummies/ frontal-impact/hybrid-iii-5th> [Accessed 28 September 2010]

FTSS. (2012) Available from: <http://www.humaneticsatd.com/crash-test-dummies/ frontal-impact/> [Accessed 25 September 2012]

Fleck, J.T., and Butler, F.E. (1975) Development of an Improved Computer Model of the Human Body and Extremity Dynamics, *Aerospace Medical Research Laboratory*, Report No.-TR-75-14

Foster, J.K., Kortge, J.O., Wolanin, M.J. (1977) Hybrid III, A Biomechanically Based Crash Test Dummy, *Society of Automotive Engineers*, Paper No. 770938

Fried, A.M. (1978) Distribution of the bulk of the normal placenta. Review and classification of 800 cases by ultrasonography, *American Journal of Obstetrics and Gynecology*, 132(6), 675-680

FT-Arup. (2005) Hybrid III 50th Dummy LS-DYNA Model, Version 5.1, User Manual

Fusco, M.A., Martin, R.S., Chang, M.C. (2001) Estimation of intra-abdominal pressure by bladder pressure measurement: Validity and methodology, *Journal of Trauma,* 2001;50:297-302

General Motors, (1934) First Crash Test. Available from: http://www.gm.com/ corporate/about/history/ [Accessed 15 September 2010]

Goodwin, T. and Breen, M. (1990) Pregnancy outcome and fetomaternal hemorrhage after noncatastrophic trauma, American Journal of Obstetrics and Gynecology. 162930: 665-671

Haapaniemi, P. (1996) Women's highway deaths on the rise, *Road Safety,* 96, 6-11

Hammond, R.H. and Edmonds, D.K. (1990) Does treatment for cervical intraepithelial neoplasia affect fertility and pregnancy? *BMJ*. 1990 Dec 15; 301(6765): 1344-5

Happee, R., Hoofman, M., van den Krooenberg, A. J., Morsink., P., and Wismans, J. (1998) A mathematical human body model for frontal and rearward seated automotive impact loading, *Proceedings of the 42nd Stapp Car Crash Conference*, Society of Automotive Engineers, SAE Paper No. 983150

Happee, R., Ridella, S., Nayef, A., Morsink, P., De Lange, R., Bours, R., Van Hoof, J. (2000) Mathematical human body models representing a mid size male and a small female for frontal, lateral and rearward impact loading, *International Conference on the Biomechanics of Impacts*, Montpellier, France

Happee, R., Wismans, J., Morsink, P. (1999) Mathematical human body modelling for impact loading", *Society of Automotive Engineers,* Paper No.1999-01-1909

Hardy, W.N., Schneider, L.W., and Rouhana, S.W. (2001) Abdominal impact response to rigid-bar, seat-belt, and airbag loading. *Stapp Car Crash Journal*, 2001, 45, 1-32

Hendler, E., O'Rourke, J., Schulman, M., Katzeff, M., Domzalaski, L. and Rodgers, S. (1974) Effect of Head and Body Position and Muscular Tensing on Response to Impact, *Society of Automotive Engineers*, Paper No. 741184

Hitosugi, M., Motozawa, Y., Kido, M., Yokoyama, T., Kawato, H., Kuroda, K., Tokudome, S. (2006) Traffic injuries of the pregnant women and fetal or neonatal outcomes, *Forensic Science International* 159 (2006) 51-54

Hitosugi, M., Motozawa, Y., Kido, M., Maegawa, M., Nagai, T., Tokudome, S. (2007) The benefits of seat belt use in pregnant drivers, Forensic Science International, volume 169, issue 2, pages 274-275

Hodgson, V. R., Thomas L. M. (1972) Comparison of head acceleration injury indices in cadaver skull fracture, *Society of Automotive Engineers*, Paper No. 710854, 190-206

Hu, J., Klinich, K.D., Miller, C.S., Nazmi, G., Pearlman, M.D., Schneider, L.W., and Rupp, J.D. (2009) Quantifying dynamic mechanical properties of human placenta tissue using optimization techniques with specimen-specific finite element models, *Journal of Biomechanics* 42(15):2528-2534

Huelke, D.F. and Moore, J.L. (1993) Field investigations of the performance of airbag deployments in frontal collisions, *Accident analysis and prevention* Vol.25, No 6, 717-730, 1993

HyperMesh 7.0 (Altair) Altair HyperWorks http://www.altairhyperworks.co.uk /Product,7,HyperMesh.aspx?AspxAutoDetectCookieSupport=1

Invent, (2010) Nills Bohlin. Available from: <http://www.invent.org/hall_of _fame/ 179.html> [Accessed 25 September 2010]

Jager K., Ratingen M., Lesire, P., Guillemot, H., Pastor, C., Schnottable, B., Tejera, G., Lepretre, J.P. (2005) Assessing new child dummies and criteria for child occupant protection in frontal impact, *19th ESV Conference*, Washington DC, USA

Jeanty, P., Rodesch, F., Delbecke, D., and Dumont, J. (1984) Estimation of gestational age from measurements of fetal long bones, *Journal Ultrasound Medicine* 3:75

Jost, R. and Nurick, G.N. (1999) Finite element modelling of the human body in vehicle side impact, *International Journal of Crashworthiness*, 4, No.1

Kaleps, I., White, R.P., Jr., Beecher, R.M., Whitestone, J., and Obergefell, L.A. (1988) Measurement of Hybrid III Dummy Properties and Analytical Simulation Data Base Development, *Armstrong Laboratory*, Report No.AAMRL-TR-88-005

Khatua, T., Chang, L., and Pizialli., (1988) ATB simulation of the Hybrid III dummy in sled tests, *Society of Automotive Engineers*, Paper No. 880646

Kirkpatrick W.S., Holmes S.B., Hollowell W.T., Gabler H.C., Trella T.J. (1993) Finite Element Modelling of the Side Impact Dummy (SID), *Human Surrogates: Design, Development and Side Impact Protection*, SAE Paper No.930104

Klinich, K.D., Schneider, L.W., Moore, J.L., and Pearlman, M.D. (1998) Injuries to pregnant occupants in automotive crashes [Abstract 98-sp-p17] *Annual Conference of the Association for the Advancement of Automotive Medicine*, Charlottesville, Va

Klinich, K.D., Schneider, L.W., Eby, B., Rupp, J.D., and Pearlman, M.D. (1999a) Investigations of crashes involving pregnant occupants, *University of Michigan Transportation Research Institute*, TRI 99-200

Klinich, K.D., Schneider, L.W., Eby, B., Rupp, J.D., and Pearlman, M.D. (1999b) Seated anthropometry during pregnancy, *University of Michigan Transportation Research Institute Final Report*, No. UMTRI 99-16

Klossner N.J. (2005) Introductory Maternity Nursing Copyright by Lippincott Williams and Wilkins

Langley, J. and Brenner, R., (2004) What is an injury? Injury Prevention 2004; 10:69-71 doi:10.1136/ip.2003.003715

Lau, I.V., Horsch, J.D., Viano, D.C., and Andrzejak, D.V. (1993) Mechanism of injury from airbag deployment loads, *Accident; Analysis and Prevention* 1993 Feb: 25 (1): 29-45

L'Abbe, R.J., Dainty, D.A., and Newman, J.A. (1982) An experimental analysis of thoracic deflection response to belt loading. *Seventh International IRCOBI Conference on the Biomechanics of Impacts*, pp. 184-194. Bron, France

Lieberman, E., Davidson, K., Lee-Parritiz, A., and Shearer, E. (2005) Changes in fetal position during labour and their association with epidural analgesia, *Obstetrics and Gynecology*, 2005 May; 105(5 Pt 1):974-82

Lizee, E., Robin, S., Song, E., Bertholon, N., Coz, J.Y.L., Besnault, B., Lavaste, F. (1998) Development of a 3D Finite Element Model of the Human Body, *Society of Automotive Engineers*, Paper No.983152

Loftis, K.L., Halsey, M.G., Anthony, E., Duma, S.M., and Stitzell, J.D. (2008) Pregnant female anthropometry from CT scans for finite element model development, *Biomedical Sciences Instrumentation* 44:355-360

Made R., Margerie L., Hovenga E., Kant R., Co J., Xu B., Sriram N.S., Laituri T. (2001) Development of a Hybrid III 5th percentile Facet Dummy Model, *Society of Automotive Engineers*, Paper No. 2001-01-2050

Madehow, (2012) How is airbag made, http://www.madehow.com/Volume-1/Air-Bag.html [Accessed 21 April 2013]

MADYMO Applications Manual (2010) Release 7.2 January 2010 Copyright by TNO https://www1.ethz.ch/biomed.ee/intranet/support/madymo/Applications.pdf [Accessed 10 April 2013]

MADYMO Model Manual. (2010). Available from: <www.tass-safe.com/public/... /MADYMO_dummy_models_Data_Sheet-v2.pdf> [Accessed 28 September 2010]

MADYMO Theory Manual. (2010). Available from http://www.advanced simtech.com/software /MADYMO/MADYMO-model-libraries />[Accessed 29 September 2010]

MADYMO Human Models Manual (2010) Release 7.2 January 2010 Copyright by TNO https://www1.ethz.ch/biomed.ee/intranet/support/madymo/HumanModels.pdf [Accessed 15 April 2013]

Manoogian, S.J., Bisplinghooff, J.A., McNally, C., Kemper, A.R., Santago, A.C., and Duma S.M (2008) Dynamic tensile properties of human placenta, *Journal of Biomechanics* 41:3436-3440

Margulies, S.S. and Thibault, K.L. (2000) Infant skull and suture properties: measurements and implications for mechanisms of pediatric brain injury, *Journal Biomechanics Engineering* 122 (4):364-371

Marklund, P.O., and Nilsson, L., (2003) Optimization of airbag inflation parameters for the minimization of Out of Position occupant injury, *Computational Mechanics*, Volume 31, pp 496-504, 2003

Martinez, L. V., Lasaga, C., Garcia, M. (1999) An Advanced 50th Percentile THOR Dummy Database, *International Conference on the Biomechanics of Impact*, Society of Automotive Engineers, Paper No. 930094

Marzougui D., Kan C. D., Bedewi N. E. (1996) Development and Validation of an NCAP Simulation Using LS-DYNA3D, *Proceedings of the Fourth International LS-DYNA3D Conference*, Minneapolis, USA

McElhaney, J.H., Fogle, J.L., Melvin, J.W., Haynes, R.R. Roberts, V.L., and Alem, N.M. (1970) Mechanical properties of cranial bone, *Journal Biomechanics* 3, 495-512

McHenry, R. R. and Naab, K. N. (1966) Computer simulation of the Automobile Crash Victim in a Frontal Collision, *Cornell Aeronautical Laboratory, Inc., A Validation Study Report*, Number YB-2126-V-IR

McHenry, R. R. (1963) Analysis of the dynamics of automobile passenger restraint systems, *Proceedings of the 7th Stapp Car Crash Conference*, Society of Automotive Engineers, Paper No.1963-12-0017.

McPherson, G.K. and Kriewall, T.J. (1980) Fetal head molding: An investigation utilizing a finite element model of the fetal parietal bone, *Journal of Biomechanics* Vol. 13, pp. 17-26

Medicinembbs (2012) fetal skull http://medicinembbs.blogspot.co.uk/2012/05/fetal-skull.html [Accessed 10 March 2013]

Melvin, J. W., Horsch, J. D., McCleary, J. D., Wideman, L. C., Jensen, J. L., and Wolanin, M. J. (1993) Assessment of Airbag Deployment Loads with the Small Female Hybrid III Dummy, *Society of Automotive Engineers*, Paper No. 933119

Metz T. D. and Abbott, J. T. (2006) Uterine trauma in pregnancy after motor vehicle crashes with airbag deployment: A 30-case series, J Trauma 2006; 61:658-661

Midoun D. E., Abramoski E., Rao M. K. and Kalidindi R. (1993) Development of a Finite Element Based Model of the Side Impact Dummy, *Society of Automotive Engineers*, Paper No.930444

Miller, R.A., and Allen, B.T. (2007) Injury optimization of the frontal crash supplemental restraint system (SRS) deployment matrix *ESV SAE International* Paper No 07-0073

Mizrahi, J. and Karni, Z. (1975) A mechanical model for uterine muscle activity during labor and delivery, *Israel Journal of Technology* 13: 185-191

Motojima H., Hasegawa J., Ogawa Y., Ando K. And Haug E. (1997) Development of a Finite Element Model of the Side Impact Dummy and Application for the Side Impact Protection, *Toyota Technical Review*, 46, No2, 25-31

Moorcroft, M., Duma, S., Stitzel, J., and Duma, G. (2003) A finite element and multi-body model of the pregnant female occupant for the analysis of restraint effectiveness, *SAE International*, 2003-01-0157

Motozawa, Y., Abe, T., Hitosugi, M., and Tokudome, S. (2009) Analysis of overall kinematics and abdominal response of pregnant drivers during frontal vehicle collisions, *SAE International* 2009-01-0380

Murao, H., Miura K., Ohata, N., Nakamoto, T., Kinjo, K., Takahashi, Y., Hashiguchi, M. (2002) Clinical study of 109 cases of injury during pregnancy, *Proceedings JSAE annual Congress*

National Highway Traffic Safety Administration (1997) Airbag design and performance characteristics in the 1900's http://www.nhtsa.gov/Research/ Crashworthiness/Advanced +Air+Bag+Technology+ Research [Accessed 10 April 2013]

NHTSA (1982) An evaluation of side structure improvements in response to federal motor vehicle safety standard 214, http://www-nrd.nhtsa.dot.gov/Pubs/806314.pdf [Accessed 20 May 2013]

NHTSA (1973) Federal Motor Vehicle Safety Standard 208. Available from: <http://www.nhtsa.gov/cars/rules/import/fmvss/index.html#SN208> [Accessed 12 April 2012]

NHTSA, (2002) Should pregnant women wear seat belts (Leaflet No. DOT HS 809 506). Washington DC, USA: NHTSA; 2002

NHTSA, (2008) Counts of frontal airbag related fatalities and seriously injured persons, Statistical Breakdown of Airbag Fatalities. http://www-nrd.nhtsa.dot.gov/Pubs/AB0108. pdf [Accessed 10 March 2013]

Nissan Global, (2007) Active bonnet system, http://www.nissan-global.com /EN/TECHNOLOGY/OVERVIEW/puehfpp.html [Accessed 20 April 2013]

Novakov, A. (2002) Ultrasound examination in the second and third trimester http://sonoworld.com/fetus/page.aspx?id=449

Nyquist, G. W., Begeman, P. C., King, A. L., and Mertz, H. J. (1980) Correlation of field injuries and GM Hybrid III responses for lap-shoulder belt restraint, *Journal of Biomechanical Engineering*, 102:103-109

Obergefell, L., Kaleps, I. and Steele, S. (1988) Part 572 and Hybrid III dummy comparisons in sled test simulations, *International Congress and Exposition*, Society of Automotive Engineers, Paper No.880639

Oshita, F., Omori, K., Nakahira, Y. and Miki, K. (2002) Development of a Finite Element Model of the Human Body, *7th International LS-DYNA User Conference*, Detroit

Patrick, L. M. (1966) Cadaver windshield research, *Plastic and Reconstructive Surgery*, 37:314-323

Pearlman, M. D. (1997) Motor vehicle crashes, pregnancy loss and preterm labour, *International Journal of Gynaecology and Obstetrics*, 57, 127-132

Pearlman, M. D., Tintinalli, J. E., Lorenz, R. P. (1990) Blunt trauma during pregnancy, N. England J. Med 1990; 323; 1609

Pearlman, M. D. and Viano, D. (1996) Automobile crash simulation with the first pregnant crash test dummy, *American Journal of Obstetrics and Gynaecology*, 175, 977–981

Pearlman, M. D., Viano, D., Jedrzejczak, E., Deng, B., Smrcka, J., and Kempf, P. (1996) Belt and airbag testing with a pregnant Hybrid III female dummy, *Society of Automotive Engineers*, Paper No. 96-S10-O-03

Pearsall, G.W. and Roberts, V.L. Passive mechanical properties of uterine muscle (myometrium) tested in vitro, J. Biomech, (UK), vol 11 no.4 (1978). pp. 167-76

Pepperell, R.J., Rubenstein, E., and MacIsaac, I.A. (1977) Motor-car accidents during pregnancy, *The Medical Journal of Australia*, 0400714

Peres, J., Behr, M., Thollon, L., Kayvantash, K. (2011) A pregnant woman model to understand injury mechanisms in frontal car crashes, *International conference simulations in biosciences and multiphysics*

Pheasant, S. (1998) *Bodyspace: Anthropometry, Ergonomics and the Design of Work*, Taylor and Francis,

Prasad, P. (1990) Comparative evaluation of the dynamic response of the dynamic response of the Hybrid II and Hybrid III dummies, *Proceedings of the 34th Stapp Conference,* Society of Automotive Engineers, Paper No.902318

Prasad, P. (1988) MADYMO 2-D Simulation of Sled Tests, Society of Automotive Engineers, Paper No.880640.

Prasad, P., King, A.I., (1974) An experimentally validated dynamic model of the spine, J. Appl. Mech., 41, 546-550

Pregnant Driver. (2004) Pregnant Women's Anthropometry Website. Available from: <http://pregnantdriver.lboro.ac.uk/> [Accessed 20 September 2010].

Q Child Dummies. (2010) Available from: <http://www.humaneticsatd.com/crash-test-dummies/children/q-series> [Accessed 20 September 2010]

RAMSIS software. (1994). Available from: <http://www.human-solutions.com /automotive /ramsis_community/index_en.php> [Accessed 29 September 2010]

Richardson, M. and O'Connell, J. (2000) Airbag injuries: The Australian scenario. Implications for trauma nurses, *AENJ* Volume 3 No. 1 April 2000

Robbins, D. H. (1970) Three-dimensional simulation of advanced automotive restraint system, Society of Automotive Engineers, Paper No.700421

Robbins, D. H., Bennett, Jr., Bowman, B. M. (1972) User-oriented mathematical crash victim simulator, *In: Proceedings 16th Stapp Car Crash Conference,* Society of Automotive Engineers, 128-148

Robbins, D. H., Bennett, Jr., R. O. and Bowman, B. M. (1974) The MVMA two-dimensional crash victim simulator, *In Proceedings 18th Stapp Car Crash Conference,* Society of Automotive Engineers, 657-678

Robbins, D. H., Melvin, J. W., and Stalnaker, R. L. (1976) The Prediction of Thoracic Impact Injuries, *In Proceedings, 20th Stapp Car Crash Conference,* Society of Automotive Engineers, 697-729. 197

Robbins, D. H., Reynolds, H. M. (1975) Position and Mobility of Skeletal Landmarks of the 50th Percentile Male in an Automotive Seating Posture, *Vehicle Research Institute Report,* VRI 7.1

Robbin, D., H., Schneider, L., W., Snyder, R., G., Pflug, M., and Haffner, M., (1983) Seated posture of vehicle occupants, SAE Paper N 831617, Proceedings of the 27th Stapp Car Crash Conference, 1983, pp. 199-223

Robin, S. (2001) HUMOS: Human model for safety- A joint effort towards the development of refined humanlike car occupant models, *17th ESV Conference*, Paper No.297

Roche, A.F. (1953) Increase in cranial thickness during growth, Human Biology, 1953;25:81-92

Romero, R., Jeanty, P., Ghidini, A., Pretorius, D.H. (1988) Prenatal diagnosis of congenital anomalies. Norwalk, CT: Appleton and Lange, 1988:295-296

Roth, S., Raul, J.S., Willinger, R. (2008) Finite element analysis of child head injuries in the field of child abuse, *Computer Methods in Biomechanics and Biomedical Engineering* 11, 199-201

Rospa, The Royal Society for the Prevention of Accidents, (2013) http://www.rospa.com/news/releases/detail/?id=266

Rupp, J.D., Scheider, L.W. Klinich, K.D., Moss, S., Zhou, J., and Pearlman, M.D. (2001) Design, development and testing of a new pregnant abdomen for the Hybrid III small female crash test dummy. Report UMTRI-2001-07, University of Michigan Transportation Research Institute, Ann Arbor, Michigan, USA, 2001

SAAB Anti Whiplash Head Restraint System. (1996) Available from: <http:// www.shadetreemechanic.com/saab%20active%20head%20restraint.htm> [Accessed 5 May 2010]

Sances, A. and Yoganandan, N. Human head injury tolerance, Mechanisms of Head and Spine Trauma. Aloray Publisher; Goshen, NY: 1986. pp. 189–218

Sankar, S., Baranski, A., Taylak-Tokcelik, E., Scarlat, G., Roswall, M., Oancea, V., Grimes, B. (2008) Development of a new finite element model for the BioRID II crash dummy, SAE 2008-01-0509

Schneider, L., Robbins, D., Pflug, M., and Snyder, R., (1993) Anthropometry of Motor Vehicle Occupants. Final Report, UMTRI-83-53-1 University of Michigan Transportation Research Institute

Schultze, P.M., Stamm, C.A., and Roger, J. (1998) Placental abruption and fetal death with airbag deployment in a motor vehicle accident, Obstet Gynecol, 1998 Oct; 92 (4 Pt 2)719

Schuster P., Franz U., Stahlschmidt S., Pleschberger M., Eichberger A. (2004) Comparison of ES-2re with ES-2 and USSID Dummy, Considerations for ES-2re model in FMVSS Tests, *3.LS-DYNA Anwenderforum*, Bamberg

Serre, T., Brunet, C., Bidal, S., Behr, M., Ghannouchi, S. E., Chabert, L., Durand, F., Cavallero, C., Bonnoit, J. (2002) The seated man; geometry acquisition and three-dimensional reconstruction, *Surgical and Radiologic Anatomy*, 24:382-387

Sims, C.J., Boardman, C.H., Fuller, S.J. (1996) Airbag deployment following a motor vehicle accident in pregnancy. *Obstetrics and Gynecology*, 88(4 pt 2):726

Snijders, R.J. and Nicolaides, K.H. (1994) Fetal biometry at 14-40 weeks' gestation, *Ultrasound Obstetrics and Gynecology*, 1994 Jan 1; 4(1) : 34-48

Standing, S., (2005) *Gray's anatomy*, 39th edition, (Elsevier Churchill Livingstone, Edinburgh)

Sugimoto, T. And Yamazaki, K. (2005) First results from the JAMA human body model project, *The 19th International ESV Conference,* ID (05-0291)

Sutton, J. (2007) *How will I be born*, Optimal foetal positioning explained, what babies wish their mothers knew

Thackray, L. A. and Blackketter, D. M. (2002) Three-point seat belt maternal comfort and foetal safety, *Proceedings of the Institution of Mechanical Engineers Part D - Journal of Automotive Engineering,* Vol.216

Thinkroadsafety (2013) buckle up for baby and you http://think.direct.gov.uk /assets/pdf/dg_ 195233.pdf

TNO, (2012) Successful demonstration cyclist airbag http://www.tno.nl/content.cfm? context =overtnoandcontent=persberichtand laag1=37anditem_id=201211070049 andTaal=2 [Accessed 15 April 2013]

TNO Crash Safety Research Centre, (1995) The EUROSID 1 Technical Information, Delft

University of Texas Medical School (UTMS) (2013) Pediatric Surgery Fetus head shape http://utsurg.uth.tmc.edu/pedisurgery/tutorials/PtEduc/Abnormal_Head_Shape. htm [Accessed 10 March 2013]

User Manual MAMA-2B Rev B (2007) First Technology Safety Systems

Verriest, J.P., Chapon, A. and Trauchessee, R. (1981) Cinephotogrammetrical study of porcine thoracic response to belt applies load in frontal impact comparison between living and dead subjects. *Proceedings of the 25th Stapp Conference*, pp. 499-545.

Vezin, P. and Verriest, J.P. (2005) Development of a set of numerical human models for safety *The 19th International ESV Conference*, ID (05-0163).

Volvo, (2002) Pregnant Dummy Model. Available from http://www.volvocars. com /uk/top/my_volvo/volvo-accessories/child-safety/pages/pregnant.aspx [Accessed: 20 April 2013]

Volvo, (2004) Laura Thackray, Volvo Pregnant Woman Finite Element Model creator. Available from: <https://www.media.volvocars.com/download/media /articles/.../4982_1_5.aspx> [Accessed 28 September 2010]

Walter, D., and James, M. (1996) An usual mechanism of airbag injury. *Injury*, v.27, n.7, pp.523-4 Oxford; Elsevier Science

Webster, G. D., Newman J.A. (1976) A comparison of the impact response of cadaver heads and anthropomorphic head forms, *Association for the Advancement of Automotive Medicine*, 221-240

Weiss, H. B. (2001) The epidemiology of traumatic injury-related foetal mortality in Pennsylvania. 1995-1997: The role of motor vehicle crashes, *Accident Analysis and Prevention*, 33, 449-54

Whitestone, J. and Kaleps, I. (1988) Hybrid III Geometrical and Inertial Properties, *Society of Automotive*, Paper No.880639

Willinger, R., Kang, H.S, and Diaw, B. (1999) Three-dimensional human head finite element model validation against two experimental impacts, *Annual Biomedical Engineering*, 1999;27: 403-10

Wismans, W., Wismans, J., and Maltha, J. (1981) Application of three-dimensional mathematical occupant model for the evaluation of side impacts, *5th International Conference on the Biomechanics of Impact*

Wisman, W., (1994), Injury Biomechanics (4j610) Course Notes, Eindhoven University of Technology, Mechanical Engineering, The Netherlands.

Wismans, J., Hermans, J. H. A. (1988) MADYMO 3D Simulations of Hybrid III Dummy Sled Tests, *Society of Automotive Engineers*, Paper No.880645

Wood, J.L. (1971) Dynamic response of human cranial bone, *Journal Biomechanics*, 4, 1-12

World Health Organization Statistics, (2013) *Global Status Report on Road Safety*

Zhang, L., Yang, K.H., Dwarampudi, R., Omori, K., Li, T., Chang, K., Hardy, W.N., Khalil, T.B., and King, A.I. (2001) Recent, advances in brain injury research: A new human head model development and validation, *Stapp Car Crash Journal*, 45, pp. 369-394

Zhao, Z. and Narwani, G. (2005) Development of a human body finite element model for restraint system RandD applications, *The 19th International ESV Conference*, ID 05-03999

APPENDIX

PUBLICATIONS AND AWARDS

Moustafa, M., Acar, B.S., Automotive Safety Design in Conjunction with ATD Development, *14th International Conference on Machine Design and Production*, Morphou, CYPRUS, 29 June - 2 July 2010.

Moustafa, M., Esat, V., Acar, B.S., Effects of Airbag Firing Times on Pregnant Driver Safety in Full-Frontal Impacts, 2nd *International Conference Simulations on Bio-Sciences and Multi physics,* (SIMBIO-M), Marseille, FRANCE, 20-22 June 2011.

Moustafa, M., 'Expecting too' A Pregnant Occupant Model, *International MasterClass 2011 in Biomechanics for Design for Injury Prevention, Computer Science Department,* Loughborough, UNITED KINGDOM, 11-14 July 2011.

Moustafa, M., **Acar, B.S., Acar, M.,** Effects of Including a Fetus in the Uterus of Pregnant Woman Model, *15th International Conference on Machine Design and Production*, Pamukkale, TURKEY, 19-22 June 2012.

Moustafa, M., Acar, B.S., Acar, M., The Role of Placental Locations on Fetus Mortality in Road Accidents, ASME 2012 *11th Biennial Conference on Engineering Systems Design and Analysis* (ESDA 2012), Nantes, FRANCE, 2-4 July 2012. doi:ESDA2012-82738

Moustafa, M., Acar, B.S., Acar, M., Implications of Including a Fetus in the Uterus of Pregnant Woman Model, *International Crashworthiness Conference*, ICrash 2012, Milan, ITALY, 18-20 July 2012.

Acar, B.S., Meric M., Acar, M., Importance of Including a Fetus in Pregnant Occupant Models, NHTSA, ESV 2013, 23th International Technical Conference on Enhanced Safety of Vehicles, Seoul, Korea, May 27-30 2013, Paper No: 13-0445

Acar, B.S., Moustafa M., Acar, M., Location of Placenta and Fetus Mortality in Pregnant Drivers, *ASME 2013 International Mechanical Engineering Congress and Exposition*, San Diego, California, USA, 15-21 November 2013.

Acar, B.S., Moustafa, M., Esat, V., Acar, M., Pregnant Occupant Model Including a Fetus for Vehicle Safety Investigations, *ASME 2014 12th Biennial Conference on Engineering Systems Design and Analysis*, Copenhagen, Denmark, 25-27 June 2014. doi:10.1115/ESDA2014-20513

Awards

- Science Student Poster Competition 2011, Winner of 'Apical Limited' Prize, Computer Science Department, Loughborough University
- Graduate School Poster Competition 2011, Finalist, Runner up Prize, Computer Science Department, Loughborough University
- Graduate School Conference Fund 2012, Loughborough University